

Well-Defined Semiconducting Materials with Stabilized Molecular Orbitals: Thiaphospholes to Polythiophenes

by

Joshua Charles Worch

A dissertation submitted in partial fulfillment of the
requirements for the degree of Doctor of Philosophy in
Chemistry at Carnegie Mellon University

Examining Doctoral Committee:

Assistant Professor **Kevin J.T. Noonan** (Advisor)

Associate Professor **Newell R. Washburn** (Chair)

Professor **Bruce Armitage**

Associate Professor **Tomislav Pintauer** (Duquesne University)

© *Joshua C. Worch*

2016

Dedication:

To my dear wife, Anna, without whom I would be terribly lost.

To my mother and father for nurturing my quest for scientific inquiry.

To my brother who cultivated my passion for higher education.

Acknowledgements

I would like to begin by thanking my advisor, Dr. Kevin Noonan. We started this journey together (I was a first-year graduate student and he was a first-year faculty member). I am extremely thankful to have had the opportunity to work in his research group and witness his professional growth over the last five years. Kevin truly is a fantastic mentor, researcher, and teacher who has prepared me exceptionally well for the next stage of my career. Perhaps his greatest attribute is his humanity; he has been as understanding as anyone could be and I am forever grateful to him. I have no doubts he will continue to thrive and lead his students in a distinguished manner. Future students will certainly be in excellent hands!

I have spent an unhealthy amount of time in the NMR facility, but it allowed me to foster great relationships with Dr. Gayathri Withers and Dr. Roberto Gil. These individuals were invaluable to my professional success, but I now consider you both to be dear friends. I always enjoyed our technical discussions that inevitably diverged to entertaining personal conversations.

Many thanks are also extended to Dr. Tomasz Kowalewski and Dr. Stefan Bernhard for their unparalleled expertise and guidance during our collaborations. I wish to thank the members of my PhD committee, Dr. Newell Washburn and Dr. Bruce Armitage, for their helpful advice through the years and Dr. Tomislav Pintauer for participating in my PhD examination. The administrative and support staff of the chemistry department were extremely helpful and accommodating to me over the years. I must recognize Brenda Chambers, Valerie Bridge, Sara Wainer, and Patsey Haddock for their support. Dr. Rea Freeland has also been particularly hospitable to me and her compassionate advisement was crucial to my success.

Even though being a teaching assistant was not my favorite activity of graduate school, the instructors that I worked with made my experiences quite enjoyable and entertaining. I would especially like to thank Dr. Gizelle Sherwood and Carolyn Neiderlander for their mentorship that ultimately grew into great friendships.

I must also recognize my lab mates who trudged along with me through the halls of Mellon. Yunyan Qiu and I also began our PhD careers together. I will remember all of the arguing and laughter while we let our reactions proceed. I will especially remember the days where we both found ourselves in the lab until 3 am, trying to finish just one more reaction. Tyler Womble and Matt Baker were amazing people to have by my side, not only in the lab, but on the field for the Isotopes softball team. I will never overlook our late night “mini-group meetings” where we would

spend hours battling in Mario Kart 64 (I am the all-time wins leader, just to clarify!). It provided the perfect, much-needed break in my day. Finally, Chia-Hua Tsai was my favorite next door neighbor in the office (sorry, Yunyan). I have always admired her amazing work ethic and timely one-liners. Last, but not least, I must recognize the honorary Noonan group member, Andria Fortney. Her cheerful willingness, to be my sounding board for both chemistry related problems and matters not-having-much-to-do with chemistry, was much appreciated. I will certainly remember *our* embarrassingly awful dance sessions. And, I must thank her for welcoming my wife and me to live with her the month preceding this writing. It is hard to imagine how I would have finished this thesis without her hospitality. There were many other amazing people I met at Mellon during the last few years and I would like to simply mention a few: Melissa Lamson, Jake Mohin, Antonina Simakova, Adam Ahern, Christian Legaspi, Eric Wu, Danielle Chirdon, Husain Kagalwala, Jonathan Porras, Anthony Brooks, Matheus Tanha, James Woods, Jon Willcox, Matha Rishwan, Tom Ribelli, Samaneh Mesbahi, Karl Shultz, Danny Davis, and Claire Dingwell. For all others not named, I want to let you know that I value our friendship greatly.

I am forever grateful to my loving parents, Mike and Linda. They always provided for me in whatever way I needed, often knowing exactly what to do when I had no clue. I must specifically thank them for nurturing my love for science as they always steered me back to my dreams. I must also thank my older brother, Derek, for leading by example. I often looked to his guidance throughout my college career as well as graduate school.

My wife, Anna, deserves more than a meager paragraph, but I will do my best here. She has been my absolute rock since we married 5 years ago, just a few short weeks before I began graduate school. I cherish the fantastic memories we created: from moving into our first apartment in a new city, to our family vacations with our beloved baby (I mean our dog) – who we adopted shortly after moving to Pittsburgh. I also cherish our struggles as they have only strengthened our commitment and passion for one another. Anna has provided me with unparalleled, unconditional encouragement and support to allow me to thrive these previous 5 years. Through all of my darkest moments, she has provided the spark for me to see the way forward. For these reasons, among others, this PhD is as much hers as it is mine. Here's to the rest of our lives!

Table of Contents

List of Figures.....	viii–xi
List of Schemes.....	xi–xii
List of Tables.....	xii–xiii
List of Charts.....	xiii
Abstract and Chapter Descriptions.....	xiv–xvi
Chapter 1. Introduction to Organic Semiconductors and State of the Art of n-Type Materials	
1.1. Features of Organic Semiconducting Materials.....	1–2
1.1.1. Applications in Organic Electronic Devices.....	2–3
1.1.3. Introduction to p-Type and n-Type Organic Semiconductors.....	4
1.2. Design Strategies for n-Type Materials.....	4–5
1.2.1. Heteroatom Substitution.....	5
1.2.2. Manipulation using Main Group Chemistry.....	5–6
1.2.3. Selenium and Tellurium-Based Semiconductors.....	6–8
1.2.4. Silole-Based Semiconductors.....	8–9
1.2.5. Boron-Based Semiconductors.....	10–11
1.2.6. Phosphorus-Based Semiconductors.....	11–14
1.2.7. Incorporation of π -Accepting or Inductively-withdrawing Groups.....	15–17
1.2.8. Curved π -Conjugated Architectures.....	17
1.2.9 Extending the Conjugation Path.....	18–19
1.3. Molecular Orbital Stabilization in Polythiophenes.....	19–21

1.4. Scope of Thesis.....21

1.5 References.....22-30

Chapter 2. Synthetic Tuning of Electronic and Photophysical Properties of 2-Aryl-1,3-Benzothiaphospholes

2.1. Introduction.....31-33

2.2. Results and Discussion.....33-44

2.3. Conclusion.....44

2.4. Experimental Section.....44-52

2.5. References.....53-59

Chapter 3. Stability and Reactivity of 1,3-Benzothiaphosphole: Metallation and Diels-Alder Chemistry

3.1. Introduction.....60-61

3.2. Results and Discussion.....61-73

3.3. Conclusion.....73-74

3.4. Experimental Section.....74-84

3.5. References.....85-88

Chapter 4. Nickel Catalyzed Suzuki Polycondensation for Controlled Synthesis of Ester-Functionalized Conjugated Polymers

4.1. Introduction.....89-91

4.2. Results and Discussion.....91-102

4.3. Conclusion.....103

4.4. Experimental Section.....103-120

4.5. References.....121-125

Chapter 5. Nickel-Catalyzed Suzuki CTP for Polythiophenes Incorporating π -Accepting Functional Groups

5.1. Introduction.....	126-128
5.2. Results and Discussion.....	128-133
5.3. Conclusion.....	133-134
5.4. Experimental Section.....	134-152
5.5. References.....	153-155

Chapter 6. Perspective and Outlook

.....	156-158
-------	---------

Appendix 1. Supplementary Information for Chapter 4

A1.1. Model Compound Studies.....	159-162
A1.2. NMR Spectra Collected for Polymers.....	162-169
A1.3. Representative GPC Traces.....	170-172

Appendix 2. Supplementary Information for Chapter 5

A2.1. NMR Spectra Collected for Polymers.....	173-175
A2.2. Representative GPC Traces.....	176-178

List of Figures

Figure 1.1. Formation of band structure from ethylene to polyacetylene.....	2
Figure 1.2. Recent progress in device technologies for electronic skin.....	3
Figure 1.3. Description of heterocyclic conjugated building blocks.....	5
Figure 1.4. DFT calculations of HOMO–LUMO energy levels for polyheteroles.....	6
Figure 1.5. Comparison of band gap between hexyl–substituted group 16 polyheteroles.....	7
Figure 1.6. Absorption spectra of group 16 (S, Se, Te) donor–acceptor copolymers.....	8
Figure 1.7. Orbital interactions between silicon σ^* orbitals and the π^* of the butadiene fragment..	8

Figure 1.8. Commonly used silole building blocks for organic semiconducting materials.....	9
Figure 1.9. Orbital interactions between trivalent boron and π -conjugated framework.....	10
Figure 1.10. Trivalent and hypervalent phosphorus bonding.....	12
Figure 1.11. Tunability of phosphole conjugated materials.....	12
Figure 1.12. Resonance stabilization of π -acceptors.....	15
Figure 1.13. Calculated LUMO levels for highly fluorinated dithienophospholes.....	16
Figure 1.14. Band gap dependence on conjugation length in polythiophenes.....	18
Figure 1.15. Molecular orbital comparison of P3HT and ester-functionalized polythiophene.....	20
Figure 2.1. π -conjugated building blocks that incorporate a 3-coordinate phosphorus atom.....	32
Figure 2.2. Extended π -conjugated materials that incorporate phosphalkene moieties.....	33
Figure 2.3. Solid state molecular structure of 2-phenyl-1,3-benzothiaphosphole.....	35
Figure 2.4. Cyclic voltammogram of 2-phenyl-1,3-benzothiaphosphole using high scan rates...36	
Figure 2.5. Cyclic voltammograms of various 2-aryl-1,3-benzothiaphospholes.....	37
Figure 2.6. DFT calculations for molecular orbitals of 2-aryl-1,3-benzothiaphospholes.....	39
Figure 2.7. Hammett constants plotted versus the reduction potentials for thiaphospholes.....	41
Figure 2.8. Correlation of experimental reduction potentials with DFT results.....	42
Figure 2.9. Optical spectroscopy of 2-(C ₆ H ₄ - <i>p</i> -OMe)-1,3-benzothiaphosphole.....	43
Figure 3.1. Crude ¹ H NMR spectrum of 1,3-benzothiaphosphole.....	62
Figure 3.2. ³¹ P NMR spectra illustrating reaction of 1,3-benzothiaphosphole and HNEt ₂	63
Figure 3.3. Left – ³¹ P NMR spectra for synthesis of compound 2-bromo-1,3-benzothiaphosphole. Right – Crude gas chromatogram of the reaction mixture to synthesize 2-bromo-1,3-benzothiaphosphole.....	65
Figure 3.4. Stack plot of the crude ³¹ P NMR spectra for benzothiaphosphole lithiation and quenching using Me ₃ SiCl.....	66
Figure 3.5. Crude ³¹ P NMR spectra for quenching of 2-lithio-1,3-benzothiaphosphole.....	67
Figure 3.6. DFT calculated HOMO and LUMO levels for the benzoheterophospholes.....	69
Figure 3.7. Solid state molecular structure of Diels–Alder cycloadduct from 1,3-benzothiaphosphole and dimethylbutadiene.....	70

Figure 3.8. Different possible isomers of Diels–Alder cycloadduct from 1,3-benzothiaphosphole and dimethylbutadiene	72
Figure 3.9. Different possible isomers of Diels–Alder cycloadduct from 1,3-benzothiaphosphole and cyclopentadiene.....	73
Figure 4.1. Cross-coupling methods used in catalyst–transfer polycondensation.....	90
Figure 4.2. MALDI-TOF mass spectrum of P3HET prepared using Ni(PPh ₃)IPrCl ₂	95
Figure 4.3. GC-MS chromatograms for catalyst initiation with ThBpin.....	98
Figure 4.4. GPC chromatograms for the P3HT homopolymer and P3HT- <i>b</i> -P3HET copolymer synthesized using Ni(PPh ₃)IPrCl ₂	100
Figure 4.5. Solution and solid–state UV–vis spectra for ester polymers with P3HT included for reference.....	101
Figure 4.6. ¹ H NMR spectrum and end group analysis of P3HET.....	102
Figure 5.1. GPC chromatograms for the block copolymers. Top – synthesizing P3HT first. Bottom – synthesizing P3DBAT first.....	131
Figure 5.2. Solution and solid–state UV–vis spectra for amide polymers with P3HT, P3HET, and P3HET- <i>a</i> -P3HT included for reference.....	132
Figure 5.3. Solution and solid–state UV–vis spectra for cyano polymers with P3HT included for reference.....	133
Figure 6.1. Main–chain and side–chain sequence control in conjugated polymers.....	158
Figure A1.1. Crude ¹ H NMR Spectrum for small molecule Suzuki–Miyaura coupling at 50 °C using methyl 2,5-dibromothiophene-3-carboxylate and Ni(PPh ₃)IPrCl ₂ (1 mol %).....	159
Figure A1.2. GC-MS chromatograms for small molecule Suzuki–Miyaura coupling at 50 °C using methyl-2,5-dibromothiophene-3-carboxylate and Ni(PPh ₃)IPrCl ₂ (1 mol %).....	160
Figure A1.3. Crude ¹ H NMR Spectrum for small molecule Suzuki–Miyaura coupling at 50 °C using methyl-2,5-dibromothiophene-3-carboxylate and PEPPSI-IPr (1 mol %).....	161
Figure A1.4. GC-MS chromatograms for small molecule Suzuki–Miyaura coupling at 50 °C using methyl-2,5-dibromothiophene-3-carboxylate and PEPPSI-IPr (1 mol %).....	162
Figure A1.5. P3HET ¹ H NMR Spectrum.....	163
Figure A1.6. P3HET ¹³ C NMR Spectrum.....	163
Figure A1.7. P3HET long–range COSY.....	164
Figure A1.8. P3HET high resolution coupled HSQC.....	165
Figure A1.9. P3HET treated with Ni(COD) ₂ followed by HCl.....	166

Figure A1.10. P3HET- <i>a</i> -P3HT ¹ H NMR Spectrum.....	167
Figure A1.11. P3HET- <i>a</i> -P3HT ¹³ C NMR Spectrum.....	167
Figure A1.12. P3HET- <i>a</i> -P3HT long-range COSY.....	168
Figure A1.13. P3HET- <i>a</i> -P3HT high resolution HSQC.....	169
Figure A1.14. GPC Chromatogram and analysis of P3HET sample. Entry 3, Table 4.2 in Chapter 4.....	170
Figure A1.15. GPC Chromatogram and analysis of P3HT sample using Ni(dppp)Cl ₂ as the catalyst without water.....	171
Figure A1.16. GPC Chromatogram and analysis of P3HT sample. Entry 9, Table 4.2 in Chapter 4.....	172
Figure A2.1. P3DBAT ¹ H NMR Spectrum.....	173
Figure A2.2. P3DBAT ¹³ C NMR Spectrum.....	174
Figure A2.3. P3DBAT- <i>a</i> -P3HT ¹ H NMR Spectrum.....	174
Figure A2.4. P3DBAT- <i>a</i> -P3HT ¹³ C NMR Spectrum.....	175
Figure A2.5. GPC Chromatogram and analysis of P3DBAT sample. Entry 3, Table 5.1 in Chapter 5.....	176
Figure A2.6. GPC Chromatogram and analysis of P3DBAT- <i>a</i> -P3HT sample. Entry 6, Table 5.1 in Chapter 5.....	177
Figure A2.7. GPC Chromatogram and analysis of P3DBAT- <i>a</i> -P3HT sample. Entry 7, Table 5.1 in Chapter 5.....	178

List of Schemes

Scheme 2.1. Reduction of diisopropyl (2-mercaptophenyl)phosphonate to prepare 1-mercapto-2-phosphinobenzene.....	34
Scheme 2.2. Synthesis of 1,3-benzothiaphospholes from 1-mercapto-2-phosphinobenzene and aryl acid chlorides.....	34
Scheme 3.1. Synthesis of 1,3-benzothiaphosphole and byproduct from N-H addition across the P=C bond.....	61
Scheme 3.2. Synthesis of 2-bromo-1,3-benzothiaphosphole.....	64
Scheme 3.3. Lithiation and electrophilic quenching of the 1,3-benzothiaphosphole.....	65
Scheme 3.4. Attempted Stille and Negishi cross-coupling of metallated thiaphosphole.....	68

Scheme 3.5. [2+4] Diels–Alder cycloadditions.....	70
Scheme 4.1. Preparation of P3HET monomer.....	93
Scheme 4.2. Ester-containing polymers prepared using nickel–catalyzed Suzuki CTP.....	94
Scheme 4.3. Hydrolysis mechanisms of Suzuki monomers.....	94
Scheme 4.4. Detailed synthesis of P3HET monomer	107
Scheme 4.5. Synthesis of P3HET- <i>a</i> -P3HT monomer.....	109
Scheme 4.6. Synthesis of P3HET.....	114
Scheme 4.7. Synthesis of P3HT.....	115
Scheme 4.8. Synthesis of P3HET- <i>a</i> -P3HT.....	116
Scheme 5.1. P3DBAT, P3DBAT- <i>a</i> -P3HT, P3CT- <i>a</i> -P3HT, and P3CT- <i>a</i> -P3HET- <i>a</i> -P3HT prepared using Ni(dppp)Cl ₂ catalyzed Suzuki CTP.....	128
Scheme 5.2. Synthesis of Monomer P3DBAT monomer.....	137
Scheme 5.3. Synthesis of P3DBAT- <i>a</i> -P3HT monomer.....	139
Scheme 5.4. Synthesis of P3CT- <i>a</i> -P3HT monomer.....	142
Scheme 5.5. Synthesis of P3CT- <i>a</i> -P3HET- <i>a</i> -P3HT monomer.....	144
Scheme 5.6. Synthesis of P3DBAT.....	148
Scheme 5.7. Synthesis of P3DBAT- <i>a</i> -P3HT.....	149
Scheme 5.8. Synthesis of P3CT- <i>a</i> -P3HT.....	150
Scheme 5.9. Synthesis of P3CT- <i>a</i> -P3HET- <i>a</i> -P3HT.....	150

List of Tables

Table 2.1. Photophysical and electrochemical properties of 2-aryl-1,3-benzothiaphospholes.....	38
Table 2.2. Crystallographic details for 2-phenyl-1,3-benzothiaphosphole.....	52
Table 3.1. Crystallographic details for Diels-Alder cycloadduct from 1,3-benzothiaphosphole and dimethylbutadiene.....	84
Table 4.1. Model compound reactions with methyl 2,5-dibromothiophene-3-carboxylate.....	92
Table 4.2. Polymerization studies for P3HET, P3HT, and P3HET- <i>a</i> -P3HT monomers.....	97
Table 4.3. Catalyst screening for dihalogenated thiophenes using Suzuki–Miyaura coupling...	113
Table 4.4. Optimization of P3HET synthesis.....	115

Table 4.5. Optimization of water content in P3HT synthesis.....	116
Table 4.6. Synthesis of P3HET- <i>a</i> -P3HT.....	117
Table 4.7. Summary of optical properties of P3HET, P3HT- <i>b</i> -P3HET, P3HET- <i>a</i> -P3HT, P3HT.....	120
Table 5.1. Polymerization studies for P3DBAT, P3DBAT- <i>a</i> -P3HT, P3CT- <i>a</i> -P3HT, and P3CT- <i>a</i> -P3HET- <i>a</i> -P3HT monomers.....	129
Table 5.2. Summary of optical properties of P3DBAT, P3DBAT- <i>a</i> -P3HT, P3CT- <i>a</i> -P3HT, and P3CT- <i>a</i> -P3HET- <i>a</i> -P3HT.....	152

List of Charts

Chart 1.1. Representative examples of trivalent boron containing semiconductors.....	11
Chart 1.2. Comparison of phosphorus, nitrogen, and carbon π -bonds.....	13
Chart 1.3. Aromatic organic heterocycles and phosphorus congeners.....	14
Chart 1.4. Common n-type organic semiconductors featuring electron-withdrawing groups.....	16
Chart 1.5. π -Conjugated curved molecules displaying n-type behavior.....	17
Chart 1.6. Thiophene-based polymers with side-chain or main-chain cyano groups.....	19
Chart 1.7. Imide-functionalized thiophenes paired with common donor units in donor-acceptor copolymers.....	20
Chart 2.1. Conjugated systems with multiple thiaphosphole units.....	44
Chart 3.1. Common aromatic phosphorus heterocycles and their nitrogen congeners.....	60
Chart 5.1. Donor-acceptor copolymers synthesized via chain-growth mechanism.....	127
Chart 6.1. Scope of controlled polymers produced using CTP.....	156
Chart 6.2. Building blocks appearing in state of the art conjugated polymers currently prepared using step-growth polycondensation.....	157

Abstract

The development of organic semiconductors for device applications has been intensely pursued over the past four decades. The active layer in such devices consists of both hole transporting (p-type) semiconductors and electron transporting (n-type) semiconductors. The development of p-type materials has progressed rapidly while n-type systems are relatively underdeveloped, primarily due to stability issues. Perhaps the most salient feature of electron transport materials is a low reduction potential, resulting from the stabilization of the lowest unoccupied molecular orbital (LUMO). Thus, current research is largely focused on molecular design strategies to reduce LUMO energy levels. An extension of the π -system (i.e. conjugated polymers) normally results in a lowering of the LUMO while simultaneously raising the highest occupied molecular orbital (HOMO), reducing the ambient stability. The incorporation of π -accepting functional groups is a convenient manner through which to stabilize molecular orbitals (HOMO and LUMO) and their incorporation into conjugated polymers should lead to materials with improved stability. This thesis explains our efforts to synthesize well-defined conjugated polymers that incorporate π -accepting functional groups. Moreover, heteroatom substitution also has a profound impact on the optoelectronic properties of semiconducting materials and the insertion of main group elements into conjugated organic scaffolds is another established approach to accomplish LUMO stabilization. Specifically, phosphorus is an attractive element to incorporate into organic semiconductors because of its inimitable bonding versatility. This thesis also highlights our efforts to synthesize aromatic phosphorus heterocycles for electron transport.

Chapter 1 provides a general introduction into organic semiconductors as well as efforts to manipulate the molecular orbitals of π -conjugated materials. The focus is on both small molecules and polymeric materials with specific attention paid to main group substitution and functional group incorporation and how these strategies can be applied to create n-type materials.

Chapter 2 describes a series of bench-stable 2-aryl-1,3-benzothiaphospholes synthesized from 1-mercapto-2-phosphinobenzene and a variety of acid chlorides. The structure of 2-phenyl-1,3-benzothiaphosphole was established using X-ray diffraction. The electrochemical and photophysical properties of each benzothiaphosphole are reported and some of these molecules exhibit reversible 1-electron reductions due to the LUMO stabilization afforded by incorporation of P=C moiety. The reduction potentials show a defined pattern: becoming incrementally more positive as the electron deficiency of the 2-aryl substituent increases and enhances LUMO

stabilization. DFT calculations corroborate the electrochemical data elucidating the more pronounced effect of electron deficient groups on reduction by showing significantly more participation of those substituents in the LUMO.

Chapter 3 discusses the synthesis and functionalization of the parent 1,3-benzothiaphosphole. The phosphole could not be isolated, but the compound could be manipulated in solution to produce several new phosphorus compounds. Metallation of the 2-position using lithium diisopropylamide proceeded smoothly according to ^{31}P NMR spectroscopy, and quenching with trimethylsilyl chloride resulted in the desired 2-(trimethylsilyl)-1,3-benzothiaphosphole. However, functional substrates for cross-coupling could not be isolated using this approach. The P=C bond of the thiaphosphole was also explored as a dienophile, owing to its low lying LUMO, in Diels-Alder reactions with isoprene, 2,3-dimethylbutadiene, 2,3-dibenzylbutadiene and cyclopentadiene. The fused ring structures were fully characterized and a solid-state molecular structure of the 2,3-dimethylbutadiene cycloadduct was obtained.

Chapter 4 highlights our initial efforts to expand the functional group scope of conjugated polymers. Controlled synthesis of conjugated polymers with functional side chains is of great importance, affording well-defined optoelectronic materials possessing enhanced stability and tunability as compared to their alkyl substituted counterparts. A chain-growth Suzuki polycondensation of an ester-functionalized thiophene is described using commercially available nickel precatalysts. Model compound studies were used to identify suitable catalysts, and these experiments provided guidance for the polymerization of the ester-substituted monomer. This is the first report of nickel-catalyzed Suzuki cross-coupling for catalyst-transfer polycondensation (CTP) and to further illustrate the versatility of this method, block and alternating copolymers with 3-hexylthiophene were synthesized. This Suzuki protocol should serve as an entry point into the controlled synthesis of other electron-deficient polymers and donor-acceptor copolymers.

Chapter 5 describes further application of our nickel-catalyzed Suzuki CTP protocol. $\text{Ni}(\text{dppp})\text{Cl}_2$ was used to polymerize an amide-functionalized polythiophene – a monomer that is structurally similar to the prominent thiophene diimide electron-acceptor. Polymer molecular weights could be modulated according to catalyst loading, thus indicating a chain-growth process. Alternating and block copolymers were also prepared with reasonable polydispersities. Cyano-functionalized dimeric and trimeric monomers were explored using the Suzuki CTP protocol, however the resultant polymers were found to be highly insoluble.

Chapter 6 provides a general outlook for CTP regarding state of the art conjugated polymers. The development of new catalysts for mild cross-coupling strategies should significantly enhance the monomer scope for CTP. Next generation conjugated polymers will be synthesized by CTP protocols providing control over topology, microstructure, and composition. Specifically, sequence controlled conjugated polymers should provide a major advancement to the field of organic electronics.

Chapter 1

Introduction to Organic Semiconductors and State of the Art of n-Type Materials

1.1 Features of Organic Semiconducting Materials

Since the discovery of organic semiconducting materials by Heeger, MacDiarmid, and Shirakawa in 1977¹ (Nobel Prize in Chemistry, 2000), research on organic semiconductors has focused on either small molecules or larger polymeric structures. The key feature of organic semiconductors is a π -conjugated framework (i.e., alternating single and double bonds) with significant p-orbital overlap. An extended conjugated network possesses a delocalized π -electron cloud with a high degree of polarizability; removal or addition of π -electrons (doping) leads to the formation of charge carriers that are capable of traversing the π -system.² In small conjugated systems, delocalization of electrons decreases the gap between the Highest Occupied Molecular Orbital (HOMO) and Lowest Unoccupied Molecular Orbital (LUMO). As the number of π -bonds increases (e.g., in conjugated polymers) and more molecular orbitals are added, the individual orbitals become less discrete to form continuous bands, akin to inorganic semiconductors (Figure 1.1).³ This band gap separation between the valence band and conduction band is determined by the difference between the respective energies of the HOMO (valence band) and the LUMO (conduction band). To be practical, organic semiconductors require a band gap < 3 eV in order to absorb visible or near-infrared radiation.⁴ When this qualification is achieved, these materials become potentially useful in electronic device applications.

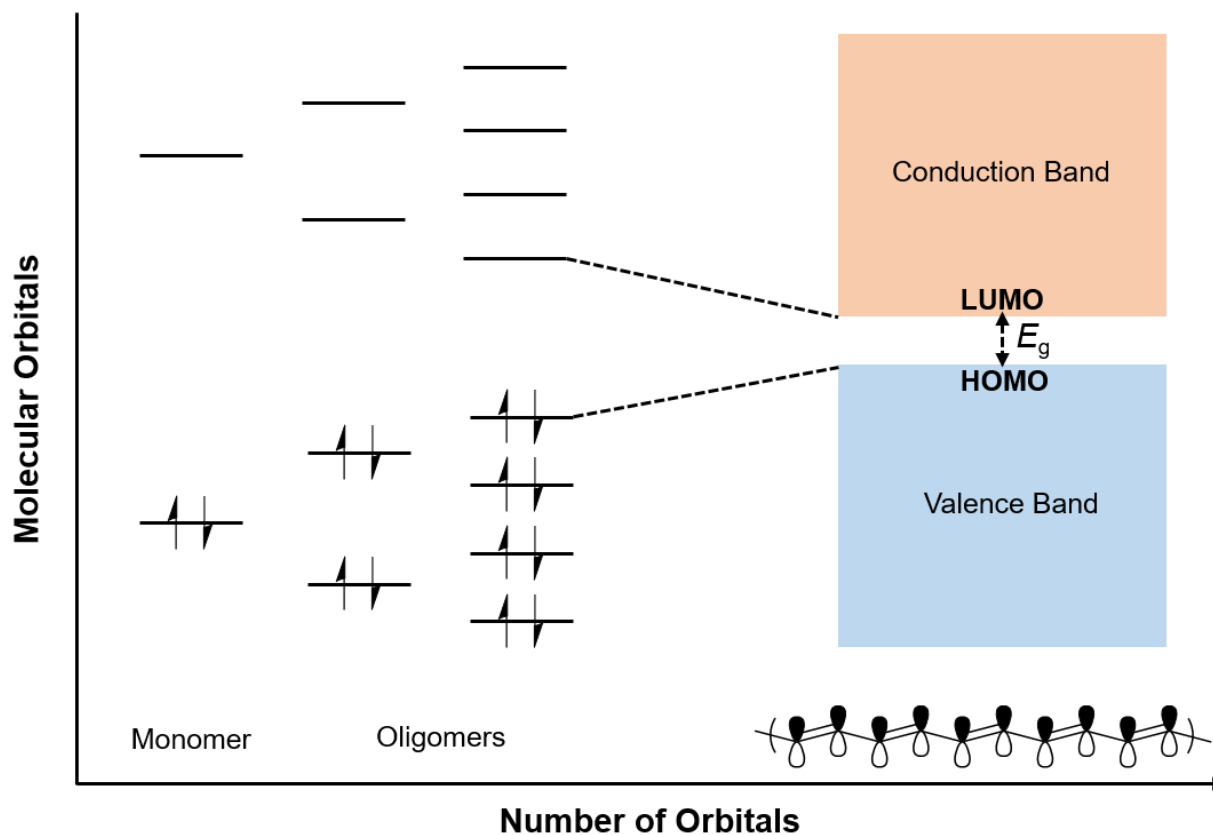


Figure 1.1. Formation of band structure from ethylene to polyacetylene.

1.1.1 Applications in Organic Electronic Devices

π -Conjugated materials⁵ have garnered enormous attention as solution processable components for photovoltaics⁶, light-emitting diodes⁷ and field-effect transistors.⁸ Organic semiconductors were initially envisioned as replacements for their inorganic counterparts due to relatively inexpensive solution processability allowing for large scale roll-to-roll manufacturing.⁹ Moreover, the lightweight nature of organic materials makes them suitable for thin and flexible devices. Perhaps the most salient feature of organic electronics is their inherent tunability through molecular engineering. As such, chemists can rationally design organic semiconductors to alter the optoelectronic and solid-state properties.¹⁰

Although some organic electronic devices have emerged into the consumer market (e.g., OLED display in televisions or smartphones) widespread development and commercialization has been sluggish. In particular, organic photovoltaics (OPV's) display comparatively lower efficiencies than inorganic analogues, stemming from inefficient charge transport.¹¹ A systemic issue for organic semiconductors is their inherent instability facilitated by chemical or photo-oxidative processes.¹² Despite these challenges, organic semiconducting materials remain intensely studied. More recently, conjugated materials have been explored for use in the biomedical field with developments focused on sensor applications¹³ or bioelectronics (Figure 1.2).¹⁴

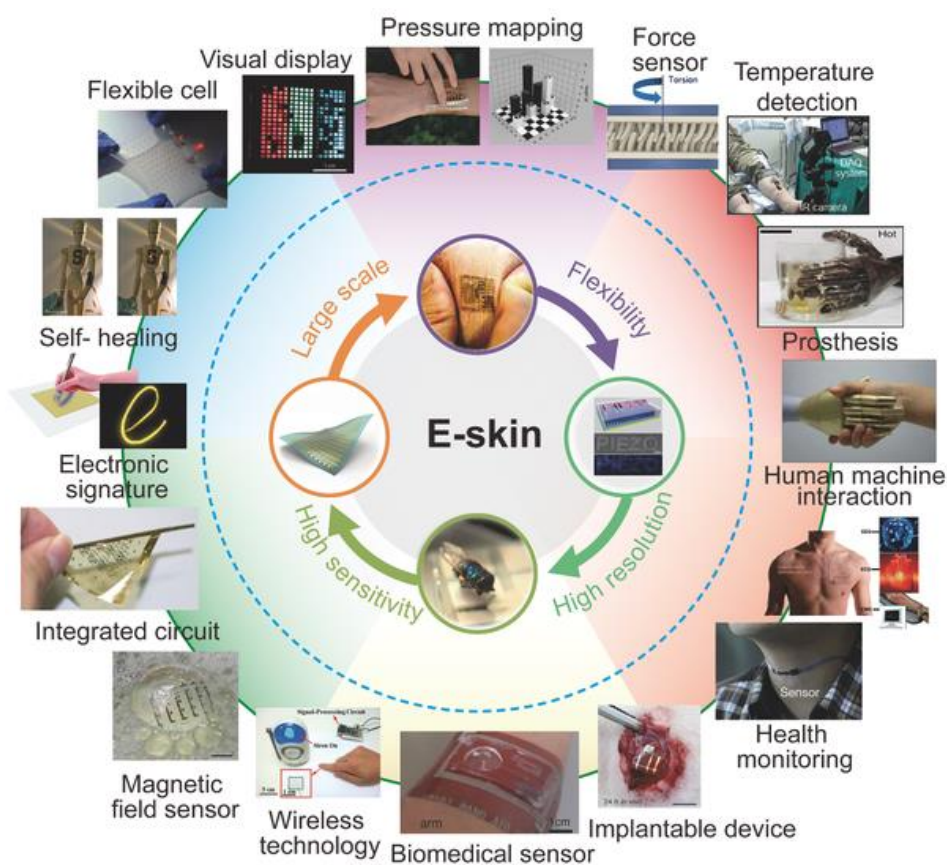


Figure 1.2. Recent progress in device technologies for electronic skin. Reproduced with permission from reference 14b. Copyright 2011 John Wiley and Sons.

1.1.3 Introduction to p-Type and n-Type Organic Semiconductors

In organic electronic devices, the active layer is composed of hole-transporting (p-type) and electron-transporting (n-type) semiconductors. P-type materials generally feature high-lying HOMO and LUMO energy levels whereby an electron can be easily removed from the HOMO (oxidation) to create a radical cation.¹⁵ On the other hand, n-type materials feature stabilized energy levels allowing for facile electron injection into the LUMO (reduction) to produce a stable radical anion.¹⁵ The presence of oxygen and water can induce trapping of the active charge carrier species (radical anions) in n-type materials.¹⁶ Generally speaking, increasing the electron affinity (lower lying LUMO) promotes ambient stability provided that the LUMO is below the reduction potential of either oxygen or water. To this end, a LUMO energy < -4 eV is generally regarded as sufficient for ambient stable electron injection and transport.¹⁷ During the last few decades, significant progress and improvements have been realized for p-type materials. However, benchmark numbers concerning important performance markers—e.g., charge mobility and ambient stability—of n-type molecules lag significantly behind p-type materials.¹⁸ This discrepancy between p-type and n-type semiconductors is undoubtedly a consequence of the relatively limited number of reports concerning n-type materials. However, achieving ambient electron transport remains challenging, thus explaining the current small supply of suitable n-type materials.

1.2 Design Strategies for n-Type Materials

The synthesis of stable organic n-type semiconductors is inherently challenging, but chemists have successfully utilized the following strategies:

- 1) Heteroatom substitution
- 2) Installation of electron-withdrawing groups

- 3) Molecular curvature
- 4) Extending conjugation length

The remainder of this section will highlight each method, with special emphasis on heteroatom manipulation with main group elements and stabilizing π -extended systems because these topics are the most relevant to the scope of the thesis.

1.2.1 Heteroatom Substitution

Familiar organic elements (nitrogen, oxygen, and sulfur) are staples in heterocyclic chemistry and their incorporation into conjugated scaffolds drastically alters the optoelectronic properties relative to all-carbon counterparts. Typically, heterocycles featuring such heteroatoms are described as electron-rich, with the exception of pyridine or pyrazine, and thus LUMO levels are insufficiently stabilized for n-type behavior (Figure 1.3).¹⁹

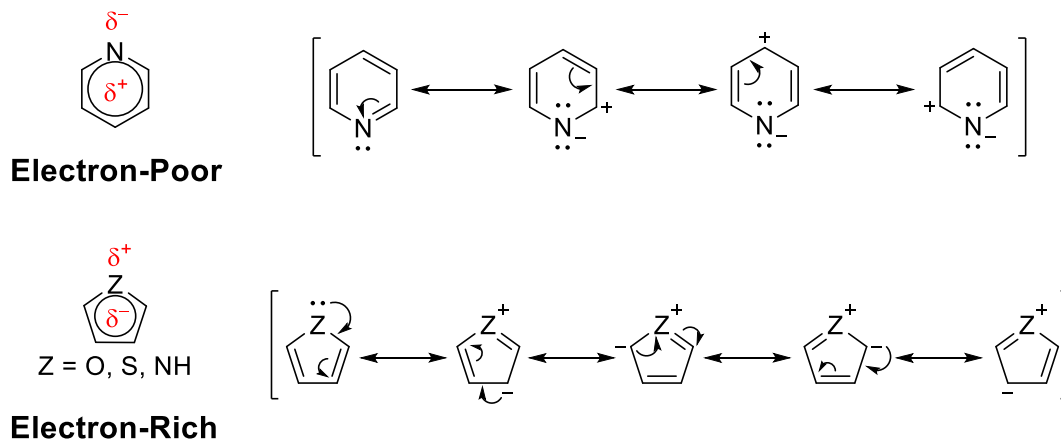


Figure 1.3. Electronic description of heterocyclic conjugated building blocks.

1.2.2 Manipulation using Main Group Chemistry

The incorporation of main group elements: including boron, silicon, selenium, tellurium, and phosphorus has emerged as a versatile strategy to enhance the electron accepting character of conjugated organic scaffolds. Atomic substitution of main group elements into classical organic

scaffolds produces interesting molecular orbital interactions, often imbuing such materials with a decreased band gap due to pronounced LUMO stabilization.²⁰ This powerful concept is conveniently illustrated *in silico* when examining heteroatom substitution in the polyheterole series (Figure 1.4).²¹ Although main group chemistry offers an attractive means for optoelectronic manipulation, the reactivity of main group-containing compounds is often different than organic systems. Consequently, alternative synthetic methods are necessary and typically challenging.

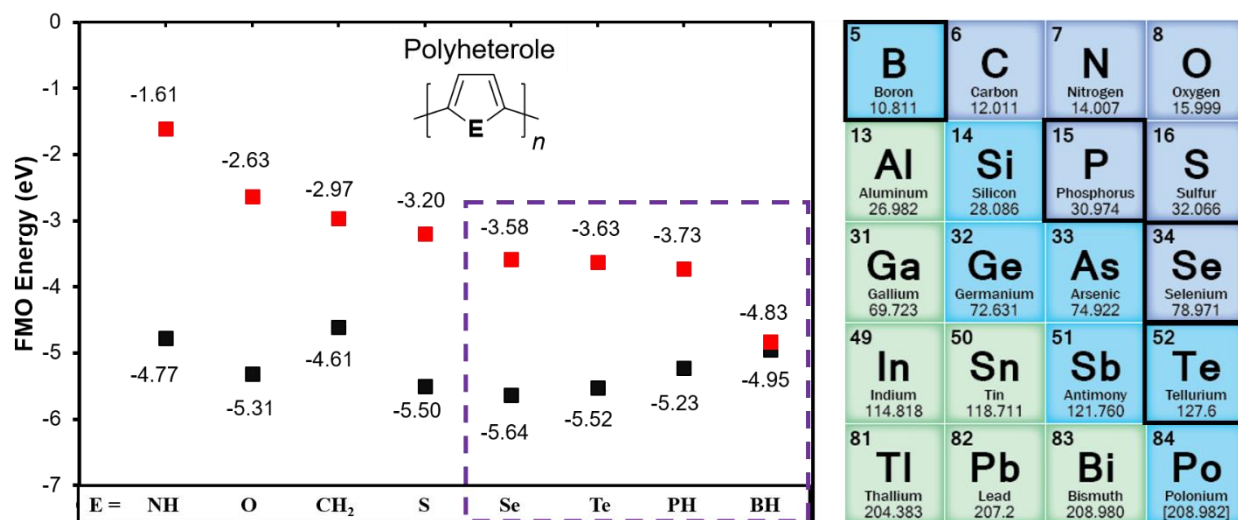


Figure 1.4. DFT calculations of HOMO-LUMO energy levels for polyheteroles based on data taken from reference 21.

The remainder of this sub-section will feature a brief introduction for each of the most important main group-containing organic semiconductors. Particular attention will be paid to the bonding environments that are responsible for the optoelectronic modulation of such materials.

1.2.3 Selenium and Tellurium-Based Semiconductors

Thiophene containing structures are among the most frequently appearing conjugated materials in organic electronic devices. In particular, polythiophenes have been thoroughly studied and the combination of poly-3-hexylthiophene (P3HT) with phenyl-C₆₁-butyric acid methyl ester

has been used as the benchmark for organic photovoltaics (OPVs) for some time.²² Optimized devices provide power conversion efficiencies (PCEs) of only ~ 5 % and this is primarily determined by the band gap of the polythiophene (1.9 eV for P3HT) because a large portion of incoming photons are not absorbed.²³ Accordingly, efforts to decrease the band gap and improve the absorption profile of conjugated materials is a point of emphasis in OPV research. The most obvious example of main group incorporation involves the heavier group 16 heterocycles, selenophene and tellurophene. Compared to polythiophene, polymers based on these heterocycles feature lower-lying LUMO energy levels, due to a lower ionization potential of the heavier elements, but similar HOMO energy levels.²⁴ Thus, polyselenophene and polytellurophene are low band gap congeners of polythiophene (Figure 1.5).

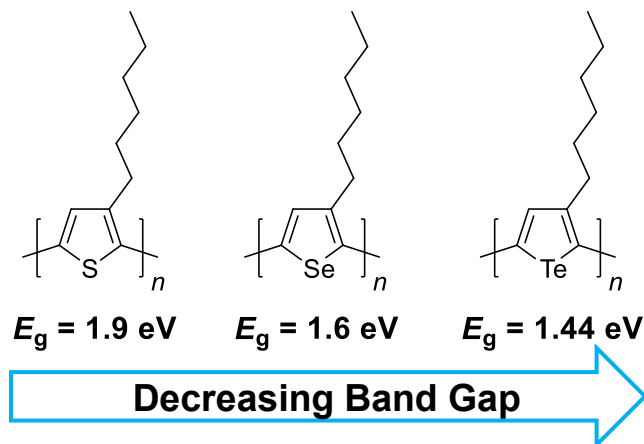


Figure 1.5. Comparison of band gap between hexyl-substituted group 16 polyheteroles.

Furthermore, the electronic properties of thiophene polymers can be drastically altered when thiophene moieties are replaced by selenophene²⁵ or tellurophene.²⁶ Additionally, selenium or tellurium atomic substitution for sulfur in other heterocycles often produces similar consequences. This concept has been referred to as “atomistic” band gap engineering and a striking example is illustrated in Figure 1.6.²⁷ Progressive substitution down group 16 (S–Se–Te)

drastically decreases the band gap in the resultant donor-acceptor polymers (E_g for S = 1.59 eV, Se = 1.46 eV, and Te = 1.06 eV).²⁷

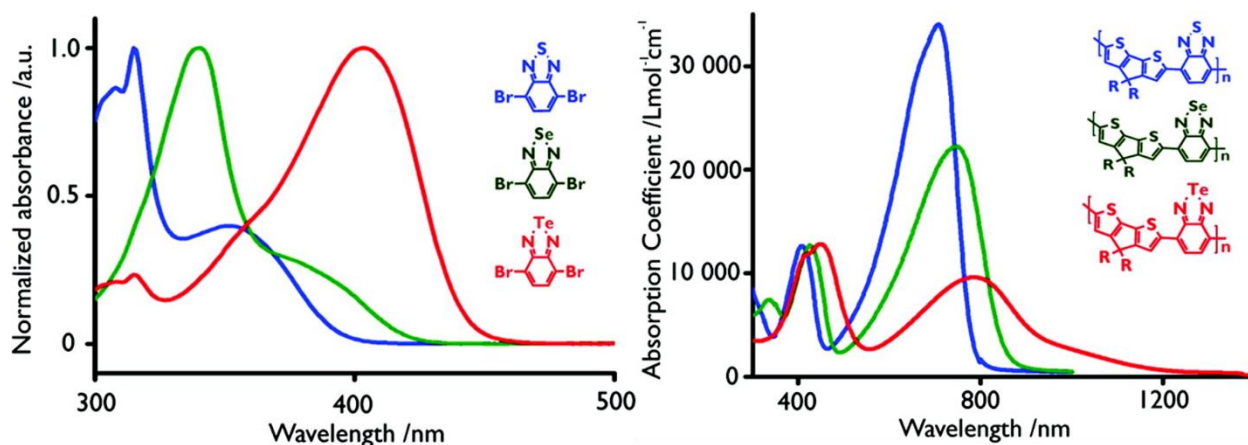


Figure 1.6. Left – absorption spectra of S, Se, Te acceptor molecules in DMSO and right – absorption spectra of corresponding group 16 donor-acceptor polymers in chloroform. Reproduced with permission from reference 27. Copyright 2012 American Chemical Society.

1.2.4 Silole-Based Semiconductors

Silicon-based compounds have also garnered attention in the organic electronic arena with the silole moiety, an inorganic cyclopentadiene analogue, appearing most frequently.²⁸ A stark change in the optoelectronic properties is observed after the simple C-Si substitution.^{20c}

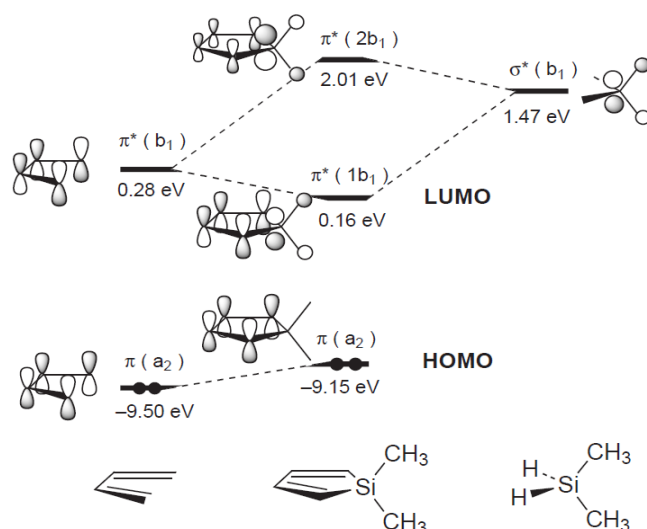


Figure 1.7. Orbital interactions between silicon σ^* bonds and the π^* butadiene fragment. Reproduced with permission from reference 29. Copyright 1998 Royal Society of Chemistry.

This electronic adjustment arises from a $\sigma^*-\pi^*$ bonding interaction, known as hyperconjugation, where the σ^* orbitals from the two exocyclic σ bonds on the silicon atom and the π^* of the butadiene fragment interact to stabilize HOMO and LUMO energy levels in the silole system (Figure 1.7).²⁹

Many silole-based organic semiconducting materials can be traced to fundamental building blocks outlined in Figure 1.8.³⁰ Several small molecules incorporating the silole moiety have displayed high charge transport mobilities and device efficiencies due to favorable electronic and solid-state morphologies rendered by the silicon atom.³¹ Furthermore, the pairing of donor silole blocks with classic accepting fragments has led to a number of valuable donor-acceptor copolymers.³²

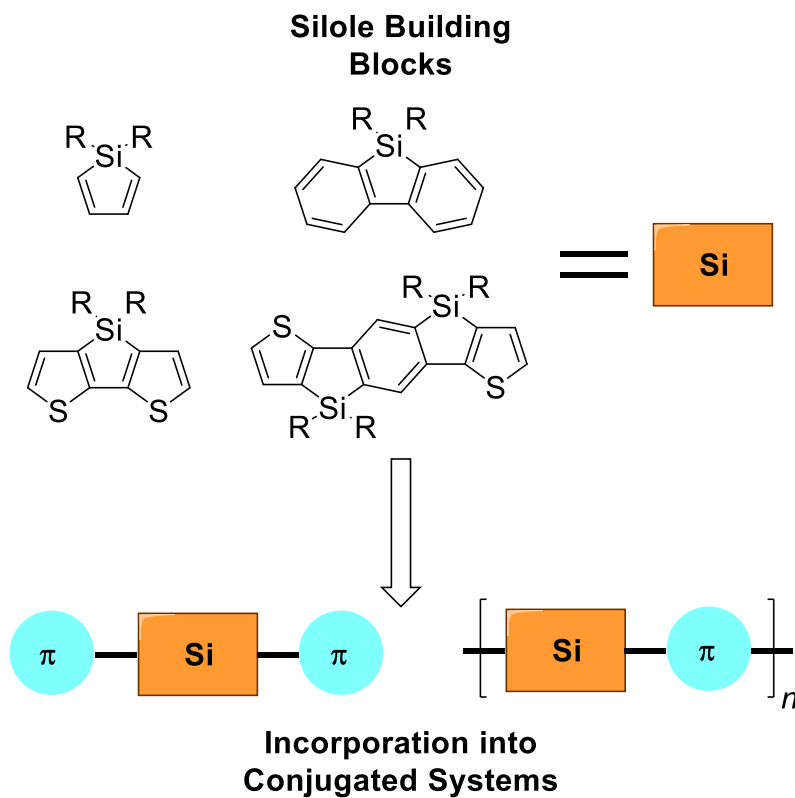


Figure 1.8. Common silole building blocks for organic semiconducting materials.

1.2.5 Boron-Based Semiconductors

Over the last decade there has been a renewed interest in organoboron π -conjugated materials due to interesting electronic features arising from boron's bonding properties.³³ Trivalent boron compounds feature a vacant p-orbital at the boron center that can communicate with the surrounding π -electron system. Specifically, a $p-\pi^*$ interaction facilitates conjugation through the boron center and simultaneously leads to strong electron accepting characteristics (Figure 1.9).^{20c}

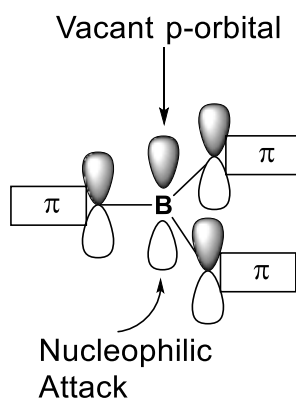


Figure 1.9. Description of orbital interactions between boron and surrounding π -conjugated framework.

Despite these interesting electronic features, trivalent organoborane species are notoriously vulnerable to nucleophilic attack on the vacant p-orbital by water, oxygen, or anions (Figure 1.9).^{33a} When the boron becomes tetracoordinate, the conjugation pathway is interrupted. Although this may seem detrimental for organic electronic applications, boron-containing semiconductors have found utility as anion sensors (e.g., fluoride sensing).³⁴ The change from tricoordinate to tetracoordinate valency produces a drastic change in either absorbance or emission due to the interruption in the conjugated network.³⁵ Additionally, some tetracoordinate boron species are highly efficient chromophores and can still be incorporated within conjugated networks to produce interesting photophysical properties.³⁶ Nevertheless, bench-stable trivalent boron compounds can be synthesized when sufficient kinetic³⁷ (steric bulk) and/or thermodynamic³⁸ (structural

constraint) stabilization exists; these concepts have also been applied to furnish stable polymeric architectures.³⁹ Several examples of trivalent organoboron semiconductors are listed in Chart 1.1.

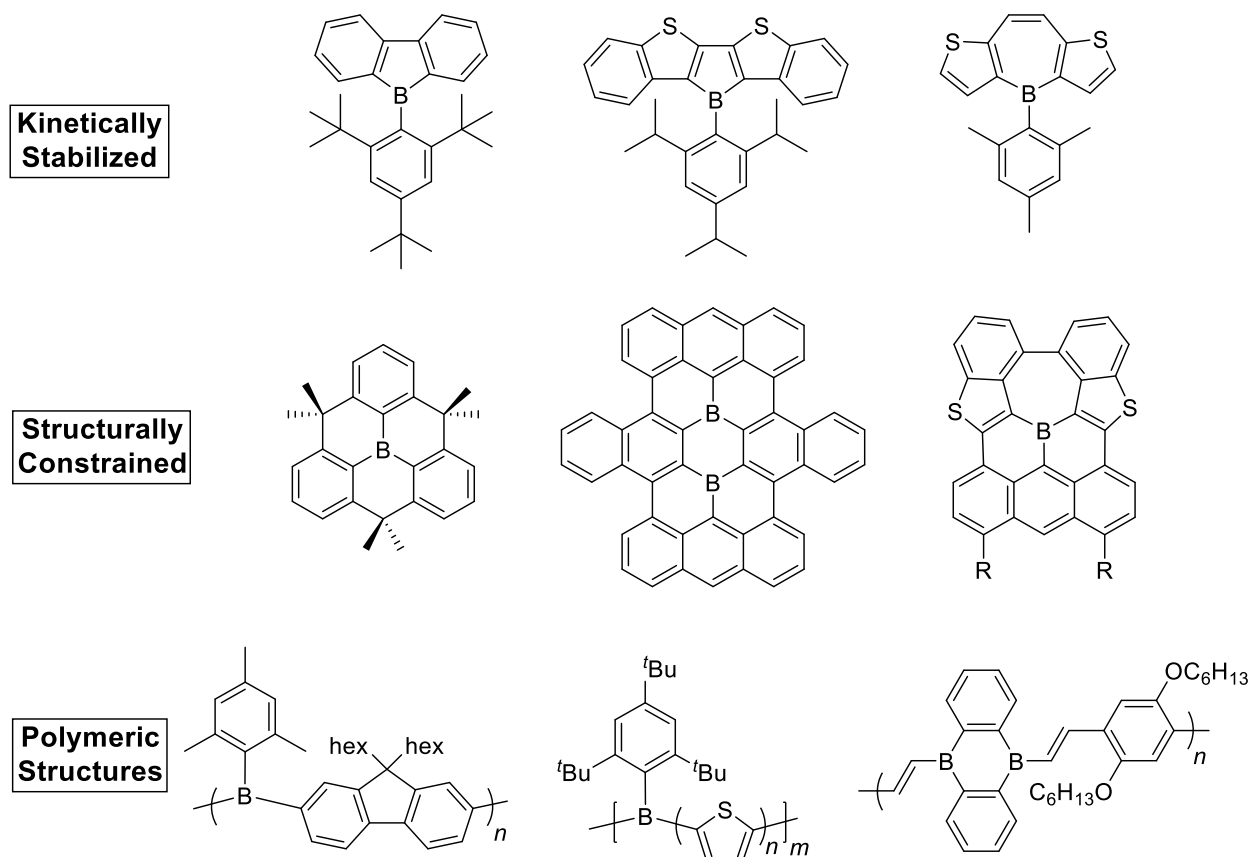


Chart 1.1. Representative examples of trivalent boron semiconductors.

1.2.6 Phosphorus-Based Semiconductors

Despite the comparatively large atomic size of phosphorus with respect to smaller organic elements, phosphorus is ubiquitous in organic chemistry (e.g., Wittig reaction or ligands for organometallic complexes).⁴⁰ Furthermore, phosphorus displays inimitable bonding versatility, making it an attractive element to incorporate into π -conjugated frameworks.⁴¹ As is the case for amines, trivalent phosphorus contains a lone-pair and is considered an electron donating species, but oxidation to the pentavalent state imbues an electron accepting character. This phenomenon, coined negative hyperconjugation, is due to π back-donation from the lone-pair on the P-

substituent (e.g., O, S, Se, NR) into the σ^* of the phosphorus atom.⁴² This creates a highly polarized moiety with enhanced electronegativity at the phosphorus atom and a pronounced electron-withdrawing quality (Figure 1.10).

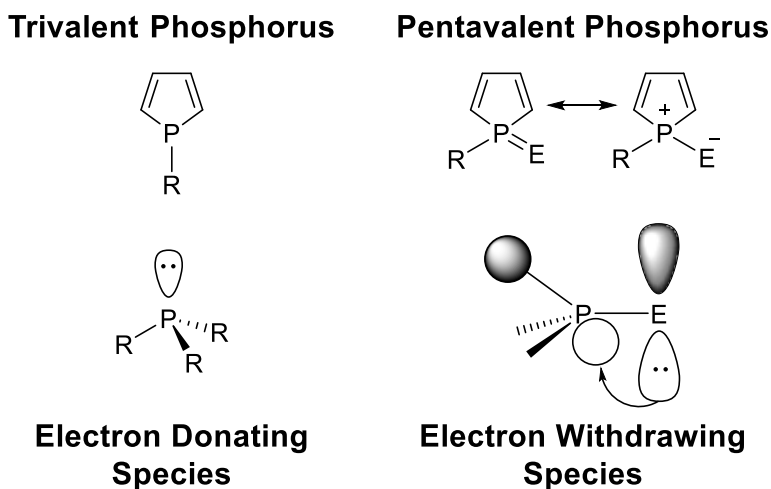


Figure 1.10. Trivalent and hypervalent phosphorus bonding.

Of the organophosphorus semiconductors, the phosphole is the most studied building block.^{41,43} Pentavalent phospholes display the aforementioned negative hyperconjugation, but the trivalent phosphole species also has electron accepting character due to positive hyperconjugation. This latter hyperconjugation is similar to the silole system and is described by a $\sigma^* - \pi^*$ bonding interaction.⁴⁴

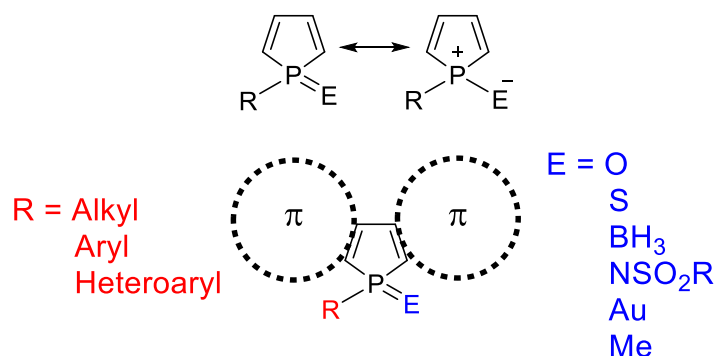
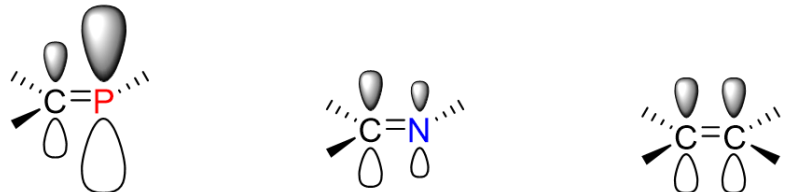


Figure 1.11. Tunability of phosphole-incorporated materials.

Thus, the unique optoelectronic properties of the phosphole moiety are enhanced by this additional orbital interaction that contributes to a more pronounced electron accepting character.⁴⁵ A high degree of tunability (manipulation of the π -scaffold or phosphorus substituents) further adds to the utility of phospholes (Figure 1.11).

Although the majority of research concerning phosphorus-based conjugated materials has involved phospholes, low-valent organophosphorus compounds – notably phosphalkenes (P=C bonds) – have also been investigated.⁴⁶ For phosphalkenes, the phosphorus atom is only partially sp^2 hybridized due to poor orbital overlap.⁴⁷ A consequence of this poor hybridization is significant s-character on the orbital describing the phosphorus lone-pair, which lowers the energy of the orbital so that the HOMO is actually the P=C π bond.^{46c,48} Thus, the phosphalkene electronic configuration is similar to the molecular orbital description of alkenes^{46e} whereas the orbital describing the nitrogen lone-pair defines the HOMO for the imine moiety. As a result, the phosphalkene is commonly referred to as the “carbon copy” since it is isoelectronic to the C=C unit and exhibits similar reactivity (Chart 1.2).⁴⁹



Bond Length	1.60 – 1.70 Å	1.28 – 1.33 Å	1.34 – 1.40 Å
Bond Strength	115 Kcal/mol	147 Kcal/mol	146 Kcal/mol
Polarization	←	→	nonpolar
Hybridization	partial sp^2	sp^2	sp^2
HOMO	C=P π	C=N _{Lone Pair}	C=C π

Chart 1.2. Comparison of phosphorus, nitrogen, and carbon π -bonds.

Despite similarities with alkenes, the P=C bond is considerably weaker than C=C or C=N moieties (Chart 1.2) and this can limit the stability of such molecules.⁵⁰ Early reports on acyclic phosphalkenes describe the installation of bulky groups on the phosphorus in order to provide kinetic stabilization.⁵¹ More recently, this strategy has been employed to furnish isolable phosphorus analogues of poly(*p*-phenylenevinylene) (PPV); these phosphorus congeners have been shown to be highly emissive with red-shifted absorption profiles compared to PPV.⁵² Some cyclic architectures lacking steric protection such as phosphinine⁵³ or heteroles (e.g., oxaphosphole, azaphosphole and thiaphosphole)^{46d,54} possess greater ambient stability than acyclic phosphalkenes due to aromatic stabilization (Chart 1.3).

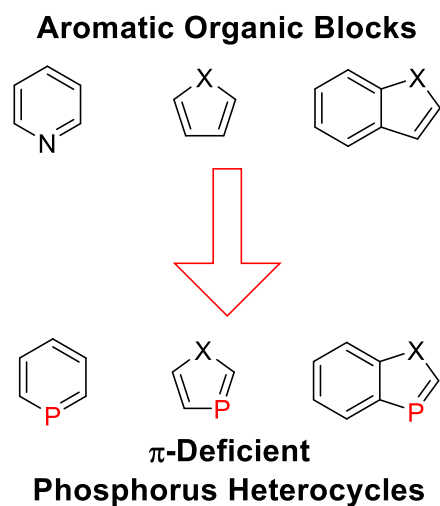


Chart 1.3. Aromatic organic heterocycles and phosphorus congeners.

Furthermore, the isolobal substitution of C-H to P in aromatic heterocycles serves to stabilize LUMO levels, thus transforming formerly electron-rich heterocycles into relatively electron-poor rings. As such, certain annelated oxaphospholes⁵⁵ and thiaphospholes⁵⁶ are n-type with reversible electron transport under an ambient atmosphere.

1.2.7 Incorporation of π -Accepting or Inductively-withdrawing Groups

The incorporation of π -accepting functional groups (e.g., carbonyl, imides, or cyano) is a convenient manner through which to stabilize molecular orbitals (HOMO and LUMO), and inductively electron withdrawing groups (such as halogens or perfluoroalkyl groups) effect a similar consequence.⁵⁷ The π -accepting or inductively withdrawing nature of these flanking functional groups results in decreased electron density within the π -system leading to higher electron affinity (Figure 1.12).

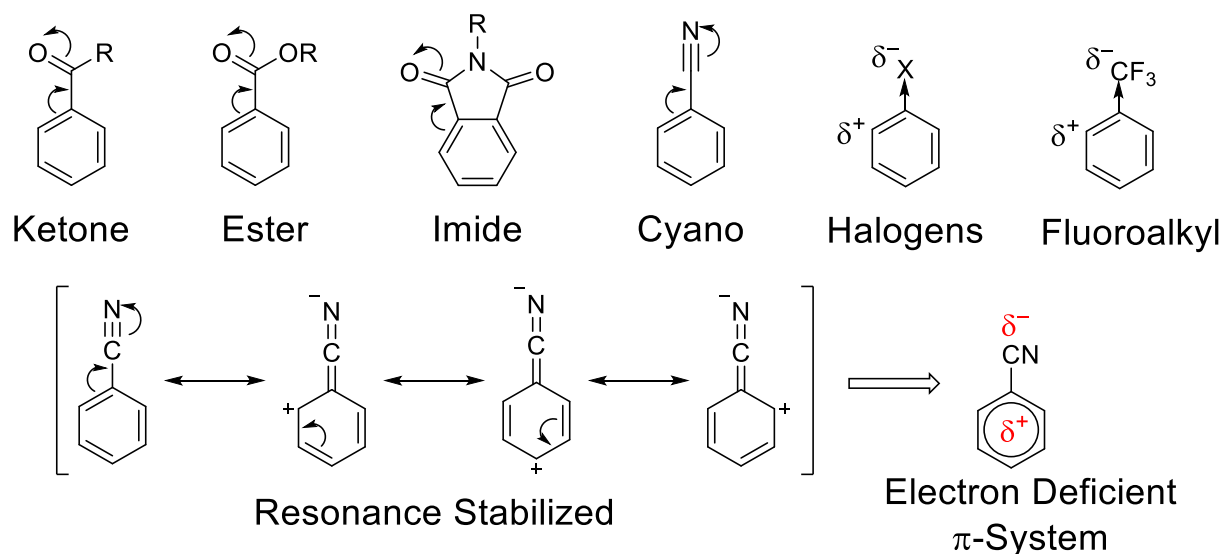


Figure 1.12. Resonance stabilization of π -acceptors and inductive effects by electronegative groups.

Additionally, molecular orbital energy levels can be dramatically influenced by substitution patterns. Concerning the LUMO, appropriate regiochemistry of electron withdrawing groups can enhance the electron affinity. The importance of substitution patterns is illustrated in a series of fluorinated dithienophospholes.⁵⁸ *Meta* substitution of the two fluorine atoms on the flanking aryl groups provides additional LUMO stabilization as compared to the *ortho* substitution pattern leading to a more facile electrochemical reduction for the former (Figure 1.13).⁵⁸ Thus, the placement of functional groups should be considered for n-type material design.

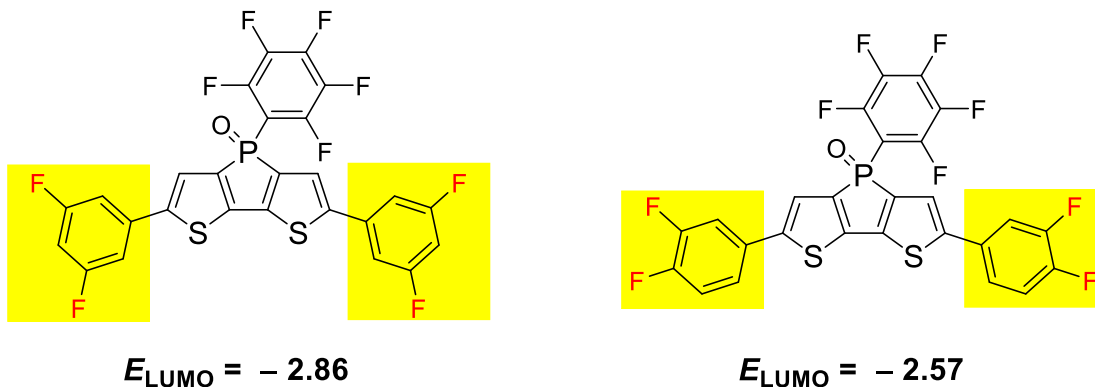
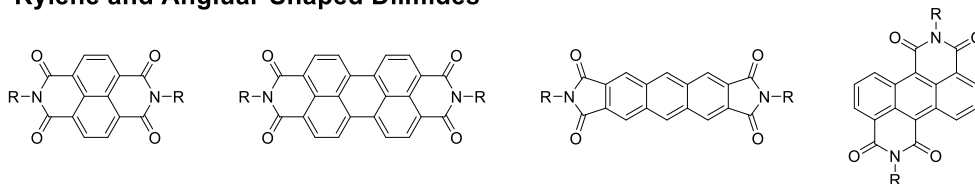


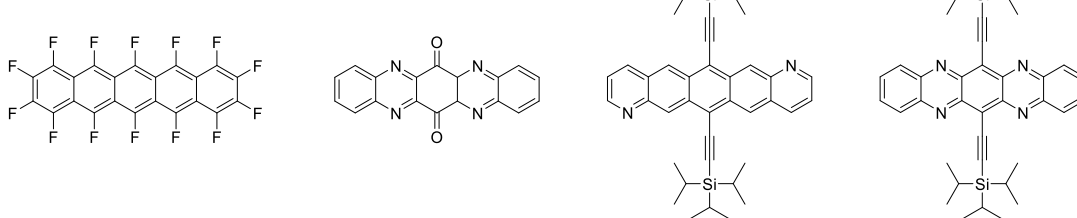
Figure 1.13. Calculated LUMO levels for highly fluorinated dithienophospholes. Data from reference 58.

A substantial number of high-performance n-type materials feature polycyclic conjugated cores flanked by imide groups; such materials are broadly referred to as rylene diimides (RDIs) and they are some of the most effective n-type semiconductors, either as small molecules or within polymeric networks.⁵⁹

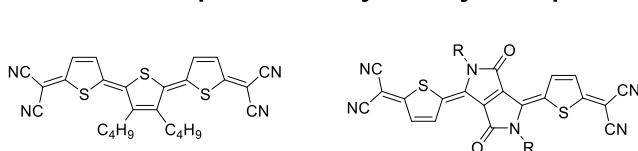
Rylene and Angluar-Shaped Diimides



Arenes and N-Heteroarenes



Quinoidal Thiophene with Cyanovinyl Groups



Donor-Acceptor Copolymers

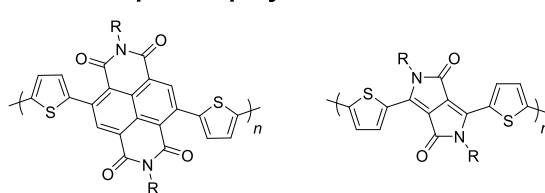


Chart 1.4. Survey of common n-type organic semiconductors that feature electron-withdrawing groups or electronegative heteroatoms.

Conjugated frameworks substituted with π -accepting or inductively electron withdrawing moieties are also common. Representative RDIs and other classes of high performance electron transport materials for transistors^{18a,18c}, photovoltaics^{18b}, or light-emitting diodes⁶⁰ are shown in Chart 1.4.

1.2.8 Curved π -Conjugated Architectures

Compounds exhibiting molecular curvature have also been investigated for electron transport. The curvature imparts unique physical properties due to nanoscale confinement of the electronic states.⁶¹ Perhaps the most widely used electron acceptor for device applications is the fullerene.^{23,62} Many bowl-shaped polycyclic aromatic hydrocarbons⁶³ composed of 6-membered rings⁶⁴ (e.g., hexabenzocoronene or helicene) and 5-membered rings⁶⁵ (e.g., cyclopenta-fused PAHs or corannulene) display n-type behavior as well. Representative curved molecular building blocks are displayed in Chart 1.5.

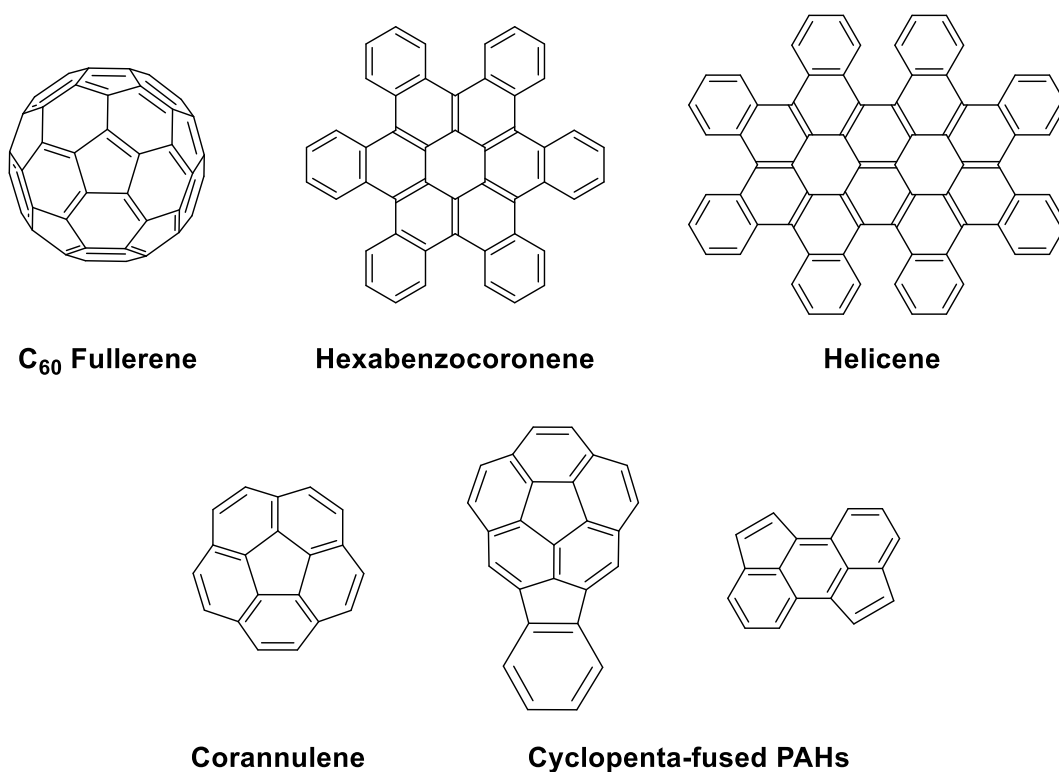


Chart 1.5. π -Conjugated curved molecules displaying n-type characteristics.

1.2.9 Extending the Conjugation Path

Small molecule organic semiconductors exhibit some degree of π -electron delocalization. However, as the conjugation path length increases further, the band gap continues to decrease up to a certain number of repeat units and this is referred to as the effective conjugation length.⁶⁶ This is important to consider in polymeric systems because inherent disorder exists and deviation from idealized planarity caused by steric interactions between monomer units can disrupt the electron overlap and restrict the effective conjugation length.⁶⁷ This concept is easily visualized when examining the effect of solubilizing groups on the band gaps of oligothiophenes and polythiophenes (Figure 1.14).⁶⁸ Despite these steric considerations, polymers generally have lower band gaps than their constituent oligomers.

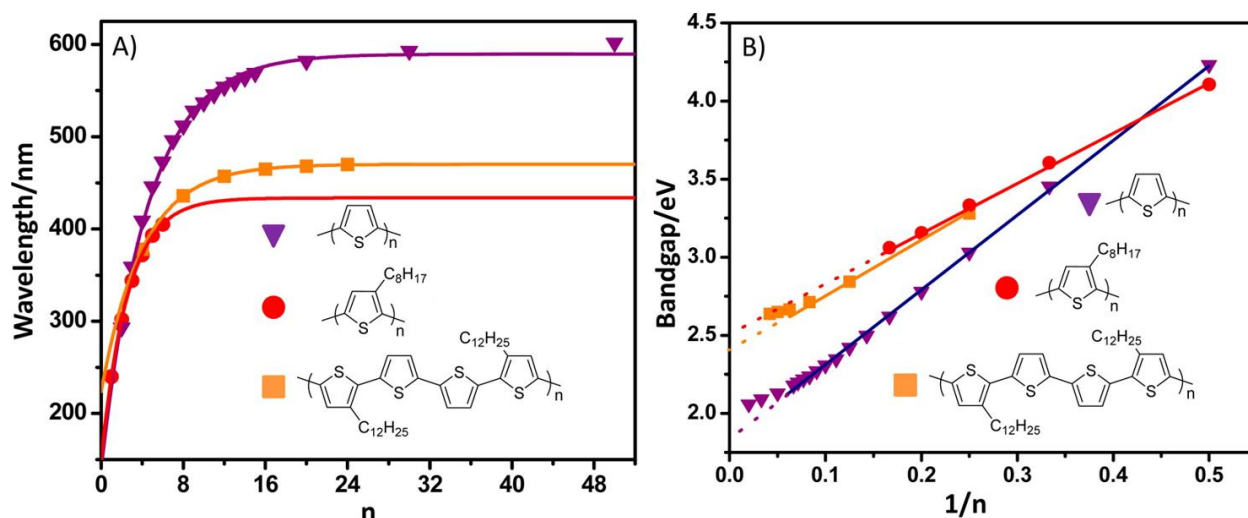


Figure 1.14. (A) Correlation between the maximum absorption (λ_{max}) and ring numbers (n) of oligothiophenes, and (B) bandgap energy vs inverse ring number (n) adapted from reference 68. Copyright 2014 American Chemical Society.

Chemists often utilize several methods (e.g., functional group alteration or heteroatom substitution) to alter the optoelectronic properties of organic semiconductors, but tuning conjugation length is arguably the simplest means for band gap manipulation (Figure 1.14–B). Semiconducting polymers often provide substantial LUMO stabilization compared to their

respective monomers, but this is at the direct cost of HOMO destabilization. Generally, high-lying HOMOs decrease ambient stability of organic semiconductors due to undesirable oxidative doping from molecular oxygen.⁴ As such, there is certainly an interest to synthesize conjugated polymers with decreased HOMO energy levels while maintaining sufficiently narrow band gaps. As noted previously, the incorporation of π -accepting functional groups within or along the polymer backbone serve to lower LUMO energy levels, but another consequence is a similar reduction in HOMO energy levels. Thus, efforts toward synthesizing semiconducting polymers with energy stabilizing functional groups remains a priority.

1.3 Molecular Orbital Stabilization in Polythiophenes

For the remainder of this section, only substituted polythiophenes will be examined in detail as to better illustrate the electronic effects from functional group substitution. Cyano substitution of alkyl thiophene-based polymers improves the ambient stability compared to pristine alkyl substituted derivatives while also adding ambipolar qualities (Chart 1.6).⁶⁹ However, cyano-substituted semiconductors are notorious for their poor solubility.

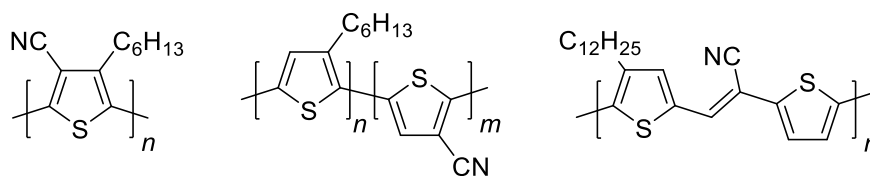


Chart 1.6. Thiophene-based polymers with side-chain or main-chain cyano groups.

The ester moiety is a satisfactory electron accepting group and imparts a good degree of solubility, thus providing an advantage to cyano substitution. When ester functionalized polythiophenes are used in organic electronic devices, they feature improved air stability—due to

stabilized molecular orbitals (Figure 1.15)—as well as superior solution processability compared to conventional alkyl substituted polythiophenes.⁷⁰

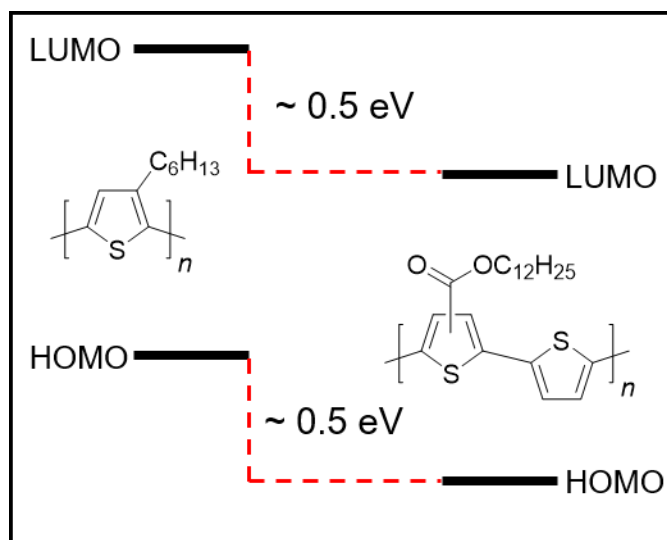


Figure 1.15. Comparison of frontier molecular orbitals in P3HT and an ester-functionalized polythiophene.^{70a}

Finally, the imide group frequently appears in n-type materials⁷¹ and one of the best-known acceptor units is the N-alkylated thieno[3,4-c]pyrrole-4,6-dione, commonly referred to as the thiophene-imide.⁷²

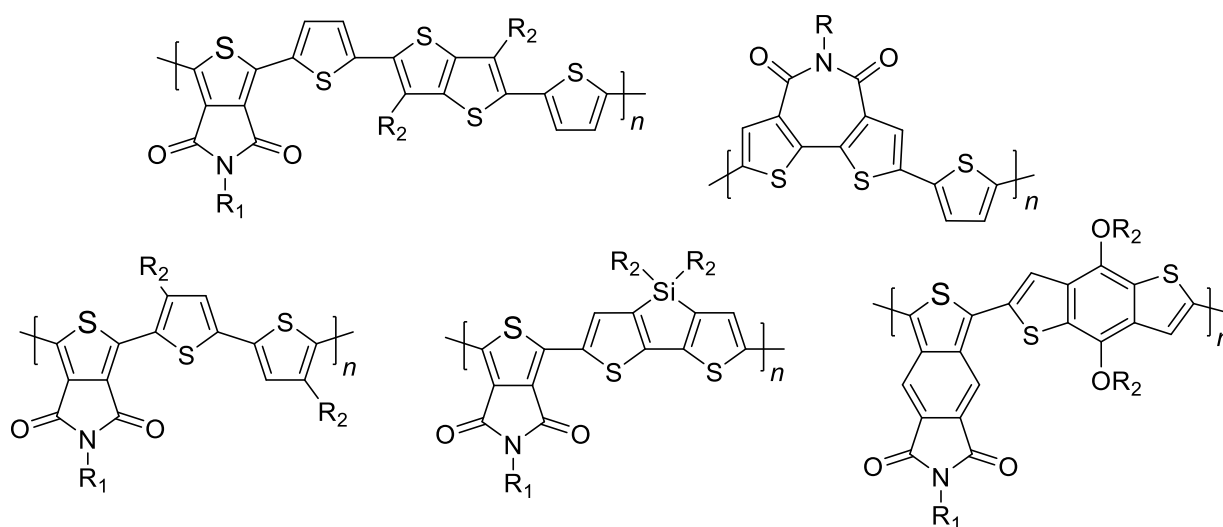


Chart 1.7. Imide-functionalized thiophenes in donor-acceptor copolymers.

These fragments, in addition to other imide functionalized thiophenes, are often paired with donor units in donor-acceptor copolymers (Chart 1.7). Such materials often feature increased charge mobility and improved performance in organic electronic devices due to the highly planarized solid-state morphology resulting from the imide functional group.^{32b,73}

1.4 Scope of Thesis

The broad focus of this thesis concerns molecular engineering as it is applied in creating materials with stabilized molecular orbitals for 1) electron transport or with 2) improved photo-oxidative stability. In Chapters 2 and 3, the incorporation of phosphorus-carbon π -bonds into conjugated scaffolds provide stabilized LUMO energy levels and, in some cases, ambient electron transport. Chapters 4 and 5 focus on the development of well-defined polythiophenes featuring enhanced stability and tunability due to the incorporation of π -accepting functional groups in conjugation with the polymer backbone. The synthesis of these materials was achieved using a nickel-catalyzed Suzuki catalyst-transfer polycondensation (CTP) protocol developed in our lab.

1.5 References

1. Chiang, C. K.; Fincher, C. R.; Park, Y. W.; Heeger, A. J.; Shirakawa, H.; Louis, E. J.; Gau, S. C.; MacDiarmid, A. G. *Phys. Rev. Lett.* **1977**, *39*, 1098-1101.
2. (a) Brédas, J. L.; Calbert, J. P.; da Silva Filho, D. A.; Cornil, J. *Proc. Natl. Acad. Sci.* **2002**, *99*, 5804-5809. (b) Bredas, J. L.; Street, G. B. *Acc. Chem. Res.* **1985**, *18*, 309-315.
3. Heeger, A. J.; Kivelson, S.; Schrieffer, J. R.; Su, W. P. *Rev. Mod. Phys.* **1988**, *60*, 781-850.
4. *Organic Electronics*; Klauk, H., Ed.; Wiley-VCH Verlag GmbH & Co. KGaA: Weinheim, 2006.
5. (a) *Handbook of Organic Materials for Optical and (Opto)Electronic Devices: Properties and Applications, 1st Ed.*; Ostroverkhova, O., Ed.; Woodhead Publishing: Cambridge, 2013. (b) *Handbook of Conducting Polymers. Conjugated Polymers: Processing and Applications*; Skotheim, T. A.; Reynolds, J. R., Eds.; CRC Press: Boca Raton, 2007.
6. *Organic Photovoltaics: Materials, Device Physics, and Manufacturing Technologies*; Brabec, C.; Scherf, U.; Dyakonov, V., Eds.; Wiley-VCH Verlag GmbH & Co. KGaA: Weinheim, 2011.
7. *Organic Light-Emitting Diodes (OLEDs): Materials, Devices and Applications. 1st Ed.*; Buckley, A., Ed.; Woodhead Publishing: Cambridge, 2013.
8. Kymissis, I. *Organic Field Effect Transistors: Theory, Fabrication and Characterization*; Springer: New York, 2009.
9. Katz, H. E. *Chem. Mater.* **2004**, *16*, 4748-4756.
10. (a) Henson, Z. B.; Mullen, K.; Bazan, G. C. *Nat. Chem.* **2012**, *4*, 699-704. (b) Roncali, J. *Macromol. Rapid Commun.* **2007**, *28*, 1761-1775.
11. Coropceanu, V.; Cornil, J.; da Silva Filho, D. A.; Olivier, Y.; Silbey, R.; Brédas, J.-L. *Chem. Rev.* **2007**, *107*, 926-952.

12. (a) Manceau, M.; Bundgaard, E.; Carle, J. E.; Hagemann, O.; Helgesen, M.; Sondergaard, R.; Jorgensen, M.; Krebs, F. C. *J. Mat. Chem.* **2011**, *21*, 4132-4141. (b) Jørgensen, M.; Norrman, K.; Krebs, F. C. *Sol. Energy Mater. Sol. Cells* **2008**, *92*, 686-714. (c) Bliznyuk, V. N.; Carter, S. A.; Scott, J. C.; Klärner, G.; Miller, R. D.; Miller, D. C. *Macromolecules* **1999**, *32*, 361-369. (d) Billingham, N. C.; Calvert, P. D.; Foot, P. J. S.; Mohammad, F. *Polym. Degrad. Stab.* **1987**, *19*, 323-341. (e) Pud, A. A. *Synth. Met.* **1994**, *66*, 1-18.

13. *Organic Semiconductors in Sensor Applications*; Bernards, D. A.; Owens, R. M.; Malliaras, G. G., Eds.; Springer-Verlag Berlin Heidelberg: Berlin, 2008.

14. (a) Wang, X.; Dong, L.; Zhang, H.; Yu, R.; Pan, C.; Wang, Z. L. *Adv. Sci.* **2015**, *2*, 1500169. (b) Chortos, A.; Liu, J.; Bao, Z. *Nat. Mater.* **2016**, *15*, 937-950. (c) Hammock, M. L.; Chortos, A.; Tee, B. C. K.; Tok, J. B. H.; Bao, Z. *Adv. Mater.* **2013**, *25*, 5997-6038.

15. Cravino, A.; Sariciftci, N. S. *Nat. Mater.* **2003**, *2*, 360-361.

16. de Leeuw, D. M.; Simenon, M. M. J.; Brown, A. R.; Einerhand, R. E. F. *Synth. Met.* **1997**, *87*, 53-59.

17. (a) Usta, H.; Facchetti, A.; Marks, T. J. *Acc. Chem. Res.* **2011**, *44*, 501-510. (b) Usta, H.; Risko, C.; Wang, Z.; Huang, H.; Deliomeroğlu, M. K.; Zhukhovitskiy, A.; Facchetti, A.; Marks, T. J. *J. Am. Chem. Soc.* **2009**, *131*, 5586-5608. (c) Jones, B. A.; Facchetti, A.; Wasielewski, M. R.; Marks, T. J. *J. Am. Chem. Soc.* **2007**, *129*, 15259-15278.

18. (a) Gao, X.; Hu, Y. *J. Mater. Chem. C* **2014**, *2*, 3099-3117. (b) Chochos, C. L.; Tagmatarchis, N.; Gregoriou, V. G. *RSC Adv.* **2013**, *3*, 7160-7181. (c) Meng, Q.; Hu, W. *Phys. Chem. Chem. Phys.* **2012**, *14*, 14152-14164. (d) Nicolai, H. T.; Kuik, M.; Wetzelaer, G. A. H.; de Boer, B.; Campbell, C.; Risko, C.; Brédas, J. L.; Blom, P. W. M. *Nat Mater* **2012**, *11*, 882-887.

19. *Handbook of Heterocyclic Chemistry, 3rd Ed.*; Katritzky, A. R.; Ramsden, C. A.; Joule, J. A.; Zhdankin, V. V., Eds.; Elsevier: Oxford, 2010.
20. (a) Parke, S. M.; Boone, M. P.; Rivard, E. *Chem. Commun.* **2016**, 52, 9485-9505. (b) He, X.; Baumgartner, T. *RSC Adv.* **2013**, 3, 11334-11350. (c) Yamaguchi, S.; Tamao, K. *Chem. Lett.* **2005**, 34, 2-7.
21. Salzner, U.; Lagowski, J. B.; Pickup, P. G.; Poirier, R. A. *Synth. Met.* **1998**, 96, 177-189.
22. Ma, W.; Yang, C.; Gong, X.; Lee, K.; Heeger, A. J. *Adv. Funct. Mater.* **2005**, 15, 1617-1622.
23. Brabec, C. J.; Gowrisanker, S.; Halls, J. J. M.; Laird, D.; Jia, S.; Williams, S. P. *Adv. Mater.* **2010**, 22, 3839-3856.
24. (a) Heeney, M.; Zhang, W.; Crouch, D. J.; Chabinyk, M. L.; Gordeyev, S.; Hamilton, R.; Higgins, S. J.; McCulloch, I.; Skabara, P. J.; Sparrowe, D.; Tierney, S. *Chem. Commun.* **2007**, 5061-5063. (b) Jahnke, A. A.; Djukic, B.; McCormick, T. M.; Buchaca Domingo, E.; Hellmann, C.; Lee, Y.; Seferos, D. S. *J. Am. Chem. Soc.* **2013**, 135, 951-954.
25. Shahid, M.; Ashraf, R. S.; Huang, Z.; Kronemeijer, A. J.; McCarthy-Ward, T.; McCulloch, I.; Durrant, J. R.; Siringhaus, H.; Heeney, M. *J. Mat. Chem.* **2012**, 22, 12817-12823.
26. Jahnke, A. A.; Howe, G. W.; Seferos, D. S. *Angew. Chem. Int. Ed.* **2010**, 49, 10140-10144.
27. Gibson, G. L.; McCormick, T. M.; Seferos, D. S. *J. Am. Chem. Soc.* **2012**, 134, 539-547.
28. Chen, J.; Cao, Y. *Macromol. Rapid Commun.* **2007**, 28, 1714-1742.
29. Yamaguchi, S.; Tamao, K. *J. Chem. Soc., Dalton Trans.* **1998**, 3693-3702.
30. (a) Lu, G.; Usta, H.; Risko, C.; Wang, L.; Facchetti, A.; Ratner, M. A.; Marks, T. J. *J. Am. Chem. Soc.* **2008**, 130, 7670-7685. (b) Ashraf, R. S.; Chen, Z.; Leem, D. S.; Bronstein, H.; Zhang, W.; Schroeder, B.; Geerts, Y.; Smith, J.; Watkins, S.; Anthopoulos, T. D.; Siringhaus, H.; de Mello, J. C.; Heeney, M.; McCulloch, I. *Chem. Mater.* **2011**, 23, 768-770.

31. Sun, Y.; Welch, G. C.; Leong, W. L.; Takacs, C. J.; Bazan, G. C.; Heeger, A. J. *Nat. Mater.* **2012**, *11*, 44-48.
32. (a) Zhang, Z.; Lin, F.; Chen, H.-C.; Wu, H.-C.; Chung, C.-L.; Lu, C.; Liu, S.-H.; Tung, S.-H.; Chen, W.-C.; Wong, K.-T.; Chou, P.-T. *Energy Environ. Sci.* **2015**, *8*, 552-557. (b) Chu, T.-Y.; Lu, J.; Beaupré, S.; Zhang, Y.; Pouliot, J.-R.; Wakim, S.; Zhou, J.; Leclerc, M.; Li, Z.; Ding, J.; Tao, Y. *J. Am. Chem. Soc.* **2011**, *133*, 4250-4253. (c) Hou, J.; Chen, H.-Y.; Zhang, S.; Li, G.; Yang, Y. *J. Am. Chem. Soc.* **2008**, *130*, 16144-16145.
33. (a) Jäkle, F. *Chem. Rev.* **2010**, *110*, 3985-4022. (b) Cheng, F.; Jakle, F. *Polym. Chem.* **2011**, *2*, 2122-2132. (c) Jäkle, F. In *Synthesis and Application of Organoboron Compounds*; Fernández, E., Whiting, A., Eds.; Springer International Publishing: Cham, 2015, 297-325.
34. Wade, C. R.; Broomsgrove, A. E. J.; Aldridge, S.; Gabbai, F. P. *Chem. Rev.* **2010**, *110*, 3958-3984.
35. Chen, P.; Jäkle, F. *J. Am. Chem. Soc.* **2011**, *133*, 20142-20145.
36. Ulrich, G.; Ziesel, R.; Harriman, A. *Angew. Chem. Int. Ed.* **2008**, *47*, 1184-1201.
37. (a) Levine, D. R.; Siegler, M. A.; Tovar, J. D. *J. Am. Chem. Soc.* **2014**, *136*, 7132-7139. (b) Iida, A.; Yamaguchi, S. *J. Am. Chem. Soc.* **2011**, *133*, 6952-6955. (c) Wakamiya, A.; Mishima, K.; Ekawa, K.; Yamaguchi, S. *Chem. Commun.* **2008**, 579-581.
38. (a) Escande, A.; Ingleson, M. J. *Chem. Commun.* **2015**, *51*, 6257-6274. (b) Shuto, A.; Kushida, T.; Fukushima, T.; Kaji, H.; Yamaguchi, S. *Org. Lett.* **2013**, *15*, 6234-6237. (c) Zhou, Z.; Wakamiya, A.; Kushida, T.; Yamaguchi, S. *J. Am. Chem. Soc.* **2012**, *134*, 4529-4532. (d) Dou, C.; Saito, S.; Matsuo, K.; Hisaki, I.; Yamaguchi, S. *Angew. Chem. Int. Ed.* **2012**, *51*, 12206-12210. (e) Saito, S.; Matsuo, K.; Yamaguchi, S. *J. Am. Chem. Soc.* **2012**, *134*, 9130-9133.

39. (a) Yin, X.; Guo, F.; Lalancette, R. A.; Jäkle, F. *Macromolecules* **2016**, *49*, 537-546. (b) Brandt, R. G.; Sveegaard, S. G.; Xiao, M.; Yue, W.; Du, Z.; Qiu, M.; Angmo, D.; Andersen, T. R.; Krebs, F. C.; Yang, R.; Yu, D. *J. Mater. Chem. C* **2016**, *4*, 4393-4401. (c) Lorbach, A.; Bolte, M.; Li, H.; Lerner, H.-W.; Holthausen, M. C.; Jäkle, F.; Wagner, M. *Angew. Chem. Int. Ed.* **2009**, *48*, 4584-4588. (d) Li, H.; Jäkle, F. *Angew. Chem. Int. Ed.* **2009**, *48*, 2313-2316.
40. Mathey, F. *Angew. Chem. Int. Ed.* **2003**, *42*, 1578-1604.
41. Baumgartner, T. *Acc. Chem. Res.* **2014**, *47*, 1613-1622.
42. Reed, A. E.; Schleyer, P. v. R. *J. Am. Chem. Soc.* **1990**, *112*, 1434-1445.
43. (a) Romero-Nieto, C.; Baumgartner, T. *Synlett* **2013**, *24*, 920-937. (b) Ren, Y.; Baumgartner, T. *Dalton Trans.* **2012**, *41*, 7792-7800.
44. (a) Wu, J.; Wu, S.; Geng, Y.; Yang, G.; Muhammad, S.; Jin, J.; Liao, Y.; Su, Z. *Theor. Chem. Acc.* **2010**, *127*, 419-427. (b) Nyulaszi, L.; Holloczki, O.; Lescop, C.; Hissler, M.; Reau, R. *Org. Biomol. Chem.* **2006**, *4*, 996-998.
45. (a) Matano, Y.; Saito, A.; Fukushima, T.; Tokudome, Y.; Suzuki, F.; Sakamaki, D.; Kaji, H.; Ito, A.; Tanaka, K.; Imahori, H. *Angew. Chem. Int. Ed.* **2011**, *50*, 8016-8020. (b) Saito, A.; Miyajima, T.; Nakashima, M.; Fukushima, T.; Kaji, H.; Matano, Y.; Imahori, H. *Chem. Eur. J.* **2009**, *15*, 10000-10004.
46. (a) *Phosphorus-Carbon Heterocyclic Chemistry: The Rise of a New Domain*; Mathey, F., Ed.; Elsevier Science Ltd: Oxford, 2001. (b) Nyulászi, L.; Benkő, Z. In *Aromaticity in Heterocyclic Compounds*; Krygowski, T. M., Cyrański, M. K., Eds.; Springer Berlin Heidelberg: Berlin, Heidelberg, 2009, 27-81. (c) Le Floch, P. *Coord. Chem. Rev.* **2006**, *250*, 627-681. (d) Bansal, R. K.; Heinicke, J. *Chem. Rev.* **2001**, *101*, 3549-3578. (e) *Multiple Bonds and Low Coordination in*

Phosphorus Chemistry; Regitz, M.; Scherer, O. J., Eds.; Georg Thieme Verlag: Stuttgart, 1990. (f)

Fischer, R. C.; Power, P. P. *Chem. Rev.* **2010**, *110*, 3877-3923.

47. Schoeller, W. In *Multiple Bonds and Low Coordination in Phosphorus Chemistry*; Regitz, M., Scherer, O. J., Eds.; Georg Thieme Verlag: Stuttgart, 1990.

48. Lacombe, S.; Gonbeau, D.; Cabioch, J. L.; Pellerin, B.; Denis, J. M.; Pfister-Guillouzo, G. *J. Am. Chem. Soc.* **1988**, *110*, 6964-6967.

49. (a) Dillon, K. B.; Mathey, F.; Nixon, J. F. *Phosphorus: The Carbon Copy: From Organophosphorus to Phospha-organic Chemistry*; Wiley, 1998. (b) Mathey, F. *Acc. Chem. Res.* **1992**, *25*, 90-96.

50. Schmidt, M. W.; Truong, P. N.; Gordon, M. S. *J. Am. Chem. Soc.* **1987**, *109*, 5217-5227.

51. (a) Klebach, T. C.; Lourens, R.; Bickelhaupt, F. *J. Am. Chem. Soc.* **1978**, *100*, 4886-4888. (b) Becker, G. *Z. Anorg. Allg. Chem.* **1976**, *423*, 242-254.

52. (a) Smith, R. C.; Protasiewicz, J. D. *J. Am. Chem. Soc.* **2004**, *126*, 2268-2269. (b) Smith, R. C.; Chen, X.; Protasiewicz, J. D. *Inorg. Chem.* **2003**, *42*, 5468-5470. (c) Wright, V. A.; Gates, D. *P. Angew. Chem. Int. Ed.* **2002**, *41*, 2389-2392.

53. (a) Le Floch, P. In *Phosphorus-Carbon Heterocyclic Chemistry*; Elsevier Science Ltd: Oxford, 2001, 485-533. (b) Batich, C.; Heilbronner, E.; Hornung, V.; Ashe, A. J.; Clark, D. T.; Copley, U. T.; Kilcast, D.; Scanlan, I. *J. Am. Chem. Soc.* **1973**, *95*, 928-930. (c) Ashe, A. J. *J. Am. Chem. Soc.* **1971**, *93*, 3293-3295.

54. (a) Heinicke, J. W. *Eur. J. Inorg. Chem.* **2016**, *2016*, 575-594. (b) Schmidpeter, A. In *Phosphorus-Carbon Heterocyclic Chemistry*; Elsevier Science Ltd: Oxford, 2001, 363-461.

55. (a) Simpson, M. C.; Protasiewicz John, D. *Pure Appl. Chem.* **2013**, *85*, 801. (b) Laughlin, F. L.; Rheingold, A. L.; Deligonul, N.; Laughlin, B. J.; Smith, R. C.; Higham, L. J.; Protasiewicz, J.

D. *Dalton Trans.* **2012**, *41*, 12016-12022. (c) Washington, M. P.; Payton, J. L.; Simpson, M. C.; Protasiewicz, J. D. *Organometallics* **2011**, *30*, 1975-1983. (d) Washington, M. P.; Gudimetla, V. B.; Laughlin, F. L.; Deligonul, N.; He, S.; Payton, J. L.; Simpson, M. C.; Protasiewicz, J. D. *J. Am. Chem. Soc.* **2010**, *132*, 4566-4567.

56. (a) Qiu, Y.; Worch, J. C.; Chirdon, D. N.; Kaur, A.; Maurer, A. B.; Amsterdam, S.; Collins, C. R.; Pintauer, T.; Yaron, D.; Bernhard, S.; Noonan, K. J. T. *Chem. Eur. J.* **2014**, *20*, 7746-7751.

(b) Worch, J. C.; Chirdon, D. N.; Maurer, A. B.; Qiu, Y.; Geib, S. J.; Bernhard, S.; Noonan, K. J. T. *J. Org. Chem.* **2013**, *78*, 7462-7469.

57. Anthony, J. E.; Facchetti, A.; Heeney, M.; Marder, S. R.; Zhan, X. *Adv. Mater.* **2010**, *22*, 3876-3892.

58. Ren, Y.; Dienes, Y.; Hettel, S.; Parvez, M.; Hoge, B.; Baumgartner, T. *Organometallics* **2009**, *28*, 734-740.

59. Zhan, X.; Facchetti, A.; Barlow, S.; Marks, T. J.; Ratner, M. A.; Wasielewski, M. R.; Marder, S. R. *Adv. Mater.* **2011**, *23*, 268-284.

60. (a) Kulkarni, A. P.; Tonzola, C. J.; Babel, A.; Jenekhe, S. A. *Chem. Mater.* **2004**, *16*, 4556-4573. (b) Zhao, X.; Zhan, X. *Chem. Soc. Rev.* **2011**, *40*, 3728-3743.

61. Zoppi, L.; Siegel, J. S.; Baldrige, K. K. *Wiley Interdisciplinary Reviews: Computational Molecular Science* **2013**, *3*, 1-12.

62. (a) Kirner, S.; Sekita, M.; Guldi, D. M. *Adv. Mater.* **2014**, *26*, 1482-1493. (b) Popov, A. A.; Yang, S.; Dunsch, L. *Chem. Rev.* **2013**, *113*, 5989-6113.

63. Wu, Y.-T.; Siegel, J. S. *Chem. Rev.* **2006**, *106*, 4843-4867.

64. Ball, M.; Zhong, Y.; Wu, Y.; Schenck, C.; Ng, F.; Steigerwald, M.; Xiao, S.; Nuckolls, C. *Acc. Chem. Res.* **2015**, *48*, 267-276.

65. (a) Li, X.; Kang, F.; Inagaki, M. *Small* **2016**, *12*, 3206-3223. (b) Plunkett, K. N. *Synlett* **2013**, *24*, 898-902.
66. Bredas, J. L.; Silbey, R.; Boudreaux, D. S.; Chance, R. R. *J. Am. Chem. Soc.* **1983**, *105*, 6555-6559.
67. (a) Ma, J.; Li, S.; Jiang, Y. *Macromolecules* **2002**, *35*, 1109-1115. (b) Meier, H.; Stalmach, U.; Kolshorn, H. *Acta Polym.* **1997**, *48*, 379-384. (c) Klaerner, G.; Miller, R. D. *Macromolecules* **1998**, *31*, 2007-2009. (d) McCullough, R. D.; Williams, S. P. *J. Am. Chem. Soc.* **1993**, *115*, 11608-11609.
68. Zhang, L.; Colella, N. S.; Cherniawski, B. P.; Mannsfeld, S. C. B.; Briseno, A. L. *ACS Appl. Mater. Interfaces* **2014**, *6*, 5327-5343.
69. (a) Rudenko, A. E.; Khlyabich, P. P.; Thompson, B. C. *ACS Macro Letters* **2014**, *3*, 387-392. (b) Khlyabich, P. P.; Rudenko, A. E.; Thompson, B. C. *J. Polym. Sci., Part A: Polym. Chem.* **2014**, *52*, 1055-1058. (c) Roth, B.; Rudenko, A. E.; Thompson, B. C.; Krebs, F. C. *J. Photon. Energy* **2014**, *5*, 057205-057205. (d) Wan, M.; Wu, W.; Sang, G.; Zou, Y.; Liu, Y.; Li, Y. *J. Polym. Sci., Part A: Polym. Chem.* **2009**, *47*, 4028-4036. (e) Chochos, C. L.; Economopoulos, S. P.; Deimede, V.; Gregoriou, V. G.; Lloyd, M. T.; Malliaras, G. G.; Kallitsis, J. K. *J. Phys. Chem. C* **2007**, *111*, 10732-10740. (f) Demanze, F.; Yassar, A.; Garnier, F. *Macromolecules* **1996**, *29*, 4267-4273.
70. (a) Murphy, A. R.; Liu, J.; Luscombe, C.; Kavulak, D.; Fréchet, J. M. J.; Kline, R. J.; McGehee, M. D. *Chem. Mater.* **2005**, *17*, 4892-4899. (b) Kazarinoff, P. D.; Shamburger, P. J.; Ohuchi, F. S.; Luscombe, C. K. *J. Mat. Chem.* **2010**, *20*, 3040-3045. (c) Hu, X.; Shi, M.; Chen, J.; Zuo, L.; Fu, L.; Liu, Y.; Chen, H. *Macromol. Rapid Commun.* **2011**, *32*, 506-511.
71. Guo, X.; Facchetti, A.; Marks, T. J. *Chem. Rev.* **2014**, *114*, 8943-9021.
72. Pron, A.; Berrouard, P.; Leclerc, M. *Macromol. Chem. Phys.* **2013**, *214*, 7-16.

73. (a) Braunecker, W. A.; Owczarczyk, Z. R.; Garcia, A.; Kopidakis, N.; Larsen, R. E.; Hammond, S. R.; Ginley, D. S.; Olson, D. C. *Chem. Mater.* **2012**, *24*, 1346-1356. (b) Berrouard, P.; Najari, A.; Pron, A.; Gendron, D.; Morin, P.-O.; Pouliot, J.-R.; Veilleux, J.; Leclerc, M. *Angew. Chem. Int. Ed.* **2012**, *51*, 2068-2071. (c) Guo, X.; Ortiz, R. P.; Zheng, Y.; Kim, M.-G.; Zhang, S.; Hu, Y.; Lu, G.; Facchetti, A.; Marks, T. J. *J. Am. Chem. Soc.* **2011**, *133*, 13685-13697. (d) Chen, G.-Y.; Cheng, Y.-H.; Chou, Y.-J.; Su, M.-S.; Chen, C.-M.; Wei, K.-H. *Chem. Commun.* **2011**, *47*, 5064-5066. (e) Letizia, J. A.; Salata, M. R.; Tribout, C. M.; Facchetti, A.; Ratner, M. A.; Marks, T. J. *J. Am. Chem. Soc.* **2008**, *130*, 9679-9694.

Chapter 2♦

Synthetic Tuning of Electronic and Photophysical Properties of 2-Aryl-1,3-Benzothiaphospholes

2.1 Introduction

Organic π -conjugated materials have garnered enormous attention over the past 40 years as solution processable components for photovoltaics, light-emitting diodes and field-effect transistors.¹ The incorporation of main group elements including: boron,^{2,3} silicon,⁴ selenium,⁵ tellurium⁶ and phosphorus⁷ has evolved as a versatile strategy for tuning the electronic properties of π -conjugated architectures.

The use of phosphorus for this purpose is particularly intriguing due to its variable oxidation states and coordination modes. Recent reports of conjugated materials bearing phosphorus heterocycles include: dithienophospholes,⁸ dibenzofuran phosphole,⁹ dibenzophosphapentaphenes,¹⁰ biphospholes,¹¹ dithienodiketophosphopins,¹² and diazadibenzophosphole oxides¹³ (several examples depicted in Figure 2.1). All of the structures shown in Figure 2.1 bear a 3-coordinate phosphorus atom and facile modulation of the solid-state packing and band gap can be achieved by oxidation, quaternization or complexation of the phosphorus. Recent device fabrication with phosphole-based dopants has yielded light-emitting diodes capable of emitting white light.¹⁴

♦ Reproduced with permission from Worch, J.C.; Chirdon, D.N.; Maurer, A.B.; Qiu, Y.; Geib, S.J.; Bernhard, S.; Noonan, K.J.T. Synthetic Tuning of Electronic and Photophysical Properties of 2-Aryl-1,3-Benzothiaphospholes. *J. Org. Chem.* **2013**, *78*, 7462-7469. Copyright 2013 American Chemical Society.

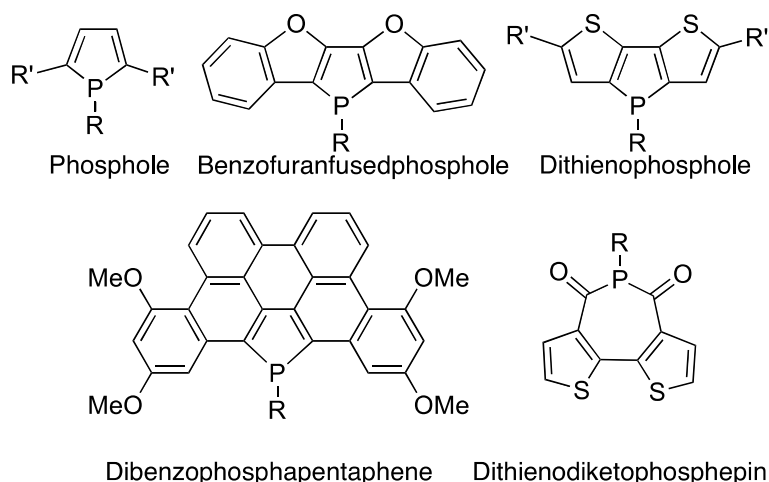


Figure 2.1. Several examples of π -conjugated building blocks that incorporate a 3-coordinate phosphorus atom.

The ability of phosphorus to form π -bonds¹⁵ has led to the investigation of phosphalkenes (P=C bonds) in extended conjugated structures. Compared to all-carbon counterparts (olefins), phosphalkenes have lower lying LUMO energy levels and many P=C species are easily reduced.¹⁶ Thus, there is the potential to develop phosphalkenes as materials for electron transport. Gates¹⁷ and Protasiewicz¹⁸ both prepared polyphenylenevinylene (PPV) analogs where the vinyl unit between the phenyl groups in the polymer main chain was replaced by a P=C bond (Figure 2.2). In Figure 2.2 (top – right), the (*E*)-poly(*p*-phenylenephosphaalkene) ($\lambda_{\text{max}} = 445 \text{ nm}$) is substantially red-shifted compared to unsubstituted *E*-PPV ($\lambda_{\text{max}} = 426 \text{ nm}$) despite the limited conjugation length of the phosphalkene polymer ($M_n = 6,500 \text{ g/mol}$).^{18c} Protasiewicz has also described a PPV analog with a diphosphene unit (P=P) between the aryl rings,^{18a} and Ott has investigated P=C bonds in conjugation with acetylenic moieties (Figure 2.2).¹⁹

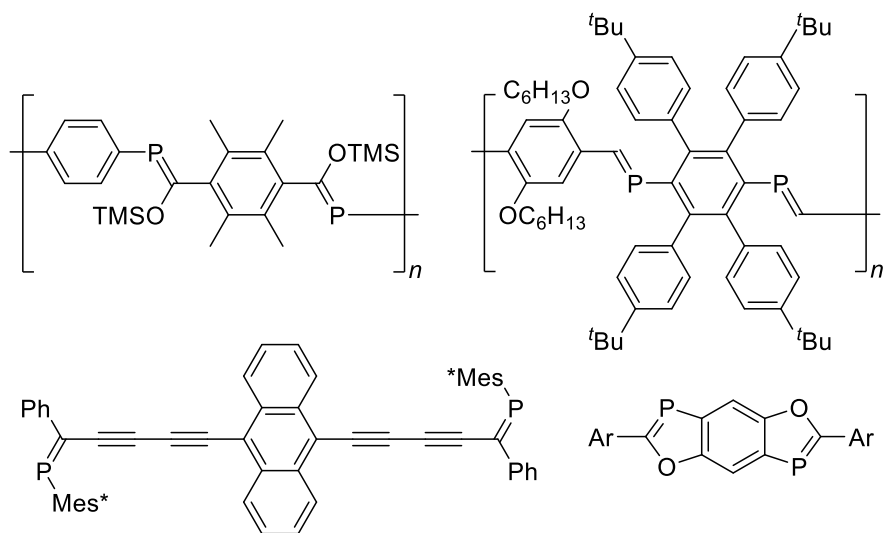


Figure 2.2. Extended π -conjugated materials that incorporate phosphalkene units.

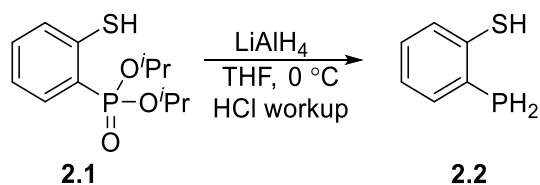
However, to our knowledge, very few reports of aromatic systems containing P=C bonds have been investigated as π -conjugated materials, though a great deal of research on aromatic heterocycles bearing phosphorus atoms has been conducted.^{15,20} Protasiewicz and co-workers recently prepared a series of photoluminescent benzoxaphospholes and benzobisoxaphospholes with the P=C bond participating in the conjugated aromatic architecture (Figure 2.2).²¹ This work provided inspiration to investigate the related benzothiaphospholes since polythiophenes are an important class of π -conjugated material. The benzothiaphosphole resembles benzothiophene except a CH moiety is replaced by a P atom. Herein, we report a new synthetic procedure to prepare 2-aryl-1,3-benzothiaphospholes and describe their electrochemical and photophysical behavior.

2.2 Results and Discussion

Several synthetic strategies to prepare the 1,3-thiaphospholes have been reported,²² however, 1,3-benzothiaphospholes have been described only once.²³ To synthesize the desired heterocycle, we prepared diisopropyl (2-mercaptophenyl)phosphonate (**2.1**) according to a

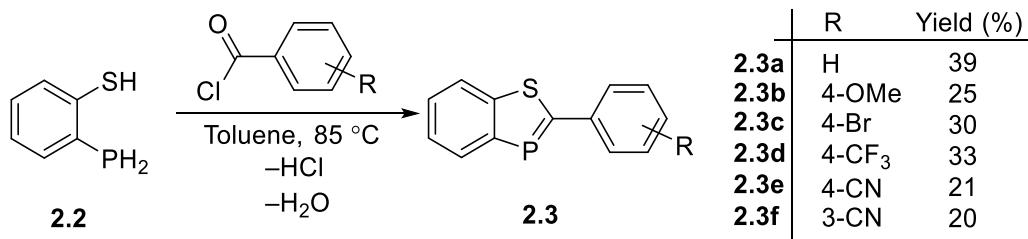
literature procedure.²⁴ Reduction of compound **2.1** using lithium aluminum hydride afforded the desired 1-mercapto-2-phosphinobenzene **2.2** (Scheme 2.1).

Scheme 2.1. Reduction of diisopropyl (2-mercaptophenyl)phosphonate to prepare 1-mercapto-2-phosphinobenzene.



Benzannulated variants of 1,3-heterophospholes can be prepared from a phosphine precursor and a variety of carboxylic acid derivatives such as imidoyl chlorides, iminoester hydrochlorides or amide acetals.^{15b,25} Issleib and co-workers reported the synthesis of 2-phenyl-1,3-benzothiaphosphole from compound **2.2** and benzaldehyde, however, efforts to reproduce this reaction proved challenging. The wide commercial availability of acid chlorides and a previous report describing 1,3-oxaphospholes from acid chlorides led us to investigate the reaction of **2** with benzoyl chloride.²⁶ The combination of **2.2** (^{31}P $\delta = -127$) with benzoyl chloride proceeded smoothly in toluene at $85\text{ }^\circ\text{C}$, with nearly quantitative conversion to a single product as evidenced by $^{31}\text{P}\{^1\text{H}\}$ NMR spectroscopy ($\delta = 192$). Upon cooling of the reaction mixture, yellow crystals formed and were collected by filtration to yield the desired 2-phenyl-1,3-benzothiaphosphole **2.3a** (Scheme 2.2).

Scheme 2.2. Synthesis of 1,3-benzothiaphospholes from 1-mercapto-2-phosphinobenzene (**2.2**) and aryl acid chlorides.



The ^{31}P NMR signal of compound **2.3a** does not match the one previously reported (^{31}P $\delta = 55.3$).²³ However, that report only includes ^{31}P NMR data without supporting evidence to prove the formation of the 2-phenyl-1,3-benzothiaphosphole. In this work, mass spectrometry data and X-ray analysis (Figure 2.3) are used to confirm the identity of the heterocycle (2-phenyl-1,3-benzothiaphosphole **2.3a**) which exhibits a $^{31}\text{P}\{\text{H}\}$ signal at 192 ppm.

The P1-C1 and P1-C2 bond lengths are 1.677(9) Å and 1.789(9) Å respectively (Figure 2.3). One of these bonds is slightly longer than a typical P=C bond (1.60-1.70 Å)^{15a} and the observed lengths are comparable to a previously reported 1,3-thiaphosphole which exhibited bond lengths of 1.691(5) Å and 1.719(5) Å.^{22e} The bond lengths for **2.3a** are in accord with the benzobisoxaphospholes reported recently that have phosphorus-carbon bond lengths of 1.694(1) Å and 1.782(1) Å.^{21a} One of the most interesting features of the structure is that very little twisting is observed between the aryl rings. The angle between the planes of the benzothiaphosphole and phenyl group is only 3.8°. This structural feature suggests that crystalline packing in extended conjugated structures may be possible and extended delocalization could result.

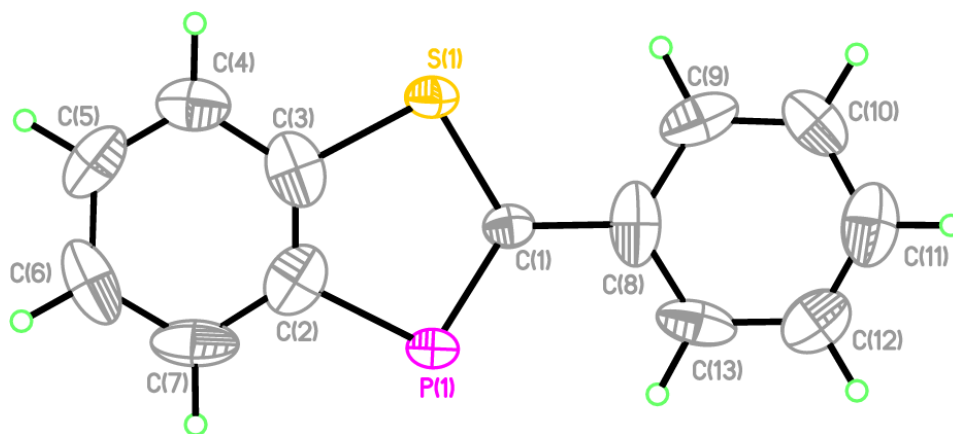


Figure 2.3. Solid-state molecular structure of **2.3a**. Thermal ellipsoids at 50 %. Selected bond lengths (Å) and bond angles (deg): S1–C1 1.757(10); S1–C3 1.800(9); P1–C1 1.677(9); P1–C2 1.789(9); C2–C3 1.289(13); C1–C8 1.473(11); C1–S1–C3 92.8(5); C1–P1–C2 95.3(5); C8–C1–P1 122.8(7); C8–C1–S1 119.7(7); P1–C1–S1 117.3(6).

Following the synthesis of **2.3a**, a series of 1,3-benzothiaphospholes were prepared (**2.3b-**, Scheme 2.2) to investigate how electron donating and electron withdrawing groups modify the electronic and photophysical properties of the ring.

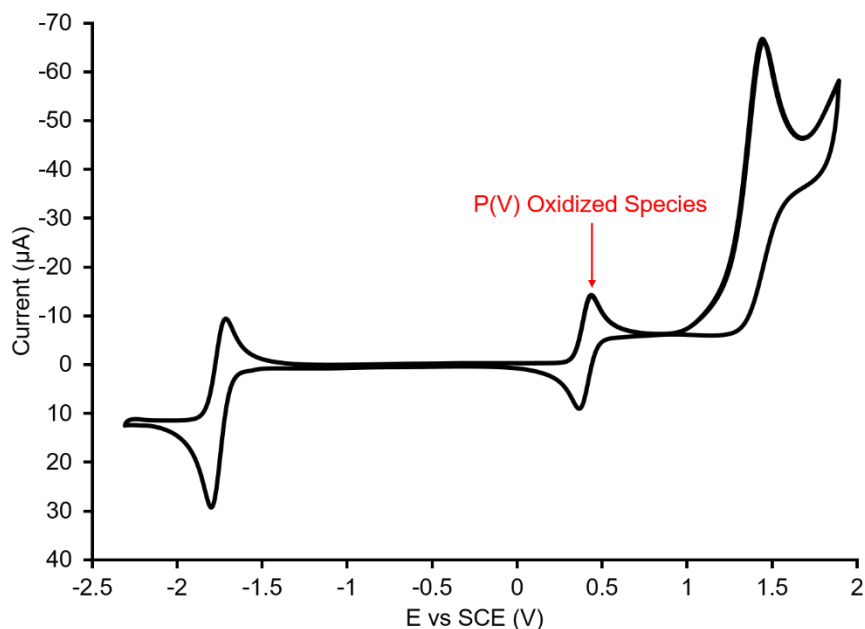


Figure 2.4. Cyclic voltammogram of **2.3a** at high-scan rate (10 V/s) indicating redox activity of the oxidized product. Voltammogram was collected in 0.10 M $N(n\text{-Bu})_4\text{PF}_6$ (MeCN) solution.

For the 2-aryl-1,3-benzothiaphospholes, redox properties and frontier orbitals were probed via cyclic voltammetry (Table 2.1). Each compound in the series exhibited an irreversible oxidation indicative of phosphalkenes (Figure 2.4–5). For the parent species (**2.3a**), the irreversibility of the process persists even at elevated scan rates (5-10 V/s) signaling that the oxidized radical cation quickly undergoes a chemical reaction. High scan rates also reveal a new reduction process near 0.17 V which is too shifted to be a reversal of the oxidation and instead is consistent with redox activity of a product formed from the oxidized species (Figure 2.4).

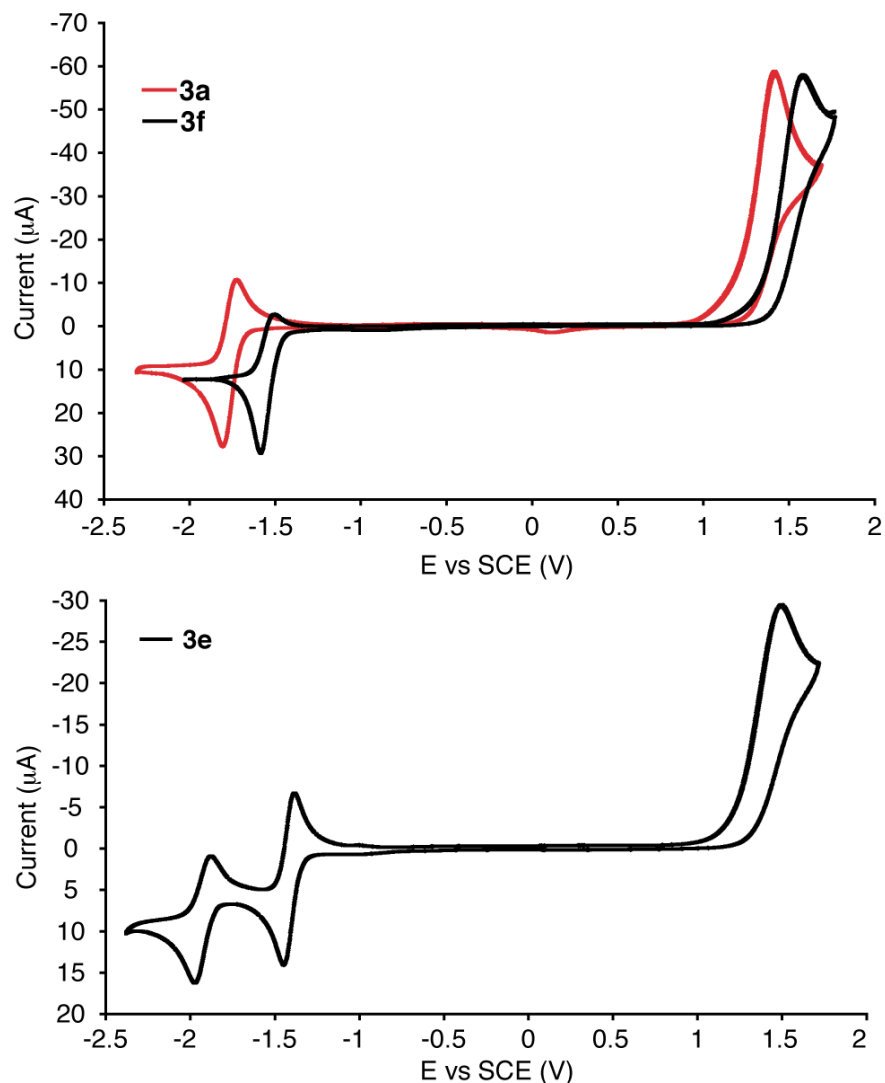


Figure 2.5. (Top) Cyclic voltammograms of **2.3a** (red) and **2.3f** (black). (Bottom) Cyclic voltammogram of **2.3e** showing the most positive first reduction of the benzothiaphosphole series and a second reduction unique to **2.3e**. All voltammograms were collected in 0.10 M $N(n\text{-Bu})_4\text{PF}_6$ (MeCN) solution.

Throughout the 2-aryl-1,3-benzothiaphosphole series, relatively high oxidation potentials (Table 2.1) highlight the electron-poor nature of these materials as compared to their oxaphosphole analogs^{21b} and C,C-diacetylenic phosphalkenes.^{19b} DFT calculations for all variants of compound **2.3** indicate that the HOMO is largely concentrated on the phosphalkene double bond.

Table 2.1. Photophysical and electrochemical properties of 2-aryl-1,3-benzothiaphospholes.

Entry	λ_{max1} abs (nm)	ϵ_1 ($\text{cm}^{-1} \text{M}^{-1}$)	λ_{max2} abs (nm)	ϵ_2 ($\text{cm}^{-1} \text{M}^{-1}$)	λ_{max} emission (nm)	Φ^a (%)	E_{ox} (V vs SCE)	E_{red} (V vs SCE)	ΔE_{red} (mV)
2.3a	271	34300	330	36800	443	4.4	1.44 ^b	-1.76	81
2.3b	279	26800	347	60500	445	5.4	1.24 ^b	-1.85	82
2.3c	273	38900	337	49900	439	3.2	1.49 ^b	-1.62 ^b	-
2.3d	271	41200	331	39400	430	1.5	1.52 ^b	-1.54 ^c	85
2.3e	272	31800	340	32000	433	1.7	1.50 ^b	-1.41, -1.91	61, 94
2.3f	270	47200	324	43800	432	1.5	1.56 ^b	-1.55 ^c	77

^(a) Quantum yields were measured according to the procedure of Abergel *et al.*²⁷ ^(b) Process is completely irreversible. ^(c) Process is quasi-reversible.

Similar HOMO assignments have been made previously with other phosphalkene systems.^{21b,28}

The lowest oxidation potential is observed for compound **2.3b** (1.24 V) due to destabilization of its HOMO via the C₆H₄-*p*-OMe group (Figure 2.6, Compound **2.3b**). Compounds **2.3c-2.3f** have higher oxidation potentials (1.49 V-1.56 V) as the HOMOs are stabilized by the electron withdrawing substituent (C₆H₄-*p*-Br, C₆H₄-*p*-CF₃, C₆H₄-*p*-CN, C₆H₄-*m*-CN). However, the oxidation potentials do not scale consistently with the electron withdrawing power of the substituent group suggesting that they exhibit limited participation in the HOMO. DFT calculations support this claim as only minor contributions to the HOMO are observed if the 2-aryl group has an electron withdrawing substituent (Figure 2.6, Compound **2.3e**).

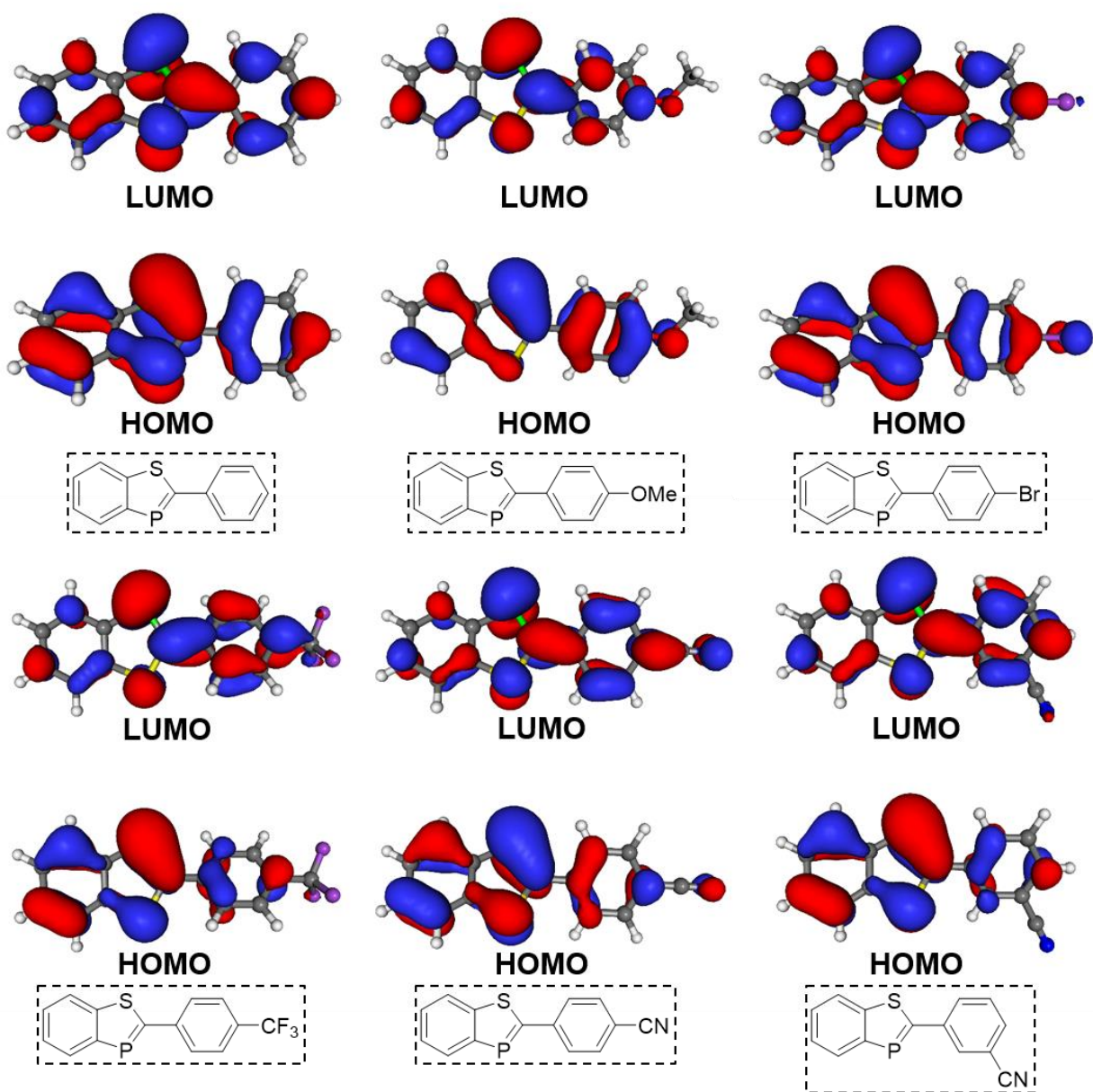


Figure 2.6. Frontier orbitals of compound **2.3a–2.3f** generated via DFT calculations performed with a B3LYP/6-31G (d,p) basis set.

In addition to oxidation, the benzothiophospholes undergo reduction with varying extents of reversibility. Reduction of compound **2.3c** is irreversible resulting most likely from elimination of its halide after radical anion formation.^{21b} Single quasi-reversible reductions are observed for **2.3d** and **2.3f** while complete reversibility is observed for the one electron reductions of compounds **2.3a**, **2.3b**, and **2.3e** (Figure 2.5). The reversibility in these compounds indicates that

the anionic radicals are stable on the time scale of the anodic and cathodic sweeps. Such stability suggests potential for these conjugated materials to conduct electrons and this behavior is not observed in many types of phosphalkenes.^{16e,19b,29}

In comparison to the oxidation peaks, the reductions are roughly half as intense. Thus, while several of the reduction processes are clearly reversible, one electron processes, the oxidation may represent a two electron process facilitated by the favorability of the P(III)/P(V) redox couple. Reduction also differs from oxidation in that its potentials show a more defined pattern: they become incrementally more positive as the electron deficiency of the 2-aryl substituent increases and enhances LUMO stabilization. DFT calculations explain the more pronounced effect of electron deficient groups on reduction by showing significantly more participation of those substituents in the LUMO than in the HOMO (Figure 2.6). The greatest LUMO stabilization is afforded by the C₆H₄-*p*-CN group which shifts **2.3e**'s reduction potential by +0.35 V compared to the parent **2.3a** and causes observation of a second reduction within the range of the solvent window (Figure 2.5-bottom). In contrast to **2.3e**, compound **2.3f** does not show two reversible reductions despite its similar C₆H₄-*m*-CN group. This observed difference in reduction occurs because conjugation allows for stabilization of radicals at the P=C bond by the cyano functionality at the *para* position but not at the *meta* position. This is also reflected in the DFT calculations which illustrate that the substituent at the *para* position of the 2-aryl group of the benzothiaphospholes exhibits orbital density in the LUMO along with the phosphorus-carbon double bond while the *meta* position does not (Figure 2.6). Additionally, DFT calculations explain the facile reduction of **2.3e** by showing that its LUMO is stabilized by distribution across its entire C₆H₄-*p*-CN group (Figure 2.6). Across the benzothiaphosphole series, each material is slightly

more easily reduced than its oxaphosphole analogue likely due to facilitation of P=C reduction by the more polarizable sulfur.^{21b}

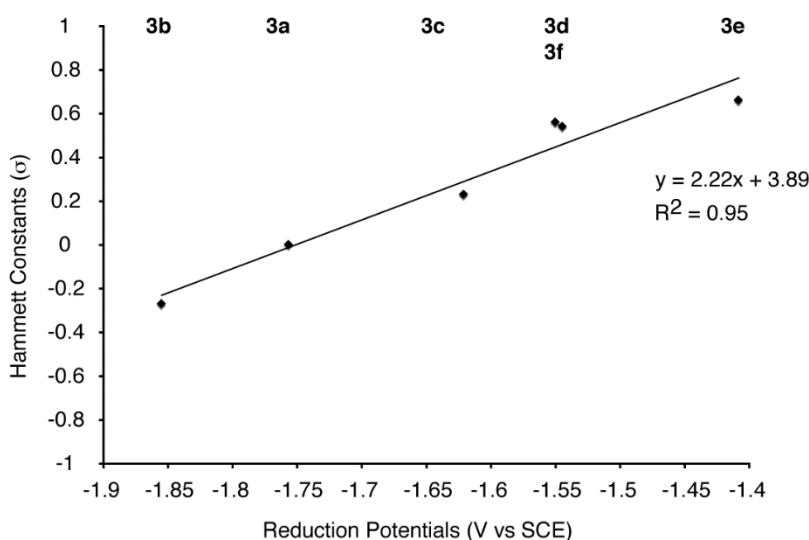


Figure 2.7. Hammett constants (σ) plotted versus the reduction potentials of compounds **2.3a-2.3f**.

The reduction potentials of the benzothiaphospholes correlate with moderate accuracy to the Hammett parameters of the employed substituents (Figure 2.7). Moreover, redox properties are in agreement with the orbital energies obtained for **2.3a-2.3f** through DFT calculations. The LUMO energies of compounds **2.3a-2.3f** form a moderately linear relationship with their related reduction potentials (Figure 2.8). Strong correlation is also seen between the reductions and the radical anion SOMO energies calculated to better model reduction products (Figure 2.8). However, perhaps the best indicator of reduction potentials is the SCF energy difference of the radical anion and the neutral molecule. Surprisingly, the calculated radical anions of the 2-aryl-1,3-benzothiaphospholes show lower absolute energies than the corresponding uncharged parent systems. This observation is likely explained by the electronegative nature of the heterocyclic phosphorus ring. Furthermore, all of the radical anions optimize to a flat geometry, which is in contrast to the 30° twisting observed in the calculated structure of the neutral species.

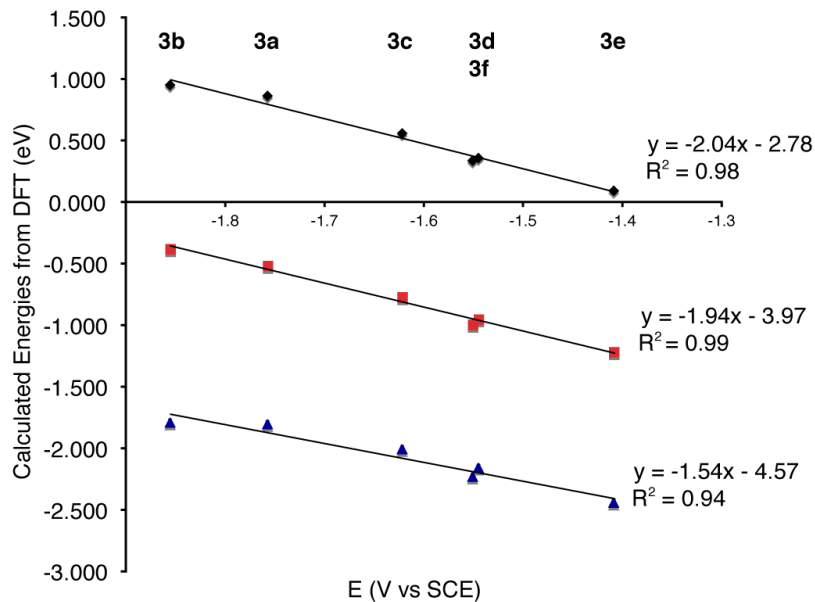


Figure 2.8: Linear correlation of experimental reduction potentials for **2.3a-2.3f** with DFT calculations. Blue triangles (\blacktriangle): LUMO energies correlated to reduction potentials. Black diamonds (\blacklozenge): SOMO energies of the radical anions correlated to reduction potentials. Red rectangles (\blacksquare): The calculated energy difference between the radical anion and neutral benzothiaphosphole species correlated to reduction potentials.

The resulting increase in aromaticity could partially explain the observed stabilization effect for the radical anions. The SCF energy difference between radical anions and neutral molecules is plotted versus reduction potential in Figure 2.8. The quality of the observed linearity is extraordinary, so reduction potentials of similar compounds can be predicted from DFT with great confidence (Figure 2.8). Interestingly, neither the HOMO energy nor the energy difference between the radical cation and the parent show any relationship with the measured oxidation potentials for the 2-aryl-1,3-benzothiaphospholes. The irreversible nature of the oxidation hints at the involvement of more complex processes, which are understandably problematic to evaluate by simple DFT calculations.

The investigated compounds exhibit strong light absorption in the UV which tails into the visible region of the spectrum explaining the yellow color of these materials in solution and in solid-state. Two absorption signals are observed at 271 nm and 330 nm for the parent compound

(Table 2.1). The λ_{max} of the lower energy signal is influenced by substituent effects and ranges from 324 nm (**2.3f**) to 347 nm (**2.3b**). TD-DFT calculations confirm the π - π^* character of this transition showing that it involves the HOMO and LUMO orbitals exclusively, with strong involvement of the P=C bond. All of the derivatives luminesce near 440 nm upon excitation at 330 nm, and the fluorescence spectrum of **2.3b** along with its absorption are depicted in Figure 2.9.

The emission of **2.3b** is the most red shifted in the series because of destabilization of the HOMO by the methoxy group. However, as with oxidation potentials, the emission maxima for more electron deficient derivatives do not follow a clear trend due to minimal participation of their substituents in the HOMO. Emission quantum yields vary greatly across the series (Table 2.1). Electron withdrawing groups diminish quantum yield while the methoxy functionality markedly increases it.

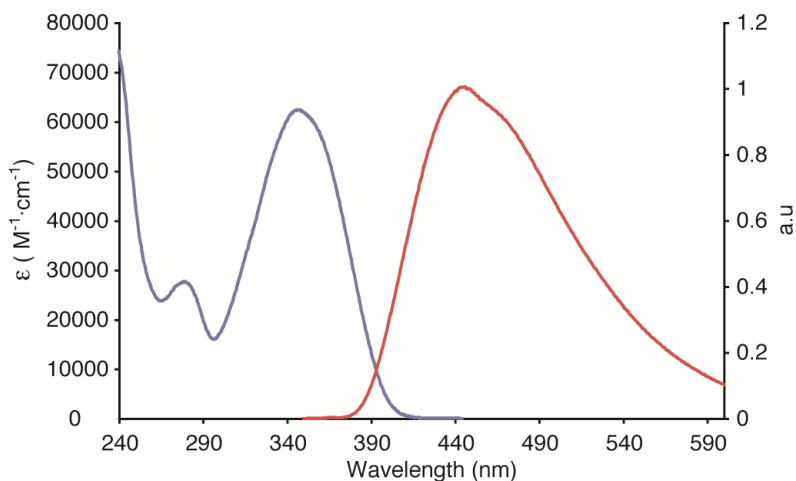


Figure 2.9. Absorption spectrum (blue) and luminescence spectrum (red) of **2.3b** collected for a 10 μM MeCN solution. Luminescence was measured following excitation at 330 nm.

To increase the π -conjugation length, a series of fused bithiaphospholes or benzobithiaphospholes (BBTPs) were investigated (Chart 2.1).³⁰ As expected, the absorption profiles are red-shifted compared to the benzothiaphosphole derivatives and some compounds

exhibit multiple reversible reduction waves. However, the additional thiaphosphole unit significantly hampers the solubility, unless appropriate solubilizing groups are installed.³⁰

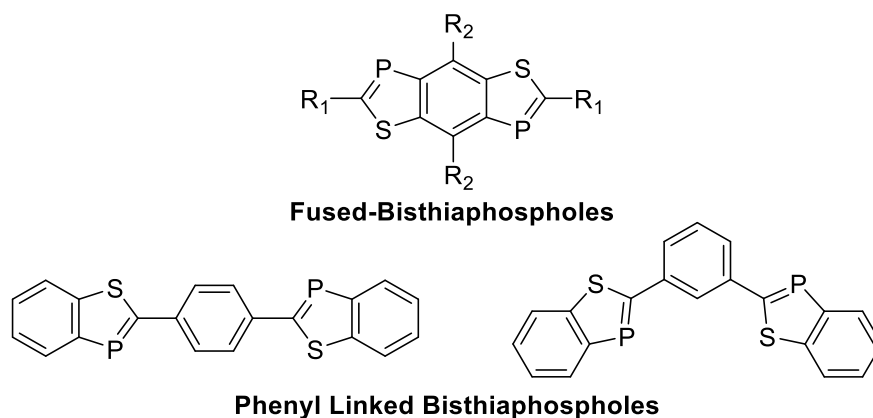


Chart 2.1. Conjugated systems with multiple thiaphosphole units.

2.3 Conclusion

The preparation of a series of 2-aryl-1,3-benzothiaphospholes has been reported and their redox and photophysical behaviors have been evaluated. Electronic modulation of the benzothiaphosphole materials was employed as a strategy to alter the reduction and oxidation potentials of the ring system. Some of the benzothiaphosphole derivatives yielded accessible, reversible reductions highlighting the potential of these compounds as n-type charge transport systems.

2.4 Experimental Section

Materials and Methods. All reactions and manipulations of air or water sensitive compounds were carried out under dry nitrogen using an mBraun glovebox or standard Schlenk techniques unless otherwise specified. Diisopropyl (2-mercaptophenyl)phosphonate (**1**) was prepared according to a published procedure from thiophenol.²⁴ In the synthesis of **1**, diisopropyl bromophosphate (prepared from triisopropyl phosphite and bromine ($^{31}\text{P}\{^1\text{H}\} \delta = -11$) was used

as opposed to diisopropyl chlorophosphate. All solvents (toluene, diethyl ether, tetrahydrofuran, hexanes) were degassed with argon and dried prior to use. Acetonitrile, used for photophysical characterization and electrochemistry measurements, was degassed prior to use. CDCl_3 was dried using P_2O_5 and distilled prior to use. C_6D_6 was dried over 4Å sieves prior to use. Melting points were obtained using a DigiMelt MPA160 from Stanford Research Systems and are uncorrected.

NMR Analysis. NMR spectra were recorded on a Bruker Avance 500 MHz Spectrometer or a Bruker Avance 300 MHz Spectrometer. The $^{31}\text{P}\{^1\text{H}\}$ NMR spectra were referenced to an external standard (85 % H_3PO_4). The ^1H NMR spectra are referenced to residual protio solvents (7.24 for CHCl_3 and 7.16 for $\text{C}_6\text{D}_5\text{H}$). In the ^1H NMR spectra of **2.3a-2.3f**, significant fine splittings (~ 1 -2 Hz) were observed from long range coupling (^1H - ^1H and ^1H - ^{31}P) on the fused aromatic rings. Signals that are listed as broad typically exhibited fine splitting that was left unassigned. The ^1H NMR spectra of all compounds, except for **2.3a** and **2.3f**, have shown the typical ABCD spin systems pattern for ring A and an AA'BB' spin system characteristic of *p*-disubstituted aromatic rings. ^{13}C NMR spectra are referenced to the solvent signal (δ 77.23 CDCl_3) and J_{PC} coupling is observed for most signals.

Photophysical Characterization. Photoluminescence measurements were performed at room temperature using 10 μM solutions in acetonitrile using a capped quartz cuvette (1.0 cm). UV-Vis absorption spectra were measured using a Shimadzu UV-1800 spectrophotometer. Photoluminescence emission spectra were measured on a Jobin-Yvon Fluorolog-3 spectrophotometer equipped with dual monochromators and a Hamamatsu-928 photomultiplier tube (PMT) at right angle geometry. The emission spectra were recorded at an excitation wavelength of 330 nm. Photoluminescent quantum yields (Φ) were measured against 100 μM

quinine sulfate in 0.5 M H₂SO₄, $\Phi = (I_s/I_{ref})(A_{ref}/A_s)(\eta_s/\eta_{ref})$,²⁷ where Φ is the quantum yield for the sample, I_s and I_{ref} represent the points of maximum intensity in the emission spectra of the sample and reference, A_s and A_{ref} are the absorbance of the sample and the reference at the excitation wavelength, and η_{ref} and η_s are the refractive indices of the solvents of the reference and of the sample used for UV-Vis absorption measurements.

Electrochemical Analyses. Electrochemical potentials were determined using a CH Instruments Model 600C Series Electrochemical Analyzer/Workstation with a potential sweep rate of 100 mV/s. A 1 mm² platinum working electrode, a platinum coil counter electrode, and a silver wire pseudo-reference electrode were employed for the measurements. Ferrocene (Aldrich) was used as an internal standard referenced against SCE at 0.4 V (E_{Fc/Fc^+}).³¹ Solutions of the benzothiaphosphole were prepared at ~1-2 mM and tetra-*n*-butylammonium hexafluorophosphate (Fluka, electrochemical grade) served as the supporting electrolyte at a concentration of 0.1 M. The MeCN solutions with the supporting electrolyte were degassed for 5 min with bubbling Ar prior to adding the benzothiaphosphole.

Computational Studies. Hybrid density functional theory (DFT) calculations were performed for compounds **2.3a-2.3f** using a B3LYP/6-31G (d,p) basis set in the Gaussian 03 suite.³²

Mass Spectrometry. High resolution mass spectrometry data was obtained using a Waters 70-VSE double focusing sector instrument.

X-ray Crystallography. Crystallographic data for 2-phenyl-1,3-benzothiaphosphole were collected at 150 (2) K using I μ S micro-focus, Cu radiation (1.54178 Å) on a Bruker Smart Apex II CCD diffractometer. Data reduction included absorption corrections by the multi-scan method

using SADABS and refined by full matrix least squares using SHELXL-2012 bundled software package.

Synthesis of 1-mercapto-2-phosphinobenzene (2.2). A 1000 mL Schlenk flask was charged with lithium aluminum hydride (14.25 g, 375 mmol) and dried *in vacuo* for 15 min. To this was added 400 mL THF and the mixture was cooled to 0 °C using an ice bath. Slow addition of **2.1** (33.40 g, 122 mmol) over a period of 8 minutes produced a vigorous reaction with significant gas evolution (the addition of **2.1** was conducted slowly so as to control the rate of gas evolution). Upon completion of the addition, the ice bath was removed and the reaction mixture was stirred overnight at room temperature. The mixture was quenched with 6 M HCl (100 mL) and the layers were allowed to separate. The organic layer was cannula transferred through a filter flask containing celite into a 1000 mL Schlenk flask containing magnesium sulfate. This extraction process was repeated using dry, degassed hexanes (75 mL, 4×). Then the dried organic layer was transferred to another 1000 mL Schlenk flask via a filter cannula. After removing volatiles *in vacuo*, the crude product was distilled using a short path column (64 °C, 0.1 Torr) to afford **2.2** as a colorless oil. The $^{31}\text{P}\{^1\text{H}\}$ and ^1H NMR spectra were compared to a previous report.³² Often, the ^1H spectrum of the distilled product contained impurities that are suspected to be aluminum isopropoxide salts. Loading the 1-mercapto-2-phosphinobenzene onto silica gel under an atmosphere of N_2 and eluting with degassed hexanes helped remove the impurity (7.51 g, 43%).

General Procedure A: synthesis of 2-aryl-1,3-benzothiaphospholes 2.3a and 2.3b. In a N_2 filled glovebox, a 50 mL Schlenk flask was charged with 1-mercapto-2-phosphinobenzene (0.375 g, 2.64 mmol), 5 g of dry toluene, and an aryl acid chloride (1 eq, 2.64 mmol). The Schlenk flask was removed from the glovebox and immersed in an oil bath at 85 °C. The solution was stirred

overnight and the colorless solution turned bright yellow. An aliquot of the reaction mixture was removed using a syringe and analyzed using ^{31}P NMR spectroscopy. Complete consumption of the starting material was confirmed by disappearance of the $^{31}\text{P}\{^1\text{H}\}$ NMR signal at -127 ppm. Formation of the desired benzothiaphosphole was confirmed by the appearance of a $^{31}\text{P}\{^1\text{H}\}$ NMR signal in the range of $185 - 203$ ppm. The reaction vessel was removed from the oil bath, and cooled to room temperature. The flask was placed in a refrigerator at 4 °C for several hours and, upon removal from the fridge, yellow crystals were observed in the reaction flask. The yellow crystals were collected via filtration and washed with cold ether (3×10 mL).

General Procedure B: synthesis of 2-aryl-1,3-benzothiaphospholes 2.3c and 2.3d. In a N_2 filled glovebox, a 50 mL Schlenk flask was charged with 1-mercapto-2-phosphinobenzene (0.375 g, 2.64 mmol), 5 g of dry toluene, and an aryl acid chloride (1 eq, 2.64 mmol). The Schlenk flask was removed from the glovebox and immersed in an oil bath at 85 °C. The solution was stirred overnight and the colorless solution turned bright yellow. An aliquot of the reaction mixture was removed using a syringe and analyzed using ^{31}P NMR spectroscopy. Complete consumption of the starting material was confirmed by disappearance of the $^{31}\text{P}\{^1\text{H}\}$ NMR signal at -127 ppm. Formation of the desired benzothiaphosphole was confirmed by the appearance of a $^{31}\text{P}\{^1\text{H}\}$ NMR signal in the range of 185 to 203 ppm. The volatiles of the reaction mixture were removed *in vacuo* and the crude mixture was brought into the glovebox. The residue was dissolved in a minimal amount of solvent, and placed in a 20 mL scintillation vial. The vial was stored in the freezer at -35 °C overnight. Yellow crystals were observed in the scintillation vial and they were collected by filtration. The filtrate was placed back in the freezer and a second batch of crystals was obtained. These were also collected by filtration.

General Procedure C: synthesis of 2-aryl-1,3-benzothiaphospholes 2.3e and 2.3f. In a N₂ filled glovebox, a 50 mL Schlenk flask was charged with 1-mercapto-2-phosphinobenzene (0.375 g, 2.64 mmol), 5 g of dry toluene, and an aryl acid chloride (1 eq, 2.64 mmol). The Schlenk flask was removed from the glovebox and immersed in an oil bath at 85 °C. After stirring overnight, the colorless solution had turned bright yellow and some precipitate was observed. The hot reaction mixture was separated from the precipitate by a hot gravity filtration. The yellow filtrate was collected and immediately transferred to a 20 mL scintillation vial. The vial was allowed to cool to room temperature and placed in a refrigerator at 4 °C for several hours and, upon removal from the fridge, yellow crystals were observed in the reaction flask. The yellow crystals were collected via filtration and washed with cold ether (3 × 10 mL).

2-phenyl-1,3-benzothiaphosphole (2.3a) was prepared following general procedure A. The combination of compound **2.2** (0.375 g, 2.64 mmol) and benzoyl chloride (0.370 g, 2.64 mmol) afforded **2.3a** as yellow crystals (0.234 g, 39%). Mp 142–145 °C dec. ³¹P{¹H} NMR (202 MHz, C₆D₆) δ 191.9. ¹H NMR (500 MHz, C₆D₆): δ 8.06 – 8.00 (m, 1H), 7.89 – 7.84 (m, 2H), 7.63 (br d, *J* = 7.8 Hz, 1H), 7.11 – 6.98 (m, 5H). ¹³C NMR (126 MHz, CDCl₃) δ 181.1 (d, *J*_{PC} = 52.8 Hz), 153.8 (d, *J*_{PC} = 39.8 Hz), 148.4 (d, *J*_{PC} = 10.2 Hz), 137.0 (d, *J*_{PC} = 16.1 Hz), 130.9 (d, *J*_{PC} = 27.5 Hz), 129.4 (d, *J*_{PC} = 3.5 Hz), 129.3, 126.9 (d, *J*_{PC} = 14.6 Hz), 126.7 (d, *J*_{PC} = 3.5 Hz), 124.1 (d, *J*_{PC} = 13.4 Hz), 123.4. HR-EIMS (*m/z*): [M]⁺ calculated for C₁₃H₉PS: 228.0163; found 228.0153.

2-(4-methoxyphenyl)-1,3-benzothiaphosphole (2.3b) was prepared following general procedure A. The combination of compound **2.2** (0.375 g, 2.64 mmol) and 4-methoxybenzoyl chloride (0.450 g, 2.64 mmol) afforded **2.3b** as yellow crystals (0.170, 25%). Mp 164–165 °C dec. ³¹P{¹H} NMR (202 MHz, CDCl₃): δ 184.6. ¹H NMR (500 MHz, CDCl₃) δ 8.23 (br t, *J* = 7.0 Hz, 1H), 8.02 (br d, *J* = 8.1 Hz, 1H), 7.83 – 7.78 (AA'BB' system, A centered on 7.82, A' centered on 7.80, 2H), 7.42

(br t, $J = 7.6$ Hz, 1H), 7.36 (br t, $J = 7.5$ Hz, 1H), 6.94 – 6.90 (AA'BB' system, B centered on 6.94, B' centered on 6.92, 2H), 3.84 (s, 3H). ^{13}C NMR (126 MHz, CDCl_3) δ 181.2 (d, $J_{\text{PC}} = 53.1$ Hz), 160.9 (d, $J_{\text{PC}} = 3.7$ Hz), 153.8 (d, $J_{\text{PC}} = 39.7$ Hz), 148.0 (d, $J_{\text{PC}} = 10.1$ Hz), 130.7 (d, $J_{\text{PC}} = 27.6$ Hz), 130.0 (d, $J_{\text{PC}} = 16.2$ Hz), 128.1 (d, $J_{\text{PC}} = 14.7$ Hz), 126.3 (d, $J_{\text{PC}} = 3.4$ Hz), 124.1 (d, $J_{\text{PC}} = 13.2$ Hz), 123.2, 114.6, 55.6. HR-EIMS (m/z): $[\text{M}]^+$ calculated for $\text{C}_{14}\text{H}_{11}\text{OPS}$: 258.0268; found 258.0260. Anal. Calcd for $\text{C}_{14}\text{H}_{11}\text{OPS}$: C, 65.10; H, 4.29. Found: C, 64.84; H, 4.15.

2-(4-bromophenyl)-1,3-benzothiaphosphole (2.3c) was prepared following general procedure B using compound **2.2** (0.375 g, 2.64 mmol) and 4-bromobenzoyl chloride (0.579 g, 2.64 mmol). **2.3c** was obtained as a yellow powder (0.246 g, 30%) after recrystallization from Toluene/THF (10:1). Mp 176–177 °C dec. $^{31}\text{P}\{^1\text{H}\}$ NMR (202 MHz, C_6D_6): δ 194.0. ^1H NMR (500 MHz, CDCl_3) δ 8.26 (br t, $J = 7.1$ Hz, 1H), 8.04 (br d, $J = 8.1$ Hz, 1H), 7.73 – 7.69 (AA'BB' system, A centered on 7.72, A' centered on 7.70, 2H), 7.53 – 7.49 (AA'BB' system, B centered on 7.52, B' centered on 7.51, 2H), 7.46 (br t, $J = 7.6$ Hz, 1H), 7.38 (br t, $J = 7.5$ Hz, 1H). ^{13}C NMR (126 MHz, CDCl_3) δ 179.1 (d, $J_{\text{PC}} = 52.6$ Hz), 153.7 (d, $J_{\text{PC}} = 39.7$ Hz), 148.4 (d, $J_{\text{PC}} = 10.4$ Hz), 136.0 (d, $J_{\text{PC}} = 16.6$ Hz), 132.3, 131.0 (d, $J_{\text{PC}} = 27.6$ Hz), 128.2 (d, $J_{\text{PC}} = 14.8$ Hz), 126.9 (d, $J_{\text{PC}} = 3.5$ Hz), 124.3 (d, $J_{\text{PC}} = 13.5$ Hz), 123.5, 123.4. HR-EIMS (m/z): $[\text{M}]^+$ calculated for $\text{C}_{13}\text{H}_8\text{BrPS}$: 305.9268; found 305.9267. Anal. Calcd for $\text{C}_{13}\text{H}_8\text{BrPS}$: C, 50.84; H, 2.63. Found: C, 50.58; H, 2.38.

2-(4-(trifluoromethyl)phenyl)-1,3-benzothiaphosphole (2.3d). Following the general procedure B using compound **2.2** (0.375 g, 2.64 mmol) and 4-(trifluoromethyl)benzoyl chloride (0.550 g, 2.64 mmol) afforded **2.3d** as yellow crystals (0.256 g, 33%) after recrystallization from THF. Mp 215–217 °C dec. $^{31}\text{P}\{^1\text{H}\}$ NMR (202 MHz, C_6D_6): δ 199.5. ^1H NMR (500 MHz, C_6D_6) δ 8.02 (br t, $J = 6.8$ Hz, 1H), 7.63 (br d, $J = 7.9$ Hz, 1H), 7.60 (br d, $J = 7.3$ Hz, 2H), 7.24 (br d, $J = 8.2$ Hz, 2H), 7.08 – 6.99 (m, 2H). ^{13}C NMR (126 MHz, CDCl_3) δ 178.4 (d, $J_{\text{PC}} = 52.7$ Hz), 153.9 (d, $J_{\text{PC}} =$

40.1 Hz), 148.8 (d, $J_{PC} = 10.5$ Hz), 140.5 (d, $J_{PC} = 16.8$ Hz), 131.2 (d, $J_{PC} = 27.7$ Hz), 127.3 (d, $J_{PC} = 3.6$ Hz), 127.1 (d, $J_{PC} = 14.7$ Hz), 126.3 and 126.2 (overlapping doublets), 124.5 (d, $J_{PC} = 13.6$ Hz), 124.3, (q, $J_{FC} = 271.5$ Hz), 123.5. HR-EIMS (m/z): $[M]^+$ calculated for $C_{14}H_8F_3PS$: 296.0036; found 296.0031. Anal. Calcd for $C_{14}H_8F_3PS$: C, 56.76; H, 2.72. Found: C, 56.48; H, 2.49.

2-(4-cyanophenyl)-1,3-benzothiaphosphole (2.3e) was prepared following general procedure C.

The combination of **2.2** (0.375 g, 2.64 mmol) and 4-cyanobenzoyl chloride (0.437 g, 2.64 mmol) afforded a crude yield of 0.254 g of **2.3e** as yellow crystals. Recrystallization from toluene yielded analytically pure **2.3e** (0.139 g, 21%). Mp 178 °C dec. $^{31}P\{^1H\}$ NMR (202 MHz, C_6D_6): δ 202.7. 1H NMR (500 MHz, C_6D_6) δ 7.98 (br t, $J = 6.9$ Hz, 1H), 7.60 (br d, $J = 7.8$ Hz, 1H), 7.44 – 7.39 (AA'BB' system, A centered on 7.43, A' centered on 7.41, 2H), 7.07 – 6.97 (m, 2H), 6.94 – 6.89 (AA'BB' system, B centered on 6.92, B' centered on 6.91, 2H). ^{13}C NMR (126 MHz, $CDCl_3$) δ 177.2 (d, $J_{PC} = 52.7$ Hz), 153.7 (d, $J_{PC} = 39.7$ Hz), 148.7 (d, $J_{PC} = 10.5$ Hz), 141.3 (d, $J_{PC} = 16.8$ Hz), 133.0, 131.3 (d, $J_{PC} = 27.6$ Hz), 127.5 (d, $J_{PC} = 3.7$ Hz), 127.1 (d, $J_{PC} = 15.4$ Hz), 124.5 (d, $J_{PC} = 13.8$ Hz), 123.6, 118.8, 112.4 (d, $J_{PC} = 4.2$ Hz). HR-EIMS (m/z): $[M]^+$ calculated for $C_{14}H_8NPS$: 253.0115; found 253.0111. Anal. Calcd for $C_{14}H_8NPS$: C, 66.39; H, 3.18; N, 5.53. Found: C, 66.09; H, 2.91; N, 5.29.

2-(3-cyanophenyl)-1,3-benzothiaphosphole (2.3f) was prepared following general procedure C.

The combination of **2.2** (0.375 g, 2.64 mmol) and 3-cyanobenzoyl chloride (0.437 g, 2.64 mmol) afforded **2.3f** as yellow crystals (0.131 g, 20%). Mp 178 °C dec. $^{31}P\{^1H\}$ NMR (121 MHz, C_6D_6) δ 198.5. 1H NMR (300 MHz, C_6D_6) δ 7.98 (br td, $J = 6.7, 1.9$ Hz, 1H), 7.80 (br d, $J = 1.8$ Hz, 1H), 7.65 – 7.57 (m, 2H), 7.09 – 6.97 (m, 2H), 6.87 (dd, $J = 7.8, 1.1$ Hz, 1H), 6.60 (br t, $J = 7.8$ Hz, 1H). ^{13}C NMR (126 MHz, $CDCl_3$) δ 177.0 (d, $J_{PC} = 52.4$ Hz), 153.6 (d, $J_{PC} = 39.8$ Hz), 148.5 (d,

$J_{PC} = 10.5$ Hz), 138.2 (d, $J_{PC} = 17.3$ Hz), 132.2 (d, $J_{PC} = 3.4$ Hz), 131.2 (d, $J_{PC} = 27.6$ Hz), 130.9 (d, $J_{PC} = 14.7$ Hz), 130.1, 130.0 (d, $J_{PC} = 14.9$ Hz), 127.4 (d, $J_{PC} = 3.7$ Hz), 124.5 (d, $J_{PC} = 13.7$ Hz), 123.6, 118.5, 113.6. HR-EIMS (m/z): $[M]^+$ calculated for $C_{14}H_8NPS$: 253.0115; found 253.0119.

Crystallographic Information

Table 2.2. Crystallographic details for 2-phenyl-1,3-benzothiaphosphole (**2.3a**)

2-phenyl-1,3-benzothiaphosphole			
Formula	$C_{13}H_9PS$	Absorption coefficient, mm^{-1}	3.780
Color	Colorless	F(000)	472
Shape	Rhomboid	Diffractometer	Bruker Smart Apex II
Formula Weight	228.23	Radiation Source	IMuS micro-focus, Cu
Crystal System	Orthorhombic	Wavelength (\AA)	1.54178
Space Group	$P2_1/c$	Crystal size, mm	$0.010 \times 0.040 \times 0.15$
Temp (K)	150 (2)	θ range, deg	$3.77 < \theta < 68.32$
a, \AA	5.9362 (3)	Range of h,k,l	-7, 6, -8, 7, -28, 26
b, \AA	7.6173 (3)	Reflections collected/unique	9823/ 1917
c, \AA	23.4584 (12)	Rint	0.0616
α , deg	90	Refinement Method	Full Matrix Least-Squares on F^2
β , deg	90	Data/Restraints/Parameters	1917 / 0 / 160
γ , deg	90	GOF on F^2	2.185
V, \AA^3	1060.74 (9)	Final R indices [$I > 2\sigma(I)$]	0.2075
Formula units/unit cell	4	R indices (all data)	0.2114
Dcal'd, gcm^{-3}	1.429	Max. Resid. Peaks ($e^* \text{\AA}^{-3}$)	0.9270 and 0.8300

2.5 References

1. Skotheim, T. A.; Reynolds, J. R. *Handbook of Conducting Polymers. Conjugated Polymers: Processing and Applications*; 3rd ed.; CRC Press: Boca Raton, 2007.
2. For recent reviews on conjugated materials containing boron see: (a) Jäkle, F. *Chem. Rev.* **2010**, *110*, 3985-4022. (b) Wade, C. R.; Broomsgrove, A. E. J.; Aldridge, S.; Gabbai, F. P. *Chem. Rev.* **2010**, *110*, 3958-3984. (c) Entwistle, C. D.; Marder, T. B. *Angew. Chem. Int. Ed.* **2002**, *41*, 2927-2931. (d) Entwistle, C. D.; Marder, T. B. *Chem. Mater.* **2004**, *16*, 4574-4585.
3. For some recent examples of conjugated small molecules and polymers bearing boron atoms see: a) Saito, S.; Matsuo, K.; Yamaguchi, S. *J. Am. Chem. Soc.* **2012**, *134*, 9130-9133. b) Araneda, J. F.; Neue, B.; Piers, W. E.; Parvez, M. *Angew. Chem. Int. Ed.* **2012**, *51*, 8546-8550. c) Chen, P.; Lalancette, R. A.; Jäkle, F. *Angew. Chem. Int. Ed.* **2012**, *51*, 7994-7998. d) Tanaka, K.; Chujo, Y. *Macromol. Rapid Commun.* **2012**, *33*, 1235-1255. e) Levine, D. R.; Caruso, A.; Siegler, M. A.; Tovar, J. D. *Chem. Commun.* **2012**, *48*, 6256-6258. f) Hoffend, C.; Schödel, F.; Bolte, M.; Lerner, H.-W.; Wagner, M. *Chem. Eur. J.* **2012**, *18*, 15394-15405. g) Lorbach, A.; Huebner, A.; Wagner, M. *Dalton Trans.* **2012**, *41*, 6048-6063. h) Marwitz, A. J. V.; Lamm, A. N.; Zakharov, L. N.; Vasiliu, M.; Dixon, D. A.; Liu, S. Y. *Chem Sci.* **2012**, *3*, 825-829. i) Chen, P.; Jäkle, F. *J. Am. Chem. Soc.* **2011**, *133*, 20142-20145. j) Chen, P.; Lalancette, R. A.; Jäkle, F. *J. Am. Chem. Soc.* **2011**, *133*, 8802-8805. k) Caruso, A.; Tovar, J. D. *Org. Lett.* **2011**, *13*, 3106-3109. l) Caruso, A.; Tovar, J. D. *J. Org. Chem.* **2011**, *76*, 2227-2239. m) Januszewski, E.; Lorbach, A.; Grewal, R.; Bolte, M.; Bats, J. W.; Lerner, H.-W.; Wagner, M. *Chem. Eur. J.* **2011**, *17*, 12696-12705. n) Wood, T. K.; Piers, W. E.; Keay, B. A.; Parvez, M. *Chem. Eur. J.* **2010**, *16*, 12199-12206. o) Caruso, A.; Siegler, M. A.; Tovar, J. D. *Angew. Chem. Int. Ed.* **2010**, *49*, 4213-4217. p) Nagai, A.; Chujo, Y. *Macromolecules* **2010**, *43*, 193-200.

4. For some examples of conjugated small molecules and polymers bearing silicon atoms see: a) Beaujuge, P. M.; Tsao, H. N.; Hansen, M. R.; Amb, C. M.; Risko, C.; Subbiah, J.; Choudhury, K. R.; Mavrinskiy, A.; Pisula, W.; Brédas, J. L.; So, F.; Müllen, K.; Reynolds, J. R. *J. Am. Chem. Soc.* **2012**, *134*, 8944-8957. b) Guo, X.; Zhou, N.; Lou, S. J.; Hennek, J. W.; Ponce Ortiz, R.; Butler, M. R.; Boudreault, P.-L. T.; Strzalka, J.; Morin, P.-O.; Leclerc, M.; Lopez Navarrete, J. T.; Ratner, M. A.; Chen, L. X.; Chang, R. P. H.; Facchetti, A.; Marks, T. J. *J. Am. Chem. Soc.* **2012**, *134*, 18427-18439. c) Fu, H.; Cheng, Y. *Curr. Org. Chem.* **2012**, *16*, 1423-1446. d) Chu, T.-Y.; Lu, J.; Beaupré, S.; Zhang, Y.; Pouliot, J.-R.; Zhou, J.; Najari, A.; Leclerc, M.; Tao, Y. *Adv. Funct. Mater.* **2012**, *22*, 2345-2351. e) Caputo, B. J. A.; Welch, G. C.; Kamkar, D. A.; Henson, Z. B.; Nguyen, T. Q.; Bazan, G. C. *Small* **2011**, *7*, 1422-1426. f) Chu, T. Y.; Lu, J.; Beaupré, S.; Zhang, Y. G.; Pouliot, J. R.; Wakim, S.; Zhou, J. Y.; Leclerc, M.; Li, Z.; Ding, J. F.; Tao, Y. *J. Am. Chem. Soc.* **2011**, *133*, 4250-4253. g) Park, J. K.; Jo, J.; Seo, J. H.; Moon, J. S.; Park, Y. D.; Lee, K.; Heeger, A. J.; Bazan, G. C. *Adv. Mater.* **2011**, *23*, 2430-2435. h) Hoven, C. V.; Dang, X. D.; Coffin, R. C.; Peet, J.; Nguyen, T. Q.; Bazan, G. C. *Adv. Mater.* **2010**, *22*, E63-E66. i) Tong, M. H.; Cho, S.; Rogers, J. T.; Schmidt, K.; Hsu, B. B. Y.; Moses, D.; Coffin, R. C.; Kramer, E. J.; Bazan, G. C.; Heeger, A. J. *Adv. Funct. Mater.* **2010**, *20*, 3959-3965. j) Welch, G. C.; Perez, L. A.; Hoven, C. V.; Zhang, Y.; Dang, X. D.; Sharenko, A.; Toney, M. F.; Kramer, E. J.; Nguyen, T.-Q.; Bazan, G. C. *J. Mater. Chem.* **2011**, *21*, 12700-12709. k) Bejan, I.; Scheschke, D. *Angew. Chem. Int. Ed.* **2007**, *46*, 5783-5786. l) Boydston, A. J.; Yin, Y. S.; Pagenkopf, B. L. *J. Am. Chem. Soc.* **2004**, *126*, 10350-10354. m) Boydston, A. J.; Pagenkopf, B. L. *Angew. Chem. Int. Ed.* **2004**, *43*, 6336-6338. n) Lee, Y.; Sadki, S.; Tsuie, B.; Reynolds, J. R. *Chem. Mater.* **2001**, *13*, 2234-2236.

5. (a) Gao, D.; Hollinger, J.; Seferos, D. S. *ACS Nano* **2012**, *6*, 7114-7121. (b) Lee, J.; Han, A.-R.; Kim, J.; Kim, Y.; Oh, J. H.; Yang, C. *J. Am. Chem. Soc.* **2012**, *134*, 20713-20721. (c) Palermo, E. F.; McNeil, A. J. *Macromolecules* **2012**, *45*, 5948-5955. (d) Treat, N. D.; Varotto, A.; Takacs, C. J.; Batara, N.; Al-Hashimi, M.; Heeney, M. J.; Heeger, A. J.; Wudl, F.; Hawker, C. J.; Chabynyc, M. L. *J. Am. Chem. Soc.* **2012**, *134*, 15869-15879. (e) Tsoi, W. C.; James, D. T.; Buchaca Domingo, E.; Kim, J. S.; Al-Hashimi, M.; Murphy, C. E.; Stingelin, N.; Heeney, M.; Kim, J.-S. *ACS Nano* **2012**, *6*, 9646-9656. (f) Hollinger, J.; DiCarmine, P. M.; Karl, D.; Seferos, D. S. *Macromolecules* **2012**, *45*, 3772-3778. (g) Ballantyne, A. M.; Chen, L.; Nelson, J.; Bradley, D. D. C.; Astuti, Y.; Maurano, A.; Shuttle, C. G.; Durrant, J. R.; Heeney, M.; Duffy, W.; McCulloch, I. *Adv. Mater.* **2007**, *19*, 4544-4547. (h) Heeney, M.; Zhang, W.; Crouch, D. J.; Chabynyc, M. L.; Gordeyev, S.; Hamilton, R.; Higgins, S. J.; McCulloch, I.; Skabara, P. J.; Sparrowe, D.; Tierney, S. *Chem. Commun.* **2007**, 5061-5063.

6. (a) Jahnke, A. A.; Djukic, B.; McCormick, T. M.; Buchaca Domingo, E.; Hellmann, C.; Lee, Y.; Seferos, D. S. *J. Am. Chem. Soc.* **2013**, *135*, 951-954. (b) He, G.; Kang, L.; Delgado, W. T.; Shynkaruk, O.; Ferguson, M. J.; McDonald, R.; Rivard, E. *J. Am. Chem. Soc.* **2013**, *135*, 5360-5363. (c) McCormick, T. M.; Jahnke, A. A.; Lough, A. J.; Seferos, D. S. *J. Am. Chem. Soc.* **2012**, *134*, 3542-3548. (d) Jahnke, A. A.; Howe, G. W.; Seferos, D. S. *Angew. Chem. Int. Ed.* **2010**, *49*, 10140-10144.

7. (a) Baumgartner, T.; Réau, R. *Chem. Rev.* **2006**, *106*, 4681-4727. (b) Baumgartner, T.; Réau, R. *Chem. Rev.* **2007**, *107*, 303-303.

8. (a) Stolar, M.; Baumgartner, T. *New J. Chem.* **2012**, *36*, 1153-1160. (b) Chua, C. J.; Ren, Y.; Baumgartner, T. *Org. Lett.* **2012**, *14*, 1588-1591. (c) Romero-Nieto, C.; Kamada, K.; Cramb, D. T.; Merino, S.; Rodríguez-López, J.; Baumgartner, T. *Eur. J. Org. Chem.* **2010**, 5225-5231. (d)

Durben, S.; Linder, T.; Baumgartner, T. *New J. Chem.* **2010**, *34*, 1585-1592. (e) Romero-Nieto, C.; Merino, S.; Rodríguez-López, J.; Baumgartner, T. *Chem. Eur. J.* **2009**, *15*, 4135-4145. (f) Ren, Y.; Dienes, Y.; Hettel, S.; Parvez, M.; Hoge, B.; Baumgartner, T. *Organometallics* **2009**, *28*, 734-740. (g) Dienes, Y.; Durben, S.; Kárpáti, T.; Neumann, T.; Englert, U.; Nyulászi, L.; Baumgartner, T. *Chem. Eur. J.* **2007**, *13*, 7487-7500. (h) Baumgartner, T.; Wilk, W. *Org. Lett.* **2006**, *8*, 503-506. (i) Baumgartner, T.; Neumann, T.; Wirges, B. *Angew. Chem. Int. Ed.* **2004**, *43*, 6197-6201.

9. Chen, H.; Delaunay, W.; Li, J.; Wang, Z.; Bouit, P.-A.; Tondelier, D.; Geffroy, B.; Mathey, F.; Duan, Z.; Réau, R.; Hissler, M. *Org. Lett.* **2013**, *15*, 330-333.

10. Bouit, P.-A.; Escande, A.; Szücs, R.; Szieberth, D.; Lescop, C.; Nyulászi, L.; Hissler, M.; Réau, R. *J. Am. Chem. Soc.* **2012**, *134*, 6524-6527.

11. (a) Chen, H.; Delaunay, W.; Yu, L.; Joly, D.; Wang, Z.; Li, J.; Wang, Z.; Lescop, C.; Tondelier, D.; Geffroy, B.; Duan, Z.; Hissler, M.; Mathey, F.; Réau, R. *Angew. Chem. Int. Ed.* **2012**, *51*, 214-217. (b) Fadhel, O.; Benkö, Z.; Gras, M.; Deborde, V.; Joly, D.; Lescop, C.; Nyulászi, L.; Hissler, M.; Réau, R. *Chem. Eur. J.* **2010**, *16*, 11340-11356.

12. He, X.; Borau-Garcia, J.; Woo, A. Y. Y.; Trudel, S.; Baumgartner, T. *J. Am. Chem. Soc.* **2013**, *135*, 1137-1147.

13. Durben, S.; Baumgartner, T. *Angew. Chem. Int. Ed.* **2011**, *50*, 7948-7952.

14. (a) Joly, D.; Tondelier, D.; Deborde, V.; Delaunay, W.; Thomas, A.; Bhanuprakash, K.; Geffroy, B.; Hissler, M.; Réau, R. *Adv. Funct. Mater.* **2012**, *22*, 567-576. (b) Fadhel, O.; Gras, M.; Lemaitre, N.; Deborde, V.; Hissler, M.; Geffroy, B.; Réau, R. *Adv. Mater.* **2009**, *21*, 1261-1265.

15. (a) Mathey, F. *Angew. Chem. Int. Ed.* **2003**, *42*, 1578-1604. (b) Mathey, F. *Phosphorus-Carbon Heterocyclic Chemistry : The Rise of A New Domain*; 1st ed.; Elsevier Science Ltd.:

Amsterdam ; New York, 2001. (c) Dillon, K. B.; Mathey, F.; Nixon, J. F. *Phosphorus: The Carbon Copy*; Wiley: West Sussex, England, 1998.

16. For some examples of reduced phosphalkenes see: (a) Pan, X.; Wang, X.; Zhao, Y.; Sui, Y.; Wang, X. *J. Am. Chem. Soc.* **2014**, *136*, 9834-9837. (b) Power, P. P. *Chem. Rev.* **2003**, *103*, 789-809. (c) Dutan, C.; Shah, S.; Smith, R. C.; Choua, S.; Berclaz, T.; Geoffroy, M.; Protasiewicz, J. D. *Inorg. Chem.* **2003**, *42*, 6241-6251. (d) Badri, A. A.; Jouaiti, A.; Geoffroy, M. *Magn. Reson. Chem.* **1999**, *37*, 735-742. (e) Jouaiti, A.; Al Badri, A.; Geoffroy, M.; Bernardinelli, G. *J. Organomet. Chem.* **1997**, *529*, 143-149. (f) Al-Badri, A.; Chentit, M.; Geoffroy, M.; Jouaiti, A. *J. Chem. Soc. Faraday Trans.* **1997**, *93*, 3631-3635. (g) Jouaiti, A.; Geoffroy, M.; Terron, G.; Bernardinelli, G. *J. Am. Chem. Soc.* **1995**, *117*, 2251-2258. (h) Jouaiti, A.; Geoffroy, M.; Terron, G.; Bernardinelli, G. *J. Chem. Soc., Chem. Commun.* **1992**, 155-156. (i) Geoffroy, M.; Jouaiti, A.; Terron, G.; Cattani-Lorente, M.; Ellinger, Y. *J. Phys. Chem.* **1992**, *96*, 8241-8245.

17. (a) Wright, V. A.; Patrick, B. O.; Schneider, C.; Gates, D. P. *J. Am. Chem. Soc.* **2006**, *128*, 8836-8844. (b) Wright, V. A.; Gates, D. P. *Angew. Chem. Int. Ed.* **2002**, *41*, 2389-2392.

18. (a) Smith, R. C.; Protasiewicz, J. D. *J. Am. Chem. Soc.* **2004**, *126*, 2268-2269. (b) Smith, R. C.; Protasiewicz, J. D. *Eur. J. Inorg. Chem.* **2004**, 998-1006. (c) Smith, R. C.; Chen, X.; Protasiewicz, J. D. *Inorg. Chem.* **2003**, *42*, 5468-5470.

19. (a) Geng, X.-L.; Hu, Q.; Schäfer, B.; Ott, S. *Org. Lett.* **2010**, *12*, 692-695. (b) Öberg, E.; Schäfer, B.; Geng, X.-L.; Pettersson, J.; Hu, Q.; Kritikos, M.; Rasmussen, T.; Ott, S. *J. Org. Chem.* **2009**, *74*, 9265-9273. (c) Schaefer, B.; Oeberg, E.; Kritikos, M.; Ott, S. *Angew. Chem. Int. Ed.* **2008**, *47*, 8228-8231.

20. Nyulászi, L. *Chem. Rev.* **2001**, *101*, 1229-1246.

21. (a) Washington, M. P.; Gudimetla, V. B.; Laughlin, F. L.; Deligonul, N.; He, S.; Payton, J. L.; Simpson, M. C.; Protasiewicz, J. D. *J. Am. Chem. Soc.* **2010**, *132*, 4566-4567. (b) Washington, M. P.; Payton, J. L.; Simpson, M. C.; Protasiewicz, J. D. *Organometallics* **2011**, *30*, 1975-1983.
22. (a) Ashe, A. J., III; Fang, X. *Chem. Commun. (Cambridge)* **1999**, 1283-1284. (b) Märkl, G.; Hölzl, W.; Kallmünzer, A.; Ziegler, M. L.; Nuber, B. *Tetrahedron Lett.* **1992**, *33*, 4421-4424. (c) Soleilhavoup, M.; Baceiredo, A.; Dahan, F.; Bertrand, G. *Inorg. Chem.* **1992**, *31*, 1500-1504. (d) Märkl, G.; Dorfmeister, G. *Tetrahedron Lett.* **1987**, *28*, 1089-1092. (e) Märkl, G.; Eckl, E.; Jakobs, U.; Ziegler, M. L.; Nuber, B. *Tetrahedron Lett.* **1987**, *28*, 2119-2122. (f) Rösch, W.; Richter, H.; Regitz, M. *Chem. Ber.* **1987**, *120*, 1809-1813.
23. Issleib, K.; Vollmer, R. *Tetrahedron Lett.* **1980**, *21*, 3483-3484.
24. Masson, S.; Saint-Clair, J. F.; Saquet, M. *Synthesis* **1993**, 485-486.
25. Bansal, R. K.; Heinicke, J. *Chem. Rev.* **2001**, *101*, 3549-3578.
26. Heinicke, J.; Tzschach, A. *Phosphorus Sulfur* **1985**, *25*, 345-356.
27. Abergel, R. J.; D'Aleo, A.; Leung, C. N. P.; Shuh, D. K.; Raymond, K. N. *Inorg. Chem.* **2009**, *48*, 10868-10870.
28. Gudimetla, V. B.; Ma, L.; Washington, M. P.; Payton, J. L.; Simpson, M. C.; Protasiewicz, J. D. *Eur. J. Inorg. Chem.* **2010**, 854-865.
29. (a) Schoeller, W. W.; Niemann, J.; Thiele, R.; Haug, W. *Chem. Ber.* **1991**, *124*, 417-421. (b) Rosa, P.; Gouverd, C.; Bernardinelli, G.; Berclaz, T.; Geoffroy, M. *J. Phys. Chem. A* **2003**, *107*, 4883-4892.
30. Qiu, Y.; Worch, J. C.; Chirdon, D. N.; Kaur, A.; Maurer, A. B.; Amsterdam, S.; Collins, C. R.; Pintauer, T.; Yaron, D.; Bernhard, S.; Noonan, K. J. T. *Chemistry – A European Journal* **2014**, *20*, 7746-7751.

31. Connelly, N. G.; Geiger, W. E. *Chem. Rev.* **1996**, *96*, 877-910.
32. Frisch, M. J. T., G. W.; Schlegel, H. B.; Scuseria, G. E.; Robb, M. A.; Cheeseman, J. R.; Montgomery, J. A. Jr.; Vreven, T; Kudin, K. N.; Burant, J. C.; Millam, J. M. ; Iyengar, S. S.; Tomasi, J.; Barone, V.; Mennucci, B.; Cossi, M.; Scalmani, G.; Rega, N.; Petersson, G. A.; Nakatsuji, H.; Hada, M.; Ehara, M.; Toyota, K.; Fukuda, R.; Hasegawa, J.; Ishida, M.; Nakajima, T.; Honda, Y.; Kitao, O.; Nakai, H.; Klene, M.; Li, X.; Knox, J. E.; Hratchian, H. P.; Cross, J. B.; Bakken, V.; Adamo, C.; Jaramillo, J.; Gomperts, R.; Stratmann, R. E.; Yazyev, O.; Austin, A. J.; Cammi, R.; Pomelli, C.; Ochterski, J. W.; Ayala, P. Y.; Morokuma, K.; Voth, G. A.; Salvador, P.; Dannenberg, J. J.; Zakrzewski, V. G.; Dapprich, S.; Daniels, A. D.; Strain, M. C.; Farkas, O.; Malick, D. K.; Rabuck, A. D.; Raghavachari, K.; Foresman, J. B. ; Ortiz, J. V.; Cui, Q.; Baboul, A. G.; Clifford, S.; Cioslowski, J.; Stefanov, B. B.; Liu, G.; Liashenko, A.; Piskorz, P.; Komaromi, I.; Martin, R. L.; Fox, D. J.; Keith, T.; Al-Laham, M. A.; Peng, C. Y.; Nanayakkara, A.; Challacombe, M.; Gill, P. M. W.; Johnson, B.; Chen, W.; Wong, M. W.; Gonzalez, C.; Pople, J. A. *Gaussian 03, Revision E.01, Gaussian, Inc., Wallingford CT, 2004.*

Chapter 3♦

Stability and Reactivity of 1,3-Benzothiaphosphole: Metalation and Diels-Alder Chemistry

3.1 Introduction

Heterocyclic structures serve as valuable synthetic precursors to π -conjugated materials and ligand frameworks for metal catalysis. While most organic heterocycles contain oxygen, nitrogen or sulfur, phosphorus-based rings have also become a popular area of exploration.¹ Aromatic phosphorus heterocycles exhibit different structural and electronic properties than their organic counterparts, making them attractive targets for further functionalization (Chart 3.1).^{1a} However, the reactivity of P=C containing rings is often different than organic systems and consequently, alternative synthetic methods are necessary for their derivatization.^{1a,2}

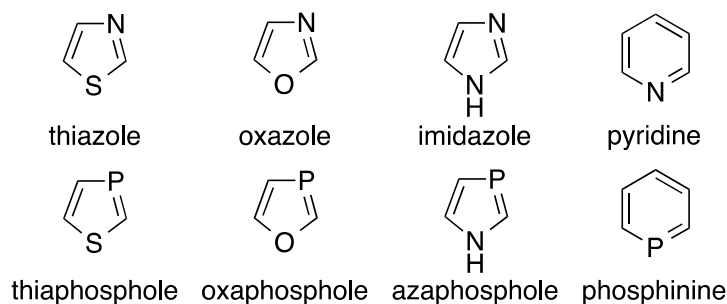


Chart 3.1. Common aromatic phosphorus heterocycles and their nitrogen congeners.

While the reactivity of phosphinines³ and azaphospholes⁴ has been explored, the functionalization of thiaphospholes and oxaphospholes is still limited. Since benzothiaphosphole

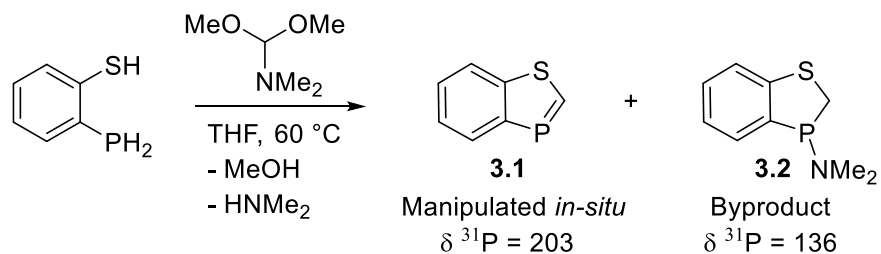
♦ Reproduced with permission from Worch, J.C.; Hellemann, E.; Pros, G.; Gayathri, C.; Pintauer, T.; Gil, R.R.; Noonan, K.J.T. Stability and Reactivity of 1,3-Benzothiaphospholes: Metalation and Diels-Alder Chemistry. *Organometallics* **2015**, *34*, 5366–5373. Copyright 2015 American Chemical Society.

derivatives can be tuned as electron-deficient materials⁵ and benzoxaphosphole derivatives are highly luminescent in solution,⁶ synthetic methods for the manipulation of these heterocycles is crucial for further exploration. Herein, we report on the synthesis of the parent 1,3-benzothiaphosphole and efforts towards functionalization of this heterocycle.

3.2 Results and Discussion

1,3-benzothiaphosphole (**3.1**) can be prepared from the combination of 1-mercapto-2-phosphinobenzene and *N,N*-dimethylformamide dimethyl acetal (Scheme 3.1). Analysis of the reaction mixture using $^{31}\text{P}\{^1\text{H}\}$ spectroscopy revealed that the phosphine ($\delta^{31}\text{P} -127$) was nearly completely consumed and a new downfield signal had appeared at $\delta^{31}\text{P} 203$ (Figure 3.2 – top spectrum).

Scheme 3.1. Synthesis of 1,3-benzothiaphosphole and byproduct from N-H addition across the P=C bond.



A previous report describing the synthesis of the parent 1,3-benzothiaphosphole has appeared however,⁷ the reported ^{31}P NMR shift ($\delta = 79.9$) is not consistent with other thiaphosphole molecules which typically have ^{31}P NMR signals near 200 ppm.⁸ The chemical shift we observed is consistent with the 2-aryl-1,3-benzothiaphospholes^{5b} ($\delta^{31}\text{P} 185\text{--}203$) and 1,3-thiaphosphole ($\delta^{31}\text{P} 211$).^{8a} Interestingly, concentration of the reaction mixture in an effort to isolate **3.1** resulted in the formation of an intractable white solid, indicative of degradation. A crude ^1H NMR spectrum of **3.1** (Figure 3.1) could be obtained from the THF reaction mixture though other unidentified species are also present. The proton of the 2-position resonates significantly

downfield at 8.86 ppm with a J_{PH} of 33.9 Hz which is very similar to 1,3-thiaphosphole with a signal at 8.87 ppm ($J_{PH} = 35.7$ Hz).^{8a}

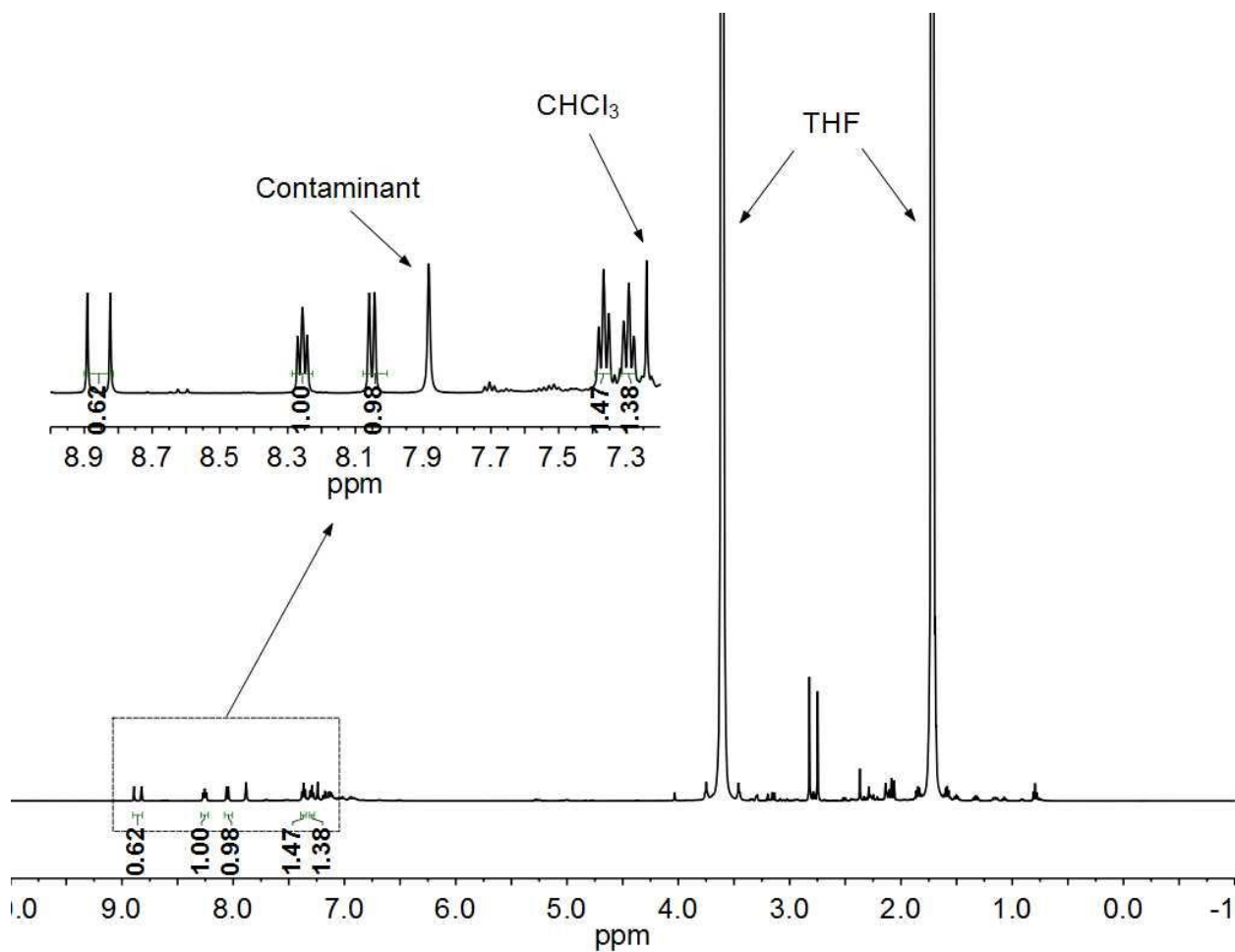


Figure 3.1. Crude ¹H NMR spectrum in CDCl₃ for compound 3.1.

After repeating the reaction to synthesize compound 3.1, a second signal was observed in the ³¹P{¹H} spectrum (136 ppm). Upon isolation of this byproduct, analysis using ¹H NMR suggested addition of dimethylamine across the P=C bond of the benzothiaphosphole (compound 3.2). The regiochemistry of the N-H addition was inferred from the absence of ¹J_{P-H} coupling (~200 Hz) in the ¹H NMR spectrum and similar reports of amine addition to acyclic P=C bonds.⁹ This result was surprising considering 1,3-benzazaphosphole is quite resistant to N-H addition.¹⁰

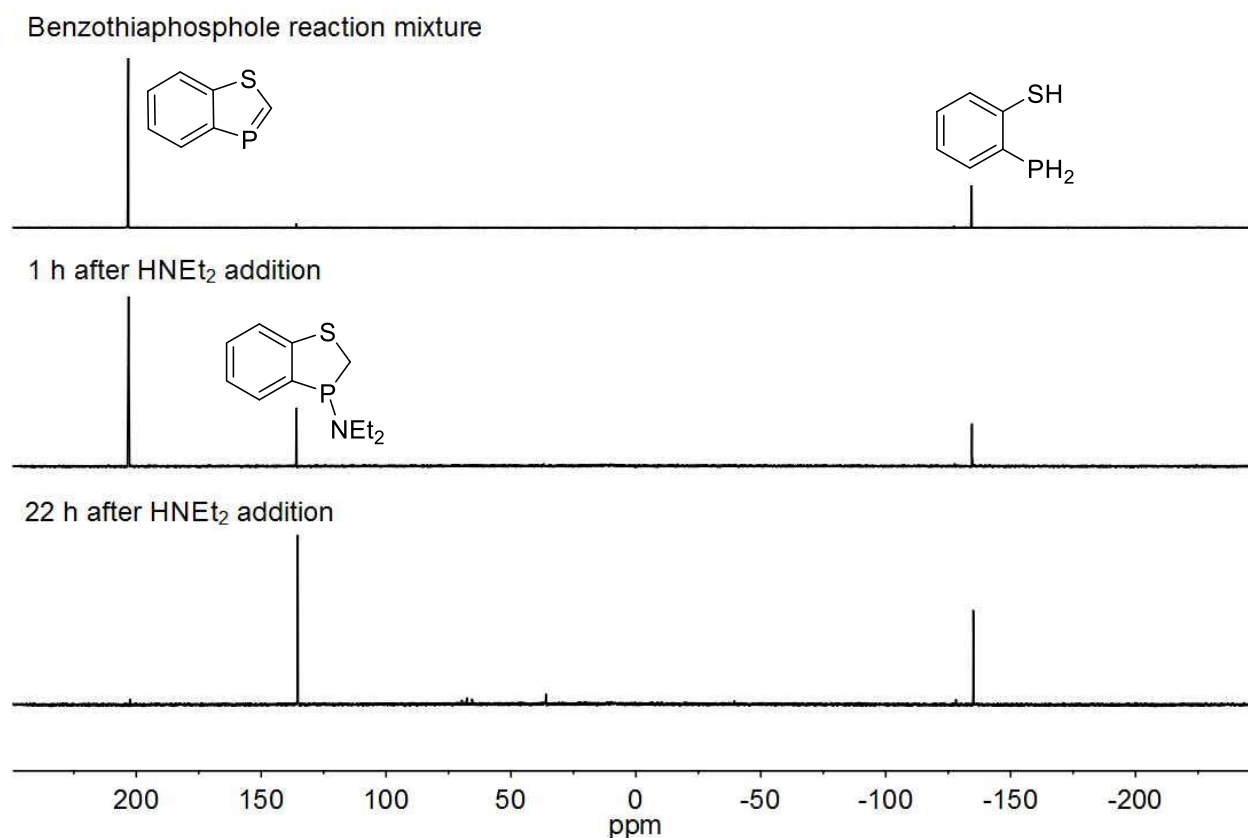


Figure 3.2. $^{31}\text{P}\{^1\text{H}\}$ NMR spectra illustrating the change in benzothiaphosphole **3.1** upon treatment with HNEt₂.

The quality of N,N-dimethylformamide dimethyl acetal used for the reaction had a significant impact on the ratio of compounds **3.1** and **3.2**. Relatively more of the byproduct (**3.2**) was formed when using technical grade diacetal (94%) as opposed to reagent grade (97%). Moreover, storage of the acetal under ambient conditions also altered the ratio of compound **3.1** and the undesired byproduct **3.2**. Utilization of freshly distilled diacetal produced **3.1** fairly cleanly with minimal N-H addition to the P=C bond.

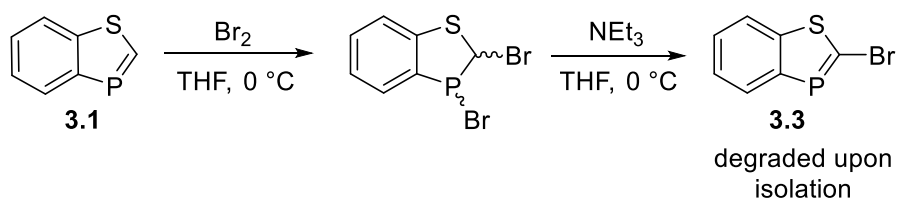
To explore the reactive nature of 1,3-benzothiaphosphole towards secondary amines, a subsequent experiment was carried out at 60 °C where compound **3.1** was synthesized and one equivalent of HNEt₂ was added to the reaction mixture. The solution darkened immediately upon addition of the amine and the reaction was sampled after 1 h and 22 h. $^{31}\text{P}\{^1\text{H}\}$ NMR spectroscopy

(Figure 3.2) of the mixture revealed consumption of compound **3.1** and the new signal (135 ppm) confirmed thiaphosphole sensitivity towards secondary amines. The P=C bond did not seem susceptible to O-H addition, since treatment of the reaction mixture with methanol produced no change in the $^{31}\text{P}\{^1\text{H}\}$ NMR spectrum.

Reactivity towards Electrophiles. The previously reported 1,3-thiaphosphole ($\text{C}_3\text{H}_3\text{P}_1\text{S}_1$) was manipulated in dilute solution,^{8a} and this strategy was adopted for functionalization of benzothiaphosphole **3.1**. To assess reactivity, several electrophiles were added to the reaction mixture. Methyl iodide was unreactive, which is in accordance with other low coordinate P=C heterocycles such as phosphinine.^{1a} The lone pair is weakly basic in low coordinate phosphorus heterocycles and alkylation of P=C bonds is quite rare.¹¹

We anticipated simple addition of HCl across the P=C bond, however, treatment of the reaction mixture with a 2M ethereal solution of HCl resulted in multiple phosphorus products after several days. A previous report described facile addition of HCl across the P=C bond in 2-*t*Bu-1,3-benzoxaphospholes,¹² but the inability to isolate **3.1** cleanly may complicate the 1,2-addition reaction.

Scheme 3.2. Synthesis of 2-(bromo)-1,3-benzothiaphosphole.



When **3.1** was treated with stoichiometric Br_2 (Scheme 3.2), $^{31}\text{P}\{^1\text{H}\}$ spectroscopy indicated a rapid attack at the P=C bond with disappearance of the signal for **3.1** ($\delta^{31}\text{P}$ 204) and the formation of three new signals ($\delta^{31}\text{P}$ 108, $\delta^{31}\text{P}$ 95, $\delta^{31}\text{P}$ 55 – Figure 3.3 – Left). Although the intermediate was not isolated, one of the former signals is postulated to be attributed to the racemic

mixture of enantiomers while the latter is unidentified. Addition of 1 equivalent of triethylamine, led to the formation of new signals ($\delta^{31}\text{P}$ 218, $\delta^{31}\text{P}$ 205) with the previously unidentified signal remaining in the mixture ($\delta^{31}\text{P}$ 55). Analysis of the reaction mixture using GC-MS revealed a major product (Figure 3.3 – Right) with a molecular ion peak at 230 amu (consistent with compound **3.3**) and the expected isotope pattern of a brominated molecule ($M+2$ peak = 232 amu).

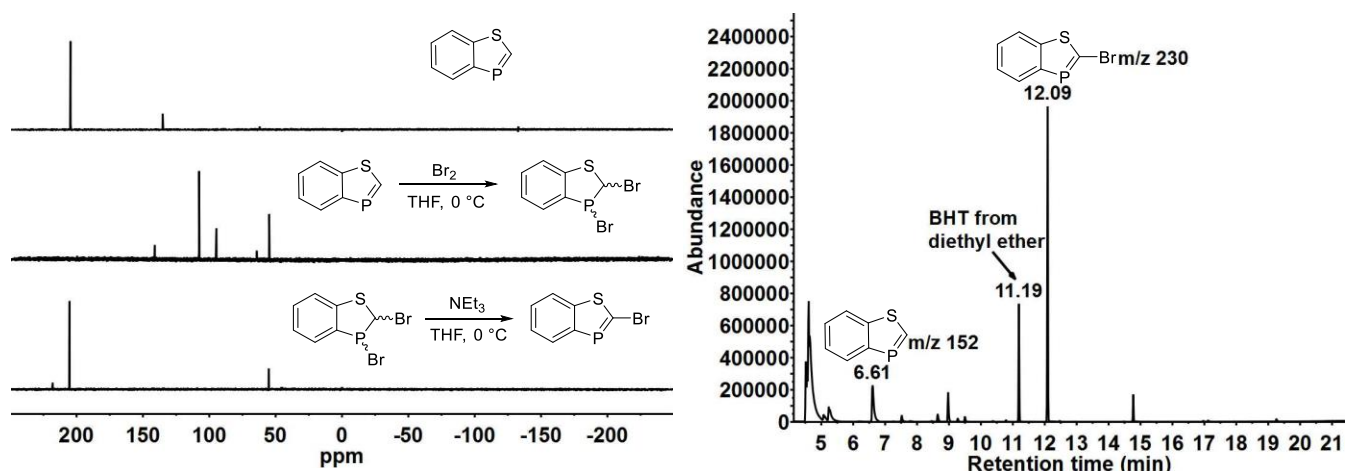
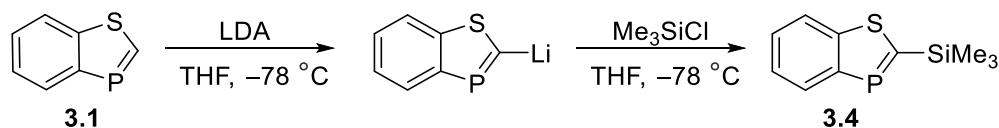


Figure 3.3. Left – Crude ^{31}P NMR spectra for synthesis of compound **3.3**. Right – Crude gas chromatogram of the reaction mixture to synthesize 2-(bromo)-1,3-benzothiaphosphole. Major signal at 12.1 min exhibits a molecular ion peak (M^+) at 230 amu and the $M+2$ isotope peak at 232 amu.

After column chromatography under N_2 , $^{31}\text{P}\{^1\text{H}\}$ spectroscopy of the diluted product fraction revealed only one signal at $\delta^{31}\text{P}$ 205. However, upon concentration, the white crystalline solid became substantially discolored within minutes and a red residue formed. Analysis of the residue using $^{31}\text{P}\{^1\text{H}\}$ spectroscopy revealed multiple signals with complete loss of the original signal, indicative of degradation.

Scheme 3.3. Lithiation and electrophilic quenching of the 1,3-benzothiaphosphole.



Metalation. To explore metalation of the parent 1,3-benzothiaphosphole, compound **3.1** was prepared in the presence of 4 Å molecular sieves (to remove dimethylamine and methanol byproducts), the reaction mixture was filtered and different bases were added. *tert*-Butyl lithium, Schlosser's base,¹³ Ph₃CLi and PhLi failed to cleanly yield the desired metalated thiaphosphole species. Nucleophilic attack on the P=C bond is a possibility since it has been observed previously in azaphospholes^{4b} and protected 2-chlorophosphinines.¹⁴

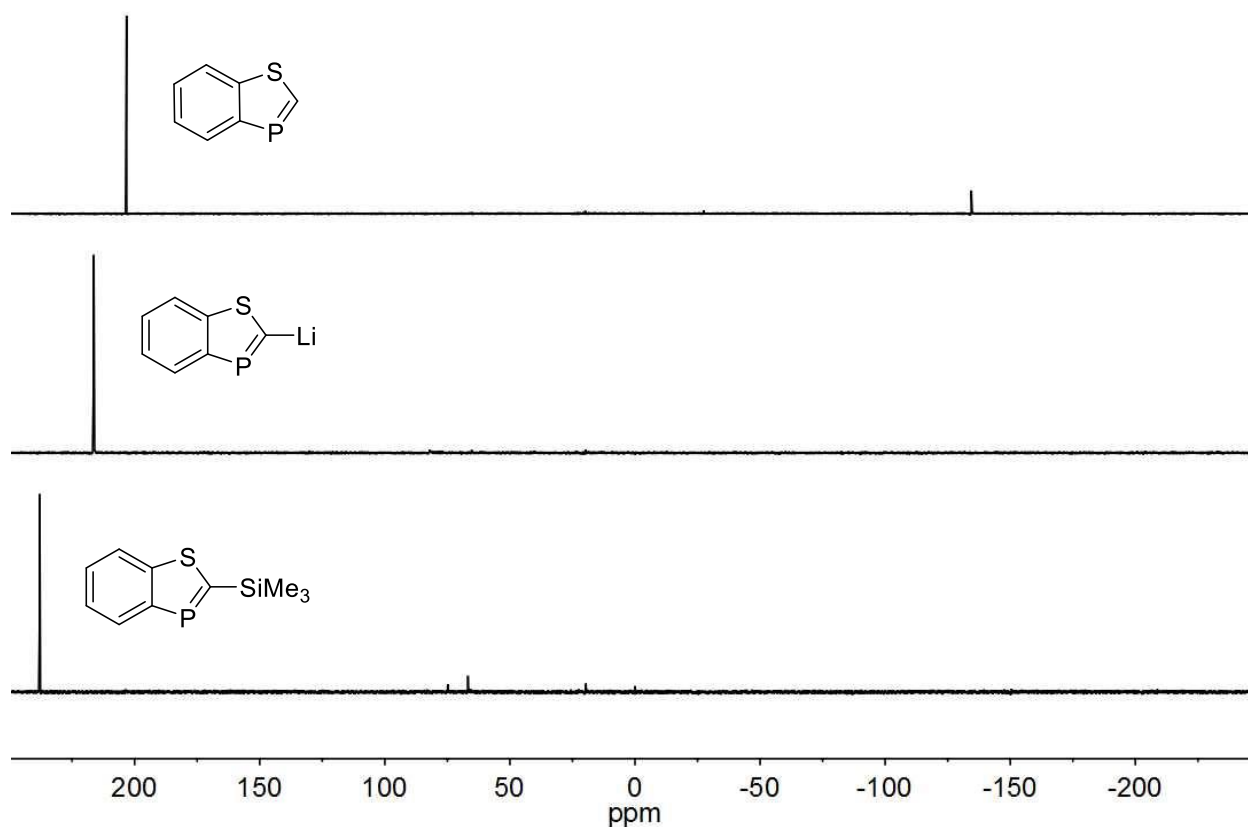


Figure 3.4. Stack plot of the crude ³¹P{¹H} NMR spectra for benzothiaphosphole lithiation and quenching using Me₃SiCl.

The proton at the 2-position should be susceptible to deprotonation using a non-nucleophilic base such as lithium diisopropyl amide (LDA) (Scheme 3.3) and, the 1,3-benzazaphospholes have already been lithiated in this manner.^{4b} Treatment of compound **3.1** with

LDA at $-78\text{ }^{\circ}\text{C}$ produced a single downfield signal in the $^{31}\text{P}\{^1\text{H}\}$ NMR spectrum ($\delta^{31}\text{P}$ 216). This downfield shift in the spectrum indicated that the P=C bond remained intact during the reaction (Figure 3.4). The lithiated species was stable for at least 3 hours in a cold bath at $-78\text{ }^{\circ}\text{C}$, but the compound decomposed within an hour upon warming the solution to room temperature.

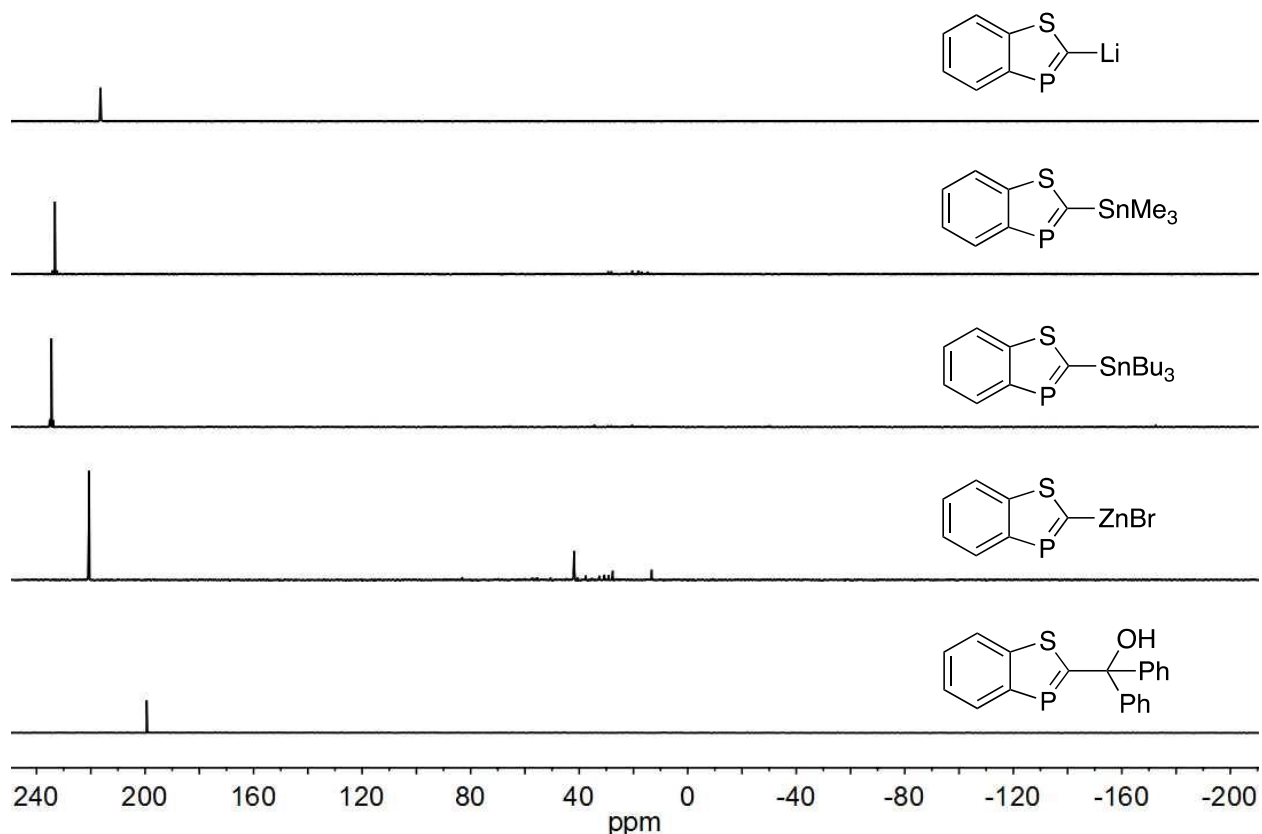


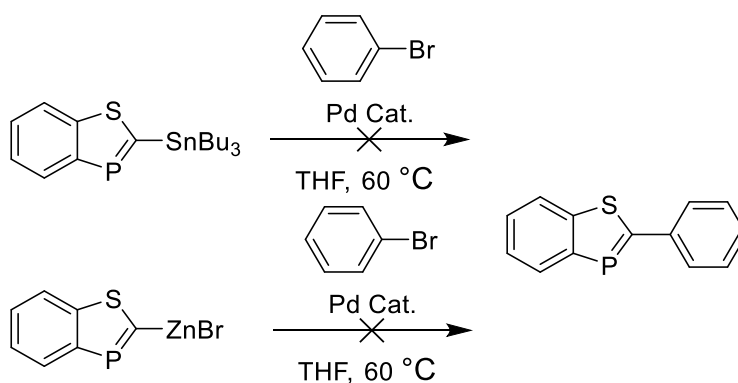
Figure 3.5. Crude $^{31}\text{P}\{^1\text{H}\}$ NMR spectra for quenching of 2-lithio-1,3-benzothiaphosphole.

The lithiated benzothiaphosphole reacted smoothly with Me_3SiCl according to $^{31}\text{P}\{^1\text{H}\}$ spectroscopy (Figure 3.4). The 2-(trimethylsilyl)-1,3-benzothiaphosphole **3.4** (Scheme 3.3) could be isolated in fairly low yield using column chromatography with ethylated silica gel under a N_2 atmosphere. Other electrophiles such as $\text{Ph}_2\text{C}=\text{O}$, Me_3SnCl , Bu_3SnCl were also explored in the functionalization of the lithiate. Replacement of the C-Li was monitored using ^{31}P NMR

spectroscopy and proceeded smoothly (Figure 3.5) however, these compounds were difficult to isolate in analytically pure form.

Nevertheless, a stannylated derivative was obtained in reasonable purity and used in Stille cross-coupling with an aryl halide. The *in situ* zinc reagent was also used under Negishi cross-coupling conditions (Scheme 3.4).

Scheme 3.4. Attempted Stille and Negishi cross-coupling of metalated thiaphosphole.



However, all cross-coupling attempts failed to produce 2-aryl-1,3-benzothia-phospholes even though the metalated thiaphosphole remained intact according to $^{31}\text{P}\{^1\text{H}\}$ spectroscopy (Scheme 3.4). It is possible that the phosphalkene fragment acts as competitive ligand to the palladium catalyst.¹⁵

Diels-Alder Reactivity. The reactivity of the parent benzothia-phosphole as a dienophile was also investigated. Cyclic and acyclic $\text{P}=\text{C}$ moieties (phosphalkenes, phosphinines, heterophospholes) are known to participate in Diels-Alder reactions.¹⁶

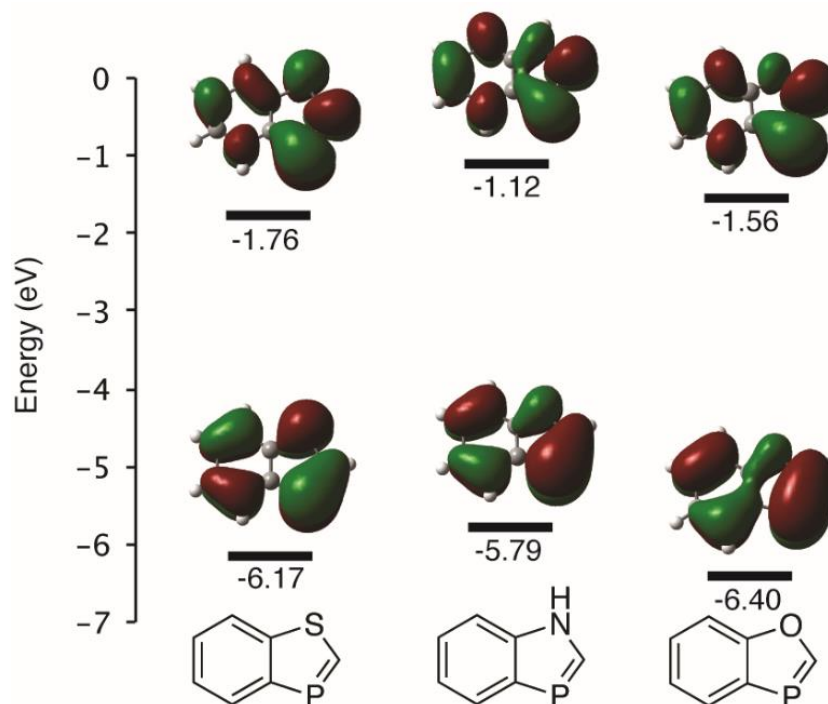
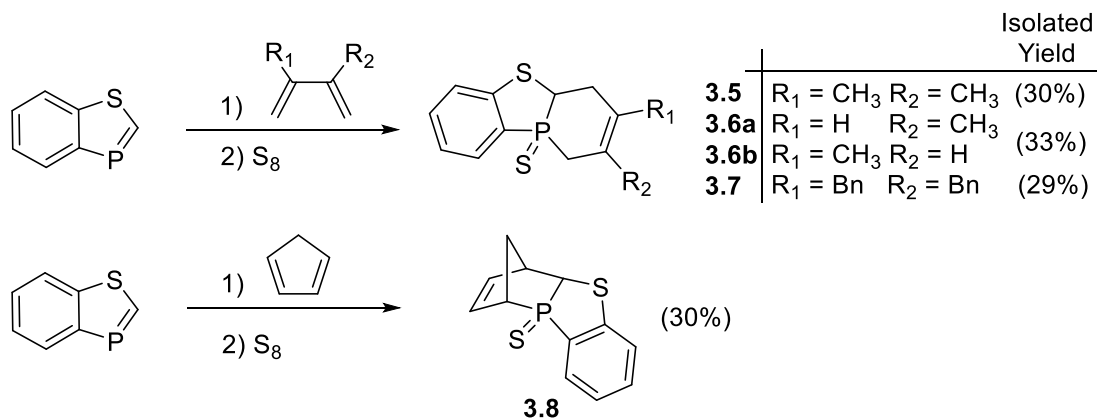


Figure 3.6. Calculated HOMO and LUMO levels for the benzoheterophospholes. DFT calculations were performed using the hybrid functional B3LYP with a 6-31G*(d,p) basis set.

When examining the series of 1,3-benzoheterophospholes using DFT calculations (Figure 3.6), the benzothiaphosphole features the greatest LUMO stabilization and should be the most reactive as a dienophile. Compound **3.1** reacts readily with various dienes to produce the desired cycloadducts (compounds **3.5-3.8**, Scheme 3.5). For 2,3-dimethylbutadiene and cyclopentadiene, the reaction was complete within 1 day at elevated temperatures while isoprene and 2,3-dibenzylbutadiene required longer reaction times with heating. Following the cycloaddition, the three coordinate phosphines could be isolated, however some undesired oxidation (~5 %) occurred under ambient conditions. Each phosphine adduct was converted to the air-stable phosphine sulfide by combination with elemental sulfur at room temperature in CHCl_3 . We suspect no isomerization of the P atom occurs under these conditions.¹⁷ The P(V) structures can be chromatographed on silica gel to obtain analytically pure products which were characterized using ^{31}P , ^1H , ^{13}C NMR spectroscopy, mass spectrometry and elemental analysis.

Scheme 3.5. [2+4] Diels-Alder cycloadditions.



Compound **3.5** was also characterized using X-ray crystallography (Figure 3.7). The geometry at the P atom is largely tetrahedral with a P=S distance of 1.9590(5) Å and P–C distances between 1.7905(11) – 1.8430(11) Å. The C–P–C angles vary from 98.47(5)° to 107.62(5)°, which is not surprising considering the puckered geometry of the cycloadduct. The S2 atom and the hydrogen atom of C7 are in a cis confirmation which is in agreement with previously reported benzoxaphosphole adducts¹⁸ and is indicative of a concerted cycloaddition.

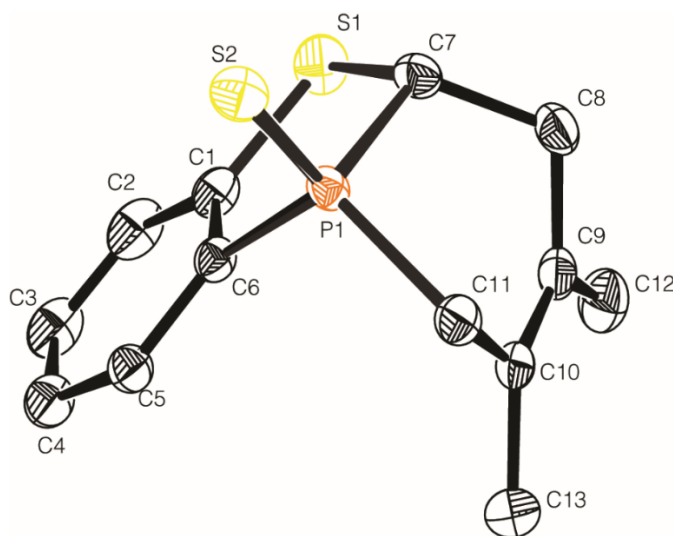


Figure 3.7. Solid state molecular structure of Diels-Alder cycloadduct **3.5** with H atoms omitted. Thermal ellipsoids at 50% probability. Selected distances (Å) and angles (deg) for **5**: P1–C6 1.7905(11); P1–C7 1.8430(11); P1–C11 1.8156(11); P1–S2 1.9590(5); S1–C1 1.7616(12); S1–C7 1.8183(12); C6–P1–C11 107.62(5); C6–P1–C7 98.47(5); C11–P1–C7 102.66(5); C1–S1–C7 98.18(5).

While compounds **3.5** and **3.7** exhibit a single set of signals in the ^1H NMR spectrum, compounds **3.6** and **3.8** exhibit two sets of signals corresponding to a major and minor product. Compound **3.6** has a pair of isomers from the two possible regio-additions of isoprene (**3.6a** and **3.6b**) and compound **3.8** exhibits endo/exo isomerism. Residual dipolar coupling (RDC) NMR experiments were used to assign the major and minor isomers obtained for both compounds.¹⁹ The RDC technique is a simple methodology for providing global orientation of spin pairs in rigid molecules and is used when NOE experiments are inconclusive in structural assignments.^{19b}

In conventional solution NMR spectroscopy, dipolar-coupling averages to zero due to isotropic molecular tumbling. However, if the sample is partially oriented in an anisotropic medium, the dipolar coupling value is non-zero and a fraction of the original dipolar coupling value is observed, known as RDC. The measured RDCs can be fitted to all the possible diastereomers of the proposed structure and an alignment tensor is obtained for each diastereomer using a singular value decomposition method.²⁰ The calculated RDCs for each diastereomer are then compared with the experimental values to assign the structure. Partial alignment of compounds **3.6** and **3.8** was achieved using PMMA gels swollen in CDCl_3 and a reversible compression/relaxation method.²¹

For completeness, the computed structures were calculated with both *cis* and *trans* orientation of the P=S and C-H bond of the bridging phosphorus and carbon atoms (formerly the P=C bond). These two orientations and the two potential regioisomers of isoprene provide a total of 4 possible structures for **3.6**. If the reaction follows a concerted cycloaddition, the two isomers present should be *cis* orientation only (Figure 3.8). Comparison of the calculated and experimental data confirmed the *cis* isomers are the only ones present in the mixture. The major and minor signals in the ^1H NMR spectrum were assigned and the major isomer has the methyl group of the

diene fragment nearest to phosphorus (**3.6a**) in a 75:25 ratio. Similar product ratios have been observed in cycloaddition reactions between isoprene and various phosphalkene moieties; the regioselectivities were rationalized by the presence of additional orbital interactions (*in silico*) between π_{diene} and $\pi^*_{\text{dienophile}}$ when the methyl group is nearest the phosphorus atom.²²

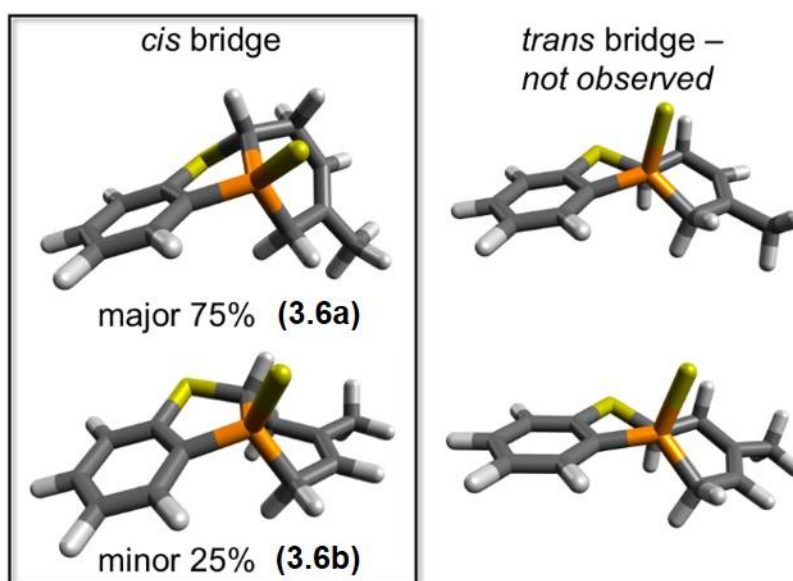


Figure 3.8. Different possible isomers of compound **3.6**. Cis and trans refer to the orientation of the P=S and C-H bond of the bridging atoms.

For compound **3.8**, endo and exo isomerism is possible for the product. Again, the cis and trans orientation of the bridging P=S and C-H bond were considered with computed structures for a total of 4 possible diastereomers (Figure 3.9). The calculated and experimental RDCs were compared and once again, only the cis isomers were present. The endo isomer was preferred and the mixture exists as a ratio of 78:22, endo:exo.

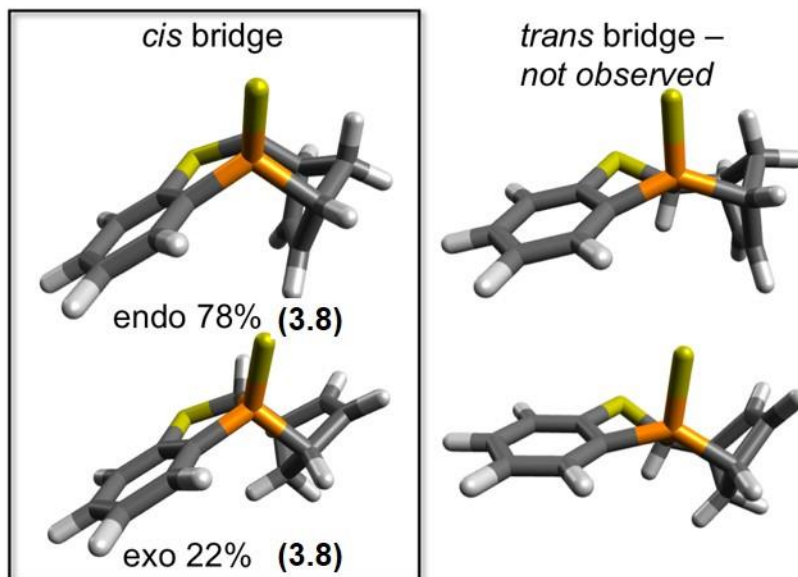


Figure 3.9. Different possible isomers of compound **3.8**. Cis and trans refer to the orientation of the P=S and C-H bond of the bridging atoms.

3.3 Conclusions

The synthesis of the parent 1,3-benzothiaphosphole was accomplished using 1-mercapto-2-phosphinobenzene and *N,N*-dimethylformamide dimethylacetal. The compound is susceptible to addition with secondary amines. The reactivity of the benzothiaphosphole was evaluated with several electrophiles (MeI, HCl, Br₂) and it can be selectively lithiated in the 2-position using LDA at -78 °C. The lithiate was trapped using trimethylsilylchloride to obtain 2-(trimethylsilyl)-1,3-benzothiaphosphole. The metalated derivatives explored in this work were targeted in an effort to further functionalize the thiaphosphole using metal-catalyzed cross coupling. However, the complex reaction mixture made it quite difficult to explore this topic in further depth. Continued work in this area will focus on an isolable organometallic or main group derivative that can be functionalized using metal mediated pathways.

The reactivity of the thiaphosphole as a dienophile was also explored. Diels-Alder cycloadditions occurred with several different dienes resulting in the formation of fused

phosphorus ring systems. Anisotropic NMR experiments (RDCs) were used to assign the isomeric mixtures. This method provides access to fused phosphorus derivatives that could potentially be explored as ligands in catalysis.

3.4 Experimental Section

General Materials and Methods. All reactions and manipulations of air and water sensitive compounds were carried out under a dry nitrogen atmosphere using an mBraun glovebox or standard Schlenk techniques. Technical grade and reagent grade *N,N*-dimethylformamide dimethyl acetal (either 94% or 97%) were obtained from commercial sources and could be used as received but prolonged storage under ambient conditions resulted in more 1,2-addition of dimethylamine to benzothiaphosphole **3.1**. Distillation of the acetal from 4Å sieves prior to use minimized byproduct formation in this reaction. Cyclopentadiene was obtained by cracking dicyclopentadiene at 180 °C. 1-Mercapto-2-phosphinobenzene was synthesized according to a published procedure.^{5b,23} All solvents (diethyl ether, tetrahydrofuran, toluene, dichloromethane, hexanes) were degassed with argon and dried prior to use. Ethylated silica gel was obtained by treatment of silica gel with EtSiCl₃ in CHCl₃ prior to use.²⁴

NMR Analysis. CDCl₃ was dried using P₂O₅ and distilled prior to use, while CD₂Cl₂ was used as received. NMR spectra were recorded on a Bruker Avance 500 MHz spectrometer or a Bruker Avance 300 MHz spectrometer and referenced (¹H NMR: 7.24 ppm for CHCl₃ and 5.32 ppm for CHDCl₂; ¹³C NMR: 77.23 ppm for CDCl₃ and 54.00 ppm for CD₂Cl₂). The ³¹P{¹H} spectra were referenced to an external standard (85 % H₃PO₄). For RDC Experiments, compounds **6** and **8** were dissolved in CDCl₃ and diffused in PMMA gels. Anisotropy was introduced using a previously reported compression/relaxation method.²¹ F1 coupled HSQC experiments were performed under

isotropic and anisotropic conditions. One bond C–H dipolar coupling (${}^1D_{\text{CH}}$) values for the major and minor components of each reaction were extracted from the difference of the splitting in anisotropic conditions and isotropic conditions (${}^1D_{\text{CH}} = {}^1T_{\text{CH}} - {}^1J_{\text{CH}}$). The geometries of the different isomers were computed using DFT methods with the hybrid functional B3LYP and 6-31+G** as basis set in the Gaussian 03 Suite.²⁵ The fit for the alignment tensor, back-calculated dipolar couplings and the Cornilescu quality factor (Q) were completed using Mspin.²⁶ The calculated and experimental RDC values were evaluated using the Q factor.²⁷ The lowest Q factor corresponds to the best fit, and hence to the correct structure.^{19a,19c}

Mass Spectrometry and Elemental Analysis. High-resolution mass spectrometry data were obtained using a Waters 70-VSE double focusing sector instrument in the School of Chemical Sciences Mass Spectrometry Laboratory at the University of Illinois, Urbana-Champaign. Elemental analysis data were collected by Robertson Microlit using a Perkin-Elmer Model 2400 CHN Analyzer.

DFT Methods. Hybrid density functional theory (DFT) calculations were performed for 1,3-benzoheterophospholes using the B3LYP functional with a 6-31G*(d,p) basis set in the Gaussian 03 suite.²⁵

X-ray Crystallography. Crystallographic data for compound **3.5** were collected at 149 (2) K using graphite-monochromated Mo-K α radiation (0.7173 Å) on a Bruker Smart Apex II CCD diffractometer. Data reduction included absorption corrections by the multi-scan method using SADABS and refined by full matrix least squares using SHELXTL 6.1 bundled software package. The H-atoms were positioned geometrically (aromatic C–H 0.93, methylene C–H 0.97, and methyl C–H 0.96) and treated as riding atoms during subsequent refinement, with $U_{\text{iso}}(\text{H}) =$

1.2U_{eq}(C) or 1.5U_{eq}(methyl C). The methyl groups were allowed to rotate about their local 3-fold axes. All other crystallographic data is available in the Supporting Information.

General Synthesis of 1,3-benzothiaphosphole (3.1). In a nitrogen-filled glove box, an oven-dried 50 mL Schlenk flask was charged with 1-mercapto-2-phosphinobenzene (0.250 g, 1.76 mmol), 6 mL of THF and sealed with a rubber septum. The flask was removed from the glove box and stirred at room temperature. *N,N*-Dimethylformamide dimethyl acetal (0.26 mL, 1.96 mmol) was added by syringe to the reaction mixture and the flask was subsequently immersed in an oil bath at 60 °C. The reaction was stirred for 16 h and the colorless solution turned dark orange as the reaction progressed. An aliquot of the reaction mixture was removed using a syringe and analyzed using ³¹P{¹H} NMR spectroscopy. Near complete consumption of the starting material was observed and a new signal had appeared at 203.2 ppm corresponding to the 1,3-benzothiaphosphole. Further manipulation of the compound was typically conducted in dilute solution (< 0.5 M). Byproduct formation ($\delta^{31}\text{P}$ 136.3) could be minimized by distillation of the acetal. A ¹H NMR spectrum was recorded for the crude reaction mixture and unidentified contaminants were present in the spectrum along with the signals attributed to the 1,3-benzothiaphosphole (**Figure 3.1**). ¹H NMR (500 MHz, CDCl₃) δ 8.86 (d, *J* = 33.9 Hz, 1H), 8.26 (t, *J* = 6.9 Hz, 1H), 8.05 (d, *J* = 8.1 Hz, 1H), 7.37 (t, *J* = 7.5 Hz, 1H), 7.29 (t, *J* = 7.6 Hz, 1H).

Synthesis of 2-bromo-1,3-benzothiaphosphole (3.3). In a nitrogen-filled glove box, an oven-dried 100 mL Schlenk flask was charged with 1-mercapto-2-phosphinobenzene (0.52 g, 3.66 mmol) and 10 mL toluene. The flask was sealed, removed from the glove box and stirred. *N,N*-Dimethylformamide dimethyl acetal (0.488 mL, 3.67 mmol) was added by syringe to the mixture and the flask was subsequently immersed in an oil bath at 85 °C. The reaction was stirred for 16 h and the colorless solution turned dark orange as the reaction progressed. An aliquot of the reaction

mixture was removed and analyzed using $^{31}\text{P}\{^1\text{H}\}$ spectroscopy to confirm product **3.1** had formed. The reaction vessel was then cooled to 0°C and 1 equivalent of Br_2 (0.19 mL, 3.71 mmol) was added drop-wise using a syringe. The reaction mixture darkened and some precipitate formed. After stirring for 1 h in the ice bath, an aliquot of the reaction mixture was analyzed using $^{31}\text{P}\{^1\text{H}\}$ NMR spectroscopy. The signal corresponding to compound **3.1** had completely disappeared and three new signals ($\delta^{31}\text{P}$ 108, $\delta^{31}\text{P}$ 95, $\delta^{31}\text{P}$ 55) had appeared. Triethylamine (0.51 mL, 3.67 mmol) was then added to the reaction mixture at 0°C . The vessel was warmed to room temperature and stirred for 2 h with the mixture turning a lighter shade of orange as the reaction progressed. Analysis of the reaction mixture using $^{31}\text{P}\{^1\text{H}\}$ NMR spectroscopy revealed new signals ($\delta^{31}\text{P}$ 218, $\delta^{31}\text{P}$ 205 (major)) along with the previously unidentified signal ($\delta^{31}\text{P}$ 55) remaining. The reaction mixture was cannula filtered into an oven-dried 100 mL Schlenk flask under N_2 . The remaining solids were washed with 10 mL toluene, which was combined with the previous organic extract. An aliquot was removed for GC-MS analysis and the major signal at 12.1 min exhibited a molecular ion peak (M^+) at 230 amu and the associated isotope peak at 232 amu. The reaction mixture was concentrated and loaded onto a N_2 flushed, silica gel short-path column. The title compound eluted using hexanes and upon concentration, a white crystalline solid was obtained. However, the solid became a red residue within minutes and $^{31}\text{P}\{^1\text{H}\}$ and ^1H NMR analyses indicated extensive decomposition with no definable structure.

Synthesis of 2-(trimethylsilyl)-1,3-benzothiaphosphole (3.4). In a nitrogen-filled glove box, an oven-dried Schlenk flask was charged with 1-mercapto-2-phosphinobenzene (1.42 g, 10.0 mmol), 30 mL THF and approximately 10 g 4\AA molecular sieves. The flask was sealed, removed from the glove box and stirred slowly. *N,N*-Dimethylformamide dimethyl acetal (1.46 mL, 11.0 mmol) was added by syringe to the mixture and the flask was subsequently immersed in an oil bath at 60°C .

The reaction mixture was stirred for 16 h after which, an aliquot was analyzed using $^{31}\text{P}\{^1\text{H}\}$ NMR spectroscopy to confirm formation of compound **3.1**. The solution was transferred by cannula filtration through a fritted filter funnel packed with celite into a 100 mL Schlenk flask. The sieves were washed with one portion of THF (10 mL), which was combined with the reaction solution. The solution containing **3.1** in 40 mL THF, was cooled to $-78\text{ }^\circ\text{C}$ using a dry-ice acetone bath, and 2.0 M lithium diisopropyl amide solution (5.0 mL, 10 mmol) was added dropwise to the solution. During the addition, the reaction mixture turned dark red. The solution was stirred for 1h at $-78\text{ }^\circ\text{C}$ at which point, an aliquot was removed from the reaction mixture and analyzed using $^{31}\text{P}\{^1\text{H}\}$ NMR spectroscopy. A new signal at 215.7 ppm was observed. Trimethylsilyl chloride (1.27 mL, 10.0 mmol) was then slowly added to the reaction vessel by syringe. The flask was not removed from the cold bath to ensure the reaction vessel returned to room temperature very slowly overnight. A final aliquot of the reaction revealed a large signal at 237.6 ppm in the $^{31}\text{P}\{^1\text{H}\}$ NMR spectrum. The solvent was removed *in vacuo*, diethyl ether (20 mL) was added, and the organic extract was cannula filtered into a 100 mL Schlenk flask. The ether solution was concentrated and the viscous dark oil was chromatographed under N_2 on ethylated silica gel using dry hexanes to afford the title compound as a white solid (0.318 g, 14%). $^{31}\text{P}\{^1\text{H}\}$ NMR (202 MHz, CD_2Cl_2) δ 237.3. ^1H NMR (500 MHz, CD_2Cl_2) δ 8.40 (ddt, $J = 7.6, 5.3, 1.0$ Hz, 1H), 8.22 (dq, $J = 8.1, 1.1$ Hz, 1H), 7.48 (ddt, $J = 8.3, 6.9, 1.4$ Hz, 1H), 7.41 (dddd, $J = 8.0, 7.0, 2.0, 1.1$ Hz, 1H), 0.52 – 0.48 (m, 9H). ^{13}C NMR (126 MHz, CD_2Cl_2) δ 178.5 (d, $J_{\text{PC}} = 76.4$ Hz), 156.6 (d, $J_{\text{PC}} = 49.3$ Hz), 154.5 (d, $J_{\text{PC}} = 8.5$ Hz), 130.7 (d, $J_{\text{PC}} = 25.9$ Hz), 126.6 (d, $J_{\text{PC}} = 3.0$ Hz), 124.0 (d, $J_{\text{PC}} = 12.5$ Hz), 123.6, 1.29 (d, $J_{\text{PC}} = 5.6$ Hz). HR-EIMS (m/z): $[\text{M}+\text{H}]^+$ calculated for $\text{C}_{10}\text{H}_{14}\text{P}_1\text{S}_1\text{Si}_1$: 225.0323; found 225.0325. Anal. Calcd. for $\text{C}_{10}\text{H}_{13}\text{P}_1\text{S}_1\text{Si}_1$: C, 53.54; H, 5.84. Found: C, 53.81; H, 5.68.

Synthesis of 2,3-dimethyl-4,4a-dihydro-1H-benzo[d]phosphinino[2,1-b][1,3]thiaphosphole

10-sulfide (3.5). 1,3-Benzothiaphosphole **3.1** was prepared according to the general procedure.

Three equivalents of 2,3-dimethyl-1,3-butadiene (0.60 mL, 5.28 mmol) were added by syringe to the reaction mixture and the flask was stirred at 65 °C for 24 h. Conversion to the Diels-Alder adduct could be monitored using $^{31}\text{P}\{^1\text{H}\}$ NMR spectroscopy. Upon completion, the reaction mixture was concentrated and chromatographed under N_2 on silica gel using degassed hexanes/dichloromethane (v/v 8:1) to afford the phosphine ($R_f \sim 0.55$) as a white crystalline solid (0.230 g, 56% yield). $^{31}\text{P}\{^1\text{H}\}$ NMR (202 MHz, CDCl_3): δ 4.1. The phosphine (0.230 g, 0.98 mmol) was placed in an oven-dried Schlenk flask and dissolved in 2 mL of chloroform. Elemental sulfur (0.047 g, 1.47 mmol) was added to the solution and the reaction was stirred overnight. The reaction mixture was concentrated and purified by chromatography on silica gel using hexanes/dichloromethane (v/v 3:1) to afford the title compound ($R_f \sim 0.55$) as a white crystalline solid (0.138 g, 53%, relative to the phosphine). $^{31}\text{P}\{^1\text{H}\}$ NMR (202 MHz, CD_2Cl_2) δ 71.4. ^1H NMR (500 MHz, CD_2Cl_2) δ 7.56 (app. t, $J = 9.2$ Hz, 1H), 7.37 (tt, $J = 7.7, 1.7$ Hz, 1H), 7.23 – 7.18 (m, 1H), 7.16 (dd, $J = 8.0, 2.9$ Hz, 1H), 3.81 (dt, $J = 10.1, 4.3$ Hz, 1H), 2.99 – 2.79 (m, 3H), 2.51 (ddd, $J = 30.1, 15.6, 4.3$ Hz, 1H), 1.77 (d, $J = 4.2$ Hz, 3H), 1.54 (s, 3H). ^{13}C NMR (126 MHz, CD_2Cl_2) δ 146.2 (d, $J_{\text{PC}} = 17.9$ Hz), 133.0 (d, $J_{\text{PC}} = 2.7$ Hz), 130.9 (d, $J_{\text{PC}} = 90.3$ Hz), 130.3 (d, $J_{\text{PC}} = 13.6$ Hz), 129.7 (d, $J_{\text{PC}} = 12.7$ Hz), 126.0 (d, $J_{\text{PC}} = 11.2$ Hz), 124.3 (d, $J_{\text{PC}} = 10.5$ Hz), 123.3 (d, $J_{\text{PC}} = 8.7$ Hz), 44.1 (d, $J_{\text{PC}} = 56.5$ Hz), 40.4 (d, $J_{\text{PC}} = 46.7$ Hz), 36.4 (d, $J_{\text{PC}} = 4.2$ Hz), 21.6 (d, $J_{\text{PC}} = 3.2$ Hz), 20.9 (d, $J_{\text{PC}} = 5.9$ Hz). HR-EIMS (m/z): $[\text{M}]^+$ calculated for $\text{C}_{13}\text{H}_{15}\text{P}_1\text{S}_2$: 266.0353; found 266.0353. Anal. Calcd. for $\text{C}_{13}\text{H}_{15}\text{P}_1\text{S}_2$: C, 58.62; H, 5.68. Found: C, 58.48; H, 5.67.

Synthesis of 2-methyl-4,4a-dihydro-1H-benzo[d]phosphinino[2,1-b][1,3]thiaphosphole 10-sulfide and 3-methyl-4,4a-dihydro-1H-benzo[d]phosphinino[2,1-b][1,3]thiaphosphole 10-

sulfide (3.6a, 3.6b). 1,3-Benzothiaphosphole **3.1** was prepared according to the general procedure. Five equivalents of isoprene (0.88 mL, 8.8 mmol) were added to the reaction mixture by syringe. The reaction was stirred at 65 °C for 5 days and at 6 h, 30 h, and 54 h, additional isoprene (0.88 mL) was added to the mixture. Conversion to the Diels-Alder adduct could be monitored using ^{31}P NMR spectroscopy. Upon completion, the reaction mixture was concentrated and chromatographed under N_2 on silica gel using degassed hexanes/dichloromethane (v/v 8:1) to afford the regioisomeric mixture ($R_f \sim 0.50$) as a colorless oil (0.154 g, 40% yield). $^{31}\text{P}\{^1\text{H}\}$ NMR (202 MHz, CDCl_3): δ -4.5 (major), -10.9 (minor). The phosphine (0.154 g, 0.70 mmol) was placed in an oven-dried 50 mL Schlenk flask and dissolved in 1.5 mL of chloroform. Elemental sulfur (0.034 g, 1.05 mmol) was added to the solution and the reaction was stirred overnight. The reaction mixture was concentrated and purified by chromatography on silica gel using hexanes/dichloromethane (v/v 3:1) to obtain the title compound ($R_f \sim 0.45$) as a mixture of regioisomers (viscous oil, 0.144 g, 82% yield, relative to the phosphine). Major and minor isomers were in a 75:25 ratio, as determined by integration of the vinyl C-H signals. **Major:** $^{31}\text{P}\{^1\text{H}\}$ NMR (202 MHz, CD_2Cl_2) δ 63.4. Aromatic signals of major and minor isomer are superimposed. ^1H NMR (500 MHz, CD_2Cl_2) δ 7.63 – 7.56 (m, 1H), 7.42 – 7.37 (m, 1H), 7.27 – 7.23 (m, 1H), 7.23 – 7.18 (m, 1H), 5.69 – 5.64 (m, 1H), 3.88 (dt, $J = 10.3, 4.3$, 1H), 3.01 – 2.91 (m, 1H), 2.91 – 2.84 (m, 1H), 2.75 – 2.65 (m, 2H), 1.69 (s, 3H). ^{13}C NMR (126 MHz, CD_2Cl_2) δ 145.0 (d, $J_{\text{PC}} = 18.5$ Hz), 137.8 (d, $J_{\text{PC}} = 15.6$ Hz, overlapping with minor isomer), 133.2 (d, $J_{\text{PC}} = 2.8$ Hz), 131.5 (d, $J_{\text{PC}} = 91.2$ Hz, overlapping with minor isomer), 130.1 (d, $J_{\text{PC}} = 12.6$ Hz), 126.2 (d, $J_{\text{PC}} = 11.0$ Hz, overlapping signal with minor isomer), 124.0 (d, $J_{\text{PC}} = 8.7$ Hz), 121.8 (d, $J_{\text{PC}} = 14.5$ Hz), 43.8 (d, $J_{\text{PC}} = 53.6$ Hz), 37.4 (d, $J_{\text{PC}} = 47.9$ Hz), 27.9 (d, $J_{\text{PC}} = 4.0$ Hz), 25.5 (d, $J_{\text{PC}} = 7.7$ Hz). **Minor:** $^{31}\text{P}\{^1\text{H}\}$ NMR (202 MHz, CD_2Cl_2) δ 63.1. Aromatic signals of major and minor isomer are

superimposed. ^1H NMR (500 MHz, CD_2Cl_2) δ 7.63 – 7.56 (m, 1H), 7.42-7.37 (m, 1H), 7.27 – 7.23 (m, 1H), 7.23 – 7.18 (m, 1H) δ 5.52 (dtt, $J = 17.9, 5.2, 1.7$ Hz, 1H), 3.96 (dt, $J = 10.5, 4.2$ Hz, 1H), 3.06 – 3.00 (m, 1H), 2.64 – 2.56 (m, 2H), 2.56 – 2.48 (m, 1H), 1.82 (s, 3H). ^{13}C NMR (126 MHz, CD_2Cl_2) δ 145.1 (d, $J_{\text{PC}} = 17.8$ Hz), 137.8 (d, $J_{\text{PC}} = 15.6$ Hz, overlapping with major isomer), 132.8 (d, $J_{\text{PC}} = 8.8$ Hz), 131.5 (d, $J_{\text{PC}} = 91.0$ Hz, overlapping with major isomer), 130.4 (d, $J_{\text{PC}} = 12.4$ Hz), 126.2 (d, $J_{\text{PC}} = 11.0$ Hz, overlapping with major isomer), 123.8 (d, $J_{\text{PC}} = 8.6$ Hz), 116.9 (d, $J_{\text{PC}} = 10.2$ Hz), 44.2 (d, $J_{\text{PC}} = 53.1$ Hz), 33.3 (d, $J_{\text{PC}} = 48.5$ Hz), 32.4 (d, $J_{\text{PC}} = 4.3$ Hz), 25.6 (d, $J_{\text{PC}} = 2.7$ Hz). HR-EIMS (m/z): $[\text{M}]^+$ calculated for $\text{C}_{12}\text{H}_{13}\text{P}_1\text{S}_2$: 252.0196; found: 252.0197. Anal. Calcd. for $\text{C}_{12}\text{H}_{13}\text{P}_1\text{S}_2$: C, 57.12; H, 5.19. Found: C, 57.03; H, 5.13.

Synthesis of 2,3-dibenzyl-4,4a-dihydro-1H-benzo[d]phosphinino[2,1-b][1,3]thiaphosphole 10-sulfide (3.7). The 1,3-benzothiaphosphole **3.1** was prepared according to the general procedure. 2,3-dibenzyl-1,3-butadiene (0.62 g, 2.64 mmol) was dissolved in 5 mL toluene in a separate 25 mL oven-dried Schlenk flask and cannula transferred to the benzothiaphosphole reaction mixture. The reaction mixture was stirred at 85 °C for 5 d. Conversion to the Diels-Alder adduct could be monitored using ^{31}P NMR spectroscopy. Upon completion, the reaction mixture was concentrated and chromatographed under N_2 on silica gel using degassed hexanes/dichloromethane (v/v 10:1) to afford the phosphine ($R_f \sim 0.50$) as a clear viscous oil (0.252 g, 37% yield). $^{31}\text{P}\{^1\text{H}\}$ NMR (202 MHz, CDCl_3): δ 5.2. The phosphine (0.252 g, 0.65 mmol) was placed in an oven-dried Schlenk flask and dissolved in 1.5 mL of chloroform. Elemental sulfur (0.031 g, 0.98 mmol) was added to the solution and the reaction was stirred overnight. The reaction mixture was concentrated and purified by chromatography on silica gel using hexanes/dichloromethane (v/v 3:1) to afford the title compound ($R_f \sim 0.52$) as a waxy white solid (0.216 g, 79%, relative to the phosphine). The compound contained residual hexanes even after concentration *in vacuo* for 12 h at 100 mTorr.

$^{31}\text{P}\{^1\text{H}\}$ NMR (202 MHz, CD_2Cl_2) δ 71.7. ^1H NMR (500 MHz, CD_2Cl_2) δ 7.36 (tt, $J = 7.6, 1.7$ Hz, 1H), 7.33 – 7.27 (m, 3H), 7.27 – 7.21 (m, 1H), 7.18 – 7.10 (m, 6H), 7.06 (tdd, $J = 7.5, 3.3, 0.9$ Hz, 1H), 6.99 – 6.94 (m, 2H), 3.89 (d, $J = 15.1$ Hz, 1H), 3.78 (dt, $J = 11.0, 4.5$ Hz, 1H), 3.57 – 3.40 (m, 3H), 3.01 (dd, $J = 16.0, 12.6$ Hz, 1H) 2.93 – 2.78 (m, 2H), 2.58 (ddd, $J = 30.0, 15.6, 4.8$ Hz, 1H). ^{13}C NMR (126 MHz, CD_2Cl_2) δ 145.8 (d, $J_{\text{PC}} = 18.7$ Hz), 139.2 (d, $J_{\text{PC}} = 3.2$ Hz) 138.6 (d, $J_{\text{PC}} = 1.4$ Hz), 134.5 (d, $J_{\text{PC}} = 12.4$ Hz), 133.1 (d, $J_{\text{PC}} = 2.7$ Hz), 130.4 (d, $J_{\text{PC}} = 90.2$ Hz), 129.8 (d, $J_{\text{PC}} = 12.4$ Hz) 129.5, 129.4 (d, $J_{\text{PC}} = 10.4$ Hz), 129.2, 129.1, 129.1 (overlapping signals), 127.0, 126.8, 126.2 (d, $J_{\text{PC}} = 11.2$ Hz), 123.3 (d, $J_{\text{PC}} = 9.0$ Hz), 43.9 (d, $J_{\text{PC}} = 54.7$ Hz), 41.0 (d, $J_{\text{PC}} = 2.8$ Hz), 40.3 (d, $J_{\text{PC}} = 5.5$ Hz), 38.6 (d, $J_{\text{PC}} = 46.9$ Hz), 34.4 (d, $J_{\text{PC}} = 4.1$ Hz). HRMS (ESI-TOF) (m/z): $[\text{M}+\text{H}]^+$ calculated for $\text{C}_{25}\text{H}_{24}\text{P}_1\text{S}_2$: 419.1057; found: 419.1052. Anal. Calcd. for $\text{C}_{25}\text{H}_{23}\text{P}_1\text{S}_2$: C, 71.74; H, 5.54. Found: C, 71.37; H, 5.79.

Synthesis of endo/exo 1,4,4a-trihydro-1,4-methanobenzo[*d*]phosphinino[2,1-*b*][1,3]thiaphosphole 10-sulfide (3.8). The 1,3-benzothiaphosphole **3.1** was prepared according to the general procedure. Cyclopentadiene (0.45 mL, 5.35 mmol) was added to the reaction vessel by syringe. The reaction was stirred at 60 °C and after 6 h, a second portion of cyclopentadiene was added (0.45 mL, 5.35 mmol). Conversion to the Diels-Alder adduct could be monitored using ^{31}P NMR spectroscopy. Upon completion, the reaction mixture was concentrated and chromatographed under N_2 on silica gel using a gradient mobile phase (degassed hexanes/dichloromethane v/v 6:1 to 2:1) to afford the phosphine as a yellow oil (0.120 g, 31% yield). $^{31}\text{P}\{^1\text{H}\}$ NMR (202 MHz, CDCl_3): δ 29.9 (endo), 23.3 (exo). The phosphine mixture (0.120 g, 0.55 mmol) was placed in an oven-dried Schlenk flask and dissolved in 1 mL of chloroform. Elemental sulfur (0.027 g, 0.84 mmol) was added to the solution and the reaction was stirred overnight. The reaction mixture was concentrated and purified by chromatography on silica gel

using hexanes/dichloromethane (v/v 3:1) to obtain the title compound ($R_f \sim 0.50$) as a mixture of endo/exo isomers (white solid, 0.132 g, 96% yield relative to the phosphine). Endo:Exo, 78:22 as determined by integration of the vinyl C-H signals. **Endo:** $^{31}\text{P}\{^1\text{H}\}$ NMR (202 MHz, CD_2Cl_2) δ 94.7. ^1H NMR (500 MHz, CD_2Cl_2) δ 7.67 – 7.61 (m, 1H), 7.36 (tt, $J = 7.6, 1.9$ Hz, 1H), 7.22 – 7.16 (m, 1H, overlapping with 1 aromatic signal from exo isomer), 7.10 (dd, $J = 8.1, 3.1$ Hz, 1H), 6.15 (ddd, $J = 8.5, 5.7, 2.9$ Hz, 1H), 5.59 (dt, $J = 6.2, 3.3$ Hz, 1H), 3.59 (dd, $J = 7.9, 4.8$ Hz, 1H), 3.54 – 3.47 (m, 1H), 3.45 (td, $J = 3.1, 1.1$ Hz, 1H), 2.41 (dd, $J = 11.0, 5.5$ Hz, 1H), 2.20 (ddt, $J = 33.2, 11.0, 2.8$ Hz, 1H). ^{13}C NMR (126 MHz, CD_2Cl_2) δ 148.7 (d, $J_{\text{PC}} = 16.5$ Hz), 135.7 (d, $J_{\text{PC}} = 12.0$ Hz), 133.1 (d, $J_{\text{PC}} = 2.7$ Hz), 132.7 (d, $J_{\text{PC}} = 13.2$ Hz), 130.0 (d, $J_{\text{PC}} = 13.1$ Hz), 129.7 (d, $J_{\text{PC}} = 91.5$ Hz) 125.5 (d, $J_{\text{PC}} = 11.4$ Hz), 123.5 (d, $J_{\text{PC}} = 8.7$ Hz), 52.8 (d, $J_{\text{PC}} = 40.5$ Hz), 48.0 (d, $J_{\text{PC}} = 2.8$ Hz), 45.4 (d, $J_{\text{PC}} = 65.0$ Hz), 44.4 (d, $J_{\text{PC}} = 12.9$ Hz). **Exo:** $^{31}\text{P}\{^1\text{H}\}$ NMR (202 MHz, CD_2Cl_2) δ 90.5. ^1H NMR (500 MHz, CD_2Cl_2) δ 7.74 – 7.69 (m, 1H), 7.43 (tt, $J = 7.7, 1.7$ Hz, 1H), 7.25 (tdd, $J = 7.5, 3.2, 1.0$ Hz, 1H), 7.22 – 7.20 (m, 1H, overlapping with 1H of the endo product), 6.42 (dt, $J = 6.2, 3.4$ Hz, 1H), 6.31 (ddd, $J = 8.1, 5.6, 3.0$ Hz, 1H), 3.43 – 3.38 (m, 1H), 3.38 – 3.35 (m, 1H) 3.25 (ddd, $J = 8.9, 2.9, 1.3$ Hz, 1H), 1.95 (ddq, $J = 38.8, 11.3, 2.9$ Hz, 1H), 1.77 (dd, $J = 11.3, 5.4$ Hz, 1H). ^{13}C NMR (126 MHz, CD_2Cl_2) δ 147.3 (d, $J_{\text{PC}} = 18.1$ Hz), 136.9 (d, $J_{\text{PC}} = 11.8$ Hz), 134.1 (d, $J_{\text{PC}} = 13.0$ Hz), 133.5 (d, $J_{\text{PC}} = 2.7$ Hz), 130.1 (d, $J_{\text{PC}} = 13.1$ Hz), 129.7 (d, $J_{\text{PC}} = 81.4$ Hz), 125.9 (d, $J_{\text{PC}} = 10.9$ Hz), 124.0 (d, $J_{\text{PC}} = 8.1$ Hz), 53.7 (d, $J_{\text{PC}} = 23.8$ Hz), 50.7 (d, $J_{\text{PC}} = 40.9$ Hz), 44.9 (d, $J_{\text{PC}} = 69.1$ Hz), 41.9 (d, $J_{\text{PC}} = 14.4$ Hz). HR-EIMS (m/z): $[\text{M}]^+$ calculated for $\text{C}_{12}\text{H}_{11}\text{P}_1\text{S}_2$: 250.0040; found: 250.0037. Anal. Calcd. for $\text{C}_{12}\text{H}_{11}\text{P}_1\text{S}_2$: C, 57.58; H, 4.43. Found: C, 57.95; H, 4.09.

Crystallographic Information

Table 3.1. Crystallographic details for compound **3.5**.

Compound 5			
Formula	C ₁₃ H ₁₅ PS ₂	Absorption coefficient, mm ⁻¹	0.500
Color	Colorless	F(000)	560
Shape	Rhomboid	Diffractometer	Bruker Smart Apex II
Formula Weight	266.34	Radiation, monochr.	graphite Mo K α (λ = 0.71073 Å)
Crystal System	Monoclinic	Crystal size, mm	0.48 × 0.30 × 0.15
Space Group	<i>P</i> 2 ₁ / <i>c</i>	θ range, deg	2.4 < θ < 33.2
Temp (K)	149 (2)	Range of h,k,l	-12, 13, -21, 22, \pm 16
a, Å	8.7462 (18)	Reflections collected/unique	17121/ 4709
b, Å	14.667 (3)	Rint	0.057
c, Å	10.868 (2)	Refinement Method	Full Matrix Least-Squares on F ²
α , deg	90	Data/Restraints/Parameters	4709/ 0/ 147
β , deg	110.551 (3)	GOF on F ²	1.13
γ , deg	90	Final R indices [<i>I</i> > 2 σ (<i>I</i>)]	0.0410
V, Å ³	1305.5 (5)	R indices (all data)	0.141
Formula units/unit cell	4	Max. Resid. Peaks (e ⁻ Å ⁻³)	0.71 and -0.92
Dcal'd, gcm ⁻³	1.355		

3.5 References

1. (a) *Phosphorus-Carbon Heterocyclic Chemistry : The Rise of A New Domain*; Mathey, F., Ed.; Elsevier Science Ltd.: Amsterdam; New York, 2001. (b) Nyulászi, L. *Chem. Rev.* **2001**, *101*, 1229-1246. (c) Bansal, R. K.; Heinicke, J. *Chem. Rev.* **2001**, *101*, 3549-3578.
2. Katritzky, A. R.; Ramsden, C. A.; Joule, J. A.; Zhdankin, V. V. *Handbook of Heterocyclic Chemistry*; 3rd ed.; Elsevier: Amsterdam, 2010.
3. (a) Pfeifer, G.; Ribagnac, P.; Le Goff, X. F.; Wiecko, J.; Mézailles, N.; Müller, C. *Eur. J. Inorg. Chem.* **2015**, 240-249. (b) Bruce, M.; Meissner, G.; Weber, M.; Wiecko, J.; Müller, C. *Eur. J. Inorg. Chem.* **2014**, 1719-1726. (c) Kostenko, N.; Ericsson, C.; Engqvist, M.; Gonzalez, S. V.; Bayer, A. *Eur. J. Org. Chem.* **2013**, 4756-4759. (d) Mao, Y.; Mathey, F. *Org. Lett.* **2012**, *14*, 1162-1163. (e) Waschbusch, K.; Le Floch, P.; Mathey, F. *Organometallics* **1996**, *15*, 1597-1603. (f) Trauner, H.; Le Floch, P.; Lefour, J.-M.; Ricard, L.; Mathey, F. *Synthesis* **1995**, 717-726. (g) Le Floch, P.; Carmichael, D.; Ricard, L.; Mathey, F. *J. Am. Chem. Soc.* **1993**, *115*, 10665-10670. (h) Le Floch, P.; Carmichael, D.; Mathey, F. *Organometallics* **1991**, *10*, 2432-2436.
4. (a) Ghalib, M.; Jones, P. G.; Lysenko, S.; Heinicke, J. W. *Organometallics* **2014**, *33*, 804-816. (b) Heinicke, J.; Aluri, B. R.; Niaz, B.; Burck, S.; Gudat, D.; Niemeyer, M.; Holloczki, O.; Nyulászi, L.; Jones, P. G. *Phosphorus, Sulfur Silicon Relat. Elem.* **2011**, *186*, 683-687. (c) Aluri, B. R.; Burck, S.; Gudat, D.; Niemeyer, M.; Holloczki, O.; Nyulászi, L.; Jones, P. G.; Heinicke, J. *Chem.–Eur. J.* **2009**, *15*, 12263-12272. (d) Aluri, B. R.; Kindermann, M. K.; Jones, P. G.; Heinicke, J. *Chem.–Eur. J.* **2008**, *14*, 4328-4335. (e) Heinicke, J.; Steinhauser, K.; Peulecke, N.; Spannenberg, A.; Mayer, P.; Karaghiosoff, K. *Organometallics* **2002**, *21*, 912-919. (f) Heinicke, J.; Tzschach, A. *Tetrahedron Lett.* **1982**, *23*, 3643-3646.

5. (a) Qiu, Y.; Worch, J. C.; Chirdon, D. N.; Kaur, A.; Maurer, A. B.; Amsterdam, S.; Collins, C. R.; Pintauer, T.; Yaron, D.; Bernhard, S.; Noonan, K. J. T. *Chem.–Eur. J.* **2014**, *20*, 7746-7751. (b) Worch, J. C.; Chirdon, D. N.; Mauer, A. B.; Qiu, Y.; Geib, S. J.; Bernhard, S.; Noonan, K. J. T. *J. Org. Chem.* **2013**, *78*, 7462-7469.
6. (a) Wu, S.; Rheingold, A. L.; Protasiewicz, J. D. *Chem. Commun.* **2014**, *50*, 11036-11038. (b) Wu, S.; Deligonal, N.; Protasiewicz, J. D. *Dalton Trans.* **2013**, *42*, 14866-14874. (c) Simpson, M. C.; Protasiewicz, J. D. *Pure Appl. Chem.* **2013**, *85*, 801-815. (d) Laughlin, F. L.; Deligonul, N.; Rheingold, A. L.; Golen, J. A.; Laughlin, B. J.; Smith, R. C.; Protasiewicz, J. D. *Organometallics* **2013**, *32*, 7116-7121. (e) Laughlin, F. L.; Rheingold, A. L.; Deligonul, N.; Laughlin, B. J.; Smith, R. C.; Higham, L. J.; Protasiewicz, J. D. *Dalton Trans.* **2012**, *41*, 12016-12022. (f) Washington, M. P.; Gudimetla, V. B.; Laughlin, F. L.; Deligonul, N.; He, S.; Payton, J. L.; Simpson, M. C.; Protasiewicz, J. D. *J. Am. Chem. Soc.* **2010**, *132*, 4566-4567.
7. Issleib, K.; Vollmer, R. *Tetrahedron Lett.* **1980**, *21*, 3483-3484.
8. (a) Ashe III, A. J.; Fang, X. *Chem. Commun.* **1999**, 1283-1284. (b) Märkl, G.; Eckl, E.; Jakobs, U.; Ziegler, M. L.; Nuber, B. *Tetrahedron Lett.* **1987**, *28*, 2119-2122.
9. (a) Appel, R.; Knoll, F.; Ruppert, I. *Angew. Chem., Int. Ed. Engl.* **1981**, *20*, 731-744. (b) Appel, R.; Kundgen, U. *Angew. Chem., Int. Ed. Engl.* **1982**, *21*, 219-220.
10. Heinicke, J. *Trends in Organomet. Chem.* **1994**, *1*, 307-322.
11. Moores, A.; Ricard, L.; Le Floch, P. *Angew. Chem., Int. Ed.* **2003**, *42*, 4940-4944.
12. Heinicke, J.; Tzschach, A. *Phosphorus, Sulfur Silicon Relat. Elem.* **1984**, *20*, 347-356.
13. Schlosser, M.; Strunk, S. *Tetrahedron Lett.* **1984**, *25*, 741-744.
14. Le Floch, P.; Ricard, L.; Mathey, F. *Polyhedron* **1990**, *9*, 991-997.
15. Le Floch, P. *Coord. Chem. Rev.* **2006**, *250*, 627-681.

16. Bansal, R. K.; Kumawat, S. K. *Tetrahedron* **2008**, *64*, 10945-10976.
17. Zon, G.; Debruin, K. E.; Naumann, K.; Mislow, K. *J. Am. Chem. Soc.* **1969**, *91*, 7023-7027.
18. Heinicke, J.; Tzschach, A. *Tetrahedron Lett.* **1983**, *24*, 5481-5484.
19. (a) Gil, R. R.; Griesinger, C.; Navarro-Vázquez, A.; Sun, H. In *Structure Elucidation in Organic Chemistry: The Search for the Right Tools*; Cid, M.-M., Bravo, J., Eds.; Wiley-VCH: Weinheim, Germany, 2015, 279-324. (b) Gil, R. R. *Angew. Chem., Int. Ed.* **2011**, *50*, 7222-7224. (c) Kummerlöwe, G.; Luy, B. *Annu. Rep. NMR Spectrosc.* **2009**, *68*, 193-230. (d) Thiele, C. M. *Eur. J. Org. Chem.* **2008**, 5673-5685.
20. Losonczi, J. A.; Andrec, M.; Fischer, M. W. F.; Prestegard, J. H. *J. Magn. Reson.* **1999**, *138*, 334-342.
21. (a) Gayathri, C.; Tsarevsky, N. V.; Gil, R. R. *Chem.–Eur. J.* **2010**, *16*, 3622-3626. (b) Gil, R. R.; Gayathri, C.; Tsarevsky, N. V.; Matyjaszewski, K. *J. Org. Chem.* **2008**, *73*, 840-848.
22. (a) Bansal, R. K.; Gupta, N.; Kumawat, S. K. *Tetrahedron* **2006**, *62*, 1548-1556. (b) Bansal, R. K.; Gupta, N.; Kumawat, S. K.; Gupta, R. *Heteroatom Chem.* **2006**, *17*, 402-410. (c) Bansal, R. K.; Karaghiosoff, K.; Gupta, N.; Gandhi, N.; Kumawat, S. K. *Tetrahedron* **2005**, *61*, 10521-10528. (d) Wannere, C. S.; Bansal, R. K.; Schleyer, P. v. R. *J. Org. Chem.* **2002**, *67*, 9162-9174.
23. Kyba, E. P.; Clubb, C. N. *Inorg. Chem.* **1984**, *23*, 4766-4768.
24. Panne, P.; Fox, J. M. *J. Am. Chem. Soc.* **2007**, *129*, 22-23.
25. Frisch, M. J.; Trucks, G. W.; Schlegel, H. B.; Scuseria, G. E.; Robb, M. A.; Cheeseman, J. R.; Montgomery, J. A. Jr.; Vreven, T.; Kudin, K. N.; Burant, J. C.; Millam, J. M.; Iyengar, S. S.; Tomasi, J.; Barone, V.; Mennucci, B.; Cossi, M.; Scalmani, G.; Rega, N.; Petersson, G. A.; Nakatsuji, H.; Hada, M.; Ehara, M.; Toyota, K.; Fukuda, R.; Hasegawa, J.; Ishida, M.; Nakajima, T.; Honda, Y.; Kitao, O.; Nakai, H.; Klene, M.; Li, X.; Knox, J. E.; Hratchian, H. P.; Cross, J. B.;

Bakken, V.; Adamo, C.; Jaramillo, J.; Gomperts, R.; Stratmann, R. E.; Yazyev, O.; Austin, A. J.; Cammi, R.; Pomelli, C.; Ochterski, J. W.; Ayala, P. Y.; Morokuma, K.; Voth, G. A.; Salvador, P.; Dannenberg, J. J.; Zakrzewski, V. G.; Dapprich, S.; Daniels, A. D.; Strain, M. C.; Farkas, O.; Malick, D. K.; Rabuck, A. D.; Raghavachari, K.; Foresman, J. B. ; Ortiz, J. V.; Cui, Q.; Baboul, A. G.; Clifford, S.; Cioslowski, J.; Stefanov, B. B.; Liu, G.; Liashenko, A.; Piskorz, P.; Komaromi, I.; Martin, R. L.; Fox, D. J.; Keith, T.; Al-Laham, M. A.; Peng, C. Y.; Nanayakkara, A.; Challacombe, M.; Gill, P. M. W.; Johnson, B.; Chen, W.; Wong, M. W.; Gonzalez, C.; Pople, J. A. *Gaussian 03, Revision E.01*; Gaussian, Inc., Wallingford CT, 2004.

26. Navarro-Vázquez, A. *Magn. Reson. Chem.* **2012**, *50*, S73-S79.

27. Cornilescu, G.; Marquardt, J. L.; Ottiger, M.; Bax, A. *J. Am. Chem. Soc.* **1998**, *120*, 6836-6837.

Chapter 4♦

Nickel Catalyzed Suzuki Polycondensation for Controlled Synthesis of Ester-Functionalized Conjugated Polymers

4.1 Introduction

Rational design of catalysts and monomers has been crucial in the development of precision polymerization protocols – affording materials with control over size, topology, and functionality.¹ Catalyst-transfer polycondensation (CTP) in particular, is used to prepare well-defined π -conjugated polymer materials.² However, the highly reactive monomers typically employed in CTP (e.g, organomagnesium or organozinc reagents) often limit the selection of solubilizing substituents tethered to the aromatic ring (Figure 4.1). The substituents appended to any π -conjugated backbone not only impart solubility, but are also crucial for tuning the chemical and physical properties of the desired polymer.³ The combination of side chain engineering with controlled polymerization will afford a wide range of new π -conjugated architectures where electronic structure and physical properties can be manipulated along with shape, size and solid-state organization.

Beyond Kumada and Negishi cross-coupling, Stille and Suzuki-Miyaura cross-coupling reactions have also attracted attention to prepare conjugated polymers with controlled molecular weights and narrow molecular weight distributions.⁴ The lower nucleophilicity of the SnMe_3 and

♦ Reproduced with permission from Qiu, Y.; Worch, J.C.; (co-first author) Fortney, A.; Gayathri, C.; Gil, R.R.; Noonan, K.J.T. Nickel Catalyzed Suzuki Polycondensation for Controlled Synthesis of Ester-Functionalized Conjugated Polymers. *Macromolecules* **2016**, 49, 4757–4762. Copyright 2016 American Chemical Society.

B(OR)₂ transmetalating agents (Figure 4.1) make these methods well-suited to enhance the substrate scope of CTP. Controlled polycondensations with these transmetalating agents are generally achieved using a Pd catalyst paired with a bulky σ -donating phosphine ligand (P^tBu₃) or an *N*-heterocyclic carbene (NHC).⁵ However, there is an interest to explore Ni catalysts for Stille and Suzuki CTP due to the lower cost as compared to Pd, and the facile oxidative addition observed with a diverse range of pseudo-halides or non-activated halides.⁶ Additionally, the chain-growth mechanism for conjugated polymers is proposed to occur via a catalyst polymer π -complex to facilitate intramolecular oxidative addition at the polymer chain-end. The stronger Ni binding interaction as compared to Pd may be important for achieving enhanced control in chain-growth polymerizations.⁷

Ni-catalyzed Suzuki cross-coupling to form biaryl compounds has been reported with relatively mild reaction conditions and moderate catalyst loadings.^{6c} This led us to investigate the possibility of Suzuki CTP with π -accepting ester groups as the side chain substituent. We chose the ester moiety since it can increase the ambient stability of polythiophene,⁸ and can also be exploited in post-polymerization modification.⁹

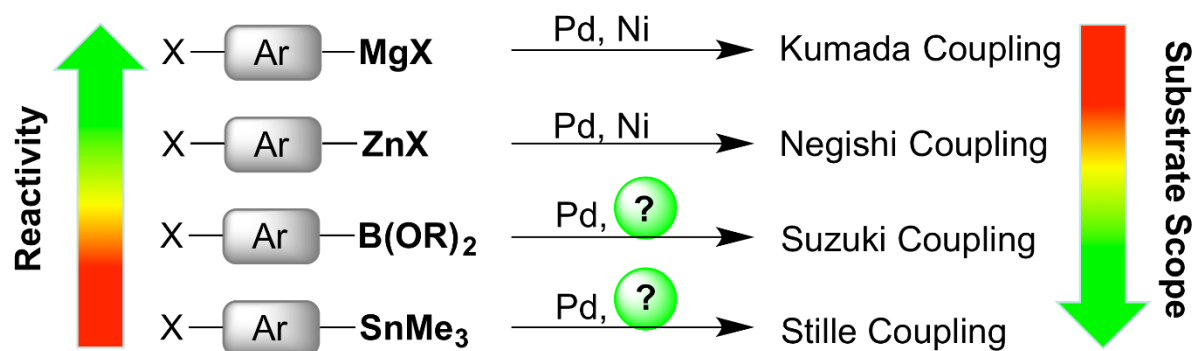


Figure 4.1. Cross-coupling methods used in catalyst-transfer polycondensation.

To our knowledge, CTP with π -accepting groups in conjugation with the monomer is unknown, though protection-deprotection strategies have been employed to synthesize similar

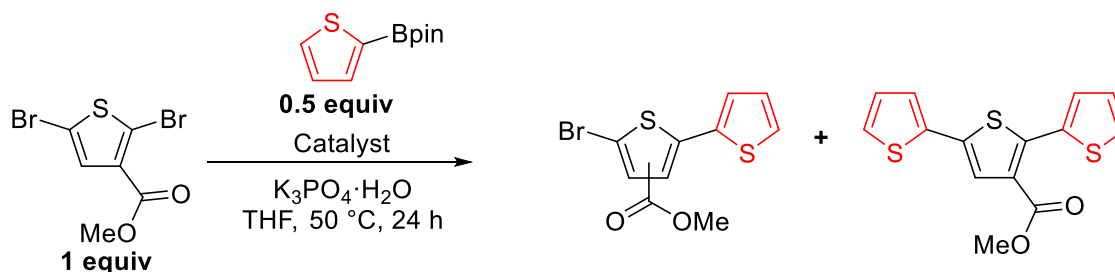
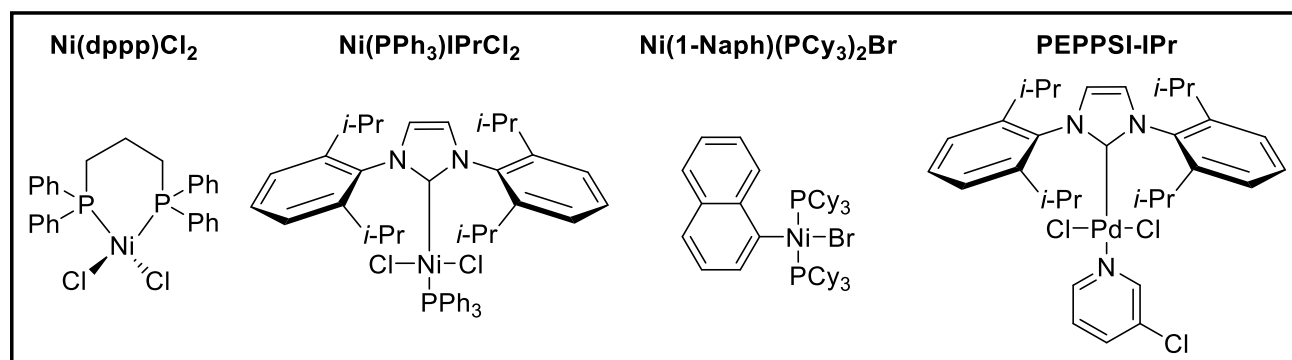
polymers.¹⁰ We used model compound studies to determine if hexyl thiophene-3-carboxylate was a suitable monomer for polycondensation. These experiments were then used as a guide for polymerization of the ester-functionalized thiophene. Finally, alternating and block copolymers of hexyl thiophene-3-carboxylate and 3-hexylthiophene were synthesized and characterized.

4.2 Results and Discussion

We first explored three nickel catalysts to couple methyl-2,5-dibromothiophene-3-carboxylate and thiophene-2-boronic acid pinacol ester (ThBpin). Ni(PPh₃)IPrCl₂ and Ni(dppp)Cl₂ were selected since both have been successful in Kumada CTP,¹¹ while Ni(1-Naph)(PCy₃)₂Br has been successfully used in Suzuki cross-coupling to form biaryl compounds.¹² Only half an equivalent of the ThBpin was used to explore whether intramolecular oxidative addition is favored and if terthiophene formation is preferred. Similar studies have been used previously to provide indirect evidence for metal π -complex formation with the substrate.^{11b}

The catalysts were screened initially at moderate loadings (5 mol %) and all reactions were conducted for 24 h. All three nickel catalysts: Ni(PPh₃)IPrCl₂, Ni(1-Naph)(PCy₃)₂Br and Ni(dppp)Cl₂ afforded the terthiophene with greater than 90% selectivity and high conversion (Table 4.1, entries 1, 3 and 5). This suggested the nickel systems have potential in Suzuki CTP with π -accepting groups. When lower catalyst loadings (1 mol %) were explored, Ni(PPh₃)IPrCl₂ and Ni(dppp)Cl₂ retained good selectivity, though complete consumption of the ThBpin was not observed with Ni(dppp)Cl₂ (Table 4.1, entry 6). By contrast, a marked decrease in conversion and selectivity was observed with 1 mol % Ni(1-Naph)(PCy₃)₂Br (Table 4.1, entry 4). Similar catalyst loading limitations with this type of catalyst have been noted previously^{12b} and suggest potential complications in polymerization.

Table 4.1. Model compound reactions with methyl 2,5-dibromothiophene-3-carboxylate.



Entry	Catalyst (mol %) ^a	% Conv. GC-MS ^b	% Terthiophene GC-MS (NMR) ^c
1	Ni(PPh ₃)IPrCl ₂ (5)	99	99 (99)
2	Ni(PPh ₃)IPrCl ₂ (1)	99	99 (99)
3	Ni(1-Naph)(PCy ₃) ₂ Br (5)	99	94 (97)
4	Ni(1-Naph)(PCy ₃) ₂ Br (1)	72	44 (72)
5	Ni(dppp)Cl ₂ (5)	99	95 (96)
6	Ni(dppp)Cl ₂ (1)	82	97 (95)
7	PEPPSI-IPr (5)	99	52 (72)
8	PEPPSI-IPr (1)	99	64 (78)

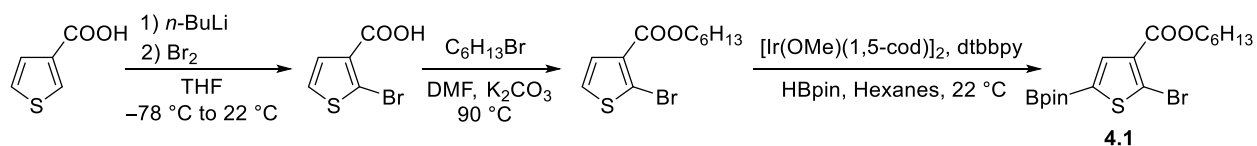
^aRelative to ThBpin. ^bConversion of ThBpin was determined by GC-MS using trimethoxybenzene as the internal standard. ^cRelative ratio of products determined via GC-MS and ¹H NMR spectroscopy.

A Pd-NHC precatalyst (PEPPSI-IPr), was also explored in these model compound studies (Table 4.1, entries 7 and 8) for comparison with Ni(PPh₃)IPrCl₂. PEPPSI-IPr produced good conversion at either 5 or 1 mol % loading, but selectivity for the terthiophene product was lower than that observed with Ni(PPh₃)IPrCl₂. This type of comparison though informative, should be

used with caution since the other ligands (3-chloropyridine for Pd and PPh₃ for Ni) may not be innocent in the catalytic cycle.¹³ To further probe the limits of the Ni-NHC catalyst,¹⁴ two separate experiments were conducted: one at 65 °C and one with a larger deficiency of the ThBpin (5:1 ratio, carboxylate:ThBpin). Greater than 90% selectivity for the terthiophene was still observed in both cases, suggesting this catalyst is highly suited for exploration in CTP with the ester-functionalized thiophene.

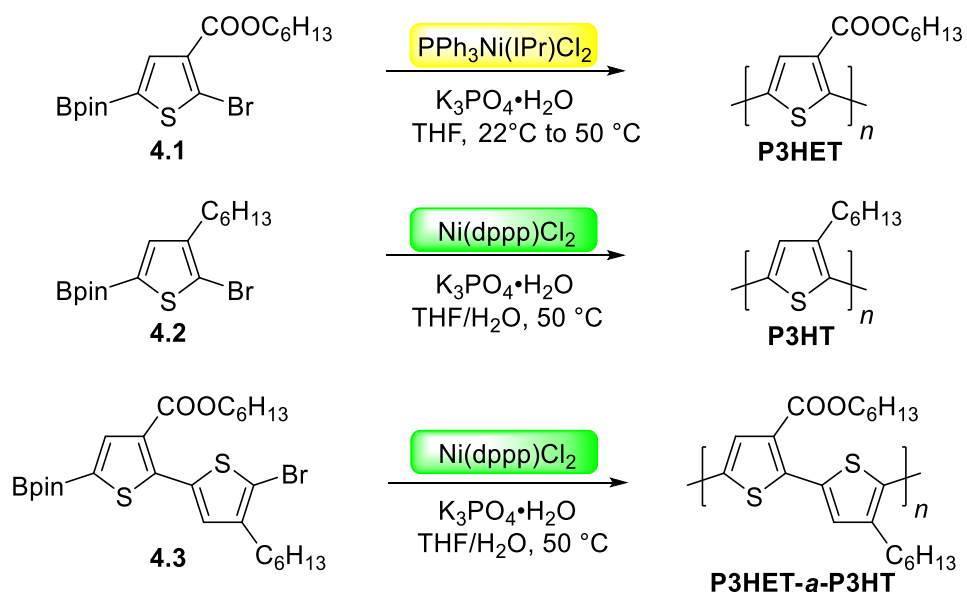
Poly(hexylthiophene-3-carboxylate) referred to as poly(3-hexylesterthiophene) (P3HET) has been prepared previously.¹⁵ However, to our knowledge, progress on the controlled synthesis of this polymer has not been reported.¹⁶ Additionally, most reports of these materials have not proceeded to higher molecular weights until recently, when a direct arylation protocol was employed.^{15a} The Suzuki monomer (**4.1**) used in this study was prepared using a three-step synthesis starting from 3-thiophenecarboxylic acid (Scheme 4.1). Borylation of the thiophene ring with pinacolborane was achieved using an iridium-catalyzed C-H borylation reaction.¹⁷

Scheme 4.1. Preparation of monomer **4.1**.



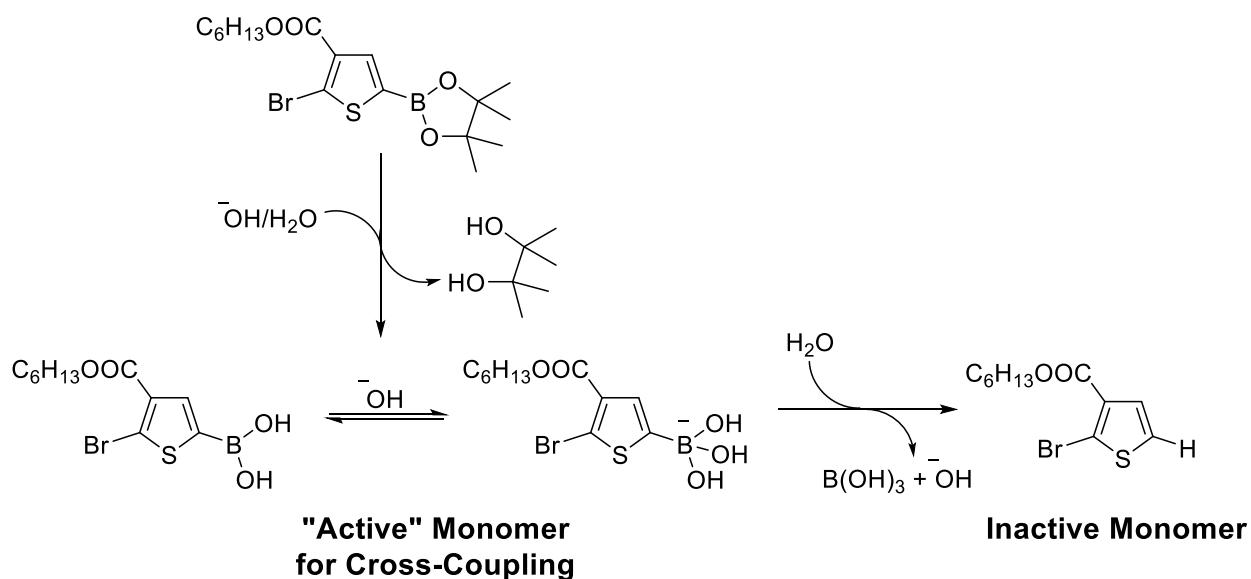
Polymerization of monomer **4.1** proceeded smoothly in THF with Ni(PPh₃)IPrCl₂ and K₃PO₄·H₂O (Scheme 4.2). A previous report from Yokozawa and coworkers on Pd-catalyzed Suzuki CTP indicated that added water was essential in promoting the controlled synthesis of poly(3-hexylthiophene) (P3HT).¹⁸ Interestingly, the water from the K₃PO₄·H₂O is sufficient to promote the controlled reaction for monomer **4.1**.

Scheme 4.2. Polymers prepared using nickel-catalyzed Suzuki CTP.



When additional water is added to the polymerization reaction, low conversion and lower molecular weight materials are obtained which we suspect is due to competitive protodeborylation.¹⁹

Scheme 4.3. Hydrolysis of starting monomer to the active boronic acid species with competitive protodeborylation mechanism.



Stability issues of 2-heterocyclic boronic acids are known,²⁰ particularly those containing electron withdrawing groups.²¹ Although boronic esters are more stable than the corresponding boronic acids, under Suzuki conditions, base-catalyzed hydrolysis of the ester yields the active cross-coupling partner (boronic acid species).²² At this point, protodeborylation to the inactive compound is in competition with productive cross-coupling for polymerization (Scheme 4.3).^{19,23} We noted some small variations in reaction rate and dispersity (1.2 – 1.3) between monomer batches and we suspect this discrepancy is linked to trace water in the monomer. Molecular weights can be modulated according to catalyst loading (Table 4.2, entries 1–3) though in the GPC traces, we sometimes observe a small shoulder which is approximately double the molecular weight of the primary distribution. We suspect this shoulder is a consequence of disproportionation.^{2b,2c} A polymer sample was also analyzed using MALDI-TOF mass spectrometry to explore the end group fidelity of the P3HET polymer. Mass spectrometry confirmed the primary distribution is H/Br (Figure 4.2) with a smaller H/H distribution also present.

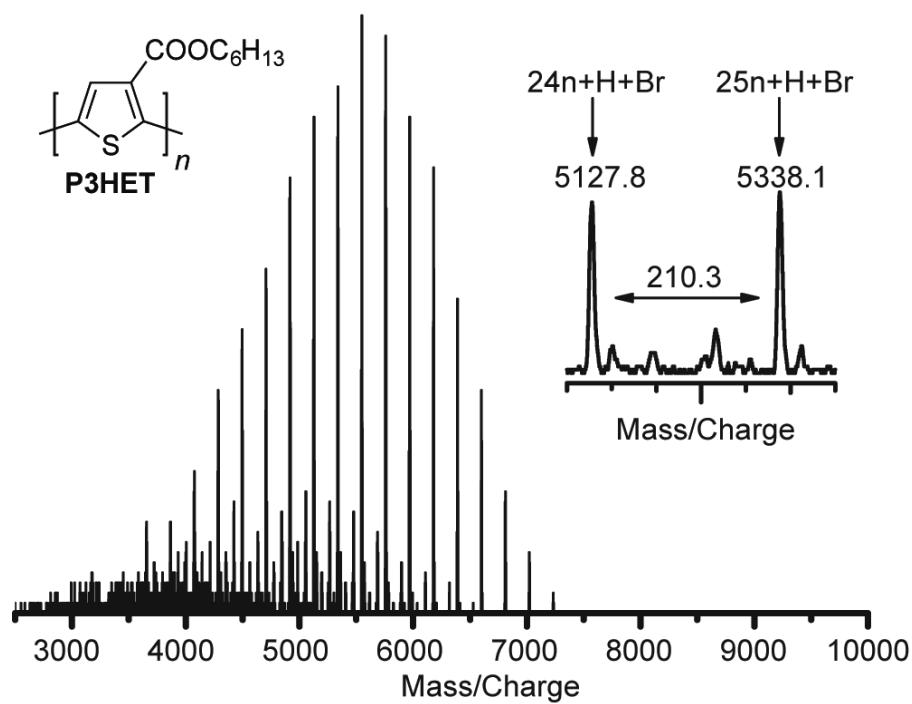


Figure 4.2. MALDI-TOF mass spectrum of P3HET prepared using $Ni(PPh_3)IPrCl_2$.

The efficiency of Ni(1-Naph)(PCy₃)₂Br was also evaluated, and low dispersity polymers were obtained using 5 mol % of the catalyst (Table 4.2, entry 4). The ¹H NMR spectrum of the final polymer exhibited the expected signals for the naphthyl endgroup. However, a broadened distribution was obtained when the catalyst loading was lowered to 2 mol %, indicative of early termination or chain transfer (Table 4.2, entry 5). This observation correlates well with the model compound studies in Table 4.1 and with the prior report.^{12b} Polymerization of **4.1** with PEPPSI-IPr and Ni(dppp)Cl₂ (Table 4.2, entries 6 and 7) resulted in relatively slow polymerization reactions and higher dispersities. The use of additional water with these two catalysts improved the dispersity of the final polymer, but produced macromolecules with lower molecular weights and low conversion, which again, is likely due to protodeborylation.

We also explored this protocol to polymerize a 3-hexylthiophene monomer (**4.2**, Scheme 4.2). When employing Ni(PPh₃)IPrCl₂ and K₃PO₄·H₂O, the reaction was dramatically different than the polymerization of monomer **4.1** and produced low molecular weight P3HT with higher dispersity (Appendix 1). The addition of water drastically increased both the reaction rate and molecular weight while narrowing the dispersity (Table 4.2, entry 8), which is consistent with the previous report.¹⁸ The differences between monomer **4.1** and **4.2** are striking. The water from the K₃PO₄·H₂O seems to be sufficient for promoting the reaction of the ester-functionalized monomer with good control. However, with the alkyl side group, additional water is needed to achieve the desired chain-growth behavior. It is plausible that the ester group in monomer **4.1** stabilizes the Ni(Ar)X intermediate via chelation, which may alter the polymerization behavior of **4.1** as compared to **4.2**.²⁴

Table 4.2. Polymerization studies for monomers **4.1**, **4.2**, and **4.3**.

Entry	M	Cat. (mol %)	Yield (%)	M_n (GPC) ^a	\bar{D}
1	1	Ni(PPh ₃)IPrCl ₂ (5)	53	7600	1.19
2	1	Ni(PPh ₃)IPrCl ₂ (2)	75	16400	1.25
3	1	Ni(PPh ₃)IPrCl ₂ (1)	79	30600	1.30
4	1	Ni(1-Naph) (PCy ₃) ₂ Br (5)	58	4500	1.14
5	1	Ni(1-Naph) (PCy ₃) ₂ Br (2)	69	10500	1.60
6	1	PEPPSI-IPr (2)	20	5500	1.28
7	1	Ni(dppp)Cl ₂ (2)	69	13600	1.55
8 ^b	2	Ni(PPh ₃)IPrCl ₂ (2)	71	74400	1.30
9 ^b	2	Ni(dppp)Cl ₂ (2)	59	18600	1.08
10	3	Ni(PPh ₃)IPrCl ₂ (2)	67	27700	1.63
11 ^b	3	Ni(dppp)Cl ₂ (2)	59	36500	1.13
12 ^b	3	Ni(dppp)Cl ₂ (1)	52	49000	1.48

^aGPC traces were recorded at 40 °C versus polystyrene standards using THF as the eluent. ^b0.1 mL of H₂O was added to the reaction mixture.

The added water also revealed a significant sensitivity of Ni(PPh₃)IPrCl₂ to the reaction conditions. The final molecular weight of P3HT was much greater than expected (Table 4.2, entry 8), likely from conversion of some precatalyst to Ni(OH)₂.²⁴⁻²⁵ In all experiments where water is added to Ni(PPh₃)IPrCl₂, polymers with higher than expected molecular weights were obtained, though controlled behavior was still observed. Recent reports have highlighted the sensitivity of Ni-NHC catalysts to water,²⁵ and this will impact Suzuki CTP reactions using this system.

To probe the combination of Ni(dppp)Cl₂ with monomer **4.2**, we conducted two experiments: with and without additional water. Without water, the polymerization of **4.2** proceeded slowly, similar to the experiment using the Ni-NHC catalyst. However, additional water with Ni(dppp)Cl₂ produced P3HT with excellent control over molecular weight and dispersity (Table 4.2, entry 9).

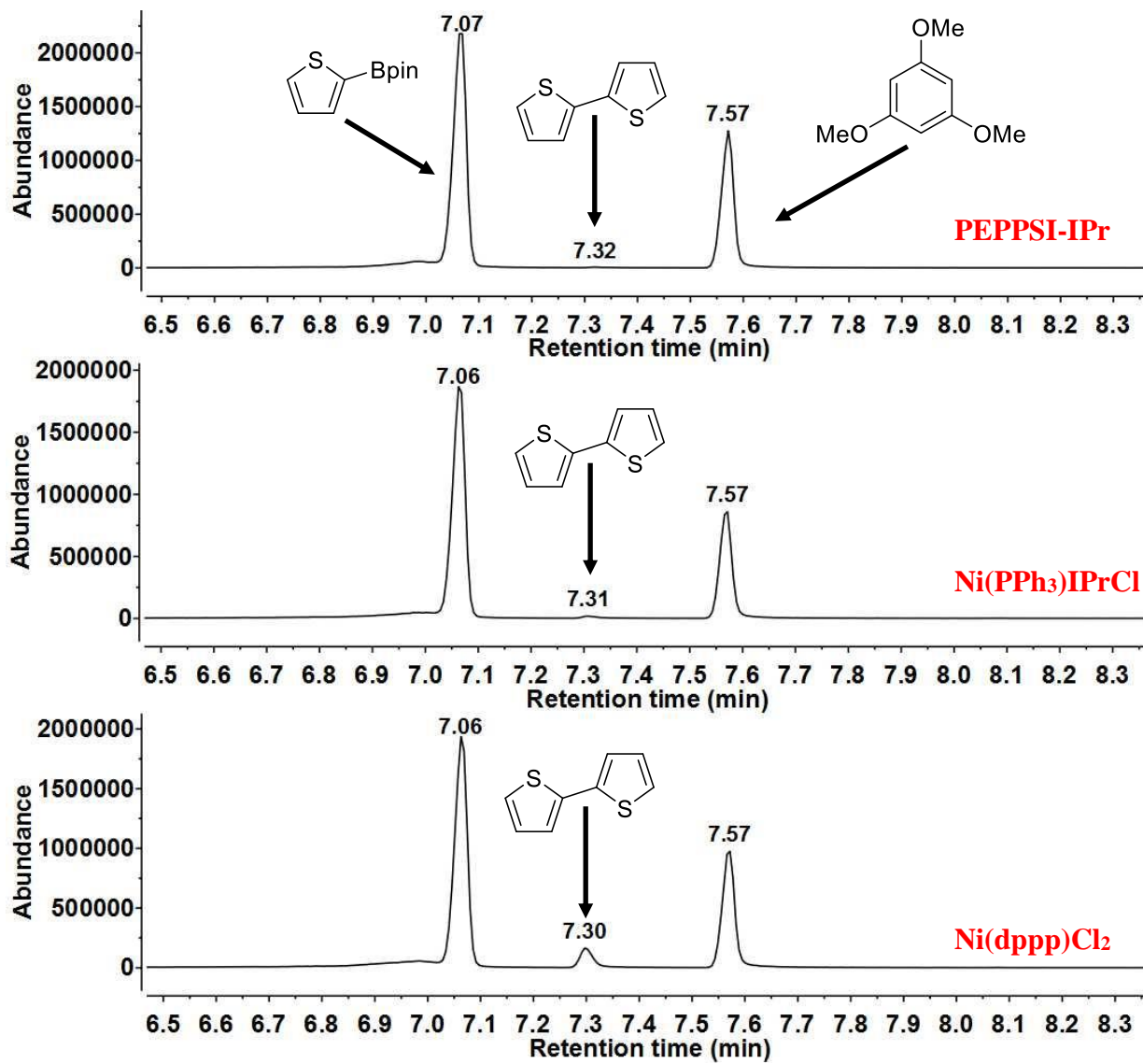


Figure 4.3. GC-MS chromatograms for catalyst initiation at 22 °C using ThBpin and catalyst (20 mol %) sampled after 5 minutes. Top – PEPPSI-IPr. Middle – Ni(PPh₃)IPrCl₂. Bottom – Ni(dppp)Cl₂. Signal at 7.3 min is bithiophene formed during precatalyst initiation.

We also evaluated how quickly these precatalysts are reduced under the polymerization conditions. A separate experiment was conducted with ThBPin, K₃PO₄ and the catalyst precursor. Upon addition of water, these reactions were monitored using GC-MS since reduction of the precatalyst should be accompanied with the formation of bithiophene. For both Ni(PPh₃)IPrCl₂ and Ni(dppp)Cl₂, bithiophene was observed within 2 minutes of water addition (Figure 4.3). Complete reduction was not quantified, but these experiments confirm that the formation of Ni(0)

is relatively facile under the polymerization conditions employed. These results are also consistent with the report from Percec and co-workers which indicated fast reduction of Ni(II) under similar conditions.^{12a} When Pd-PEPPSI-IPr was explored, reduction to the active Pd(0) seemed to be slower, though more studies are needed to examine this in detail.

An alternating copolymer consisting of P3HET and P3HT was also synthesized (Scheme 4.2). This type of material is related to donor-acceptor copolymers, a common target for organic electronic devices. Precision synthesis of donor-acceptor materials with tunable molecular weight and narrow distributions has been realized only recently,²⁶ but the scope of acceptor moieties is limited. Benzotriazole has been explored due to excellent compatibility with Grignard reagents,^{26a,26b} and benzothiadiazole containing monomers have also been polymerized using Suzuki CTP.^{26d} However, π -accepting functional groups which are often present in donor-acceptors;²⁷ are incompatible with Grignard reagents, though diimide monomers have attracted attention with Zn^{26c,26e} and Sn²⁸ as the transmetallating agent.

An alternating copolymer consisting of P3HET and P3HT was prepared using Suzuki CTP with Ni(dppp)Cl₂ as the precatalyst (Table 4.2, entries 11 and 12). Results suggest a controlled polymerization and, in the presence of additional water, high molecular weight P3HET-*a*-P3HT polymers were obtained with relatively short reaction times (1 – 2 h). Ni(PPh₃)IPrCl₂ performed quite poorly without added water and proceeded in an uncontrolled fashion (entry 10). Employing additional water and subsequent GPC analysis revealed a bimodal distribution.

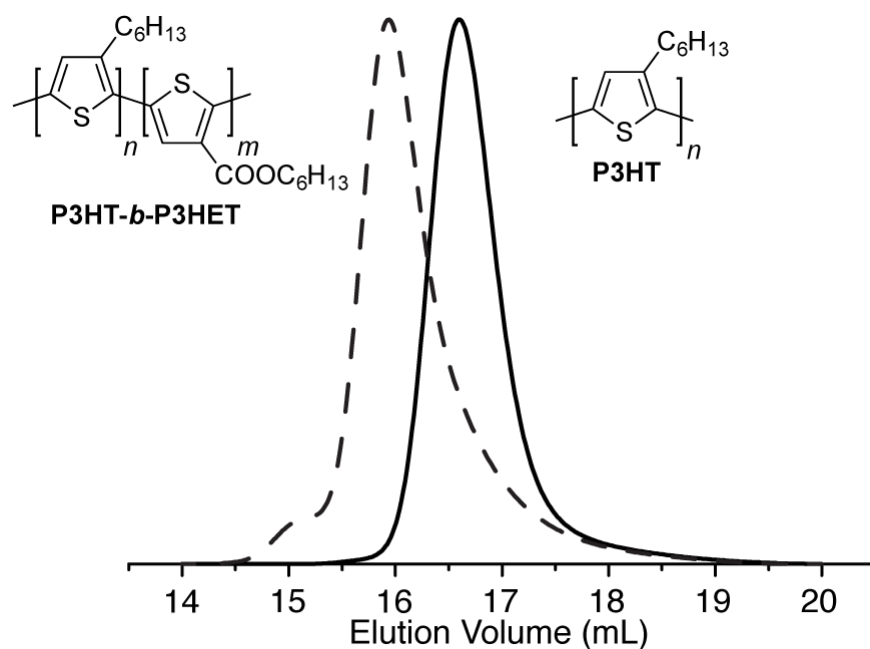


Figure 4.4. GPC chromatograms for the P3HT homopolymer and P3HT-*b*-P3HET copolymer synthesized using Ni(PPh₃)IPrCl₂.

Finally, a block copolymer of P3HET and P3HT was prepared. Both Ni(PPh₃)IPrCl₂ and Ni(dppp)Cl₂ can generate diblock architectures regardless of the order of monomer addition, though high molecular weights cannot always be generated. Water was a complicating factor since it is needed for controlled P3HT synthesis but can promote protodeborylation of the more electron-deficient **4.1** and moreover, the Ni-NHC catalyst is sensitive to water. P3HT can be prepared using 4 mol % Ni(PPh₃)IPrCl₂ and 0.1 mL of water ($M_n = 21100$, $D = 1.14$) after which, addition of monomer **4.1** to the reaction mixture afforded the desired block copolymer in a controlled manner (P3HT-*b*-P3HET, $M_n = 29500$, $D = 1.28$, Figure 4.4). Detailed experimental procedures and other block copolymer syntheses varying the starting block and catalyst are provided in the experimental section.

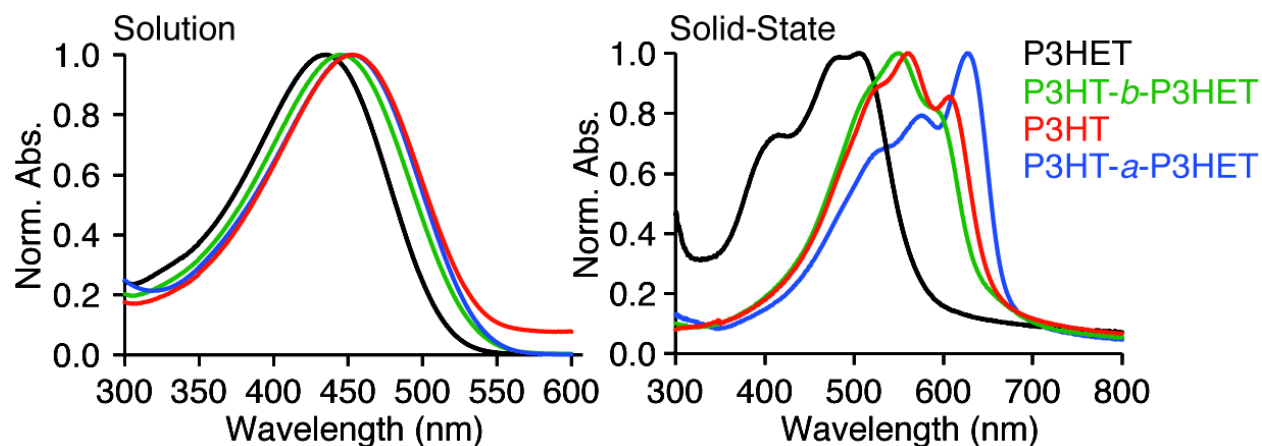


Figure 4.5. Solution (CHCl_3) and solid-state UV-vis spectra for all polymers with P3HT included for reference.

The optical properties of P3HET, P3HT, P3HET-*a*-P3HT and P3HT-*b*-P3HET were probed both in solution and in the solid-state (Figure 4.5). P3HET is significantly blue-shifted as compared to P3HT, suggesting the ester side chain may be causing a more twisted polymer backbone as compared to the linear alkyl chain.

The absorption profile of P3HT-*b*-P3HET ($\lambda_{\text{max}} = 445 \text{ nm}$) is quite close to that of P3HT ($\lambda_{\text{max}} = 453 \text{ nm}$) in solution and also in the solid state (P3HT-*b*-P3HET, $\lambda_{\text{max}} = 550 \text{ nm}$). The absorption profile of P3HET-*a*-P3HT ($\lambda_{\text{max}} = 452 \text{ nm}$) is also nearly identical to P3HT ($\lambda_{\text{max}} = 453 \text{ nm}$) in solution. However, P3HET-*a*-P3HT ($\lambda_{\text{max}} = 627 \text{ nm}$, $E_{\text{g}}^{\text{opt}} = 1.85 \text{ eV}$) is red-shifted compared to both homopolymers in the solid-state as the vibronic band becomes the dominant absorption in this spectrum, indicative of ordered π -stacking. The perfectly alternating P3HET-*a*-P3HT is also red-shifted compared to a previously synthesized random 50:50 P3HET:P3HT copolymer ($\lambda_{\text{max}} = 556 \text{ nm}$, $E_{\text{g}}^{\text{opt}} = 1.90 \text{ eV}$).²⁹

End group analysis of P3HET and P3HET-*a*-P3HT was completed using 2D NMR spectroscopy. For P3HET, a tail-to-tail (TT) defect from precatalyst initiation (H_A , Figure 4.6) is present in the spectrum along with signals that result from the H/Br polymer end groups (H_B , H_C

and H_D, Figure 4.6). The H terminated thiophene end group (H_C, Figure 4.6) appears at 8.17 ppm and is correlated with a signal at 7.81 ppm (H_D, Figure 4.6). The signal attributed to the tail-to-tail (TT) defect appears at 7.60 ppm (H_A) and the Br terminated chain-end produced one ¹H NMR signal (H_B, Figure 4.6 at 7.68 ppm). Additionally, integration of the chain-end signals and the TT defect approximately produced a 2:1:1 ratio (H_A:H_B:H_C) indicating good control over the end groups. This is consistent with the analysis by MALDI-TOF mass spectrometry (Figure 4.2).

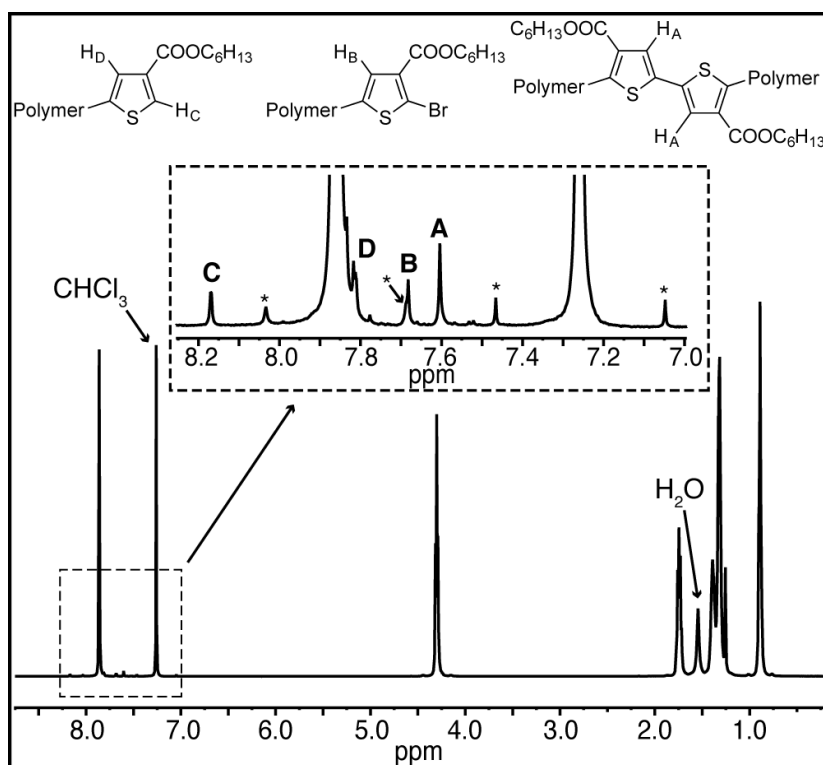


Figure 4.6. ¹H NMR spectrum and end group analysis of P3HET. The star symbols (*) correspond to ¹³C satellites for the aromatic signal of the polymer and the solvent.

Signal H_B did not show the expected correlations in the HMBC spectrum and to confirm its identity, an experiment was carried out where the polymer was reacted with Ni(COD)₂ followed by reaction with acid to selectively functionalize the C-Br bond. The signal attributed to H_B nearly disappeared after the reaction, and provided good evidence for the assignment.

2D NMR spectroscopy was also used to confirm the highly alternating nature of P3HET-*a*-P3HT (Appendix 1). Similar to P3HET, the TT defect for P3HET-*a*-P3HT appears at 7.55 ppm. The H terminated end group at 7.01 ppm is correlated with another signal at 7.32 ppm and these signals correspond to a regioregular 3-hexylthiophene chain-end. The Br terminated chain-end produced one signal in the ¹H NMR spectrum at 7.17 ppm, again corresponding to a regioregular 3-hexylthiophene.

4.3 Conclusion

In summary, we have demonstrated the first example of a Suzuki catalyst-transfer polycondensation (CTP) using Ni precatalysts and explored this protocol with ester-functionalized monomers. The ester-functionalized polythiophene could be obtained with molecular weight control, and block copolymers were synthesized with 3-hexylthiophene. Furthermore, the controlled synthesis of an alternating polymer is highly valuable and this Suzuki CTP protocol will be used to explore more sophisticated donor-acceptor polymers. Expanding this protocol to other monomers with different functional groups while further investigating the crucial role of water in the Suzuki CTP process is currently under investigation.

4.4 Experimental Section

Materials and Methods. All reactions and manipulations of air and water sensitive compounds were carried out under a dry nitrogen atmosphere using an mBraun glovebox or standard Schlenk techniques. All compounds were purchased from commercial sources and used as received. 2,5-Dibromothiophene-3-carboxylic acid³⁰, 2-(4-hexylthiophen-2-yl)-4,4,5,5-tetramethyl-1,3,2-dioxaborolane³¹ and monomer **4.2**^{4e,32} were synthesized according to literature procedures. All reaction solvents (tetrahydrofuran, dichloromethane, hexanes and dioxane) were degassed with

argon and dried prior to use. All solvents and chemicals used for extraction and column chromatography were used as received. Polymer samples were precipitated with 6 M methanolic HCl and washed with both methanol and acetone for GPC, NMR, and UV-vis analysis. Monomer conversion in polymerization experiments was typically monitored by GC-MS comparing the protodeborylated monomer to an internal standard. Since deborylation was not always quantitative (mixtures of monomer and protodeborylated monomer) and since it can occur either as a side reaction or also during GC analysis, conversion values were not reported. This was used as a rough estimate for monomer conversion.

NMR analysis. All NMR experiments were collected at 300 K on a two-channel Bruker Avance III NMR instrument equipped with a Broad Band Inverse (BBI) probe, operating at 500 MHz for ^1H (126 MHz for ^{13}C). ^1H NMR spectra are referenced to residual protio solvent (7.26 for CHCl_3 , 5.32 for CH_2Cl_2 , and 7.16 for $\text{C}_6\text{D}_5\text{H}$) and ^{13}C NMR spectra are referenced to the solvent signal (δ 77.23 for CDCl_3 , 54.00 for CD_2Cl_2 and 128.39 for C_6D_6). The F2 proton-coupled HSQC was performed using the recently published Perfect-HSQC pulse program.³³ The HMBC experiments were optimized for 4 and 8 Hz long-range proton-coupling ($^nJ_{\text{CH}}$).

Mass Spectrometry. High Resolution Electron Impact Mass Spectrometry (HRMS), Electrospray Mass Spectrometry (ESI-MS) and MALDI-TOF Mass Spectrometry were performed in the School of Chemical Sciences Mass Spectrometry Laboratory at the University of Illinois, Urbana-Champaign.

GC-MS Analysis. GC-MS analysis was performed on a Hewlett-Packard Agilent 6890-5973 GC-MS workstation. The GC column was a Hewlett-Packard fused silica capillary column crosslinked with 5% phenylmethylsiloxane. Helium was used as the carrier gas. The following conditions were

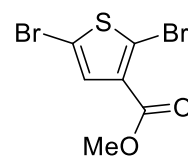
used for all GC-MS analyses: injector temperature, 250 °C; initial temperature, 70 °C; temperature ramp, 10 °C/min; final temperature, 280 °C. Polymer aliquots were typically subjected to GC-MS analysis to provide rough estimates of monomer conversion by comparing the protodeborylated monomer to an internal standard. Since deborylation was not always quantitative and since it can occur either as a side reaction or also during GC analysis, conversion values were not reported. Polymer aliquots were prepared by quenching ~0.2 mL of the polymer solution with ~1.0 mL of methanol in a 20 mL scintillation vial. This was diluted with ~1.0 mL of diethyl ether and ~0.1 mL of this resultant solution was filtered through a 0.22 µm PTFE syringe filter into a 2 mL vial and diethyl ether was added to fill the vial.

UV-vis Spectroscopy. UV-vis spectra of polymers were recorded on a Varian Cary 5000 spectrophotometer. Solution measurements were conducted in CHCl₃ at 0.01 mg/mL concentration. Thin film samples were prepared from a spin-coating process. 22 × 22 mm glass cover slips were cleaned by spraying with fresh acetone, isopropanol and dried under a jet of filtered, dry nitrogen. Polymer solutions (5 mg/mL) in dry toluene were heated to 80 °C in amber glass vials for 10 min, filtered through a 0.22 µm PTFE syringe filter using a glass syringe, and reheated for 5 min prior to spin-casting from hot solutions. The spin-coating conditions consisted of three cycles, a 400 RPM spreading cycle for 5 s, a 1000 RPM main cycle for 30 s and a 2000 RPM wicking cycle for 15 s. The films were annealed at 150°C for 1 h under N₂.

Gel-Permeation Chromatography. GPC measurements were performed on a Waters Instrument equipped with a 717 plus autosampler, a Waters 2414 refractive index (RI) detector and two SDV columns (Porosity 1000 and 100000 Å; Polymer Standard Services) with THF as the eluent (flow rate 1 mL/min, 40 °C). A 10-point calibration based on polystyrene standards (Polystyrene, ReadyCal Kit, Polymer Standard Services) was applied for determination of molecular weights.

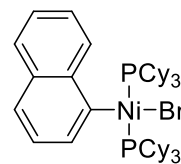
All polymer aliquots subjected to GPC analysis were prepared by quenching ~0.2 mL of the polymer solution with ~2.0 mL of 6 M methanolic HCl. The precipitate was filtered and washed with methanol and acetone to remove any monomer and low molecular weight oligomers. The resultant polymer was dissolved in ~1 mL of THF, filtered through a 0.22 μm PTFE syringe filter and analyzed.

Synthesis of methyl-2,5-dibromothiophene-3-carboxylate. An oven-dried 250 mL Schlenk flask was charged with 2,5-dibromothiophene-3-carboxylic acid (4.56 g, 15.9 mmol), 15 mL of thionyl chloride and catalytic dimethylformamide



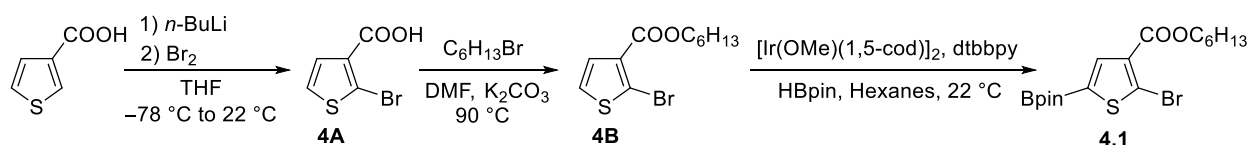
(~0.05 mL). The solution was heated to 40 $^{\circ}\text{C}$ and stirred overnight. Excess thionyl chloride was removed *in vacuo* and the residue was triturated with diethyl ether to afford an off-white solid that was used without further purification. An oven-dried 100 mL Schlenk flask was charged with a portion of the crude acid chloride (3.04 g, 10.0 mmol) and 25 mL of dichloromethane. The flask was cooled to 0 $^{\circ}\text{C}$ using an ice bath, then methanol (0.8 mL, 19.8 mmol) and triethylamine (2.78 mL, 19.9 mmol) were added to the flask. The mixture was stirred at room temperature for 2 h and, an aliquot was removed and analyzed using GC-MS to confirm formation of the product. The reaction mixture was then transferred to a separatory funnel and 1 M HCl solution (30 mL) was added. The organic layer was separated and the aqueous layer was extracted twice more with dichloromethane (2 \times 30 mL). The combined organic extracts were washed with a saturated NaHCO_3 solution (10 mL), dried over MgSO_4 and concentrated to yield an off-white solid. The compound was purified on a short path of silica, eluting with hexanes:ethyl acetate (5:1), affording the title compound as a white crystalline solid (2.72 g, 91%). ^1H NMR (500 MHz, CDCl_3) δ 7.34 (s, 1H), 3.86 (s, 3H). ^{13}C NMR (126 MHz, CDCl_3) δ 161.4, 131.9, 131.8, 119.5, 111.6, 52.3. HRMS (ESI-TOF) (m/z): $[\text{M} + \text{H}]^+$ calculated for $\text{C}_6\text{H}_5\text{Br}_2\text{O}_2\text{S}$, 298.8377; found, 298.8382.

Synthesis of Ni(1-Naph)(PCy₃)₂Br. This compound was prepared according to a modified literature procedure.^{12a} In a nitrogen filled glove box, a 20 mL scintillation vial was charged with Ni(COD)₂ (0.10 g, 0.36 mmol),



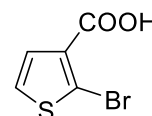
tricyclohexylphosphine (0.30 g, 1.07 mmol), and THF (1.5 mL). The solution was stirred at room temperature for 30 min, turning deep red, at which time, 1-bromonaphthalene (0.075 g, 0.36 mmol) was added to the reaction mixture. The mixture was stirred overnight and a yellow precipitate formed. The precipitate was collected using vacuum filtration and washed with hexanes (5 × 5 mL). The yellow solid was transferred to a scintillation vial and dried *in vacuo* (0.16 g, 54%). ³¹P{¹H} NMR (202 MHz, C₆D₆) δ 11.6. ¹H NMR (500 MHz, C₆D₆) δ 10.68 (d, *J* = 8.3 Hz, 1H), 7.71 (d, *J* = 7.0 Hz, 1H), 7.62 (br t, *J* = 7.3 Hz, 1H), 7.53 (d, *J* = 8.2 Hz, 1H), 7.32 (br t, *J* = 9.6 Hz, 2H), 7.14 (d, *J* = 7.5 Hz, 1H), 2.75 – 0.35 (m, 66H). Note: the signal at 7.14 ppm overlaps with the solvent signal. ¹³C NMR (126 MHz, C₆D₆) δ 157.2 (t, *J*_{PC} = 32.7 Hz), 142.9, 137.7 (t, *J*_{PC} = 3.7 Hz), 135.4, 133.5 (t, *J*_{PC} = 2.6 Hz), 128.8 (d, *J*_{PC} = 26.1 Hz), 125.6, 125.2 (t, *J*_{PC} = 2.7 Hz), 123.6, 122.5 (t, *J*_{PC} = 2.3 Hz), 34.8 (t, *J*_{PC} = 8.5 Hz), 31.2, 30.7, 28.7 (t, *J*_{PC} = 5.4 Hz), 28.4 (t, *J*_{PC} = 4.3 Hz), 27.4. HR-EIMS (*m/z*): [M – Br]⁺ calculated for C₄₆H₇₃P₂Ni, 745.4541; found, 745.4533.

Scheme 4.4. Synthesis of monomer 4.1.



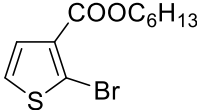
Synthesis of 2-bromothiophene-3-carboxylic acid (4A). An oven-dried 500 mL

Schlenk flask was charged with thiophene-3-carboxylic acid (15.9 g, 124 mmol) and



300 mL of THF. The solution was cooled to –78 °C using a dry-ice acetone bath and 2.5 M *n*-butyllithium in hexanes (100 mL, 250 mmol) was added via cannula over a 20 min period. During the addition, a white precipitate formed. The reaction mixture was stirred for 30 min at –78 °C and

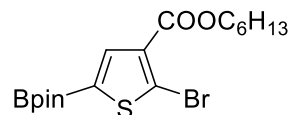
then, bromine (6.67 mL, 130 mmol) was added dropwise by syringe. The flask was not removed from the cold bath to ensure the reaction vessel returned to room temperature slowly overnight. A small amount of 1 M HCl solution (5 – 10 mL) was added to quench the reaction mixture and then, the mixture was concentrated to approximately 50 mL. The remaining solution was transferred to a separatory funnel, diluted with 150 mL of 1 M HCl solution and, extracted with ethyl acetate (3 × 150 mL). The combined organic extracts were washed with brine, dried over MgSO₄ and concentrated to afford an off-white solid. The compound was recrystallized twice using a water:ethanol mixture (4:1) to furnish the title compound as faint yellow needles (16.53 g, 64%). The ¹H and ¹³C NMR spectra were compared to a previous report.³⁴

Synthesis of hexyl 2-bromothiophene-3-carboxylate (4B). An oven-dried 100 mL Schlenk flask was charged with 2-bromothiophene-3-carboxylic acid (**4A**)  (6.00 g, 29.0 mmol), K₂CO₃ (12.0 g, 86.8 mmol) and 40 mL of dimethylformamide. 1-Bromohexane (9.60 g, 58.2 mmol) was subsequently added by syringe. The flask was immersed in an oil bath at 90 °C and the solution was stirred for 12 h under a N₂ atmosphere. The reaction mixture was cooled to room temperature, diluted with 50 mL of water and transferred to a 500 mL separatory funnel. The aqueous layer was extracted with diethyl ether (3 × 100 mL) and the combined organic extracts were washed with water (50 mL) and brine (50 mL), then dried over Na₂SO₄ and concentrated using rotary evaporation. The crude product was purified using column chromatography on silica gel eluting with hexanes:ethyl acetate (50:1) to afford the final product as a clear liquid (6.06 g, 72%). The *R_f* of the product is ~0.7 in hexanes:ethyl acetate = 9:1. ¹H NMR (500 MHz, CDCl₃) δ 7.37 (d, *J* = 5.8 Hz, 1H), 7.21 (d, *J* = 5.8 Hz, 1H), 4.28 (t, *J* = 6.7 Hz, 2H), 1.75 (dq, *J* = 7.9, 6.7 Hz, 2H), 1.49 – 1.40 (m, 2H), 1.38 – 1.28 (m, 4H), 0.94 – 0.85 (m, 3H).

^{13}C NMR (126 MHz, CDCl_3) δ 162.3, 131.6, 129.7, 126.0, 119.8, 65.4, 31.6, 28.8, 25.9, 22.8, 14.2.

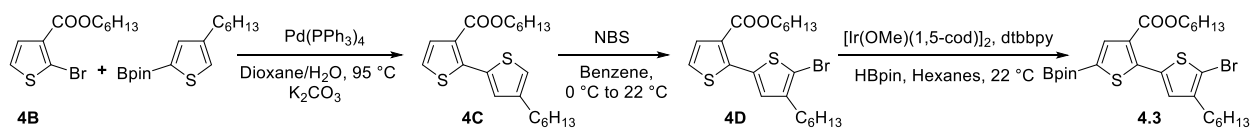
HRMS (ESI-TOF) (m/z): $[\text{M} + \text{H}]^+$ calculated for $\text{C}_{11}\text{H}_{16}\text{O}_2\text{SBr}$, 291.0054; found, 291.0062.

Synthesis of hexyl 2-bromo-5-(4,4,5,5-tetramethyl-1,3,2-dioxaborolan-2-yl)thiophene-3-carboxylate (4.1).



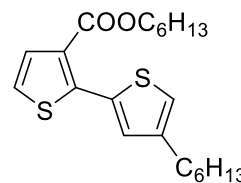
In a N_2 filled glovebox, a 40 mL scintillation vial was charged with pinacolborane (HBpin) (1.16 g, 9.06 mmol), di- μ -methoxobis(1,5-cyclooctadiene)diiridium (0.045 g, 0.068 mmol) and 3 mL of dry hexanes. To this stirring mixture, 4,4'-Bis(di-*t*-butyl)-2,2'-bipyridine (dtbbpy) (0.036 g, 0.13 mmol) in 3 mL of hexanes was added in portions and the mixture was stirred for 15 min. The color of the reaction mixture went from yellow to dark brown during that period. Compound **4B** (1.32 g, 4.53 mmol) was then dissolved in 4 mL of hexanes and added to the mixture slowly (H_2 gas evolves in this step). The solution was kept in the glovebox and stirred overnight. The crude mixture was then removed from the glovebox, loaded directly onto silica gel, and eluted with hexanes:dichloromethane (1:1). The R_f of the product is ~ 0.4 in hexanes:dichloromethane = 1:1. The final product was collected as a clear oil and slowly solidified after drying *in vacuo* to afford an off-white powder (1.40 g, 74%). ^1H NMR (500 MHz, CDCl_3) δ 7.85 (s, 1H), 4.27 (t, $J = 6.7$ Hz, 2H), 1.73 (dq, $J = 9.1, 6.7$ Hz, 2H), 1.47 – 1.39 (m, 2H), 1.36 – 1.28 (m, 16H), 0.93 – 0.87 (m, 3H). ^{13}C NMR (126 MHz, CDCl_3) δ 162.2, 139.2, 132.7, 126.3, 84.9, 65.4, 31.7, 28.8, 25.9, 25.0, 22.8, 14.2. Note: one aromatic signal is missing in the ^{13}C NMR spectrum due to quadrupolar relaxation. HR-EIMS (m/z): $[\text{M}]^+$ calculated for $\text{C}_{17}\text{H}_{26}\text{O}_4\text{BrSB}$, 416.0828; found, 416.0832.

Scheme 4.5. Synthesis of Monomer 4.3.



Synthesis of hexyl 4'-hexyl-[2,2'-bithiophene]-3-carboxylate (4C). In a N₂

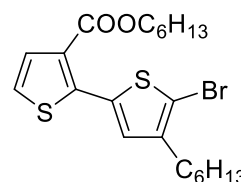
filled glovebox, a 20 mL scintillation vial was charged with compound **4B** (0.50 g, 1.72 mmol), 2-(4-hexylthiophen-2-yl)-4,4,5,5-tetramethyl-1,3,2-



dioxaborolane (0.51 g, 1.73 mmol), Pd(PPh₃)₄ (0.10 g, 0.087 mmol), K₂CO₃ (0.71 g, 5.14 mmol) and 10 mL of dioxane. The vial was removed from the glovebox and 2 mL of water was added into the vial by syringe. The vial was then immersed in an oil bath at 95 °C and the solution was stirred for 12 h before cooling to room temperature. The mixture was transferred to a separatory funnel, diluted with 100 mL of diethyl ether and washed with water and brine. The organic layer was dried using Na₂SO₄, and concentrated using rotary evaporation. The crude material was purified using column chromatography on silica gel, eluting with hexanes:dichloromethane (3:1) to afford the final product as a clear oil (0.58 g, 89%). The *R_f* of the product is ~0.6 in hexanes:dichloromethane = 1:1. ¹H NMR (500 MHz, CD₂Cl₂) δ 7.45 (d, *J* = 5.5 Hz, 1H), 7.26 (d, *J* = 1.4 Hz, 1H), 7.20 (d, *J* = 5.4 Hz, 1H), 7.01 (q, *J* = 1.1 Hz, 1H), 4.20 (t, *J* = 6.7 Hz, 2H), 2.61 (t, *J* = 7.7 Hz, 2H), 1.70 – 1.59 (m, 4H), 1.41 – 1.25 (m, 12H), 0.94 – 0.84 (m, 6H). ¹³C NMR (126 MHz, CD₂Cl₂) δ 163.7, 144.1, 143.6, 134.0, 131.1, 130.9, 128.7, 124.4, 122.8, 65.5, 32.3, 32.1, 31.1, 31.0, 29.6, 29.2, 26.3, 23.22 and 23.15 (2 overlapping signals), 14.44 and 14.37 (2 overlapping signals). HRMS (ESI-TOF) (*m/z*): [M + H]⁺ calculated for C₂₁H₃₁O₂S₂, 379.1765; found, 379.1772.

Synthesis of hexyl 5'-bromo-4'-hexyl-[2,2'-bithiophene]-3-carboxylate

(4D). Compound **4C** (0.58 g, 1.53 mmol) was dissolved in 100 mL of benzene and the solution was cooled to 0 °C. N-Bromosuccinimide (0.30 g, 1.69

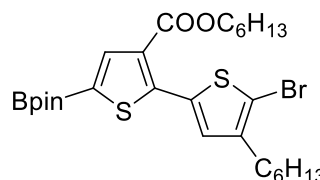


mmol) was then added to the reaction mixture in portions while maintaining a temperature of 0 °C. The reaction mixture was slowly warmed to room temperature and stirred overnight. The

mixture was quenched with 50 mL of a saturated NaHCO₃ solution and the entire contents of the flask were transferred to a separatory funnel. The aqueous layer was extracted with diethyl ether (3 × 50 mL) and the combined organic extracts were washed with a saturated NaHCO₃ solution and brine. The extracts were then dried over Na₂SO₄ and concentrated using rotary evaporation. The crude product was purified using column chromatography on silica gel, eluting with hexanes:dichloromethane (15:1) to afford the final product as a clear oil (0.45 g, 64%). The *R_f* of the product is ~0.4 in hexanes:dichloromethane = 7:3. ¹H NMR (500 MHz, CDCl₃) δ 7.46 (d, *J* = 5.4 Hz, 1H), 7.17 (d, *J* = 5.4 Hz, 1H), 7.11 (s, 1H), 4.24 (t, *J* = 6.7 Hz, 2H), 2.56 (t, *J* = 7.7 Hz, 2H), 1.73 – 1.64 (m, 2H), 1.64 – 1.56 (m, 2H), 1.41 – 1.24 (m, 12H), 0.94 – 0.84 (m, 6H). ¹³C NMR (126 MHz, CDCl₃) δ 163.4, 142.8, 142.2, 133.6, 130.7, 130.1, 128.2, 124.0, 112.1, 65.3, 31.8, 31.7, 29.9, 29.8, 29.2, 28.8, 25.9, 22.82 and 22.78 (2 overlapping signals), 14.3, 14.2. HRMS (ESI-TOF) (*m/z*): [M + H]⁺ calculated for C₂₁H₃₀O₂S₂Br, 457.0871; found, 457.0869.

Synthesis of hexyl 5'-bromo-4'-hexyl-5-(4,4,5,5-tetramethyl-1,3,2-

dioxaborolan-2-yl)-[2,2'-bithiophene]-3-carboxylate (4.3). In a N₂ filled glovebox, a 40 mL scintillation vial was charged with



pinacolborane (HBPIn) (0.50 g, 3.9 mmol), Di- μ -methoxobis(1,5-cyclooctadiene)diiridium (0.033 g, 0.050 mmol) and 2 mL of dry hexanes. To this stirring mixture, 4,4'-Bis(di-*t*-butyl)-2,2'-bipyridine (dtbbpy) (0.026 g, 0.097 mmol) in 2 mL of hexanes was added in portions and the mixture was stirred for 15 min. The color of the reaction mixture went from yellow to dark brown during that period. Compound **4D** (1.50 g, 3.28 mmol) was then dissolved in 4 mL of hexanes and added to the reaction mixture slowly (H₂ gas evolves in this step). The solution was kept in the glovebox and stirred overnight. The crude mixture was then removed from the glovebox, loaded directly onto silica gel, and eluted with gradient solvent conditions (hexanes:dichloromethane =

1:1, followed by dichloromethane). The R_f of the product is ~ 0.5 in hexanes:dichloromethane = 1:1. The final product was collected as a green oil and, upon drying, slowly solidified to a light-green solid (1.41 g, 74%). ^1H NMR (500 MHz, CDCl_3) δ 7.95 (s, 1H), 7.22 (s, 1H), 4.24 (t, $J = 6.8$ Hz, 2H), 2.55 (t, $J = 7.7$ Hz, 2H), 1.75 – 1.64 (m, 2H), 1.64 – 1.53 (m, 2H), 1.43 – 1.20 (m, 24H), 0.95 – 0.83 (m, 6H). ^{13}C NMR (126 MHz, CDCl_3) δ 163.4, 149.0, 142.3, 140.6, 133.6, 130.4, 128.7, 113.0, 84.8, 65.3, 31.8, 31.7, 29.8, 29.7, 29.1, 28.9, 25.9, 25.0, 22.79 and 22.76 (2 overlapping signals), 14.3, 14.2. Note: one aromatic signal is missing in the ^{13}C NMR spectrum due to quadrupolar relaxation. HRMS (ESI-TOF) (m/z): $[\text{M} + \text{H}]^+$ calculated for $\text{C}_{27}\text{H}_{41}\text{O}_4\text{S}_2\text{BrB}$, 583.1723; found, 583.1719.

Model Compound Studies

Representative procedure. In a N_2 filled glove box, a 20 mL scintillation vial was charged with the dihalogenated thiophene (0.50 mmol), 4,4,5,5-tetramethyl-2-(thiophen-2-yl)-1,3,2-dioxaborolane (ThBPin) (0.053 g, 0.25 mmol), $\text{K}_3\text{PO}_4 \cdot \text{H}_2\text{O}$ (0.14 g, 0.61 mmol) and either 1,3,5-trimethoxybenzene (0.042 g, 0.25 mmol) or nonadecane (0.067 g, 0.25 mmol) as an internal standard. Finally, the catalyst (mol % relative to ThBPin) was added along with 3 mL of THF. The vial was sealed, and removed from the glovebox and an aliquot was analyzed using GC-MS ($t = 0$ h). The vial was then placed in an oil bath at $50\text{ }^\circ\text{C}$ and stirred for 24 h. An aliquot (0.1 mL) was then removed and subjected to GC-MS analysis while another aliquot (0.3 mL) was concentrated, dissolved in CDCl_3 , filtered through a $0.22\text{ }\mu\text{m}$ PTFE filter, and analyzed using ^1H NMR spectroscopy. For the ^1H NMR spectra, the methyl [2,2':5',2''-terthiophene]-3'-carboxylate was isolated from one of the reaction mixtures for comparison. ^1H NMR (500 MHz, CDCl_3) δ 7.53 (s, 1H), 7.49 (dd, $J = 3.7, 1.2$ Hz, 1H), 7.42 (dd, $J = 5.1, 1.2$ Hz, 1H), 7.27 (dd, $J = 5.3, 1.2$ Hz, 1H), 7.20 (dd, $J = 3.6, 1.2$ Hz, 1H), 7.06 (ddd, $J = 11.9, 5.1, 3.7$ Hz, 2H), 3.85 (s, 3H). Note: the signal

at 7.27 ppm overlapped with the solvent signal. Integration of the methyl carboxylate signal was used to determine the ratio of terthiophene:bithiophene. For the monosubstituted bithiophene product, two regioisomers are possible, but we did not identify the regioisomer formed. Conversion was determined in GC-MS by integration of the ThBPIn signal to the internal standard. In the ^1H NMR spectrum, the methyl groups of the borane moiety were integrated versus the internal standard. Representative crude NMR spectra and GC-MS chromatograms are shown below in Appendix 1.

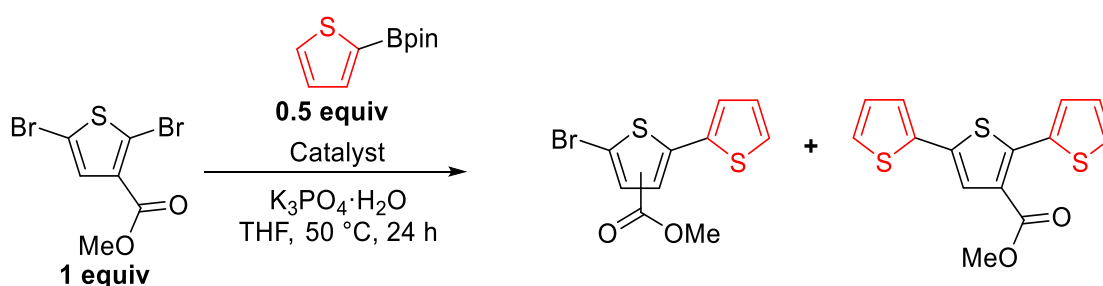
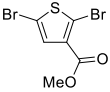
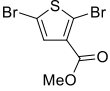
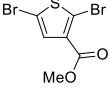
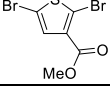
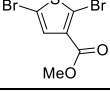
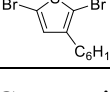


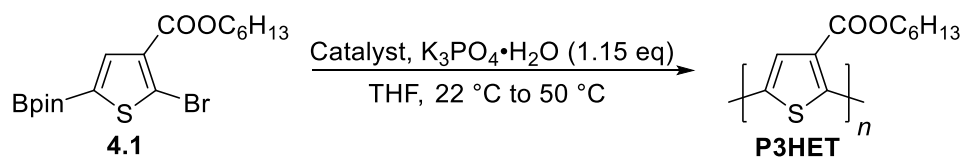
Table 4.3. Catalyst screening for dihalogenated thiophenes using Suzuki-Miyaura coupling.

Dihalogen	Catalyst	Temp. (°C)	mol % Cat.	% Conv. GC-MS ^a	% Terthiophene GC-MS (NMR)
	Ni(PPh ₃)IPrCl ₂	50	5	99	99 (99)
		50	1	99	99 (99)
	Ni(1-Naph)(PCy ₃) ₂ Br	50	5	99	94 (97)
		50	1	72	44 (72)
	Ni(dppp)Cl ₂	50	5	99	95 (96)
		50	1	82	97 (95)
	PEPPSI-IPr	50	5	99	52 (72)
		50	1	99	64 (78)
	Ni(PPh ₃)IPrCl ₂	65	5	99	95
		50 ^b	5	99	94
	Ni(PPh ₃)IPrCl ₂	50	5	99	87
		50 ^c	5	79	94

^aConversion is calculated based on the consumption of ThBPIn. ^bRelative molar ratio of methyl-2,5-dibromothiophene-3-carboxylate:ThBPIn was 5:1. ^c0.2 mL of water was added to the reaction mixture at t = 0 h.

Polymerization Studies

Scheme 4.6. Synthesis of P3HET.

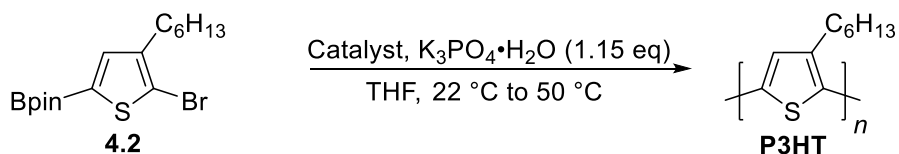


Representative procedure for P3HET synthesis. In a N₂ filled glovebox, a 20 mL scintillation vial equipped with a Teflon screw cap was charged with a calculated amount of catalyst (mol % listed in Table 4.4), K₃PO₄·H₂O (0.080 g, 0.35 mmol), nonadecane (0.080 g, 0.30 mmol) as the internal standard, and 5 mL of THF. The vial was capped, removed from the glovebox and the reaction mixture was stirred at room temperature. Monomer **4.1** (0.13 g, 0.31 mmol) in 2 mL of THF was injected into the solution to initiate the polymerization. After 30 s of stirring, an aliquot (0.2 mL) was withdrawn from the solution, quenched with methanol (1 mL), diluted with diethyl ether (1 mL) and subjected to GC-MS analysis. The reaction mixture was stirred at room temperature for 30 min before being placed in an oil bath at 50 °C. A final aliquot (0.2 mL) was withdrawn to determine the monomer conversion and the polymerization was quenched using 6 M methanolic HCl solution. The precipitate was collected using vacuum filtration, then washed with methanol and acetone to remove any unreacted monomer and oligomers. The final polymer was collected as a red solid and dried *in vacuo*. ¹H NMR (500 MHz, CDCl₃) δ 7.86 (br s, 1H), 4.30 (t, *J* = 6.8 Hz, 2H), 1.81 – 1.67 (m, 2H), 1.44 – 1.22 (m, 6H), 0.95 – 0.83 (m, 3H). ¹³C NMR (126 MHz, CDCl₃) δ 162.9, 143.1, 132.6, 132.4, 128.4, 65.6, 31.7, 28.9, 25.9, 22.8, 14.3.

Table 4.4. Optimization of P3HET synthesis from monomer **4.1**.

Catalyst	% Cat. (mol)	Time (min) ^a	<i>M_n</i> (GPC)	<i>D</i>	Yield (%)
Ni(PPh ₃)IPrCl ₂	5	630	7600	1.19	53
Ni(PPh ₃)IPrCl ₂	2	80	16400	1.25	75
Ni(PPh ₃)IPrCl ₂	1	140	30600	1.30	79
Ni(1-Naph)(PCy ₃) ₂ Br	5	90	4500	1.14	58
Ni(1-Naph)(PCy ₃) ₂ Br	2	300	10500	1.60	69
PEPPSI-IPr	2	780	5500	1.28	20
Ni(dppp)Cl ₂	2	720	13600	1.55	69

^aAll times listed were started when the vial was placed in the 50 °C oil bath.

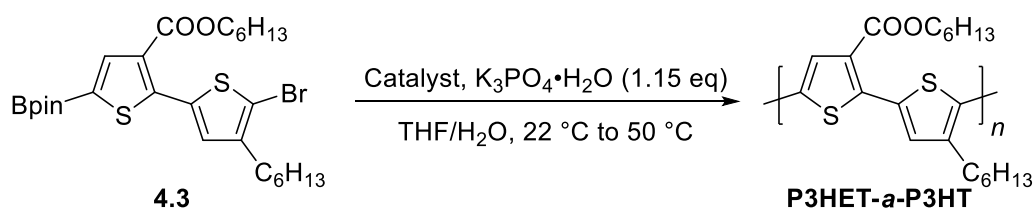
Scheme 4.7. Synthesis of P3HT.

Representative procedure for P3HT synthesis. In a N₂ filled glove box, a 20 mL scintillation vial equipped with a Teflon screw cap was charged with a calculated amount of catalyst (mol % listed in Table 4.5), K₃PO₄·H₂O (0.080 g, 0.35 mmol), nonadecane (0.080 g, 0.30 mmol) as the internal standard, and 5 mL of THF. The vial was sealed, removed from the glovebox and the reaction mixture was stirred at room temperature. Monomer **4.2** (0.114 g, 0.31 mmol) in 2 mL of THF was injected into the reaction mixture followed by degassed H₂O then, the vial was immersed in an oil bath at 50 °C. The reaction mixture was sampled periodically and polymer aliquots were prepared by quenching ~0.2 mL of the polymer solution with ~2.0 mL of 6 M methanolic HCl. The precipitate was filtered and washed with methanol and acetone to remove any monomer and low molecular weight oligomers. The resultant polymer was dissolved in ~1 mL of THF with gentle heating, filtered through a 0.22 μm PTFE syringe filter, and analyzed using GPC (relative to polystyrene) with THF as the eluent.

Table 4.5. Optimization of water content in P3HT synthesis from monomer **4.2**.

Catalyst	% Cat. (mol)	H ₂ O (mL)	Time (min)	<i>M_n</i> (GPC)	<i>D</i>
Ni(PPh ₃)IPrCl ₂	2	0	1200	6200	1.65
Ni(PPh ₃)IPrCl ₂	2	0.02	35	8100	1.54
Ni(PPh ₃)IPrCl ₂	2	0.05	35	8700	1.50
Ni(PPh ₃)IPrCl ₂	2	0.08	35	42100	1.37
Ni(PPh ₃)IPrCl ₂	2	0.10	15	61300	1.13
Ni(PPh ₃)IPrCl ₂ ^a	2	0.10	45	74400	1.30
Ni(dppp)Cl ₂	2	0	1110	8200	1.54
Ni(dppp)Cl ₂	2	0.05	140	16000	1.15
Ni(dppp)Cl ₂	2	0.10	30	17100	1.09
Ni(dppp)Cl ₂ ^b	2	0.10	60	18600	1.08

^a Isolated yield = 71%. ^b Isolated yield = 59%.

Scheme 4.8. Synthesis of P3HET-*a*-P3HT.

Representative procedure for P3HET-*a*-P3HT synthesis. In a N₂ filled glovebox, a 20 mL scintillation vial equipped with a Teflon screw cap was charged with a calculated amount of catalyst (listed in Table 4.6 below), K₃PO₄·H₂O (0.080 g, 0.35 mmol) and 5 mL of THF. The vial was capped, removed from the glovebox and the reaction mixture was stirred at room temperature. Monomer **4.3** (0.18 g, 0.31 mmol) in 2 mL of THF was injected into the reaction mixture followed by degassed H₂O then, the vial was immersed in an oil bath at 50 °C. The reaction mixture was stirred for period of time and then, the polymerization was quenched using 6 M methanolic HCl solution. The precipitate was collected using vacuum filtration, then washed with methanol and acetone to remove any unreacted monomer and oligomers. The final polymer was collected as a purple solid and dried *in vacuo*. ¹H NMR (500 MHz, CDCl₃) δ 7.54 (s, 1H), 7.38 (s, 1H), 4.30 (t, *J* = 6.7 Hz, 2H), 2.80 (t, *J* = 7.9 Hz, 2H), 1.81 – 1.57 (m, 4H), 1.49 – 1.27 (m, 12H), 0.97 – 0.83

(m, 6H). ^{13}C NMR (126 MHz, CDCl_3) δ 163.3, 142.3, 140.9, 133.9, 132.5, 132.0, 129.1, 128.1, 65.5, 31.9, 31.7, 30.8, 29.6, 29.5, 28.9, 26.0, 22.9, 22.8, 14.34 and 14.26 (2 overlapping signals).

Note: only 7 of the 8 possible signals from the thiophene rings are visible due to similarities between chemical environments.

Table 4.6. Synthesis of P3HET-*a*-P3HT from monomer **4.3**.

Catalyst	% Cat. (mol)	H_2O (mL)	Time (min)	M_n (GPC)	D	Yield (%)
Ni(PPh ₃)IPrCl ₂	2	0	210	27700	1.63	67
Ni(PPh ₃)IPrCl ₂	2	0.10	60	22600	6.08	52
Ni(dppp)Cl ₂	2	0.10	60	36500	1.13	59
Ni(dppp)Cl ₂	1	0.10	120	49000	1.48	52

Synthesis of Block Copolymers

Using Ni(PPh₃)IPrCl₂ as the catalyst and synthesizing P3HT first.

In a N_2 filled glovebox, a 20 mL scintillation vial equipped with a Teflon screw cap was charged with Ni(PPh₃)IPrCl₂ (9.5 mg, 4 mol %), $\text{K}_3\text{PO}_4 \cdot \text{H}_2\text{O}$ (0.080 g, 0.35 mmol), nonadecane (0.080 g, 0.30 mmol) as the internal standard, monomer **4.2** (0.114 g, 0.31 mmol) and 7 mL of THF. The vial was capped and removed from the glovebox. Degassed water (0.1 mL) was then injected and the mixture was stirred at room temperature. After 10 s of stirring, an aliquot (0.2 mL) was withdrawn from the solution and subjected to GC-MS analysis. The reaction mixture was stirred at room temperature for 30 min before another aliquot (0.4 mL) was withdrawn to determine the monomer conversion and molecular weight of resultant polymer ($M_n = 21100$, $D = 1.14$). Monomer **4.1** (0.13 g, 0.31 mmol) in 2 mL of THF was then injected into the solution and the mixture was stirred at 40 °C for another 30 min. A final aliquot was withdrawn to determine the monomer conversion and molecular weight of the block copolymer ($M_n = 29500$, $D = 1.28$). The polymerization was quenched using 6 M methanolic HCl solution. The precipitate was collected

using vacuum filtration, then washed with methanol and acetone to remove any unreacted monomer and oligomers. The final polymer was collected as a purple solid and dried *in vacuo* (54.3 mg, 46%).

Using Ni(PPh₃)IPrCl₂ as the catalyst and synthesizing P3HET first.

In a N₂ filled glovebox, a 20 mL scintillation vial equipped with a Teflon screw cap was charged with Ni(PPh₃)IPrCl₂ (9.5 mg, 4 mol %), K₃PO₄·H₂O (0.080 g, 0.35 mmol), nonadecane (0.080 g, 0.30 mmol) as the internal standard, and 5 mL of THF. The vial was sealed and removed from the glovebox. Monomer **4.1** (0.13 g, 0.31 mmol) in 2 mL of THF was injected into the solution. After 10 s of stirring at room temperature, an aliquot (0.2 mL) was withdrawn from the solution and subjected to GC-MS analysis. The reaction mixture was stirred at room temperature for 30 min before being placed in an oil bath at 50 °C. After 80 min, another aliquot (0.4 mL) was withdrawn to determine the monomer conversion and molecular weight of the resultant polymer ($M_n = 4500$, $D = 1.19$). The solution was then transferred via syringe to another vial containing monomer **4.2** (0.114 g, 0.31 mmol) and K₃PO₄·H₂O (0.080 g, 0.35 mmol). Degassed water (0.1 mL) was added to the mixture and, after stirring for 1 h at 50 °C, a final aliquot was withdrawn to determine the monomer conversion and molecular weight of the block copolymer ($M_n = 12700$, $D = 1.28$). The polymerization was quenched using 6 M methanolic HCl solution. The precipitate was collected using vacuum filtration, then washed with methanol and acetone to remove any unreacted monomer and oligomers. The final polymer was collected as a purple solid and dried *in vacuo* (76.3 mg, 65%).

Using Ni(dppp)Cl₂ as the catalyst and growing P3HT first.

In a N₂ filled glovebox, a 20 mL scintillation vial equipped with a Teflon screw cap was charged with Ni(dppp)Cl₂ (6.6 mg, 4 mol %), K₃PO₄·H₂O (0.080 g, 0.35 mmol), nonadecane (0.080 g, 0.30

mmol) as the internal standard, and 5 mL of THF. The vial was capped and removed from the glovebox. Monomer **4.2** (0.114 g, 0.31 mmol) in 2 mL of THF was injected into the solution followed by degassed water (0.1 mL). After 10 s, an aliquot (0.2 mL) was withdrawn from the solution and subjected to GC-MS analysis. The vial was then placed in an oil bath at 40 °C and the reaction mixture was stirred for 1 h before another aliquot (0.4 mL) was withdrawn to determine the monomer conversion and molecular weight of resultant polymer ($M_n = 11900$, $D = 1.08$). The solution was then transferred via syringe to another vial containing monomer **4.1** (0.13 g, 0.31 mmol) and $K_3PO_4 \cdot H_2O$ (0.08 g, 0.35 mmol). The reaction mixture was stirred at 40 °C for 1 h and a final aliquot was withdrawn to determine the monomer conversion and molecular weight of the block copolymer ($M_n = 15700$, $D = 1.21$). The polymerization was quenched using 6 M methanolic HCl solution. The precipitate was collected using vacuum filtration, then washed with methanol and acetone to remove any unreacted monomer and oligomers. The final polymer was collected as a purple solid and dried *in vacuo* (41 mg, 35%).

Using Ni(dppp)Cl₂ as the catalyst and growing P3HET first.

In a N₂ filled glovebox, a 20 mL scintillation vial equipped with a Teflon screw cap was charged with Ni(dppp)Cl₂ (6.6 mg, 4 mol %), $K_3PO_4 \cdot H_2O$ (0.08 g, 0.35 mmol), nonadecane (0.08 g, 0.30 mmol) as the internal standard, and 5 mL of THF. The vial was capped and removed from the glovebox. Monomer **4.1** (0.13 g, 0.31 mmol) in 2 mL of THF was injected into the solution, followed by degassed water (0.1 mL). After 10 s of stirring at room temperature, an aliquot (0.2 mL) was withdrawn from the solution and subjected to GC-MS analysis. The vial was then placed in an oil bath at 40 °C and the reaction mixture was stirred for 1 h before another aliquot (0.4 mL) was withdrawn to determine the monomer conversion and molecular weight of resultant polymer ($M_n = 3600$, $D = 1.10$). The solution was then transferred via syringe to another vial containing

monomer **4.2** (0.114 g, 0.31 mmol) and $\text{K}_3\text{PO}_4\cdot\text{H}_2\text{O}$ (0.08 g, 0.35 mmol). Water (0.1 mL) was added and the mixture was stirred at 40 °C for 1 h when a final aliquot was withdrawn to determine the monomer conversion and molecular weight of the block copolymer ($M_n = 10500$, $D = 1.28$). The polymerization was quenched using 6 M methanolic HCl solution. The precipitate was collected using vacuum filtration, then washed with methanol and acetone to remove any unreacted monomer and oligomers. The final polymer was collected as a purple solid and dried *in vacuo* (40 mg, 34%).

Optical Properties

Table 4.7. Summary of optical properties of P3HET, P3HT-*b*-P3HET, P3HET-*a*-P3HT, P3HT.

Polymer	λ_{max} CHCl_3	λ_{max} film	E_g^{opt} (eV) ^a
P3HET	435	505	2.17
P3HT- <i>b</i> -P3HET	445	550	1.92
P3HET- <i>a</i> -P3HT	452	627	1.85
P3HT	453	560	1.89

^aDetermined by onset of absorption (UV-Vis).

4.5 References

1. Müller, A. H. E.; Matyjaszewski, K. *Controlled and Living Polymerizations: From Mechanisms to Applications*; Wiley-VCH Verlag GmbH & Co. KGaA: Weinheim, Germany., 2009.
2. (a) Yokozawa, T.; Ohta, Y. *Chem. Rev.* **2016**, *116*, 1950-1968. (b) Grisorio, R.; Suranna, G. P. *Polym. Chem.* **2015**, *6*, 7781-7795. (c) Bryan, Z. J.; McNeil, A. J. *Macromolecules* **2013**, *46*, 8395-8405. (d) Okamoto, K.; Luscombe, C. K. *Polym. Chem.* **2011**, *2*, 2424-2434. (e) Kiriya, A.; Senkovskyy, V.; Sommer, M. *Macromol. Rapid Commun.* **2011**, *32*, 1503-1517. (f) Yokozawa, T.; Yokoyama, A. *Chem. Rev.* **2009**, *109*, 5595-5619.
3. Mei, J.; Bao, Z. *Chem. Mater.* **2014**, *26*, 604-615.
4. (a) Zhang, H.-H.; Peng, W.; Dong, J.; Hu, Q.-S. *ACS Macro Lett.* **2016**, *5*, 656-660. (b) Zhang, H.-H.; Xing, C.-H.; Hu, Q.-S.; Hong, K. *Macromolecules* **2015**, *48*, 967-978. (c) Qiu, Y.; Mohin, J.; Tsai, C.-H.; Tristram-Nagle, S.; Gil, R. R.; Kowalewski, T.; Noonan, K. J. T. *Macromol. Rapid Commun.* **2015**, *36*, 840-844. (d) Grisorio, R.; Mastroilli, P.; Suranna, G. P. *Polym. Chem.* **2014**, *5*, 4304-4310. (e) Sui, A.; Shi, X.; Tian, H.; Geng, Y.; Wang, F. *Polym. Chem.* **2014**, *5*, 7072-7080. (f) Kang, S.; Ono, R. J.; Bielawski, C. W. *J. Am. Chem. Soc.* **2013**, *135*, 4984-4987. (g) Yokoyama, A.; Suzuki, H.; Kubota, Y.; Ohuchi, K.; Higashimura, H.; Yokozawa, T. *J. Am. Chem. Soc.* **2007**, *129*, 7236-7237.
5. Hopkinson, M. N.; Richter, C.; Schedler, M.; Glorius, F. *Nature* **2014**, *510*, 485-496.
6. (a) Prakasham, A. P.; Ghosh, P. *Inorg. Chim. Acta* **2015**, *431*, 61-100. (b) Tasker, S. Z.; Standley, E. A.; Jamison, T. F. *Nature* **2014**, *509*, 299-309. (c) Han, F.-S. *Chem. Soc. Rev.* **2013**, *42*, 5270-5298. (d) Rosen, B. M.; Quasdorf, K. W.; Wilson, D. A.; Zhang, N.; Resmerita, A.-M.; Garg, N. K.; Percec, V. *Chem. Rev.* **2011**, *111*, 1346-1416. (e) Hu, X. *Chem. Sci.* **2011**, *2*, 1867-

1886. (f) Jana, R.; Pathak, T. P.; Sigman, M. S. *Chem. Rev.* **2011**, *111*, 1417-1492. (g) Phapale, V. B.; Cárdenas, D. J. *Chem. Soc. Rev.* **2009**, *38*, 1598-1607.

7. (a) Willot, P.; Koeckelberghs, G. *Macromolecules* **2014**, *47*, 8548-8555. (b) Bhatt, M. P.; Magurudeniya, H. D.; Sista, P.; Sheina, E. E.; Jeffries-EL, M.; Janesko, B. G.; McCullough, R. D.; Stefan, M. C. *J. Mater. Chem. A* **2013**, *1*, 12841-12849.

8. (a) Hu, X.; Shi, M.; Chen, J.; Zuo, L.; Fu, L.; Liu, Y.; Chen, H. *Macromol. Rapid Commun.* **2011**, *32*, 506-511. (b) Murphy, A. R.; Liu, J.; Luscombe, C.; Kavulak, D.; Fréchet, J. M. J.; Kline, R. J.; McGehee, M. D. *Chem. Mater.* **2005**, *17*, 4892-4899.

9. (a) Smith, Z. C.; Meyer, D. M.; Simon, M. G.; Staii, C.; Shukla, D.; Thomas III, S. W. *Macromolecules* **2015**, *48*, 959-966. (b) Liu, J.; Kadnikova, E. N.; Liu, Y.; McGehee, M. D.; Fréchet, J. M. J. *J. Am. Chem. Soc.* **2004**, *126*, 9486-9487.

10. (a) Bridges, C. R.; Guo, C.; Yan, H.; Miltenburg, M. B.; Li, P.; Li, Y.; Seferos, D. S. *Macromolecules* **2015**, *48*, 5587-5595. (b) Wang, C.; Kim, F. S.; Ren, G.; Xu, Y.; Pang, Y.; Jenekhe, S. A.; Jia, L. *J. Polym. Sci., Part A: Polym. Chem.* **2010**, *48*, 4681-4690.

11. (a) Tamba, S.; Shono, K.; Sugie, A.; Mori, A. *J. Am. Chem. Soc.* **2011**, *133*, 9700-9703. (b) Sheina, E. E.; Liu, J.; Iovu, M. C.; Laird, D. W.; McCullough, R. D. *Macromolecules* **2004**, *37*, 3526-3528. (c) Yokoyama, A.; Miyakoshi, R.; Yokozawa, T. *Macromolecules* **2004**, *37*, 1169-1171.

12. (a) Jezorek, R. L.; Zhang, N.; Leowanawat, P.; Bunner, M. H.; Gutsche, N.; Pesti, A. K. R.; Olsen, J. T.; Percec, V. *Org. Lett.* **2014**, *16*, 6326-6329. (b) Leowanawat, P.; Zhang, N.; Safi, M.; Hoffman, D. J.; Fryberger, M. C.; George, A.; Percec, V. *J. Org. Chem.* **2012**, *77*, 2885-2892.

13. (a) Chen, M.-T.; Vicic, D. A.; Turner, M. L.; Navarro, O. *Organometallics* **2011**, *30*, 5052-5056. (b) Nasielski, J.; Hadei, N.; Achonduh, G.; Kantchev, E. A. B.; O'Brien, C. J.; Lough, A.;

Organ, M. G. *Chem.-Eur. J.* **2010**, *16*, 10844-10853. (c) Diebolt, O.; Jurčík, V.; Correa da Costa, R.; Braunstein, P.; Cavallo, L.; Nolan, S. P.; Slawin, A. M. Z.; Cazin, C. S. J. *Organometallics* **2010**, *29*, 1443-1450.

14. Bryan, Z. J.; Hall, A. O.; Zhao, C. T.; Chen, J.; McNeil, A. J. *ACS Macro Lett.* **2016**, *5*, 69-72.

15. (a) Gobalasingham, N. S.; Noh, S.; Thompson, B. C. *Polym. Chem.* **2016**, *7*, 1623-1631. (b) Zhou, C. Y.; Yan, L. T.; Zhang, L. N.; Ai, X. D.; Li, T. X.; Dai, C. A. *J. Macromol. Sci., Part A: Pure Appl. Chem.* **2012**, *49*, 293-297. (c) Amarasekara, A. S.; Pomerantz, M. *Synthesis* **2003**, 2255-2258. (d) Pomerantz, M.; Cheng, Y.; Kasim, R. K.; Elsenbaumer, R. L. *J. Mater. Chem.* **1999**, *9*, 2155-2163. (e) Pomerantz, M.; Cheng, Y.; Kasim, R. K.; Elsenbaumer, R. L. *Synth. Met.* **1997**, *85*, 1235-1236. (f) Pomerantz, M.; Yang, H.; Cheng, Y. *Macromolecules* **1995**, *28*, 5706-5708.

16. Thiophenes with an ester group in the side chain have been polymerized in a controlled manner using Kumada and Negishi CTP, though the ester was not in conjugation with the aromatic ring. See for example: (a) Kudret, S.; Van den Brande, N.; Defour, M.; Van Mele, B.; Lutsen, L.; Vanderzande, D.; Maes, W. Synthesis of Ester Side Chain Functionalized All-Conjugated Diblock Copolythiophenes via the Rieke Method. *Polym. Chem.* **2014**, *5*, 1832-1837. (b) Suspène, C.; Miozzo, L.; Choi, J.; Gironde, R.; Geffroy, B.; Tondelier, D.; Bonnassieux, Y.; Horowitz, G.; Yassar, A. Amphiphilic Conjugated Block Copolymers for Efficient Bulk Heterojunction Solar Cells. *J. Mater. Chem.* **2012**, *22*, 4511-4518. (c) Ho, C.-C.; Liu, Y.-C.; Lin, S.-H.; Su, W.-F. Synthesis, Morphology, and Optical and Electrochemical Properties of Poly(3-hexylthiophene)-*b*-poly(3-thiophene hexylacetate). *Macromolecules* **2012**, *45*, 813-820. (d) Vallat, P.; Lamps, J.-P.; Schosseler, F.; Rawiso, M.; Catala, J.-M. Quasi-Controlled Polymerization through a Nickel

Catalyst Process of a Functionalized Thiophene Monomer: Kinetic Studies and Application to the Synthesis of Regioregular Poly(thiophene-3-acetic acid). *Macromolecules* **2007**, *40*, 2600-2602.

17. Chotana, G. A.; Kallepalli, V. A.; Maleczka Jr., R. E.; Smith III, M. R. *Tetrahedron* **2008**, *64*, 6103-6114.

18. Kosaka, K.; Ohta, Y.; Yokozawa, T. *Macromol. Rapid Commun.* **2015**, *36*, 373-377.

19. Kuivila, H. G.; Reuwer Jr, J. F.; Mangravite, J. A. *Can. J. Chem.* **1963**, *41*, 3081-3090.

20. (a) Cox, P. A.; Leach, A. G.; Campbell, A. D.; Lloyd-Jones, G. C. *J. Am. Chem. Soc.* **2016**, *138*, 9145-9157. (b) Tyrrell, E.; Brookes, P. *Synthesis* **2003**, 469-483.

21. (a) Lozada, J.; Liu, Z.; Perrin, D. M. *J. Org. Chem.* **2014**, *79*, 5365-5368. (b) Brandão, M. A. F.; Braga de Oliveira, A.; Snieckus, V. *Tetrahedron Lett.* **1993**, *34*, 2437-2440.

22. *Boronic acids*; Hall, D. G., Ed.; Wiley-VCH Verlag GmbH & Co. KGaA: Weinheim, Germany, 2005.

23. Lennox, A. J. J.; Lloyd-Jones, G. C. *Chem. Soc. Rev.* **2014**, *43*, 412-443.

24. Inada, K.; Miyaura, N. *Tetrahedron* **2000**, *56*, 8657-8660.

25. Astakhov, A. V.; Khazipov, O. V.; Degtyareva, E. S.; Khrustalev, V. N.; Chernyshev, V. M.; Ananikov, V. P. *Organometallics* **2015**, *34*, 5759-5766.

26. (a) Pollit, A. A.; Bridges, C. R.; Seferos, D. S. *Macromol. Rapid Commun.* **2015**, *36*, 65-70. (b) Todd, A. D.; Bielawski, C. W. *ACS Macro Lett.* **2015**, *4*, 1254-1258. (c) Tkachov, R.; Karpov, Y.; Senkovskyy, V.; Raguzin, I.; Zessin, J.; Lederer, A.; Stamm, M.; Voit, B.; Beryozkina, T.; Bakulev, V.; Zhao, W.; Facchetti, A.; Kiriy, A. *Macromolecules* **2014**, *47*, 3845-3851. (d) Elmalem, E.; Kiriy, A.; Huck, W. T. S. *Macromolecules* **2011**, *44*, 9057-9061. (e) Senkovskyy, V.; Tkachov, R.; Komber, H.; Sommer, M.; Heuken, M.; Voit, B.; Huck, W. T. S.; Kataev, V.; Petr, A.; Kiriy, A. *J. Am. Chem. Soc.* **2011**, *133*, 19966-19970.

27. Guo, X.; Baumgarten, M.; Müllen, K. *Prog. Polym. Sci.* **2013**, *38*, 1832-1908.
28. Goto, E.; Ando, S.; Ueda, M.; Higashihara, T. *ACS Macro Lett.* **2015**, *4*, 1004-1007.
29. Noh, S.; Gobalasingham, N. S.; Thompson, B. C. *Macromolecules* **2016**, 10.1021/acs.macromol.1026b01178.
30. Huo, L.; Chen, T. L.; Zhou, Y.; Hou, J.; Chen, H.-Y.; Yang, Y.; Li, Y. *Macromolecules* **2009**, *42*, 4377-4380.
31. Li, J.-C.; Lee, S.-H.; Hahn, Y.-B.; Kim, K.-J.; Zong, K.; Lee, Y.-S. *Synth. Met.* **2008**, *158*, 150-156.
32. (a) Yokozawa, T.; Suzuki, R.; Nojima, M.; Ohta, Y.; Yokoyama, A. *Macromol. Rapid Commun.* **2011**, *32*, 801-806. (b) Liversedge, I. A.; Higgins, S. J.; Giles, M.; Heeney, M.; McCulloch, I. *Tetrahedron Lett.* **2006**, *47*, 5143-5146.
33. Castañar, L.; Sistaré, E.; Virgili, A.; Williamson, R. T.; Parella, T. *Magn. Reson. Chem.* **2015**, *53*, 115-119.
34. Pomerantz, M.; Amarasekara, A. S.; Rasika Dias, H. V. *J. Org. Chem.* **2002**, *67*, 6931-6937.

Chapter 5

Nickel-Catalyzed Suzuki CTP for Polythiophenes Incorporating π -Accepting Functional Groups

5.1 Introduction

Since the discovery of organic semiconductors in 1977 by Shirakawa, MacDiarmid, and Heeger¹, the majority of synthetic paths to semiconducting polymers have relied on transition-metal-mediated step-growth polymerizations. In 2004, the first chain-growth polymerization process for conjugated polymers, now referred to as catalyst-transfer polycondensation (CTP), was reported.² During the last decade a number of π -conjugated architectures featuring controlled molecular weights and topologies have been synthesized.³ The most widely studied CTP process employs a Kumada cross-coupling protocol where the propagating monomer is an organomagnesium species.⁴ In addition to being highly reactive, organomagnesium reagents are quite nucleophilic and limit the range of suitable monomers. Thus, one glaring limitation of CTP has been functional group scope.^{3c} More mild cross-coupling strategies, such as Stille⁵ and Suzuki-Miyaura⁶ reactions, have also been utilized to prepare conjugated polymers with molecular weight control and low polydispersity. Despite reports of Stille and Suzuki-Miyaura CTP, functional group scope has remained restricted until recently, when an ester functionalized thiophene monomer was polymerized in a controlled fashion using nickel-catalyzed Suzuki CTP.⁷

The poor photo-oxidative stability of conjugated polymers, especially alkyl substituted polythiophenes, originates from a low ionization potential or high-lying highest occupied molecular orbital (HOMO).⁸ Tuning of the alkyl side-chain substitution pattern or incorporation of co-monomers that disrupt the conjugation pathway have led to increasingly stable

polythiophenes.⁹ Additionally, the incorporation of HOMO stabilizing π -accepting groups has been reported to increase ambient stability.¹⁰ Furthermore, π -accepting groups are also prevalent in many donor-acceptor polymers¹¹ or macromolecules capable of electron transport.¹² To date, the controlled synthesis of conjugated copolymers featuring electron-deficient blocks has been limited to a few reports on benzotriazole¹³, benzothiadiazole¹⁴ and naphthalene diimide (via a radical Negishi process)¹⁵ (Chart 5.1) but the homopolymerization of n-type monomers has not been realized. Thus, the controlled synthesis of electron-deficient or n-type polymeric semiconductors remains intensely investigated.

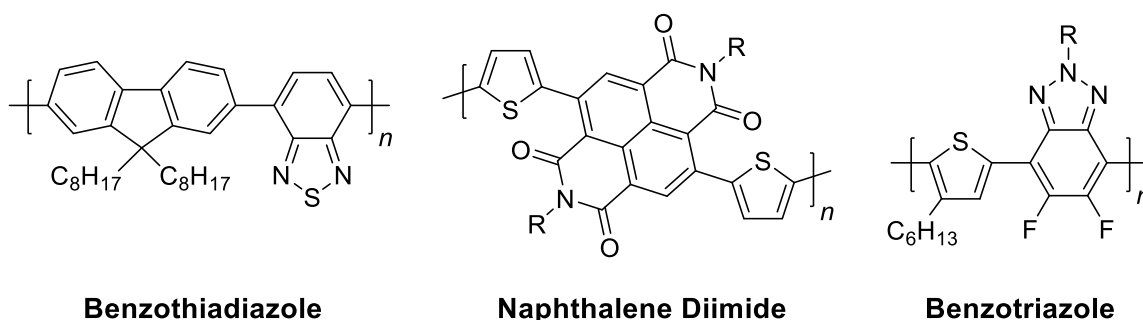


Chart 5.1. Donor-acceptor copolymers synthesized via chain-growth mechanism. The polymers are labeled according to their respective acceptor unit.

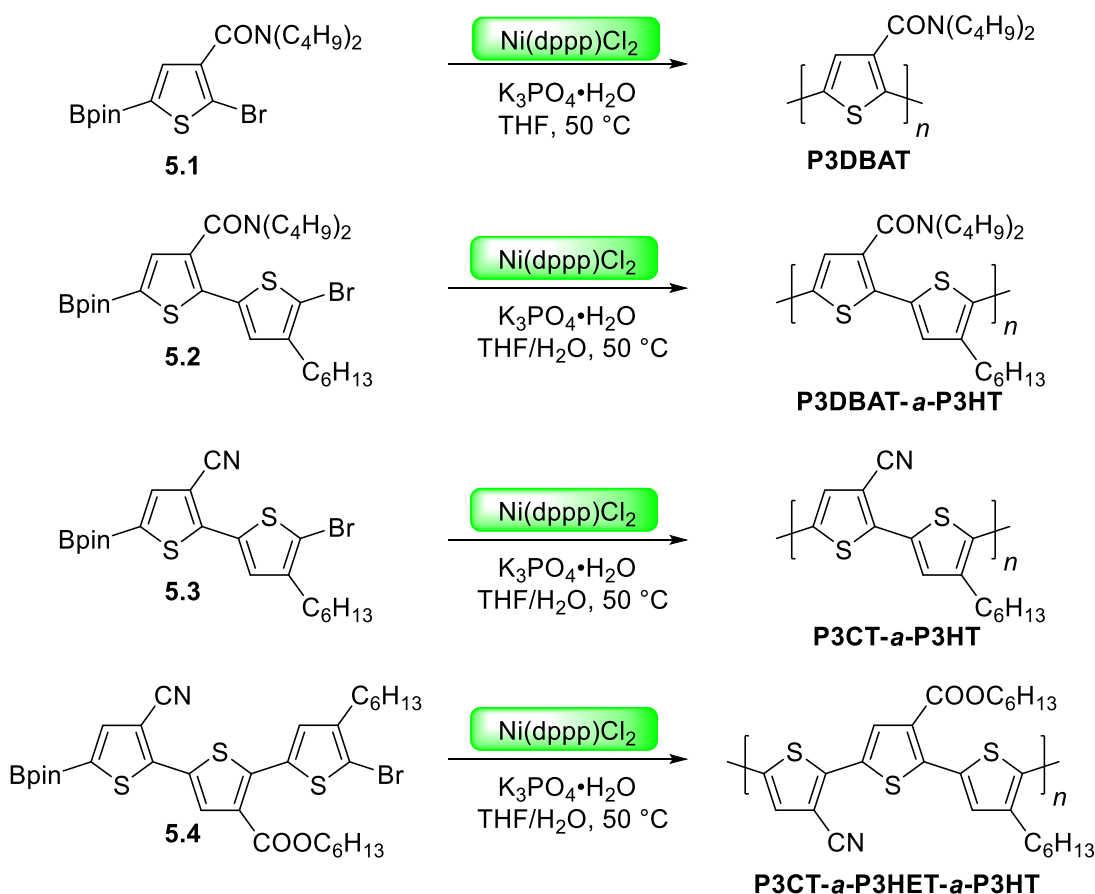
A substantial number of n-type materials feature the imide functional group.¹⁶ Rylene diimides¹⁷ and thiophene diimides¹⁸ are some of the most frequently appearing building blocks in low band gap donor-acceptor copolymers. However, the controlled synthesis of polymers featuring thiophene diimide blocks has not yet been realized. To investigate the suitability of imide functional groups in CTP, we envisioned the amide functional group as an appropriate starting point. Additionally, cyano substituted polythiophenes are known, though they have been prepared using uncontrolled step-growth polymerizations.¹⁹ Random poly(3-hexylthiophene) (P3HT)-based copolymers containing 5-20 mol % 3-cyanothiophene (CN-P3HT) presented increasingly stabilized HOMOs that correlated with 3-cyanothiophene content.^{19a,19b} Furthermore, the

photochemical stability of CN-P3HT is significantly better than pristine P3HT, clearly highlighting the advantage of electron-withdrawing groups.²⁰

To our knowledge, CTP with amide or cyano functional groups in conjugation with the monomer is unknown. Herein, we describe the controlled polymerization of amide-functionalized monomers and cyano-functionalized monomers using commercially available Ni(dppp)Cl₂ in a Suzuki CTP process.

5.2 Results and Discussion

Scheme 5.1. Polymers prepared using Ni(dppp)Cl₂ catalyzed Suzuki CTP.



Poly(N,N-dibutylthiophene-3-carboxamide) referred to as poly(3-dibutylamidethiophene) (P3DBAT) has not been reported (Scheme 5.1). Other amide substituted polythiophenes have been

prepared, but the polymers had low molecular weights with large polydispersities.²¹ The amide monomer (**5.1**) used in the study was prepared using a three-step synthesis starting from 3-thiophenecarboxylic acid. Borylation of the thiophene ring with pinacolborane was achieved using an iridium-catalyzed direct borylation.²²

The controlled synthesis of poly(3-hexylesterthiophene) (P3HET) was accomplished using nickel-catalyzed Suzuki coupling in THF with K₃PO₄·H₂O at 50 °C.⁷ Monomer **5.1** is structurally similar to the ester monomer so a similar protocol was employed for the Suzuki-mediated synthesis of P3DBAT. Ni(PPh₃)IPrCl₂, Ni(1-Naph)(PCy₃)₂Br and Ni(dppp)Cl₂ were screened, however, only Ni(dppp)Cl₂ was active for monomer **5.1**. Additionally, other bidentate phosphine ligated nickel catalysts were active, but Ni(dppp)Cl₂ was superior in regards to reactivity and polydispersity. When employing 4 mol % Ni(dppp)Cl₂, P3DBAT was obtained in reasonable yield (Table 5.1, entry 1).

Table 5.1. Polymerization studies for monomers **5.1**, **5.2**, **5.3**, and **5.4**.

Entry	Monomer	Ni (mol %)	Yield (%)	<i>M_n</i> (GPC) ^a	Đ	Time (min)
1	1	(4)	59	8,060	1.34	360
2	1	(2)	78	13,500	1.28	180
3	1	(1)	69	19,400	1.44	180
4 ^b	1	(2)	13	4,500	1.14	90
5 ^b	2	(4)	30	13,300	1.12	120
6 ^b	2	(2)	24	23,600	1.31	120
7	2	(2)	81	13,700	1.61	720
8 ^c	3	(10)	65	1,500	1.09	45
9 ^c	4	(10)	39	1,800	1.13	50

^aGPC traces were recorded at 40 °C versus polystyrene standards using THF as the eluent. ^b0.05 mL of H₂O was added. ^c0.10 mL of H₂O was added.

Lowering the catalyst loading (Table 5.1, entries 2-3) allowed for molecular weight modulation while maintaining control of polydispersity. However, a small shoulder was sometimes observed

in the GPC profiles which is approximately double the molecular weight of the primary distribution and we believe this is a consequence of disproportionation.^{3b,3c} When additional water is added to the polymerization reaction, a low molecular weight material is obtained in poor yield. We suspect this is due to competitive protodeborylation of the thiophene-based monomer.^{7,23}

We also explored a similar protocol to polymerize **5.2**, an alternating P3DBAT and P3HT comonomer (Scheme 5.1). Using Ni(dppp)Cl₂ and K₃PO₄·H₂O at 50 °C, the polymerization proceeded in a relatively uncontrolled fashion (Table 5.1, entry 7). The addition of water drastically increased both the reaction rate and molecular weight, while also narrowing the polydispersity (Table 5.1, entries 5-6); this effect is consistent with previous reports.^{7,24} Nevertheless, the sensitivity of **5.2** to aqueous alkaline conditions was noted as low yields were always obtained when additional water was added to the polymerization.

Block copolymers of P3DBAT and P3HT were also prepared, but the final copolymers had higher polydispersities than the initial polymer chains (Figure 5.1). The copolymerization can proceed starting from either block, despite the fact that water is a complicating factor as it is needed for controlled P3HT synthesis, but induces protodeborylation of monomer **5.1**.^{7,24} P3DBAT can be prepared using 2 mol % Ni(dppp)Cl₂ ($M_w = 13000$, $D = 1.15$) after which, addition of the hexyl thiophene monomer and 0.1 mL of water to the reaction mixture afforded the desired block copolymer (P3DBAT-*b*-P3HT, $M_w = 19200$, $D = 1.49$, 49%, Figure 5.1 – Top). P3HT can be prepared using 2 mol % Ni(dppp)Cl₂ and 0.1 mL of water ($M_w = 23100$, $D = 1.10$) after which, addition of monomer **5.1** to the reaction mixture afforded the block copolymer (P3HT-*b*-P3DBAT, $M_n = 27200$, $D = 1.44$, 30%, Figure 5.1 – Bottom).

Monomers **5.3** and **5.4** were polymerized with similar conditions used for monomer **5.2** (Scheme 5.1). P3CT-*a*-P3HT can be prepared using 10 mol % Ni(dppp)Cl₂ (Table 5.1, entry 8).

Efforts to obtain higher molecular weight materials at lower catalyst loadings were unsuccessful, likely due to the strong aggregation of the polymer during the polymerization. The trimeric monomer (**5.4**) was also polymerized at high catalyst loadings (Table 5.1, entry 9), but similarly failed when targeting higher molecular weights. Similar to a previous report^{19b}, the cyano containing polymers are plagued by poor solubility, thus preventing further analysis.

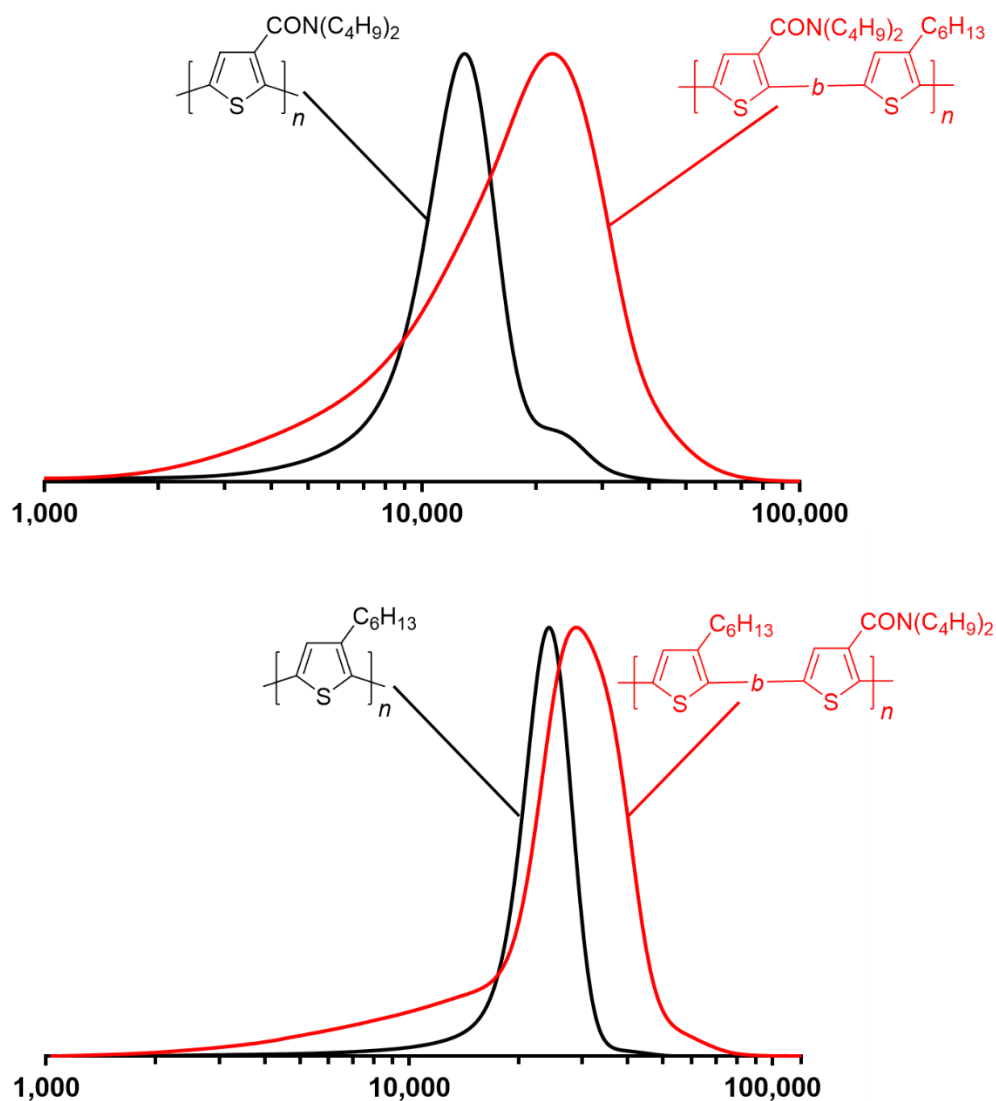


Figure 5.1. GPC chromatograms for the block copolymers. Top – synthesizing P3HT first. Bottom – synthesizing P3DBAT first.

The optical properties of P3DBAT, P3DBAT-*a*-P3HT, P3CT-*a*-P3HT, and P3CT-*a*-P3HET-*a*-P3HT were probed both in solution and in the solid-state. The amide-thiophene polymers were compared to P3HT, P3HET, and P3HET-*a*-P3HT for reference (Figure 5.2).⁷ P3DBAT ($\lambda_{\text{max}} = 490 \text{ nm}$) is significantly red-shifted as compared to both P3HT ($\lambda_{\text{max}} = 452 \text{ nm}$) and P3HET ($\lambda_{\text{max}} = 435 \text{ nm}$) in solution. However, in the solid-state, P3DBAT ($E_{\text{g}}^{\text{opt}} = 2.09 \text{ eV}$) is blue-shifted to P3HT ($E_{\text{g}}^{\text{opt}} = 1.89 \text{ eV}$) with a similar band gap to P3HET ($E_{\text{g}}^{\text{opt}} = 2.17 \text{ eV}$). Interestingly, the solid-state absorption profile of P3DBAT is featureless (Figure 5.3), indicating a lack of order likely caused by significant steric twisting due to the amide group. The absorption profile of P3DBAT-*a*-P3HT ($\lambda_{\text{max}} = 462 \text{ nm}$) is slightly red-shifted to P3HT ($\lambda_{\text{max}} = 453 \text{ nm}$) and P3HET-*a*-P3HT ($\lambda_{\text{max}} = 452 \text{ nm}$). However, similarly to P3DBAT, the alternating copolymer ($\lambda_{\text{max}} = 540 \text{ nm}$, $E_{\text{g}}^{\text{opt}} = 1.99 \text{ eV}$) is somewhat blue-shifted compared to P3HT ($\lambda_{\text{max}} = 560 \text{ nm}$, $E_{\text{g}}^{\text{opt}} = 1.89 \text{ eV}$) and P3HET-*a*-P3HT ($\lambda_{\text{max}} = 627 \text{ nm}$, $E_{\text{g}}^{\text{opt}} = 1.85 \text{ eV}$) in the solid-state.

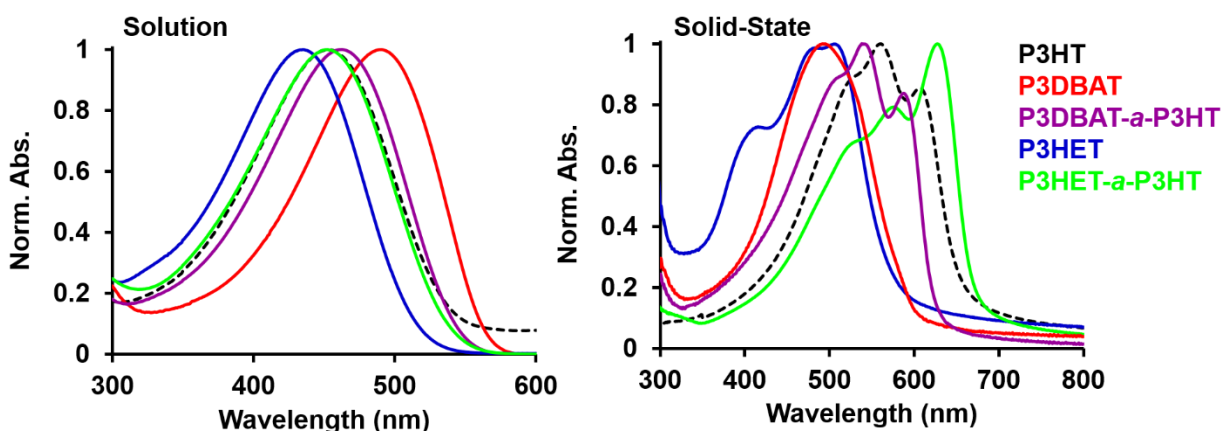


Figure 5.2. Solution (CHCl_3) and solid-state UV-vis spectra for amide polymers with P3HT, P3HET, and P3HET-*a*-P3HT included for reference.

The cyano-thiophene polymers were compared to P3HT (Figure 5.3). P3CNT-*a*-P3HT ($\lambda_{\text{max}} = 473 \text{ nm}$) is significantly red-shifted ($\sim 21 \text{ nm}$) to P3HT in solution. Yet, P3CNT-*a*-P3HT ($E_{\text{g}}^{\text{opt}} = 1.90 \text{ eV}$) has an absorption profile nearly identical to P3HT in the solid-state. A previously

reported random copolymer of P3HT:P3CT (5:1) ($E_g^{\text{opt}} = 1.86$ eV) has a slightly lower band gap than our alternating polymer, likely explained by the larger molecular weight ($M_n = 14,000$) for the random copolymer.^{19a,19b} The solution absorption of P3CT-*a*-P3HET-*a*-P3HT ($\lambda_{\text{max}} = 460$ nm) is slightly red-shifted to P3HT. In the solid-state, the band gap of P3CT-*a*-P3HET-*a*-P3HT is nearly identical to P3HT; however, the vibronic band ($\lambda_{\text{max}} = 605$ nm) becomes the dominant absorption feature. Impressively, the band gaps of P3CNT-*a*-P3HT and P3CT-*a*-P3HET-*a*-P3HT are quite similar to P3HT despite their significantly lower molecular weights.

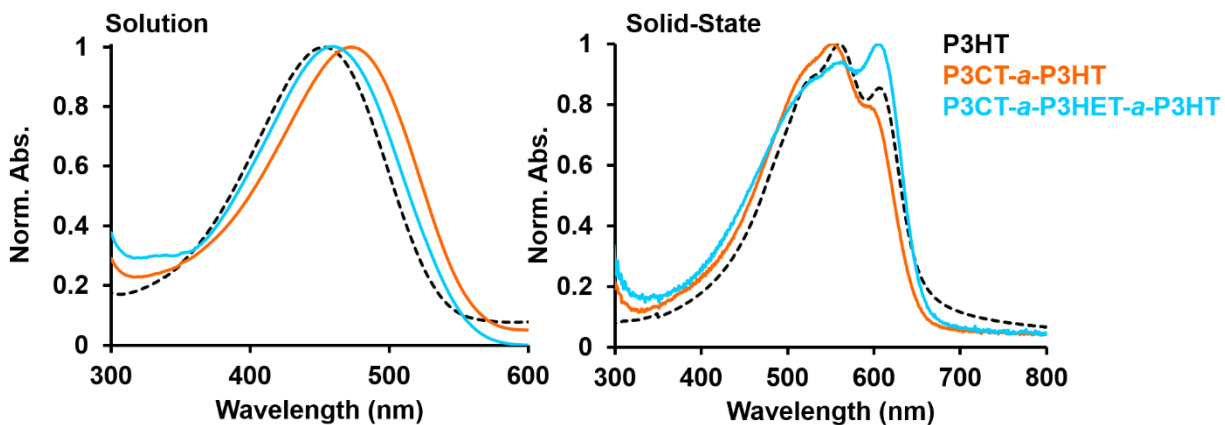


Figure 5.3. Solution (*o*-dichlorobenzene–cyano polymers, CHCl_3 –P3HT) and solid-state UV-vis spectra for cyano polymers with P3HT included for reference.

5.3 Conclusion

We have demonstrated the first example of controlled polythiophenes bearing π -accepting amide and cyano groups. Using a Suzuki catalyst-transfer polycondensation (CTP) with readily available $\text{Ni}(\text{dppp})\text{Cl}_2$, the amide-functionalized polythiophene could be obtained with molecular weight control, and block copolymers were synthesized with 3-hexylthiophene. The cyano-functionalized comonomers were also polymerized, but the resultant materials were found to be highly insoluble. Our nickel-catalyzed Suzuki protocol has now been applied to a diverse range

of functional groups. Using this protocol, the controlled synthesis of more sophisticated donor-acceptor copolymers or n-type homopolymers should be achievable.

5.4 Experimental Section

Materials and Methods. All reactions and manipulations of air and water sensitive compounds were carried out under a dry nitrogen atmosphere using an mBraun glovebox or standard Schlenk techniques. All compounds were purchased from commercial sources and used as received. 2-(4-3-Bromohexylthiophen-2-yl)-4,4,5,5-tetramethyl-1,3,2-dioxaborolane (hexyl thiophene monoer)^{7,25}, 2-bromo-3-thiophene carboxylic acid⁷ and 2-bromothiophene-3-carbonitrile^{19b} were synthesized according to literature procedures. All reaction solvents (tetrahydrofuran, dichloromethane, diethyl ether) were degassed with argon and dried prior to use. All solvents and chemicals used for extraction and column chromatography were used as received. Polymer samples were precipitated with 6 M methanolic HCl and washed with only methanol before GPC, NMR, and UV-vis analysis.

NMR analysis. All NMR experiments were collected at 300 K on a two-channel Bruker Avance III NMR instrument equipped with a Broad Band Inverse (BBI) probe, operating at 500 MHz for ¹H (126 MHz for ¹³C). ¹H NMR spectra are referenced to residual protio solvent (7.26 for CHCl₃, 5.32 for CHDCl₂, and 7.16) and ¹³C NMR spectra are referenced to the solvent signal (δ 77.23 for CDCl₃, 54.00 for CD₂Cl₂).

Mass Spectrometry. High Resolution Electron Impact Mass Spectrometry (HRMS), Electrospray Mass Spectrometry (ESI-MS) and MALDI-TOF Mass Spectrometry were performed in the School of Chemical Sciences Mass Spectrometry Laboratory at the University of Illinois, Urbana-Champaign.

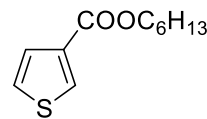
UV-Vis Spectroscopy. UV-vis spectra of polymers were recorded on a Varian Cary 5000 spectrophotometer. Solution measurements were conducted in CHCl_3 at 0.01 mg/mL concentration for P3DBAT, P3DBAT-*a*-P3HT and in *o*-dichlorobenzene at 0.01 mg/mL concentration for P3CT-*a*-P3HT and P3CT-*a*-P3HET-*a*-P3HT. Thin film samples were prepared from a spin-coating process. 22×22 mm glass cover slips were cleaned by spraying with fresh acetone, isopropanol and dried under a jet of filtered, dry nitrogen. P3DBAT and P3DBAT-*a*-P3HT solutions (2.5 mg/mL) in dry toluene were heated to 80 °C in amber glass vials for 10 min, filtered through a 0.22 μm PTFE syringe filter using a glass syringe, and re-heated for 5 min prior to spin-casting from hot solutions. The same conditions were used for P3CT-*a*-P3HT and P3CT-*a*-P3HET-*a*-P3HT except films were cast from *o*-dichlorobenzene (1 mg/mL) after heating to 150 °C. The spin-coating conditions consisted of three cycles, a 400 RPM spreading cycle for 5 s, a 1000 RPM main cycle for 30 s and a 2000 RPM wicking cycle for 15 s. The films were annealed at 150°C for 1 h under N_2 .

Gel-Permeation Chromatography. GPC measurements were performed on a Waters Instrument equipped with a 717 plus autosampler, a Waters 2414 refractive index (RI) detector and two SDV columns (Porosity 1000 and 100000 Å; Polymer Standard Services) with THF as the eluent (flow rate 1 mL/min, 40 °C). For P3CT-*a*-P3HT and P3CT-*a*-P3HET-*a*-P3HT (0.5 mg/mL sample concentration), *o*-dichlorobenzene was used as the eluent (flow rate 1 mL/min, 140 °C). A 10-point calibration based on polystyrene standards (Polystyrene, ReadyCal Kit, Polymer Standard Services) was applied for determination of molecular weights. All polymer aliquots subjected to GPC analysis were prepared by quenching ~0.2 mL of the polymer solution with ~2.0 mL of 6 M methanolic HCl. The precipitate was filtered and washed with methanol to remove any monomer.

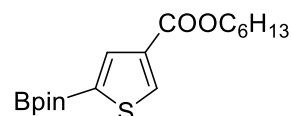
The resultant polymer was dissolved in ~1 mL of THF, filtered through a 0.22 μm PTFE syringe filter and analyzed.

Experimental Procedures

Synthesis of hexyl thiophene-3-carboxylate. An oven-dried 250 mL Schlenk flask was charged with thiophene-3-carboxylic acid (6.41 g, 50.0 mmol), K_2CO_3 (20.73 g, 150 mmol) and 60 mL of dimethylformamide. 1-Bromohexane (16.51 g, 100 mmol) was subsequently added by syringe. The flask was immersed in an oil bath at 90 $^\circ\text{C}$ and the solution was stirred for 12 h under a N_2 atmosphere. The reaction mixture was cooled to room temperature, diluted with 200 mL of water and transferred to a 500 mL separatory funnel. The aqueous layer was extracted with diethyl ether (4×100 mL) and the combined organic extracts were washed with water (2 x 50 mL) and brine (50 mL), then dried over MgSO_4 and concentrated using rotary evaporation. The crude product was purified using column chromatography on silica gel eluting with hexanes, followed by hexanes:dichloromethane (2:1) to afford the final product as a light yellow oil. The R_f of the product is ~0.7 in hexanes:dichloromethane = 2:1. The impure compound was then distilled (150 mTorr, 95 $^\circ\text{C}$ (Bath Temp.)) to afford the product as a clear oil (10.34 g, 97%). The ^1H and ^{13}C NMR spectra were compared to a previous report.²⁶

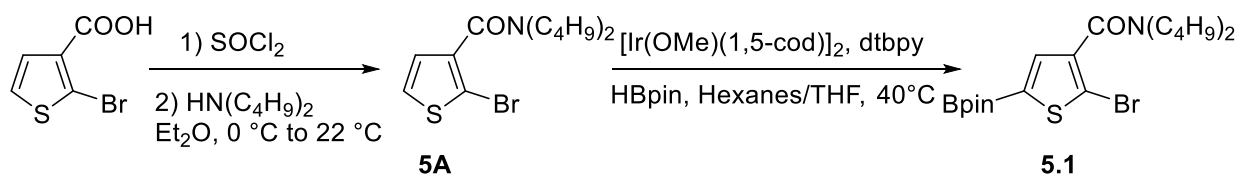


Synthesis of hexyl 5-(4,4,5,5-tetramethyl-1,3,2-dioxaborolan-2-yl)thiophene-3-carboxylate. In a N_2 filled glovebox, a 100 mL round bottom flask was charged with pinacolborane (HBpin) (4.61 g, 36.00 mmol), di- μ -methoxobis(1,5-cyclooctadiene)diiridium (0.298 g, 0.45 mmol) and 15 mL of dry hexanes. To this stirring mixture, 4,4'-Bis(di-*t*-butyl)-2,2'-bipyridine (dtbbpy) (0.241 g, 0.90 mmol) in 15 mL of hexanes was added in portions and the mixture was stirred for 5 min. The color of the reaction mixture went from



yellow to dark brown during that period. Hexyl thiophene-3-carboxylate (6.37 g, 30.0 mmol) was then dissolved in 15 mL of hexanes and added to the mixture slowly (H_2 gas evolves in this step). The solution was kept in the glovebox and stirred overnight. The crude mixture was then removed from the glovebox, loaded directly onto silica gel, and eluted using gradient solvent conditions (hexanes:dichloromethane = 1:1 to dichloromethane). The R_f of the product is ~ 0.3 in dichloromethane. The final product was collected as a clear, viscous oil (9.42 g, 93%). ^1H NMR (500 MHz, CDCl_3) δ 8.33 (d, $J = 0.8$ Hz, 1H), 8.02 (m, $J = 0.8$ Hz, 1H), 4.25 (t, $J = 6.7$ Hz, 1H), 1.76 – 1.67 (m, 1H), 1.45 – 1.36 (m, 1H), 1.35 (s, 6H), 1.36 – 1.25 (m, 3H), 0.93 – 0.86 (m, 1H). ^{13}C NMR (126 MHz, CDCl_3) 163.0, 139.1, 138.0, 135.5, 84.7, 65.1, 31.7, 28.9, 25.9, 25.0, 22.8, 14.2. Note: one aromatic signal is missing in the ^{13}C NMR spectrum due to quadrupolar relaxation. HR-EIMS (m/z): $[\text{M} + \text{H}]^+$ calculated for $\text{C}_{17}\text{H}_{28}\text{O}_4\text{BS}$, 339.1801; found, 339.1788.

Scheme 5.2. Synthesis of Monomer **5.1**.



Synthesis of 2-bromo-N,N-dibutylthiophene-3-carboxamide (5A). An

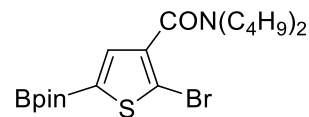
oven-dried 100 mL Schlenk flask was charged with 2-bromo-thiophene-3-



carboxylic acid (3.10 g, 15.0 mmol) and 10 mL thionyl chloride. The reaction mixture was heated to 65 °C and stirred for 2 h. Excess thionyl chloride was removed *in vacuo*, followed by the addition of 30 mL diethyl ether. The flask was cooled to 0 °C using an ice bath and dibutylamine (6.1 mL, 36.0 mmol) was slowly added to the flask. The mixture was stirred at room temperature for 1 h and, an aliquot was removed and analyzed using GC-MS to confirm formation of the product. The reaction mixture was then transferred to a separatory funnel and 1 M HCl solution

(30 mL) was added. The organic layer was separated and the aqueous layer was extracted with diethyl ether (2 × 30 mL). The combined organic extracts were washed with brine (30 mL), dried over MgSO₄ and concentrated to yield a dark brown oil. The compound was purified by column chromatography on silica gel eluting with hexanes:ethyl acetate = 5:1 to afford the title compound as a light brown oil (4.29 g, 90%). The *R_f* of the product is ~0.4 with hexanes:ethyl acetate = 5:1. ¹H NMR (500 MHz, CD₂Cl₂) δ 7.31 (d, *J* = 5.6 Hz, 1H), 6.88 (d, *J* = 5.6 Hz, 1H), 3.46 (t, *J* = 7.4 Hz, 2H), 3.16 (t, *J* = 7.4 Hz, 2H), 1.63 (p, *J* = 7.6 Hz, 2H), 1.43 (dp, *J* = 22.3, 7.4 Hz, 4H), 1.15 (q, *J* = 7.3 Hz, 2H), 0.97 (t, *J* = 7.3 Hz, 3H), 0.79 (t, *J* = 7.3 Hz, 3H). ¹³C NMR (126 MHz, CD₂Cl₂) δ 165.8, 139.0, 127.9, 127.5, 110.2, 48.8, 45.0, 31.4, 30.2, 20.9, 20.3, 14.3, 13.9. HRMS (ESI-TOF) (*m/z*): [M + H]⁺ calculated for C₁₃H₂₁NOSBr, 318.0527; found, 318.0533.

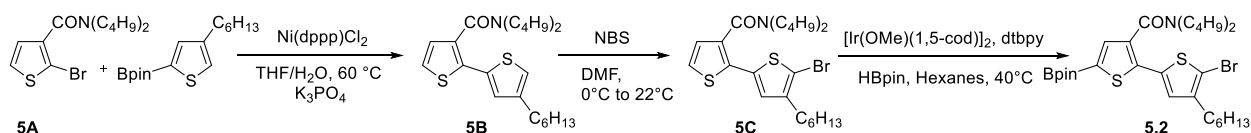
Synthesis of N,N-dibutyl 2-bromo-5-(4,4,5,5-tetramethyl-1,3,2-dioxaborolan-2-yl)thiophene-3-carboxamide (5.1). In a N₂ filled



glovebox, a 40 mL scintillation vial was charged with pinacolborane (HBpin) (1.20 g, 9.38 mmol), di- μ -methoxobis(1,5-cyclooctadiene)diiridium (0.062 g, 0.094 mmol) and 4 mL of dry hexanes. To this mixture, 4,4'-Bis(di-*t*-butyl)-2,2'-bipyridine (dtbbpy) (0.051 g, 0.19 mmol) in 4 mL of hexanes was added in portions and the mixture was stirred for 5 min. The color of the reaction mixture went from yellow to dark brown during that period. Compound **A** (2.0 g, 6.28 mmol) was then dissolved in 4 mL of THF and added to the mixture slowly (H₂ gas evolves in this step). The reaction vial was sealed, transferred from the glovebox into an oil bath at 40 °C, and stirred overnight. After cooling to room temperature, the crude mixture was loaded directly onto silica gel, and eluted using gradient solvent conditions (dichloromethane, followed by dichloromethane:ethyl acetate = 5:1). The *R_f* of the product is ~0.3 in dichloromethane:ethyl acetate = 5:1. The final product was isolated as a maroon oil (2.68 g, 96 %). ¹H NMR (500 MHz,

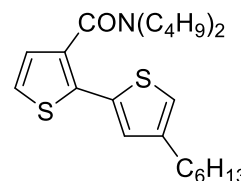
CDCl₃) δ 7.35 (s, 1H), 3.52 – 3.45 (m, 2H), 3.19 – 3.11 (m, 2H), 1.62 (p, J = 7.5 Hz, 2H), 1.43 (dp, J = 22.4, 7.4 Hz, 4H), 1.32 (s, 12H), 1.15 (h, J = 8.1, 7.3 Hz, 2H), 0.96 (t, J = 7.4 Hz, 3H), 0.79 (t, J = 7.4 Hz, 3H). ¹³C NMR (126 MHz, CDCl₃) δ 165.6, 139.8, 136.5, 117.3, 84.7, 48.5, 44.5, 31.0, 29.8, 24.9, 20.5, 20.0, 14.1, 13.8. Note: one aromatic signal is missing in the ¹³C NMR spectrum due to quadrupolar relaxation. HR-EIMS (m/z): [M]⁺ calculated for C₁₉H₃₂BNO₃SBr, 444.1379; found, 444.1389.

Scheme 5.3. Synthesis of Monomer 5.2.



Synthesis of N,N-dibutyl-4'-hexyl-[2,2'-bithiophene]-3-carboxamide

(5B). An oven-dried 100 mL Schlenk flask was charged with Compound 5A (2.67 g, 8.39 mmol), 2-(4-hexylthiophen-2-yl)-4,4,5,5-tetramethyl-1,3,2-

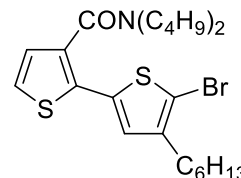


dioxaborolane (2.59 g, 8.80 mmol), Ni(dppp)Cl₂ (0.091 g, 0.17 mmol), K₃PO₄·H₂O (3.86 g, 16.8 mmol) and 20 mL of THF. The flask was then immersed in an oil bath at 60 °C and the solution was stirred 24 hours before cooling to room temperature. The mixture was diluted with 20 mL of dichloromethane and gravity filtered. The flask was washed with 3 portions of dichloromethane (30 mL) and the filtrate collected. The combined organic portions were dried with MgSO₄ and concentrated using rotary evaporation. The crude material was purified using column chromatography on silica gel, eluting with hexanes:ethyl acetate = 4:1 to afford the final product as a yellow oil (1.31 g, 39%). The R_f of the product is ~0.4 in hexanes:ethyl acetate (4:1). ¹H NMR (500 MHz, CDCl₃) δ 7.19 (d, J = 5.2 Hz, 1H), 7.04 (d, J = 1.4 Hz, 1H), 6.96 (d, J = 5.2 Hz, 1H), 6.85 (d, J = 1.3 Hz, 1H), 3.50 – 3.40 (m, 2H), 3.06 – 2.96 (m, 2H), 2.61 – 2.48 (m, 2H), 1.60 (dq, J = 15.0, 7.5 Hz, 4H), 1.40 – 1.21 (m, 10H), 1.05 (h, J = 7.4 Hz, 2H), 0.95 (t, J = 7.4 Hz, 3H), 0.92

–0.84 (m, 3H), 0.72 (t, $J = 7.4$ Hz, 3H). ^{13}C NMR (126 MHz, CDCl_3) δ 167.6, 144.3, 134.6, 133.9, 133.5, 127.8, 127.6, 124.8, 120.8, 48.6, 45.0, 31.9, 30.8, 30.7, 30.6, 29.5, 29.2, 22.8, 20.6, 20.0, 14.2, 13.8. HRMS (ESI-TOF) (m/z): $[\text{M} + \text{H}]^+$ calculated for $\text{C}_{23}\text{H}_{36}\text{NOS}_2$, 406.2238; found, 406.2247.

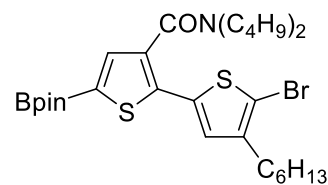
Synthesis of 5'-bromo-N,N-dibutyl-4'-hexyl-[2,2'-bithiophene]-3-

carboxamide (5C). Compound **5B** (1.14 g, 2.81 mmol) was dissolved in 10 mL of DMF and the solution was cooled to 0 °C. N-Bromosuccinimide



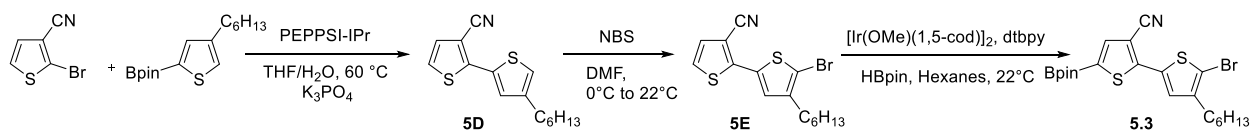
(0.55 g, 3.09 mmol), dissolved in 4 mL DMF was added to the reaction mixture dropwise over 20 minutes while maintaining a temperature of 0 °C. The reaction mixture was slowly warmed to room temperature in the bath and stirred overnight. The mixture was quenched with 50 mL of a saturated NaHCO_3 solution and the entire contents of the flask were transferred to a separatory funnel. The aqueous layer was extracted with diethyl ether (3×50 mL) and the combined organic extracts were washed with a saturated NaHCO_3 solution (20 mL) and brine (20 mL). The combined organic extracts were then dried over Na_2SO_4 and concentrated using rotary evaporation. The crude material was purified using column chromatography on silica gel, eluting with hexanes:ethyl acetate = 4:1 to afford the final product as a yellow oil (1.11 g, 82%). The R_f of the product is ~0.4 in hexanes:ethyl acetate (4:1). ^1H NMR (500 MHz, CDCl_3) δ 7.22 (d, $J = 5.2$ Hz, 1H), 6.95 (d, $J = 5.2$ Hz, 1H), 6.91 (s, 1H), 3.52 – 3.36 (m, 2H), 3.08 – 2.96 (m, 2H), 2.56 – 2.45 (m, 2H), 1.58 (dp, $J = 23.6, 7.5$ Hz, 4H), 1.32 (dp, $J = 22.6, 7.8$ Hz, 10H), 1.06 (h, $J = 7.4$ Hz, 2H), 0.96 (t, $J = 7.4$ Hz, 3H), 0.92 – 0.84 (m, 3H), 0.73 (t, $J = 7.4$ Hz, 3H). ^{13}C NMR (126 MHz, CDCl_3) δ 167.3, 143.1, 134.5, 133.9, 133.0, 127.8, 127.1, 125.2, 109.7, 77.2, 48.7, 45.1, 31.8, 30.9, 29.9, 29.8, 29.6, 29.1, 22.8, 20.6, 20.0, 14.3, 14.2, 13.8. HRMS (ESI-TOF) (m/z): $[\text{M} + \text{H}]^+$ calculated for $\text{C}_{23}\text{H}_{35}\text{NOS}_2\text{Br}$, 484.1348; found, 484.1343.

Synthesis of 5'-bromo-N,N-dibutyl-4'-hexyl-5-(4,4,5,5-tetramethyl-1,3,2-dioxaborolan-2-yl)-[2,2'-bithiophene]-3-



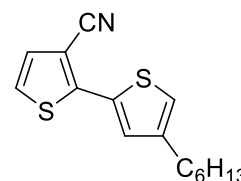
carboxamide (5.2). In a N₂ filled glovebox, a 40 mL scintillation vial was charged with pinacolborane (HBPin) (0.412 g, 3.2 mmol), Di- μ -methoxobis(1,5-cyclooctadiene)diiridium (0.043 g, 0.065 mmol) and 3 mL of dry hexanes. To this mixture, 4,4'-Bis(di-*t*-butyl)-2,2'-bipyridine (dtbbpy) (0.035 g, 0.13 mmol) in 3 mL of hexanes was added in portions and the mixture was stirred for 15 min. The color of the reaction mixture went from yellow to dark brown during that period. Compound **5C** (1.04 g, 2.15 mmol) was then dissolved in 2 mL of hexanes and added to the reaction mixture slowly (H₂ gas evolves in this step). The reaction vial was sealed, transferred out of the glovebox to an oil bath at 40 °C, and stirred overnight. After cooling to room temperature, the crude mixture was loaded directly onto silica gel, and eluted with a gradient solvent conditions (dichloromethane, followed by dichloromethane:acetone = 40:1). The *R_f* of the product is ~0.3 in dichloromethane. The final product was collected as a brown oil (0.98 g, 75%). ¹H NMR (500 MHz, CDCl₃) δ 7.41 (s, 1H), 6.96 (s, 1H), 3.50 – 3.40 (m, 2H), 3.07 – 2.96 (m, 2H), 2.55 – 2.44 (m, 2H), 1.64 – 1.50 (m, 4H), 1.40 – 1.20 (m, 24H), 1.04 (h, *J* = 7.3 Hz, 2H), 0.96 (t, *J* = 7.4 Hz, 3H), 0.91 – 0.82 (m, 3H), 0.71 (t, *J* = 7.3 Hz, 3H). ¹³C NMR (126 MHz, CDCl₃) δ 167.2, 143.2, 139.5, 137.3, 135.0, 134.6, 127.4, 110.4, 84.6, 48.8, 45.0, 31.8, 30.9, 29.8, 29.7, 29.6, 29.1, 25.0, 22.8, 20.6, 20.0, 14.3, 14.1, 13.8. Note: one aromatic signal is missing in the ¹³C NMR spectrum due to quadrupolar relaxation. HRMS (ESI-TOF) (*m/z*): [M]⁺ calculated for C₂₉H₄₅BBrNO₃S₂, 609.2117; found, 609.2106.

Scheme 5.4. Synthesis of Monomer 5.3.



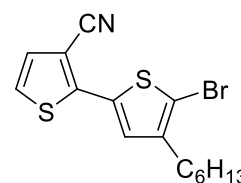
Synthesis of 4'-hexyl-[2,2'-bithiophene]-3-carbonitrile (5D).

An oven-dried 100 mL Schlenk flask was charged with 2-bromo-thiophene-3-carbonitrile (1.22 g, 6.47 mmol), 2-(4-hexylthiophen-2-yl)-4,4,5,5-tetramethyl-1,3,2-dioxaborolane (2.00 g, 6.79 mmol), PEPPSI-IPr (0.439 g, 0.065 mmol), K₃PO₄ (2.74 g, 12.9 mmol), 20 mL of THF and 2.5 mL of degassed water. The flask was then immersed in an oil bath at 60 °C and the solution was stirred overnight before cooling to room temperature. The mixture was diluted with 30 mL of dichloromethane and gravity filtered. The flask was washed with 3 portions of dichloromethane (30 mL) and the filtrate collected. The combined organic solution was dried using MgSO₄ and concentrated using rotary evaporation. The crude material was purified using column chromatography on silica gel, eluting with hexanes:ethyl acetate = 20:1 to afford the final product as a light yellow oil (1.60 g, 90%). The *R_f* of the product is ~0.25 in hexanes:ethyl acetate = 20:1. ¹H NMR (500 MHz, CDCl₃) δ 7.43 (s, 1H), 7.19 (s, 2H), 7.00 (s, 1H), 2.67 – 2.58 (m, 2H), 1.64 (p, *J* = 7.5 Hz, 2H), 1.41 – 1.23 (m, 6H), 0.89 (t, *J* = 6.7 Hz, 3H). ¹³C NMR (126 MHz, CDCl₃) δ 147.5, 144.9, 132.9, 130.2, 128.7, 124.4, 122.6, 116.0, 105.1, 31.9, 30.9, 29.2, 22.8, 14.3. HRMS (ESI-TOF) (*m/z*): [M]⁺ calculated for C₁₅H₁₇NS₂, 275.0800; found, 275.0802.



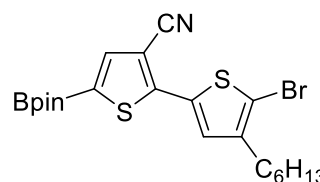
Synthesis of 5'-bromo-4'-hexyl-[2,2'-bithiophene]-3-carbonitrile (5E).

Compound 5D (1.60 g, 5.81 mmol) was dissolved in 20 mL of DMF and the solution was cooled to 0 °C. N-Bromosuccinimide (1.49 g, 8.37 mmol),



dissolved in 5 mL DMF was added to the reaction mixture dropwise over 20 minutes while maintaining a temperature of 0 °C. The reaction mixture was slowly warmed to room temperature and stirred overnight. The mixture was quenched with 50 mL of a saturated NaHCO₃ solution and the entire contents of the flask were transferred to a separatory funnel. The aqueous layer was extracted with diethyl ether (3 × 50 mL) and the combined organic extracts were washed with a saturated NaHCO₃ solution (20 mL) and brine (20 mL). The combined extracts were then dried over Na₂SO₄ and concentrated using rotary evaporation. The crude product was purified using column chromatography on silica gel, eluting with hexanes:dichloromethane (3:1). A subsequent purification with column chromatography on silica gel using the same conditions afforded the final product as a light yellow oil that solidified upon standing (1.39 g, 67%). The *R_f* of the product is ~0.4 in hexanes:dichloromethane = 1:1. ¹H NMR (500 MHz, CD₂Cl₂) δ 7.28 (t, *J* = 2.7 Hz, 2H), 7.22 (d, *J* = 5.4 Hz, 1H), 2.63 – 2.55 (m, 2H), 1.62 (p, *J* = 7.4 Hz, 2H), 1.41 – 1.28 (m, 6H), 0.96 – 0.83 (m, 3H). ¹³C NMR (126 MHz, CD₂Cl₂) δ 146.5, 144.3, 133.2, 130.7, 128.7, 125.6, 115.9, 112.1, 106.0, 32.2, 30.2, 30.1, 29.4, 23.2, 14.4. HRMS (ESI-TOF) (*m/z*): [M]⁺ calculated for C₁₅H₁₆NS₂Br, 352.9908; found, 352.9920.

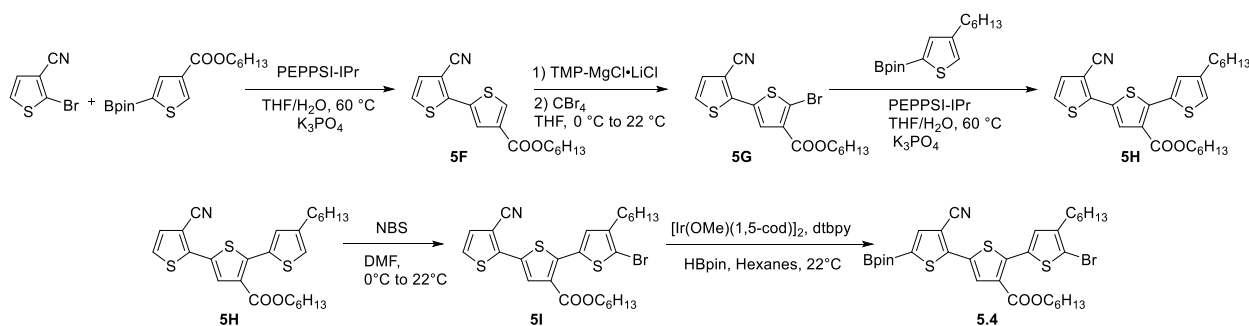
Synthesis of 5'-bromo-4'-hexyl-5-(4,4,5,5-tetramethyl-1,3,2-dioxaborolan-2-yl)-[2,2'-bithiophene]-3-carbonitrile (5.3).



In a N₂ filled glovebox, a 40 mL scintillation vial was charged with pinacolborane (HBPin) (0.56 g, 4.4 mmol), Di-μ-methoxybis(1,5-cyclooctadiene)diiridium (0.036 g, 0.054 mmol) and 4 mL of dry hexanes. To this mixture, 4,4'-Bis(di-*t*-butyl)-2,2'-bipyridine (dtbbpy) (0.030 g, 0.11 mmol) in 4 mL of hexanes was added in portions and the mixture was stirred for 15 min. The color of the reaction mixture went from yellow to dark brown during that period. Compound **5E** (1.30 g, 3.67 mmol) was then dissolved in 4 mL of THF and added to the

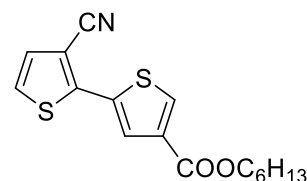
reaction mixture slowly (H_2 gas evolves in this step). The solution was kept in the glovebox and stirred overnight. The crude mixture was then removed from the glovebox, loaded directly onto silica gel, and eluted with a gradient solvent conditions (hexanes:dichloromethane = 1:1, followed by dichloromethane). The R_f of the product is ~ 0.5 in dichloromethane. The final product was collected as a light yellow oil and, upon drying, solidified to a light-brown solid (1.40 g, 95%). 1H NMR (500 MHz, $CDCl_3$) δ 7.65 (s, 1H), 7.33 (s, 1H), 2.60 – 2.54 (m, 2H), 1.59 (q, $J = 7.6$ Hz, 2H), 1.38 – 1.28 (m, 18H), 0.93 – 0.85 (m, 3H). ^{13}C NMR (126 MHz, $CDCl_3$) δ 151.4, 143.9, 139.9, 133.0, 128.5, 115.6, 112.6, 106.4, 85.2, 31.8, 29.8, 29.1, 25.0, 22.8, 14.3. Note: one aromatic signal is missing in the ^{13}C NMR spectrum due to quadrupolar relaxation. HRMS (ESI-TOF) (m/z): $[M + H]^+$ calculated for $C_{21}H_{27}NO_2S_2BBr$, 479.0760; found, 479.0768.

Scheme 5.5. Synthesis of Monomer 5.4.



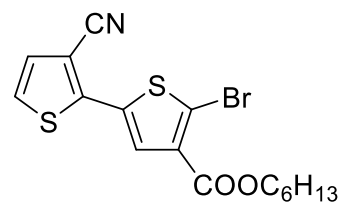
Synthesis of hexyl 3'-cyano-[2,2'-bithiophene]-4-carboxylate (5F).

An oven-dried 100 mL Schlenk flask was charged with 2-bromothiophene-3-carbonitrile (2.26 g, 12.00 mmol), hexyl 5-(4,4,5,5-tetramethyl-1,3,2-dioxaborolan-2-yl)thiophene-3-carboxylate (4.47 g, 1.73 mmol), PEPPSI-IPr (0.163 g, 0.24 mmol), K_3PO_4 (5.09 g, 24.01 mmol), 40 mL of THF and 5 mL of degassed water. The flask was then immersed in an oil bath at 60 °C and the solution was stirred overnight before cooling to room temperature. The mixture was diluted with 30 mL of dichloromethane and gravity



filtered. The flask was washed with 3 portions of dichloromethane (30 mL) and the filtrate was collected. The combined organic fractions were dried using MgSO_4 and concentrated using rotary evaporation. The crude material was purified using column chromatography on silica gel, eluting with hexanes:ethyl acetate (7:1) to afford the final product as a clear oil (3.33 g, 87%). The R_f of the product is ~ 0.3 in hexanes:ethyl acetate = 7:1. ^1H NMR (500 MHz, CDCl_3) δ 8.16 – 8.13 (m, 1H), 7.89 (d, $J = 1.2$ Hz, 1H), 7.29 (d, $J = 5.4$ Hz, 1H), 7.24 (d, $J = 5.4$ Hz, 1H), 4.29 (t, $J = 6.8$ Hz, 2H), 1.75 (p, $J = 6.9$ Hz, 2H), 1.43 (p, $J = 6.9$ Hz, 2H), 1.34 (dt, $J = 7.3, 3.7$ Hz, 4H), 0.97 – 0.85 (m, 3H). ^{13}C NMR (126 MHz, CDCl_3) δ 162.3, 145.8, 135.0, 133.9, 133.8, 130.4, 127.9, 125.7, 115.3, 106.6, 65.5, 31.7, 28.8, 25.9, 22.8, 14.2. HRMS (ESI-TOF) (m/z): $[\text{M} + \text{H}]^+$ calculated for $\text{C}_{16}\text{H}_{18}\text{NO}_2\text{S}_2$, 320.0779; found, 320.0768.

Synthesis of hexyl 5-bromo-3'-cyano-[2,2'-bithiophene]-4-carboxylate (5G). Compound **5F** (1.65 g, 5.17 mmol) was dissolved

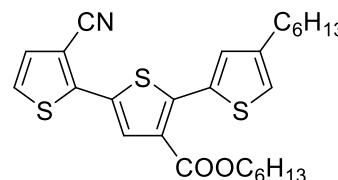


in 100 mL of THF and the solution was cooled to 0 °C. 1.0 M $\text{TMP}\cdot\text{MgCl}\cdot\text{LiCl}$ (7.1 mL, 7.1 mmol) was added to the reaction mixture dropwise over 10 minutes while maintaining a temperature of 0 °C. The reaction mixture was stirred for 30 minutes at 0 °C before adding carbon tetrabromide (1.88 g, 5.67 mmol) in one portion. The mixture was stirred at room temperature overnight before quenching with 20 mL of 2 M HCl solution and the entire contents of the flask were transferred to a separatory funnel. The aqueous layer was extracted with diethyl ether (3×50 mL) and the combined organic extracts were washed with 2 M HCl solution (20 mL) and brine (20 mL). The combined organic extracts were then dried over Na_2SO_4 and concentrated using rotary evaporation. The crude product was purified via recrystallization from hot hexanes followed by column chromatography on silica gel, eluting with hexanes:ethyl acetate (15:1) to afford the final product as an off-white solid (0.99 g, 48%). The R_f of the product is ~ 0.4

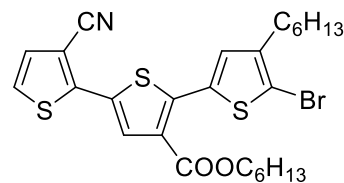
in hexanes: ethyl acetate = 7:1. ^1H NMR (500 MHz, CDCl_3) δ 7.73 (s, 1H), 7.31 (s, 1H), 7.24 (d, $J = 5.3$ Hz, 1H), 4.31 (t, $J = 6.7$ Hz, 2H), 1.77 (dt, $J = 14.6, 6.8$ Hz, 2H), 1.45 (p, $J = 7.2$ Hz, 2H), 1.34 (dq, $J = 7.1, 3.7$ Hz, 4H), 0.94 – 0.86 (m, 3H). ^{13}C NMR (126 MHz, CDCl_3) δ 161.6, 144.8, 133.1, 132.5, 130.5, 129.0, 126.0, 121.6, 115.1, 106.9, 65.8, 31.63, 28.8, 25.9, 22.8, 14.2. HRMS (ESI-TOF) (m/z): $[\text{M}]^+$ calculated for $\text{C}_{16}\text{H}_{17}\text{NBrS}_2\text{O}_2$, 397.9884; found, 397.9881.

Synthesis of Hexyl 3''-cyano-4-hexyl-[2,2':5',2''-terthiophene]-3'-

carboxylate (**5H**). In a N_2 filled glovebox, a 20 mL scintillation vial was charged with compound **5G** (0.57 g, 1.43 mmol), 2-(4-hexylthiophen-2-yl)-4,4,5,5-tetramethyl-1,3,2-dioxaborolane (0.42 g, 1.43 mmol), PEPPSI-IPr (0.01 g, 0.015 mmol), K_3PO_4 (0.61 g, 2.87 mmol), and 5 mL of THF. The vial was brought out from the glovebox and immersed in an oil bath at 60 °C, and then 1 mL of water was added via syringe. The solution was stirred overnight at 60 °C before cooling to room temperature. The mixture was diluted with 30 mL of diethyl ether and gravity filtered. The flask was washed with 3 portions of diethyl ether (10 mL) and the filtrate was collected. The combined organic fractions were dried using MgSO_4 and concentrated using rotary evaporation. The crude material was purified using column chromatography on silica gel, eluting with hexanes:ethyl acetate (20:1) to afford the final product as a viscous, yellow oil (0.57 g, 81%). The R_f of the product is ~0.3 in hexanes: ethyl acetate = 7:1. ^1H NMR (500 MHz, CDCl_3) δ 7.86 (s, 1H), 7.36 (d, $J = 1.4$ Hz, 1H), 7.27 (d, $J = 5.4$ Hz, 1H), 7.23 (d, $J = 5.4$ Hz, 1H), 4.26 (t, $J = 6.8$ Hz, 2H), 2.66 – 2.56 (m, 2H), 1.67 (ddt, $J = 30.3, 15.4, 7.3$ Hz, 4H), 1.42 – 1.25 (m, 12H), 0.89 (td, $J = 6.9, 3.1$ Hz, 6H). ^{13}C NMR (126 MHz, CDCl_3) δ 162.9, 145.5, 145.1, 143.9, 132.6, 131.6, 130.5, 130.5, 130.3, 128.4, 125.4, 123.8, 115.5, 106.2, 65.5, 31.9, 31.7, 30.6, 29.2, 28.8, 25.9, 22.8, 22.8, 14.3, 14.2. HRMS (ESI-TOF) (m/z): $[\text{M}]^+$ calculated for $\text{C}_{26}\text{H}_{32}\text{NO}_2\text{S}_3$, 486.1595; found, 486.1581.



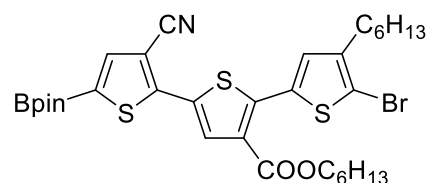
Synthesis of hexyl 5-bromo-3''-cyano-4-hexyl-[2,2':5',2''-terthiophene]-3'-carboxylate (5I). Compound **5H** (0.57 g, 1.17



mmol) was dissolved in 10 mL of DMF and the solution was cooled

to 0 °C. N-Bromosuccinimide (0.23 g, 1.29 mmol) was added to the reaction mixture portionwise while maintaining a temperature of 0 °C. The reaction mixture was slowly warmed to room temperature and stirred overnight. The mixture was quenched with 50 mL of a saturated NaHCO₃ solution and the entire contents of the flask were transferred to a separatory funnel. The aqueous layer was extracted with diethyl ether (3 × 50 mL) and the combined organic extracts were washed with a saturated NaHCO₃ solution (20 mL) and brine (20 mL). The combined organic extracts were then dried over Na₂SO₄ and concentrated using rotary evaporation. The crude product was purified using column chromatography on silica gel, eluting with hexanes:ethyl acetate (25:1) to afford the final product as a clear oil (0.57 g, 86%). The *R_f* of the product is ~0.4 in hexanes:ethyl acetate = 7:1. ¹H NMR (500 MHz, CDCl₃) δ 7.85 (s, 1H), 7.29 (d, *J* = 5.4 Hz, 1H), 7.24 (d, *J* = 5.4 Hz, 1H), 7.21 (s, 1H), 4.28 (t, *J* = 6.7 Hz, 2H), 2.61 – 2.52 (m, 2H), 1.72 (p, *J* = 6.8 Hz, 2H), 1.61 (p, *J* = 7.4 Hz, 2H), 1.43 – 1.26 (m, 12H), 0.90 (t, *J* = 6.5 Hz, 6H). ¹³C NMR (126 MHz, CDCl₃) δ 162.8, 145.2, 144.2, 142.6, 132.5, 130.9, 130.6, 130.5, 130.3, 128.3, 125.6, 115.4, 113.8, 106.4, 65.7, 31.8, 31.7, 29.9, 29.7, 29.2, 28.8, 25.9, 22.8, 22.8, 14.3, 14.2. HRMS (ESI-TOF) (*m/z*): [M]⁺ calculated for C₂₆H₃₁NO₂S₃Br, 564.0700; found, 564.0684.

Synthesis of hexyl 5-bromo-3''-cyano-4-hexyl-5''-(4,4,5,5-tetramethyl-1,3,2-dioxaborolan-2-yl)-[2,2':5',2''-



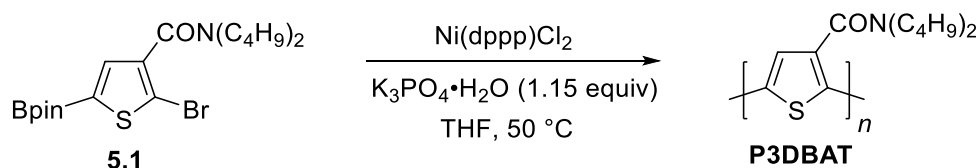
terthiophene]-3'-carboxylate (5.4). In a N₂ filled glovebox, a

40 mL scintillation vial was charged with pinacolborane (HBPin) (0.19 g, 1.48 mmol), Di-μ-methoxobis(1,5-cyclooctadiene)diiridium (0.01 g, 0.015 mmol) and 2 mL of dry hexanes. To this

mixture, 4,4'-Bis(di-*t*-butyl)-2,2'-bipyridine (dtbbpy) (0.008 g, 0.030 mmol) in 2 mL of hexanes was added in portions and the mixture was stirred for 15 min. The color of the reaction mixture went from yellow to dark brown during that period. Compound **5I** (0.57 g, 1.01 mmol) was then dissolved in 4 mL of hexanes and added to the reaction mixture slowly (H₂ gas evolves in this step). After H₂ gas evolution ceased, a second batch of catalyst solution – HBpin (1.48 mmol), diiridium catalyst (0.015 mmol) and dtbbpy (0.030 mmol) – prepared in 4 mL hexanes was added dropwise to the reaction mixture over 20 min. The reaction mixture was stirred at room temperature inside the glovebox overnight. The crude mixture was removed from the glovebox, loaded directly onto silica gel, and eluted with dichloromethane. The *R_f* of the product is ~0.2 in dichloromethane. The final product was collected as a viscous oil (0.53 g, 76%). ¹H NMR (500 MHz, CDCl₃) δ 7.91 (s, 1H), 7.69 (s, 1H), 7.22 (s, 1H), 4.27 (t, *J* = 6.7 Hz, 2H), 2.64 – 2.50 (m, 2H), 1.72 (p, *J* = 6.8 Hz, 2H), 1.61 (p, *J* = 7.5 Hz, 2H), 1.34 (d, *J* = 10.3 Hz, 24H), 0.90 (t, *J* = 6.7 Hz, 6H). ¹³C NMR (126 MHz, CDCl₃) δ 162.7, 150.3, 144.6, 142.6, 140.0, 132.5, 130.9, 130.7, 130.6, 128.3, 115.4, 113.9, 107.3, 85.3, 65.7, 31.8, 31.7, 29.9, 29.7, 29.2, 28.8, 25.9, 25.0, 22.8, 22.8, 14.3, 14.2. Note: one aromatic signal is missing in the ¹³C NMR spectrum due to quadrupolar relaxation. HRMS (ESI-TOF) (*m/z*): [M]⁺ calculated for C₃₂H₄₂BNBrO₄S₃, 690.1552; found, 690.1546.

Polymerization Studies

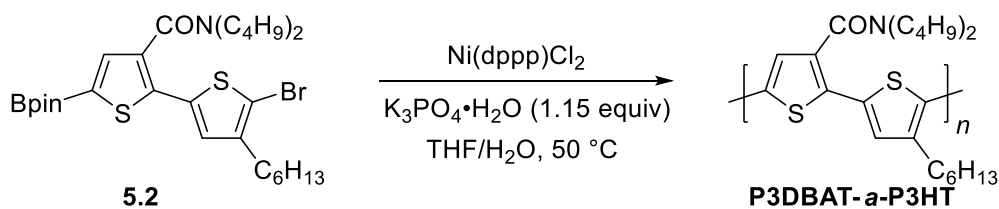
Scheme 5.6. Synthesis of P3DBAT.



Representative procedure for PDBAT synthesis. In a N₂ filled glovebox, a 20 mL scintillation vial equipped with a Teflon screw cap was charged with a calculated amount of catalyst (mol %

listed in Table 5.1), $\text{K}_3\text{PO}_4 \cdot \text{H}_2\text{O}$ (0.080 g, 0.35 mmol), and 5 mL of THF. The vial was capped, removed from the glovebox and the reaction mixture was stirred at room temperature. Monomer **5.1** (0.14 g, 0.31 mmol) in 2 mL of THF was injected into the solution to initiate the polymerization and the reaction mixture was placed in an oil bath at 50 °C. After an indicated amount of time (Table 5.1) the reaction was quenched using 6 M methanolic HCl solution. The precipitate was collected using vacuum filtration, then washed with methanol. The final polymer was collected as a red solid and dried *in vacuo*. ^1H NMR (500 MHz, CDCl_3) δ 7.08 (s, 1H), 3.48 (t, $J = 7.7$ Hz, 2H), 3.12 (t, $J = 7.7$ Hz, 2H), 1.73 – 1.61 (m, 2H), 1.39 (dq, $J = 16.8, 8.1$ Hz, 4H), 1.11 (h, $J = 7.3$ Hz, 2H), 0.99 (t, $J = 7.3$ Hz, 3H), 0.76 (t, $J = 7.3$ Hz, 3H). ^{13}C NMR (126 MHz, CDCl_3) δ 166.2, 134.8, 134.2, 132.7, 126.2, 48.9, 45.4, 31.0, 29.6, 20.7, 20.0, 14.2, 13.8.

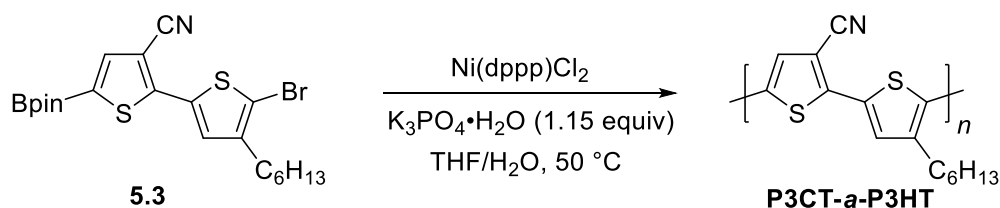
Scheme 5.7. Synthesis of P3DBAT-*a*-P3HT.



Representative procedure for P3HET-*a*-P3HT synthesis. In a N_2 filled glovebox, a 20 mL scintillation vial equipped with a Teflon screw cap was charged with a calculated amount of catalyst (mol % listed in Table 5.1), $\text{K}_3\text{PO}_4 \cdot \text{H}_2\text{O}$ (0.080 g, 0.35 mmol) and 5 mL of THF. The vial was capped, removed from the glovebox and the reaction mixture was stirred at room temperature. Monomer **5.2** (0.19 g, 0.31 mmol) in 2 mL of THF was injected into the reaction mixture followed by degassed H_2O and then the vial was immersed in an oil bath at 50 °C. The reaction mixture was stirred for period of time (Table 5.1) and quenched using 6 M methanolic HCl solution. The precipitate was collected using vacuum filtration, then washed with methanol. The final polymer was collected as a maroon solid and dried *in vacuo*. ^1H NMR (500 MHz, CDCl_3) δ 7.07 (s, 1H),

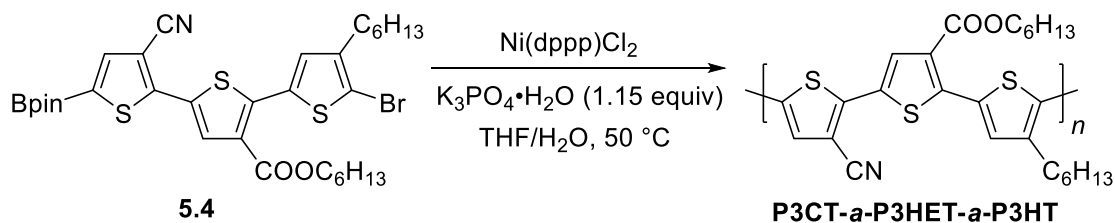
6.97 (s, 1H), 3.50 (t, $J = 8.1$ Hz, 2H), 3.14 (t, $J = 7.7$ Hz, 2H), 2.83 – 2.49 (m, 2H), 1.74 – 1.61 (m, 4H), 1.45 – 1.29 (m, 10H), 1.13 (q, $J = 7.4$ Hz, 2H), 1.00 (t, $J = 7.3$ Hz, 3H), 0.93 – 0.87 (m, 3H), 0.77 (t, $J = 7.4$ Hz, 3H). ^{13}C NMR (126 MHz, CDCl_3) δ 166.9, 141.3, 135.3, 134.1, 133.1, 132.5, 130.6, 129.1, 126.1, 48.9, 45.3, 31.9, 31.0, 30.7, 29.7, 29.7, 29.5, 22.8, 20.7, 20.1, 14.3, 14.3, 13.9.

Scheme 5.8. Synthesis of P3CT-*a*-P3HT.



P3CT-*a*-P3HT synthesis. In a N_2 filled glovebox, a 20 mL scintillation vial equipped with a Teflon screw cap was charged with Ni(dppp)Cl_2 (16.5 mg, 0.03 mmol), $\text{K}_3\text{PO}_4 \cdot \text{H}_2\text{O}$ (0.08 g, 0.35 mmol), and 5 mL of THF. The vial was capped, removed from the glovebox and the reaction mixture was stirred at room temperature. Monomer **5.3** (0.15 g, 0.31 mmol) in 2 mL of THF was injected into the solution followed by degassed H_2O (0.1 mL). The reaction mixture was placed in an oil bath at $50\text{ }^\circ\text{C}$. After 45 min, the polymerization was quenched using 6 M methanolic HCl. The precipitate was collected using vacuum filtration and washed with methanol. The final polymer was collected as a black solid and dried *in vacuo* (54.1 mg, 65%). Due to the limited solubility of the polymer, NMR analysis was not performed. The polymer was subjected to high-temperature ($140\text{ }^\circ\text{C}$) GPC analysis using *o*-dichlorobenzene ($M_n = 1500$, $D = 1.09$).

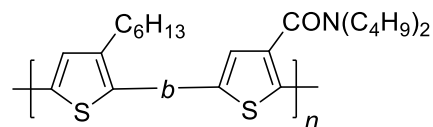
Scheme 5.9. Synthesis of P3CT-*a*-P3HET-*a*-P3HT.



P3CT-*a*-P3HET-*a*-P3HT synthesis. In a N₂ filled glovebox, a 20 mL scintillation vial equipped with a Teflon screw cap was charged with Ni(dppp)Cl₂ (10.4 mg, 0.02 mmol), K₃PO₄·H₂O (0.05 g, 0.22 mmol), and 3 mL of THF. The vial was capped, removed from the glovebox and the reaction mixture was stirred at room temperature. Monomer **5.4** (0.13 g, 0.19 mmol) in 2 mL of THF was injected into the solution followed by degassed H₂O (0.07 mL). The reaction mixture was placed in an oil bath at 50 °C. After 50 min, the polymerization was quenched using 6 M methanolic HCl. The precipitate was collected using vacuum filtration, then washed with methanol. The final polymer was collected as a black solid and dried *in vacuo* (36.2 mg, 39%). Due to the limited solubility of the polymer, NMR analysis was not performed. The polymer was subjected to high-temperature (140 °C) GPC analysis using *o*-dichlorobenzene (bimodal distribution: $M_n = 1800$, $D = 1.13$, $M_n = 650$, $D = 1.01$).

Synthesis of P3HT-*b*-P3DBAT, growing P3HT first.

In a N₂ filled glovebox, a 20 mL scintillation vial equipped with a Teflon screw cap was charged with Ni(dppp)Cl₂ (3.3

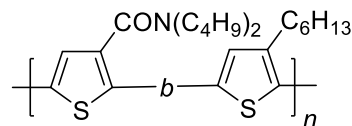


mg, 2 mol %), K₃PO₄·H₂O (0.080 g, 0.35 mmol), and 5 mL of THF. The vial was capped and removed from the glovebox. The hexyl thiophene monomer (0.11 g, 0.31 mmol) in 2 mL of THF was injected into the solution followed by degassed water (0.1 mL). The vial was then placed in an oil bath at 50 °C and the reaction mixture was stirred for 60 min. An aliquot (0.2 mL) was withdrawn to determine the molecular weight of resultant polymer (P3HT, $M_w = 23100$, $D = 1.10$). The solution was then transferred via syringe to another vial containing monomer **5.1** (0.14 g, 0.31 mmol) and K₃PO₄·H₂O (0.08 g, 0.35 mmol). The reaction mixture was stirred at 50 °C for 90 min. A final aliquot was withdrawn to determine the final molecular weight of the block copolymer (P3HT-*b*-P3DBAT, $M_w = 27200$, $D = 1.44$). The polymerization was quenched using 6M

methanolic HCl solution. The precipitate was collected using vacuum filtration, then washed with methanol. The final polymer was collected as a dark purple solid and dried *in vacuo* (38 mg, 30%).

Synthesis of P3DBAT-*b*-P3HT, growing P3DBAT first.

In a N₂ filled glovebox, a 20 mL scintillation vial equipped with a Teflon screw cap was charged with Ni(dppp)Cl₂ (3.3 mg, 2 mol %),



K₃PO₄·H₂O (0.080 g, 0.35 mmol), and 5 mL of THF. The vial was capped and removed from the glovebox. Monomer **5.1** (0.14 g, 0.31 mmol) in 2 mL of THF was injected into the solution. The vial was then placed in an oil bath at 50 °C and the reaction mixture was stirred for 150 min. An aliquot (0.2 mL) was withdrawn to determine the molecular weight of resultant polymer (P3DBAT, $M_w = 13000$, $D = 1.15$). The solution was then transferred via syringe to another vial containing the hexyl thiophene monomer (0.11 g, 0.31 mmol) and K₃PO₄·H₂O (0.08 g, 0.35 mmol). Degassed water (0.1 mL) was injected and the reaction mixture was placed in the bath and stirred at 50 °C for 60 min. A final aliquot was withdrawn to determine the final molecular weight of the block copolymer (P3DBAT-*b*-P3HT, $M_w = 19200$, $D = 1.49$). The polymerization was quenched using 6M methanolic HCl solution. The precipitate was collected using vacuum filtration, then washed with methanol. The final polymer was collected as a maroon solid and dried *in vacuo* (60 mg, 49%).

Optical Properties

Table 5.2. Summary of optical properties of P3DBAT, P3DBAT-*a*-P3HT, P3CT-*a*-P3HT, and P3CT-*a*-P3HET-*a*-P3HT.

Polymer	λ_{\max} CHCl ₃	λ_{\max} film	E_g^{opt} (eV) ^a
P3DBAT	490	493	2.09
P3DBAT- <i>a</i> -P3HT	462	540	1.99
P3CT- <i>a</i> -P3HT	473	552	1.90
P3CT- <i>a</i> -P3HET- <i>a</i> -P3HT	460	605	1.90

^aDetermined by onset of absorption

5.5 References

1. Chiang, C. K.; Fincher, C. R.; Park, Y. W.; Heeger, A. J.; Shirakawa, H.; Louis, E. J.; Gau, S. C.; MacDiarmid, A. G. *Phys. Rev. Lett.* **1977**, *39*, 1098-1101.
2. (a) Sheina, E. E.; Liu, J.; Iovu, M. C.; Laird, D. W.; McCullough, R. D. *Macromolecules* **2004**, *37*, 3526-3528. (b) Yokoyama, A.; Miyakoshi, R.; Yokozawa, T. *Macromolecules* **2004**, *37*, 1169-1171.
3. (a) Yokozawa, T.; Ohta, Y. *Chem. Rev.* **2016**, *116*, 1950-1968. (b) Grisorio, R.; Suranna, G. P. *Polym. Chem.* **2015**, *6*, 7781-7795. (c) Bryan, Z. J.; McNeil, A. J. *Macromolecules* **2013**, *46*, 8395-8405. (d) Okamoto, K.; Luscombe, C. K. *Polym. Chem.* **2011**, *2*, 2424-2434. (e) Yokozawa, T.; Yokoyama, A. *Chem. Rev.* **2009**, *109*, 5595-5619.
4. Kiriya, A.; Senkovskyy, V.; Sommer, M. *Macromol. Rapid Commun.* **2011**, *32*, 1503-1517.
5. (a) Qiu, Y.; Mohin, J.; Tsai, C.-H.; Tristram-Nagle, S.; Gil, R. R.; Kowalewski, T.; Noonan, K. J. T. *Macromol. Rapid Commun.* **2015**, *36*, 840-844. (b) Kang, S.; Ono, R. J.; Bielawski, C. W. *J. Am. Chem. Soc.* **2013**, *135*, 4984-4987.
6. (a) Zhang, H.-H.; Peng, W.; Dong, J.; Hu, Q.-S. *ACS Macro Lett.* **2016**, *5*, 656-660. (b) Zhang, H.-H.; Xing, C.-H.; Hu, Q.-S.; Hong, K. *Macromolecules* **2015**, *48*, 967-978. (c) Grisorio, R.; Mastroilli, P.; Suranna, G. P. *Polym. Chem.* **2014**, *5*, 4304-4310. (d) Sui, A.; Shi, X.; Tian, H.; Geng, Y.; Wang, F. *Polym. Chem.* **2014**, *5*, 7072-7080. (e) Yokoyama, A.; Suzuki, H.; Kubota, Y.; Ohuchi, K.; Higashimura, H.; Yokozawa, T. *J. Am. Chem. Soc.* **2007**, *129*, 7236-7237.
7. Qiu, Y.; Worch, J. C.; Fortney, A.; Gayathri, C.; Gil, R. R.; Noonan, K. J. T. *Macromolecules* **2016**, *49*, 4757-4762.
8. Hintz, H.; Egelhaaf, H. J.; Lüer, L.; Hauch, J.; Peisert, H.; Chassé, T. *Chem. Mater.* **2011**, *23*, 145-154.

9. (a) Heeney, M.; Bailey, C.; Genevicius, K.; Shkunov, M.; Sparrowe, D.; Tierney, S.; McCulloch, I. *J. Am. Chem. Soc.* **2005**, *127*, 1078-1079. (b) Ong, B. S.; Wu, Y.; Liu, P.; Gardner, S. *J. Am. Chem. Soc.* **2004**, *126*, 3378-3379.
10. (a) Noh, S.; Gobalasingham, N. S.; Thompson, B. C. *Macromolecules* **2016**, *ASAP*. (b) Kazarinoff, P. D.; Shamburger, P. J.; Ohuchi, F. S.; Luscombe, C. K. *J. Mater. Chem.* **2010**, *20*, 3040-3045. (c) Murphy, A. R.; Liu, J.; Luscombe, C.; Kavulak, D.; Fréchet, J. M. J.; Kline, R. J.; McGehee, M. D. *Chem. Mater.* **2005**, *17*, 4892-4899.
11. Zhang, Z.-G.; Wang, J. *J. Mater. Chem.* **2012**, *22*, 4178-4187.
12. (a) Olivier, Y.; Niedzialek, D.; Lemaur, V.; Pisula, W.; Müllen, K.; Koldemir, U.; Reynolds, J. R.; Lazzaroni, R.; Cornil, J.; Beljonne, D. *Adv. Mater.* **2014**, *26*, 2119-2136. (b) Zhao, X.; Zhan, X. *Chem. Soc. Rev.* **2011**, *40*, 3728-3743. (c) Anthony, J. E.; Facchetti, A.; Heeney, M.; Marder, S. R.; Zhan, X. *Adv. Mater.* **2010**, *22*, 3876-3892.
13. (a) Pollit, A. A.; Bridges, C. R.; Seferos, D. S. *Macromol. Rapid Commun.* **2015**, *36*, 65-70. (b) Todd, A. D.; Bielawski, C. W. *ACS Macro Lett.* **2015**, *4*, 1254-1258.
14. Elmalem, E.; Kiriya, A.; Huck, W. T. S. *Macromolecules* **2011**, *44*, 9057-9061.
15. (a) Tkachov, R.; Karpov, Y.; Senkovskyy, V.; Raguzin, I.; Zessin, J.; Lederer, A.; Stamm, M.; Voit, B.; Beryozkina, T.; Bakulev, V.; Zhao, W.; Facchetti, A.; Kiriya, A. *Macromolecules* **2014**, *47*, 3845-3851. (b) Senkovskyy, V.; Tkachov, R.; Komber, H.; Sommer, M.; Heuken, M.; Voit, B.; Huck, W. T. S.; Kataev, V.; Petr, A.; Kiriya, A. *J. Am. Chem. Soc.* **2011**, *133*, 19966-19970.
16. Guo, X.; Facchetti, A.; Marks, T. J. *Chem. Rev.* **2014**, *114*, 8943-9021.
17. Zhan, X.; Facchetti, A.; Barlow, S.; Marks, T. J.; Ratner, M. A.; Wasielewski, M. R.; Marder, S. R. *Adv. Mater.* **2011**, *23*, 268-284.

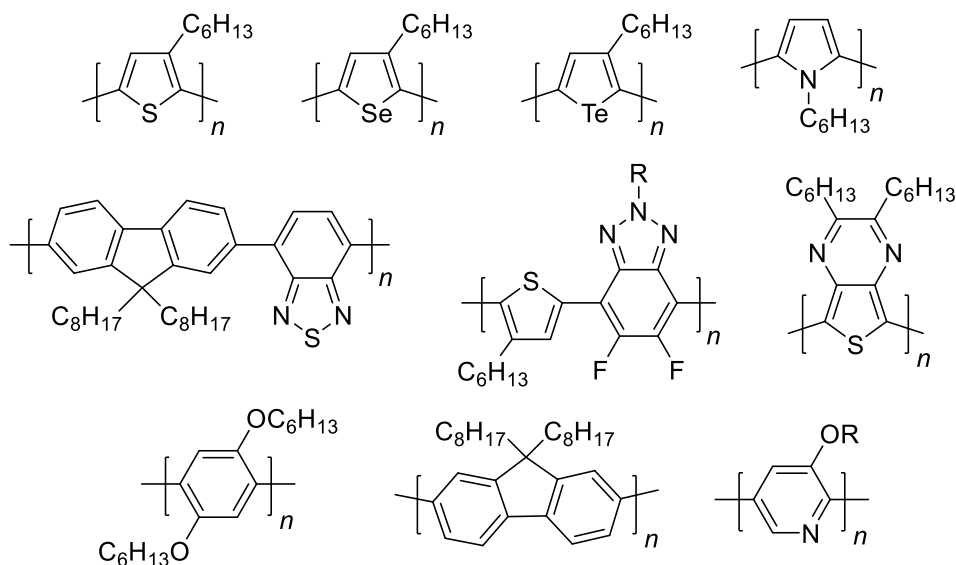
18. Pron, A.; Berrouard, P.; Leclerc, M. *Macromol. Chem. Phys.* **2013**, *214*, 7-16.
19. (a) Rudenko, A. E.; Khlyabich, P. P.; Thompson, B. C. *ACS Macro Lett.* **2014**, *3*, 387-392.
(b) Khlyabich, P. P.; Rudenko, A. E.; Thompson, B. C. *J. Polym. Sci., Part A: Polym. Chem.* **2014**, *52*, 1055-1058. (c) Wan, M.; Wu, W.; Sang, G.; Zou, Y.; Liu, Y.; Li, Y. *J. Polym. Sci., Part A: Polym. Chem.* **2009**, *47*, 4028-4036. (d) Chochos, C. L.; Economopoulos, S. P.; Deimede, V.; Gregoriou, V. G.; Lloyd, M. T.; Malliaras, G. G.; Kallitsis, J. K. *J. Phys. Chem. C* **2007**, *111*, 10732-10740.
20. Roth, B.; Rudenko, A. E.; Thompson, B. C.; Krebs, F. C. *J. Photon. Energy* **2014**, *5*, 0572051-0572057.
21. (a) Nicolas, M.; Guittard, F.; G ribaldi, S. *J. Polym. Sci., Part A: Polym. Chem.* **2007**, *45*, 4707-4719. (b) Bryce, M. R.; Chissel, A.; Kathirgamanathan, P.; Parker, D.; Smith, N. R. M. *J. Chem. Soc., Chem. Commun.* **1987**, 466-467. (c) Bryce, M. R.; Chissel, A. D.; Smith, N. R. M.; Parker, D.; Kathirgamanathan, P. *Synth. Met.* **1988**, *26*, 153-168.
22. Chotana, G. A.; Kallepalli, V. A.; Maleczka Jr, R. E.; Smith III, M. R. *Tetrahedron* **2008**, *64*, 6103-6114.
23. Carrillo, J. A.; Ingleson, M. J.; Turner, M. L. *Macromolecules* **2015**, *48*, 979-986.
24. Kosaka, K.; Ohta, Y.; Yokozawa, T. *Macromol. Rapid Commun.* **2015**, *36*, 373-377.
25. Liversedge, I. A.; Higgins, S. J.; Giles, M.; Heeney, M.; McCulloch, I. *Tetrahedron Lett.* **2006**, *47*, 5143-5146.
26. Gobalasingham, N. S.; Noh, S.; Thompson, B. C. *Polym. Chem.* **2016**, *7*, 1623-1631.

Chapter 6

Perspective and Outlook

The search for new organic semiconductors remains intensely pursued even after 4 decades of research. Although there are many active focus areas in organic electronics, the synthesis of new materials will arguably provide the bulk of innovation to the field. The concept of molecular engineering (introduced in Chapter 1) will be crucial to the development of next-generation materials, as such, chemists are the vanguard in this endeavor. Although, there are still many crucial challenges to be sorted, the development of controlled conjugated polymers via catalyst-transfer polycondensation (CTP) provided a noticeable advancement to the field and will certainly continue to do so if current issues related to monomer scope are resolved.

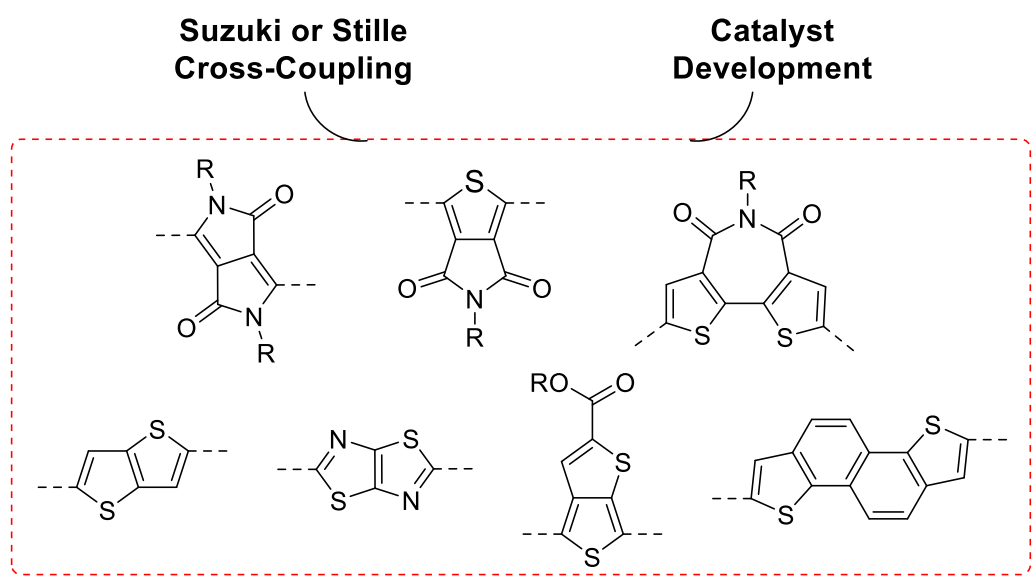
Chart 6.1. Scope of controlled polymers produced using CTP.



Presently, the CTP monomer scope is quite narrow (Chart 6.1) and state of the art semiconducting polymers (the most efficient in device applications) are still prepared using rudimentary step-growth protocols. Semiconducting polymers prepared by step-growth protocols display large batch-to-batch variability, concerning molecular weight and polydispersity, and this often leads to inconsistent device performance. The lack of reproducibility is perhaps the most significant hindrance to more widespread commercial interest in organic electronics. Thus, application of CTP to high performance building blocks is widely sought after and it would lead to more reproducible device efficiencies.

Many of the best performing polymers incorporate sensitive functional groups and/or complex fused-ring architectures. The path to the controlled synthesis of high-value conjugated polymers will certainly involve: 1) utilization of mild cross-coupling protocols (Stille or Suzuki–Miyaura) to expand the functional group scope and 2) continued catalyst development to access fused-ring systems (Chart 6.2). Our efforts in these areas were highlighted in Chapters 4 & 5.

Chart 6.2. Building blocks appearing in state of the art conjugated polymers that are currently produced using step-growth polycondensation.



In addition to providing tunable molecular weight and low polydispersity, CTP allows for control over polymer composition, microstructure, or topology. For conjugated polymers, manipulation of monomer sequence (e.g., donor-acceptor) can profoundly impact bulk properties (optoelectronic and physical). Thus, the development of sequence controlled conjugated polymers has the ability to drastically advance the field of organic electronics. The application of CTP to sequenced monomers can provide precise monomer incorporation into conjugated polymers. In our group, we are seeking to combine our Suzuki-CTP protocol (Chapter 4) with continued catalyst development to produce precise conjugated polymers with control of main-chain (heteroatom) sequence and side-chain (functional group) sequence.

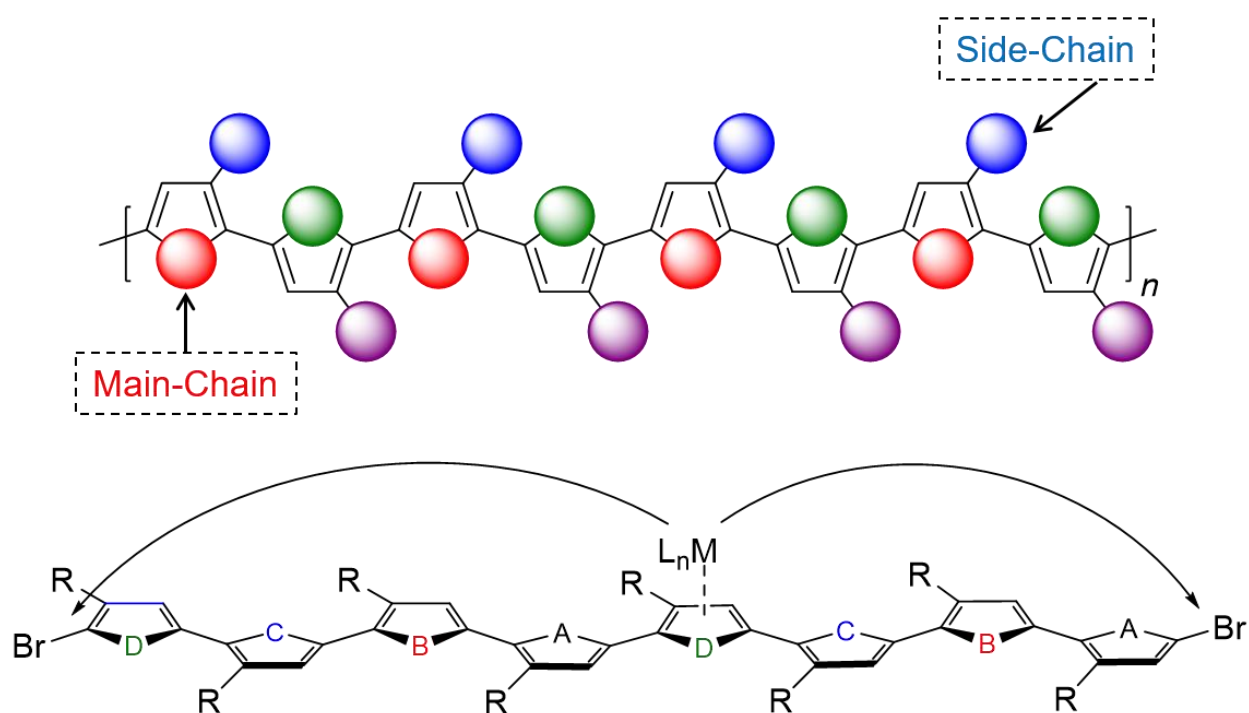


Figure 6.1. Main-chain and side-chain sequence control in conjugated polymers

Appendix 1

Supplementary Material for Chapter 4

A1.1 Model Compound Studies

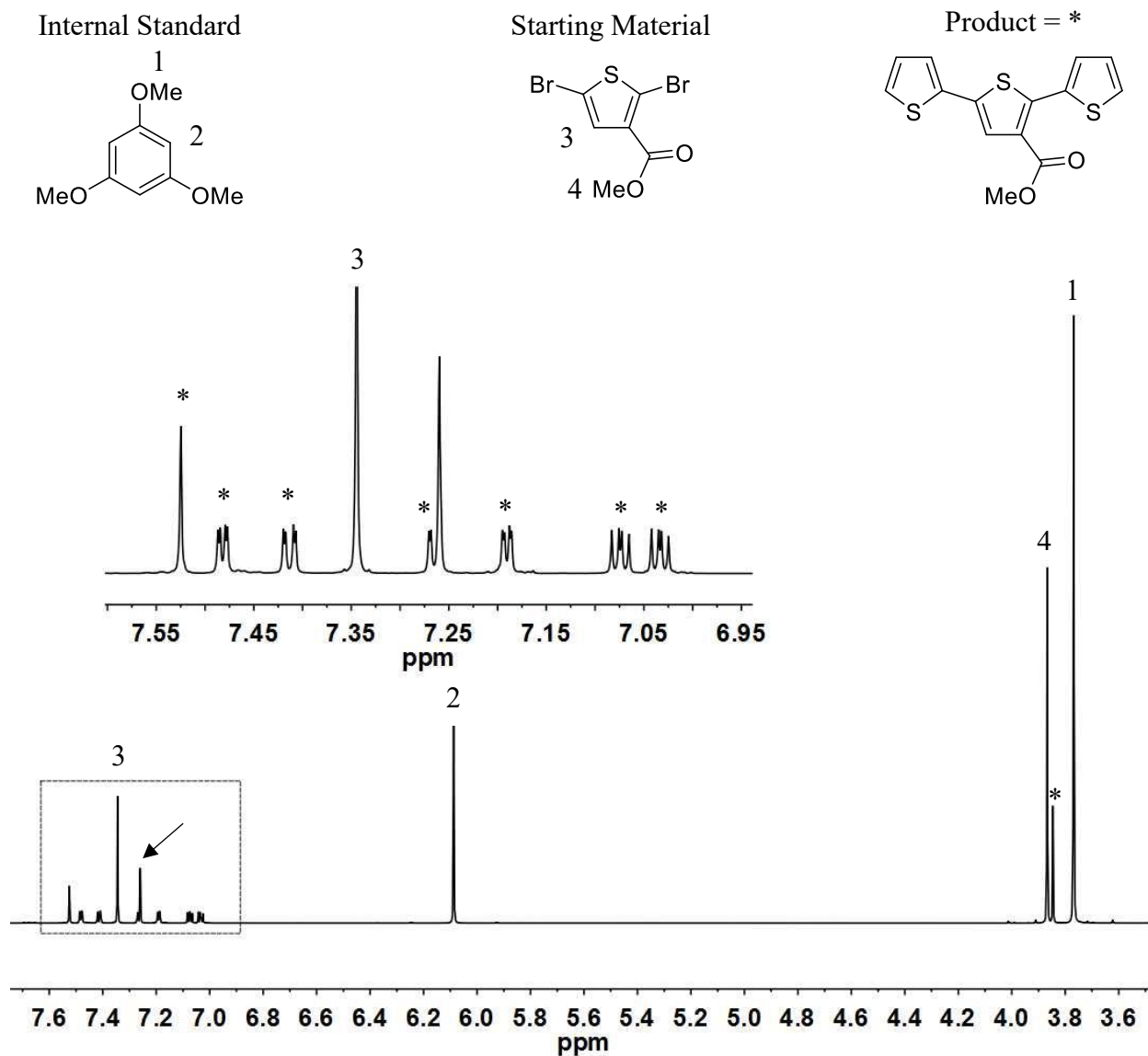


Figure A1.1. Crude ¹H NMR Spectrum (500 MHz, CDCl₃) for small molecule Suzuki-Miyaura coupling at 50 °C using methyl 2,5-dibromothiophene-3-carboxylate and Ni(PPh₃)IPrCl₂ (1 mol %). The star symbols correspond to the terthiophene product.

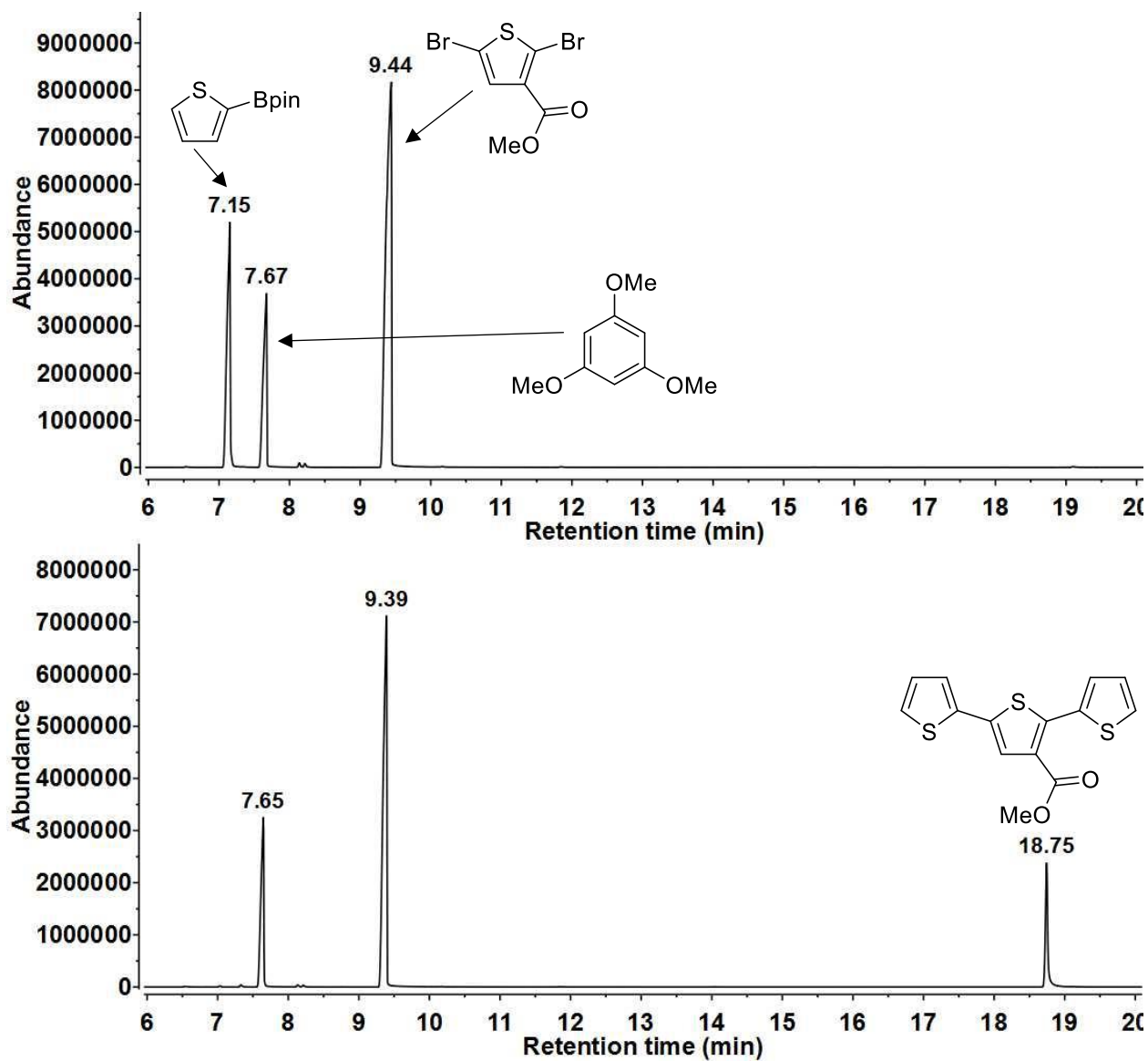


Figure A1.2. GC-MS chromatograms for small molecule Suzuki-Miyaura coupling at 50 °C using methyl-2,5-dibromothiophene-3-carboxylate and $\text{Ni}(\text{PPh}_3)\text{IPrCl}_2$ (1 mol %). Top – reaction mixture at time = 0 h. Bottom – reaction mixture after 24 h.

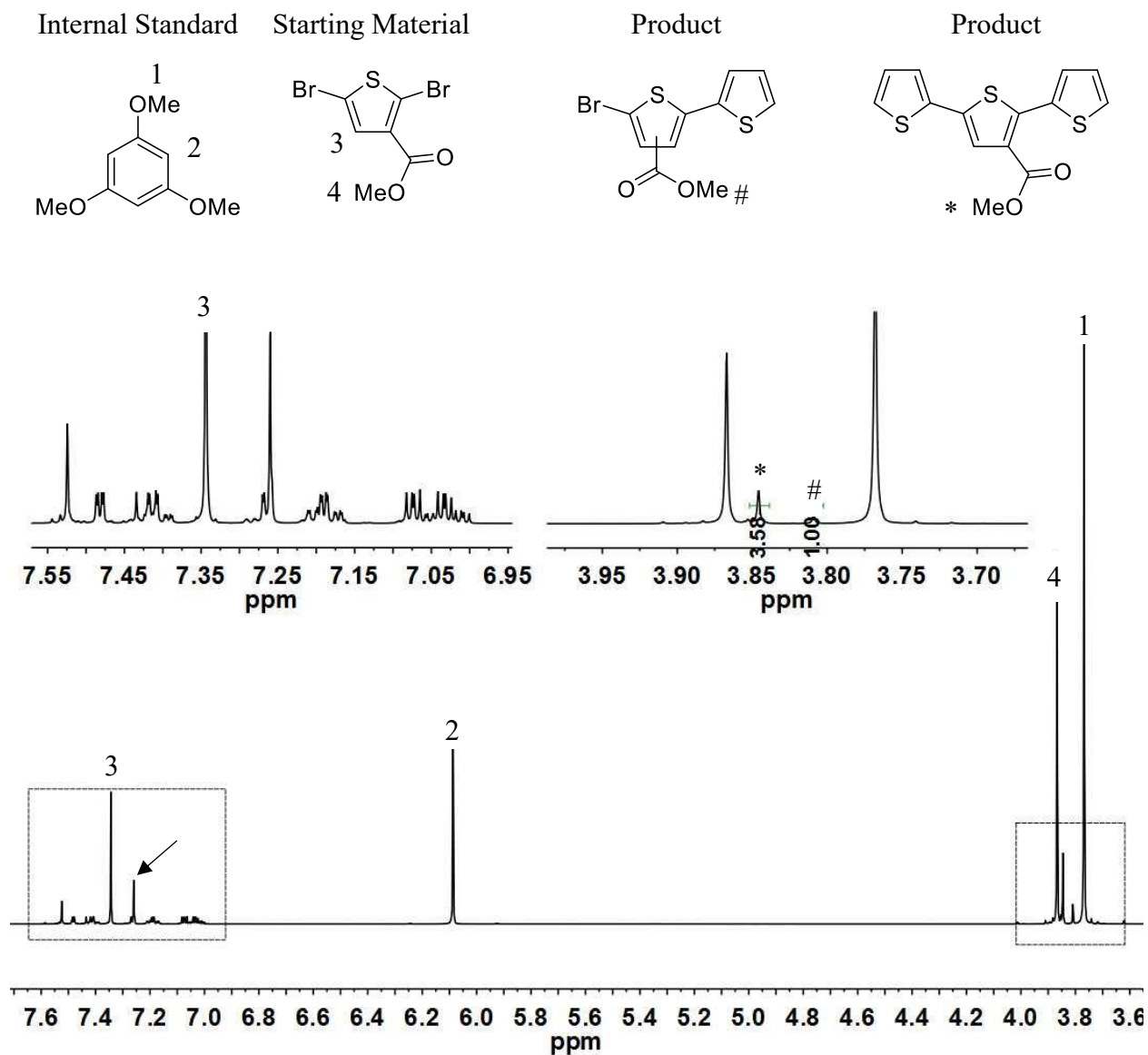


Figure A1.3. Crude ^1H NMR Spectrum (500 MHz, CDCl_3) for small molecule Suzuki-Miyaura coupling at 50 °C using methyl-2,5-dibromothiophene-3-carboxylate and PEPPSI-IPr (1 mol %). Ratio of products was determined from integration of the carboxylate signal.

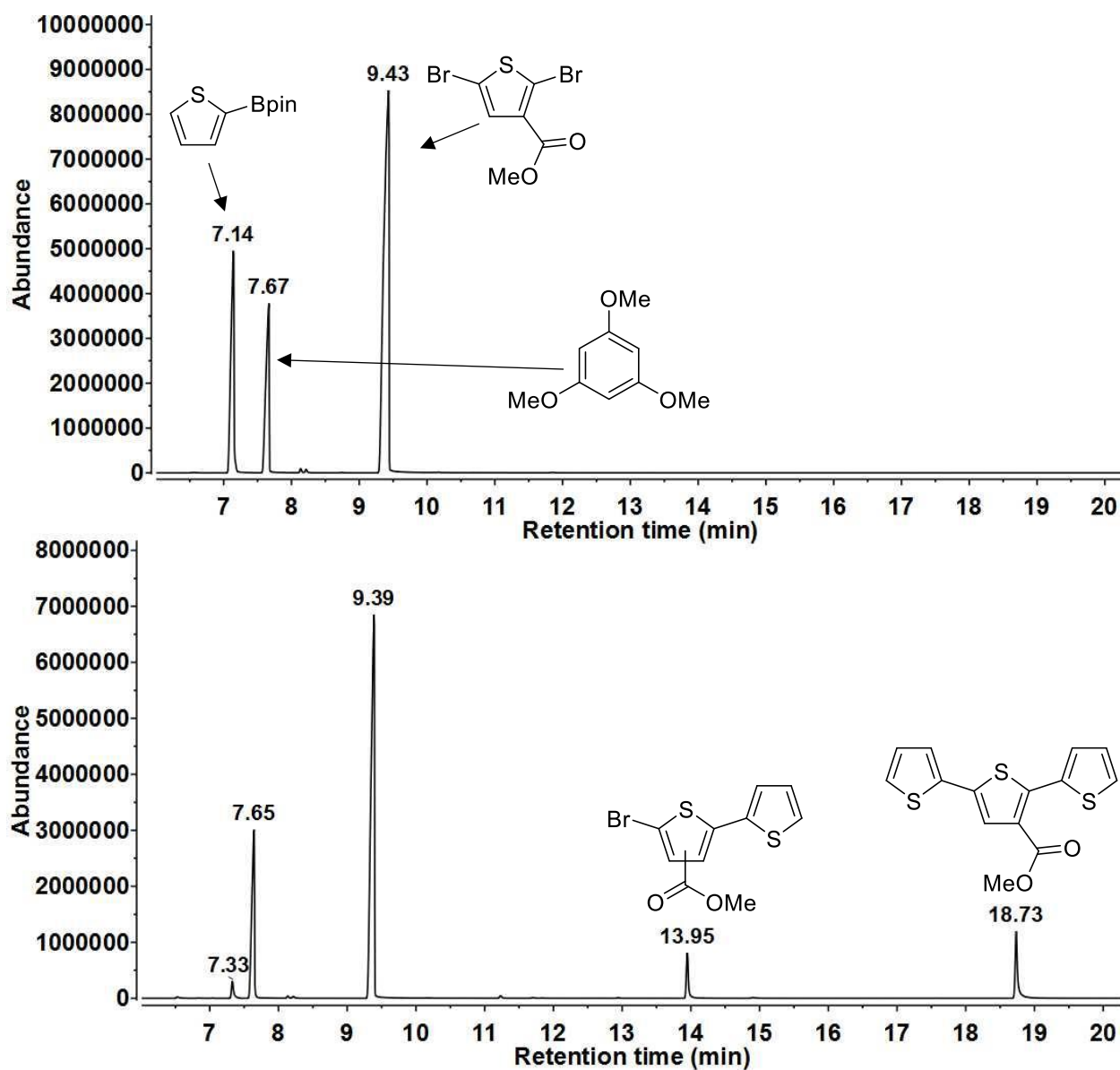


Figure A1.4. GC-MS chromatograms for small molecule Suzuki-Miyaura coupling at 50 °C using methyl-2,5-dibromothiophene-3-carboxylate and PEPPSI-IPr (1 mol %). Top – reaction mixture at time = 0 h. Bottom – reaction mixture after 24 h. Signal at 7.33 min is bithiophene formed from precatalyst initiation.

A1.2 NMR Spectra Collected for Polymers

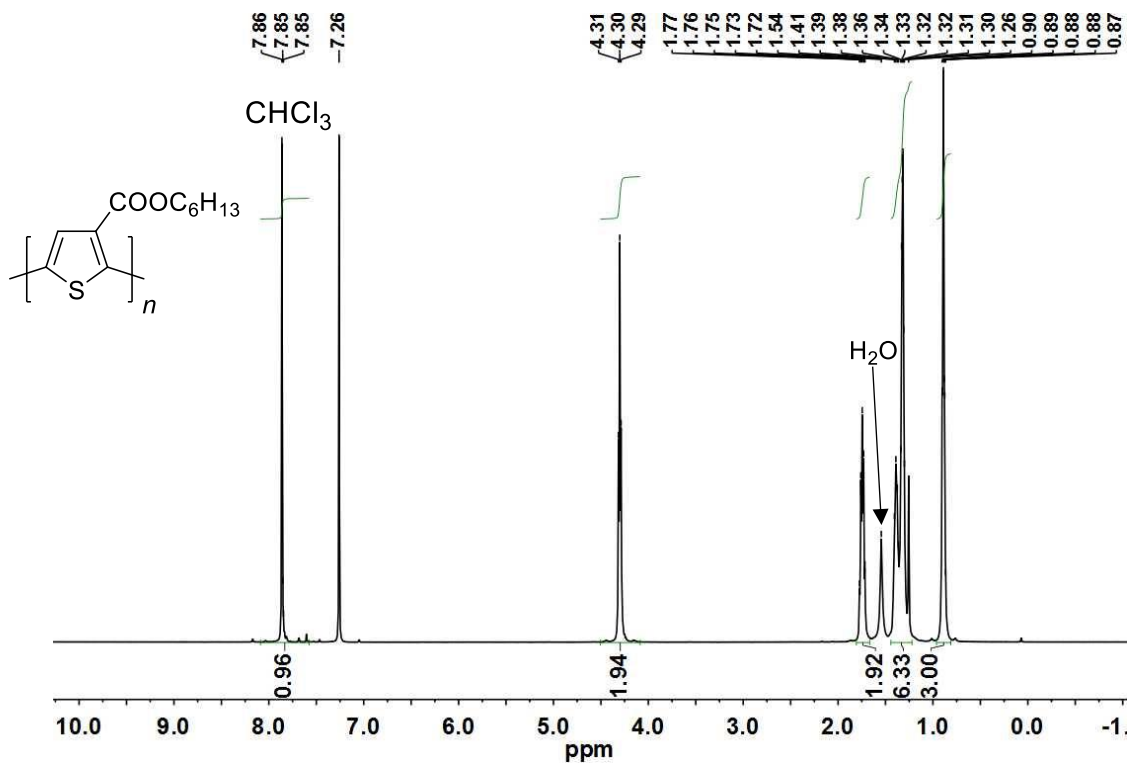


Figure A1.5. P3HET ^1H NMR Spectrum – 500 MHz, CDCl_3 .

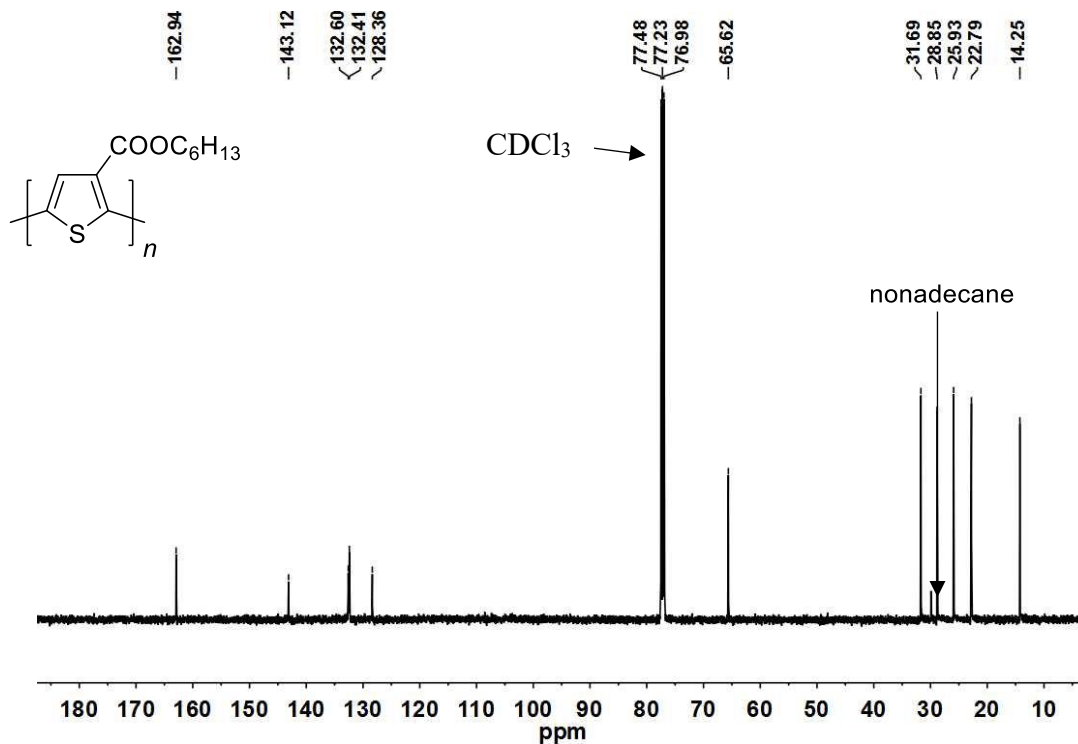


Figure A1.6. P3HET ^{13}C NMR Spectrum – 126 MHz, CDCl_3 .

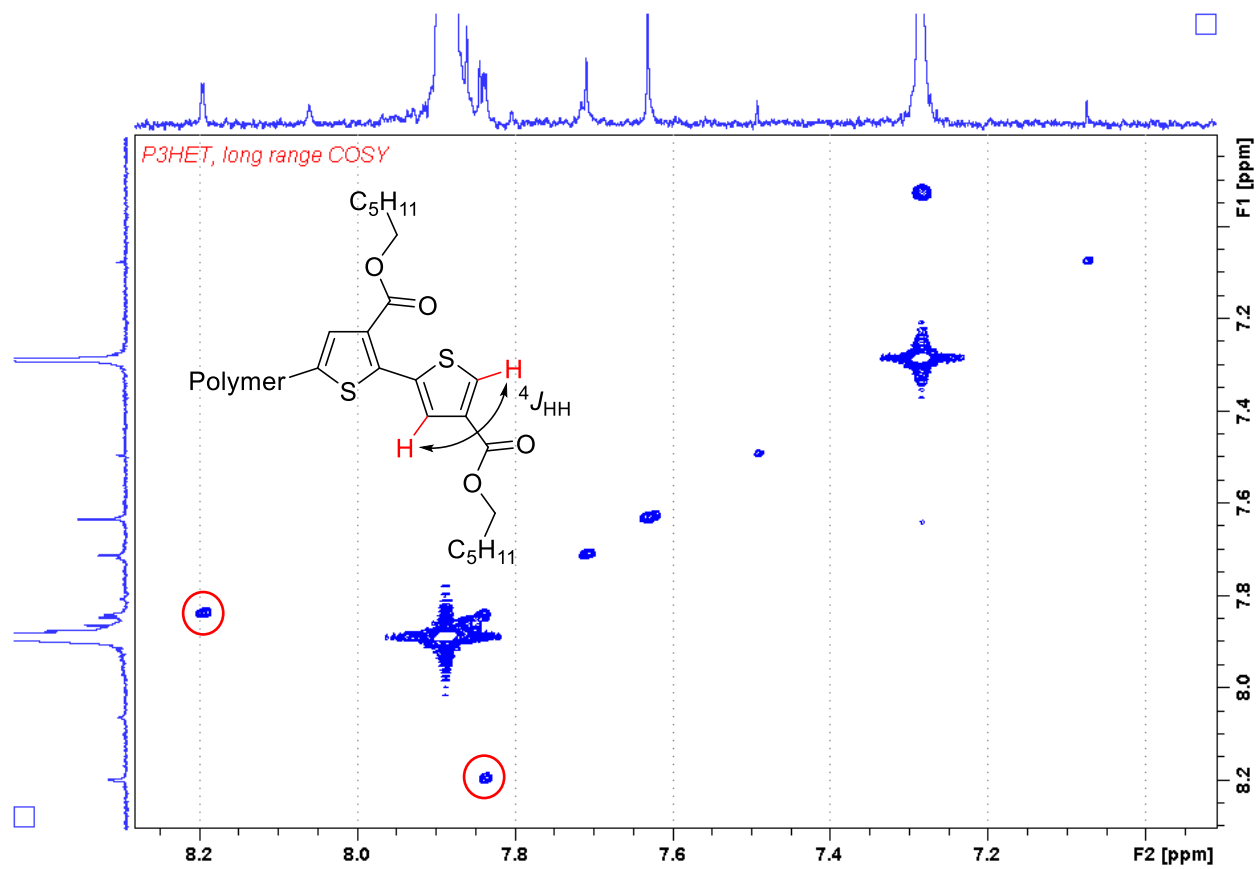


Figure A1.7. P3HET long-range COSY illustrating the coupling for the H-terminated end-group.

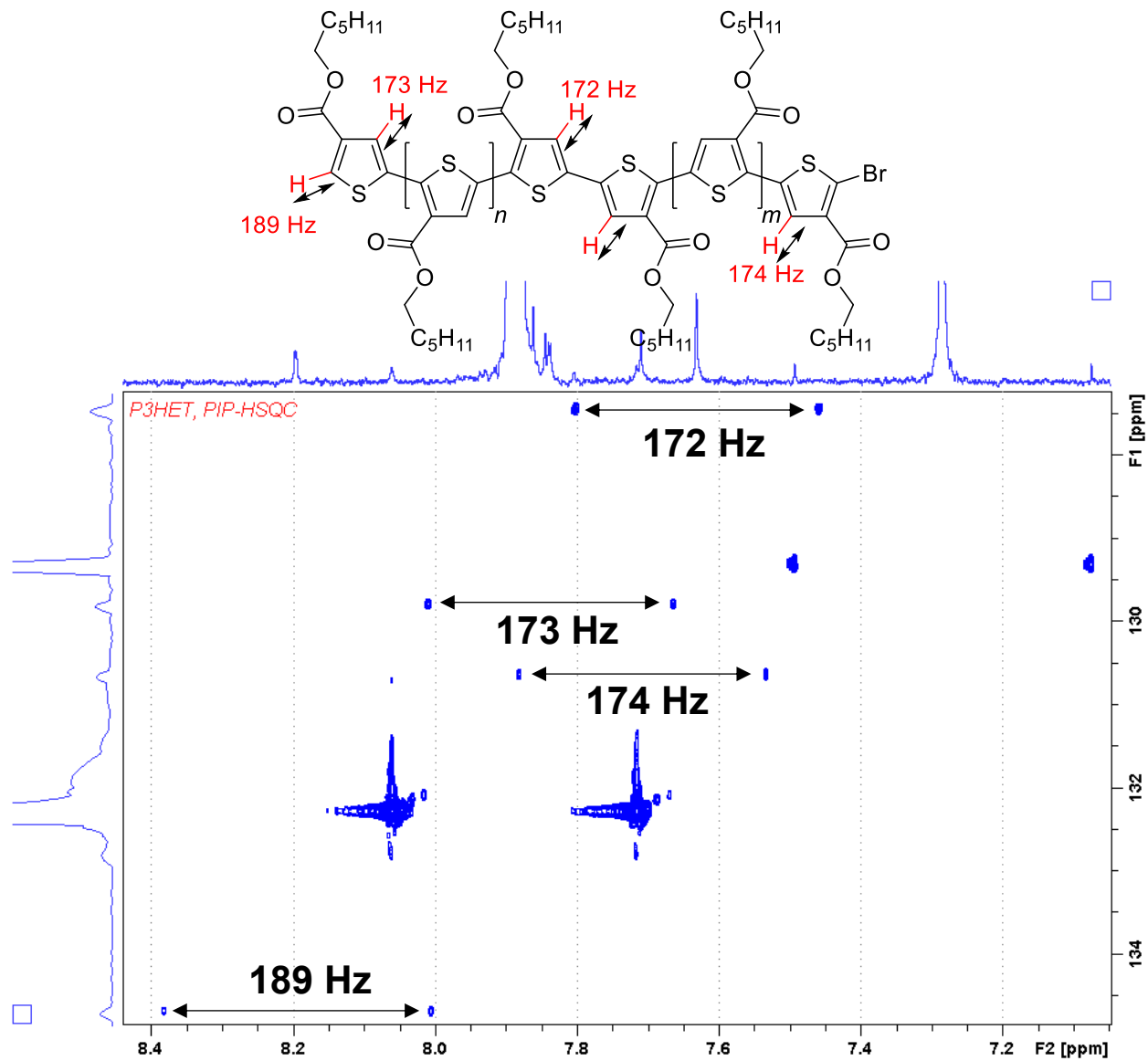


Figure A1.8. P3HET high resolution coupled HSQC illustrating the regioregular polymer backbone.

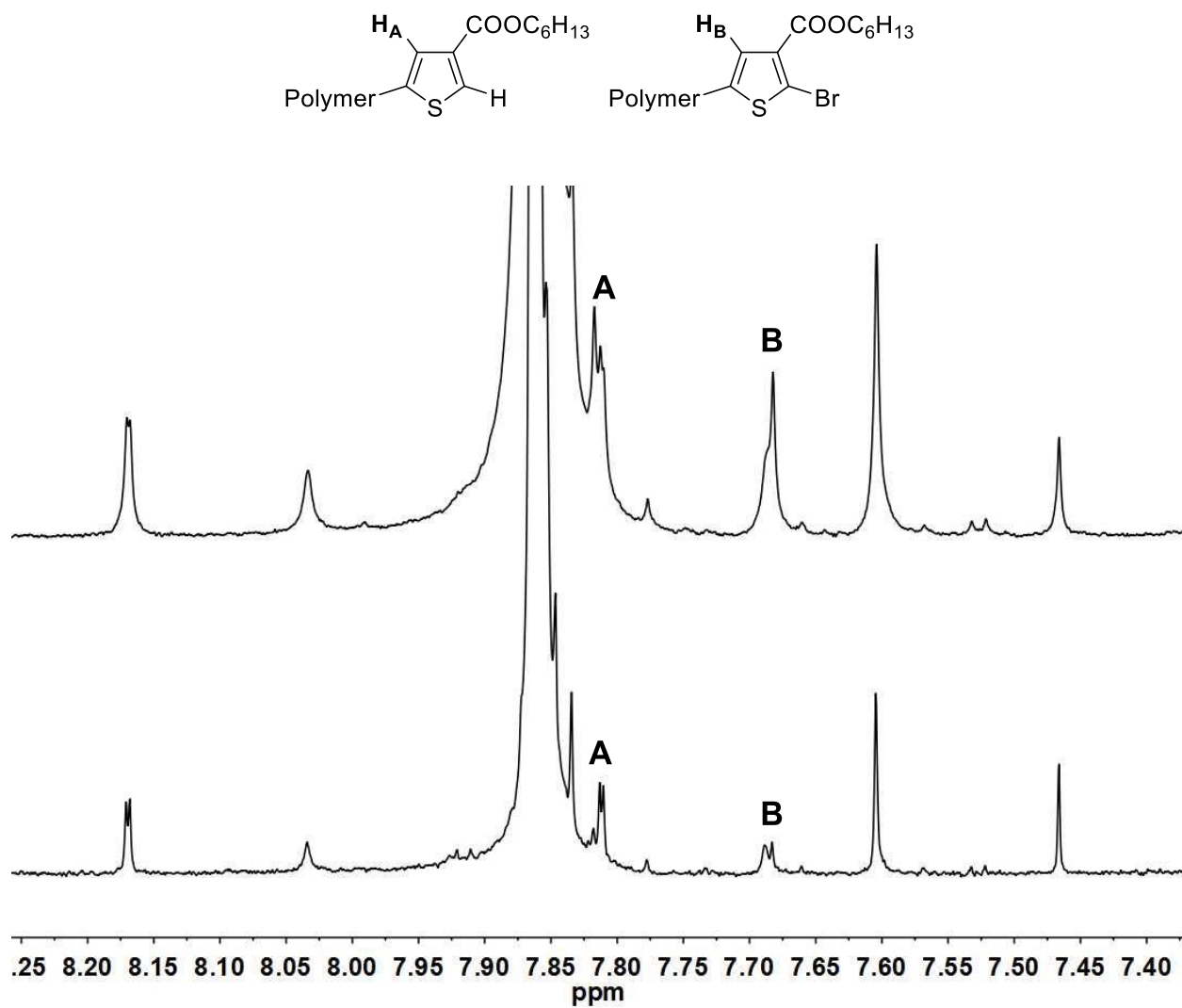


Figure A1.9. Top – ¹H NMR Spectrum of P3HET. Bottom – P3HET treated with Ni(COD)₂ followed by HCl illustrating the loss of the Br-terminated end group.

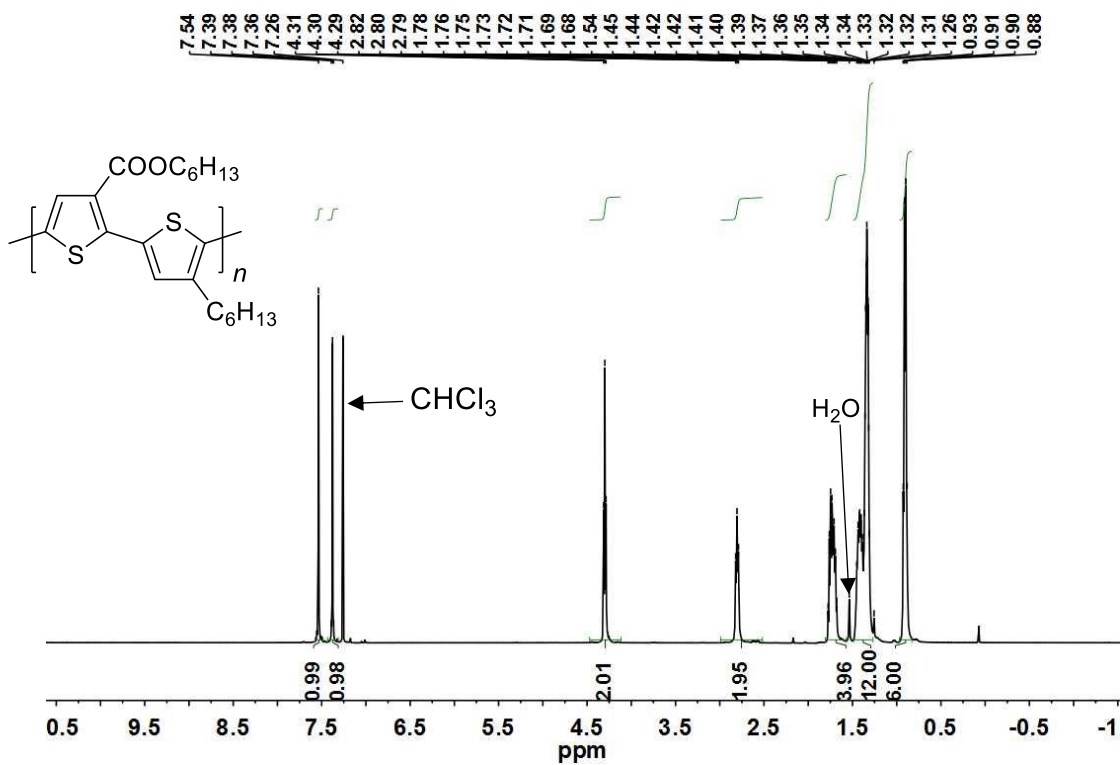


Figure A1.10. P3HET-*a*-P3HT ^1H NMR Spectrum – 500 MHz, CDCl_3 .

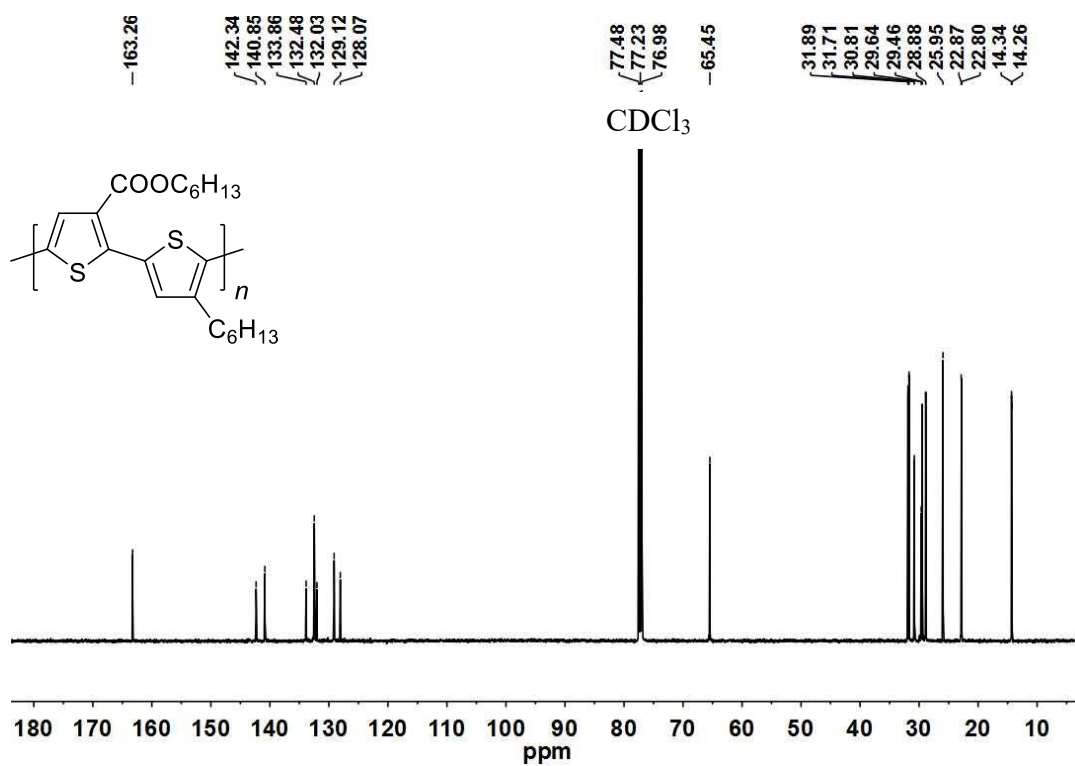


Figure A1.11. P3HET-*a*-P3HT ^{13}C NMR Spectrum – 126 MHz, CDCl_3 .

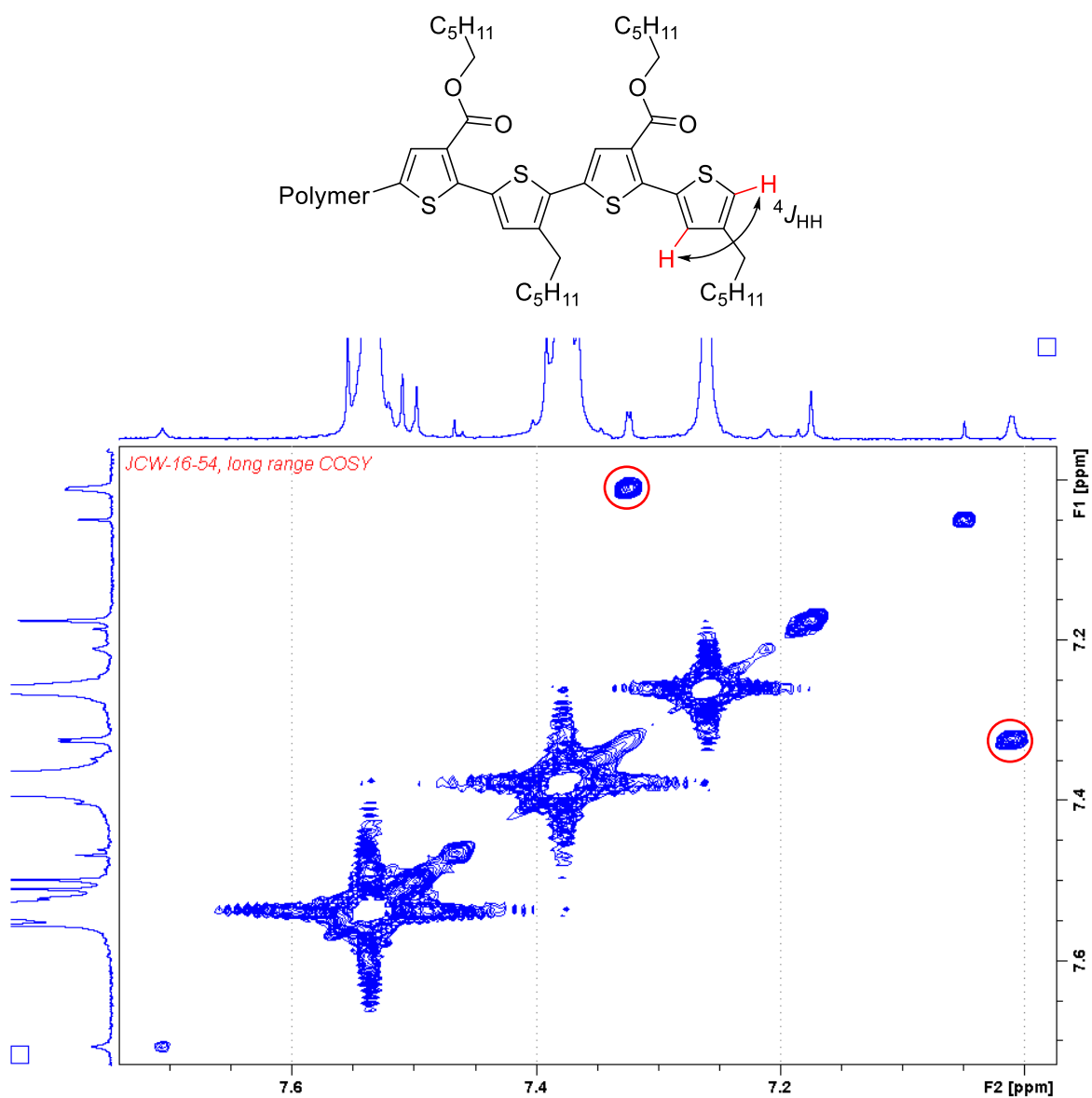


Figure A1.12. P3HET- α -P3HT long-range COSY illustrating the coupling of both aromatic protons of the end-group.

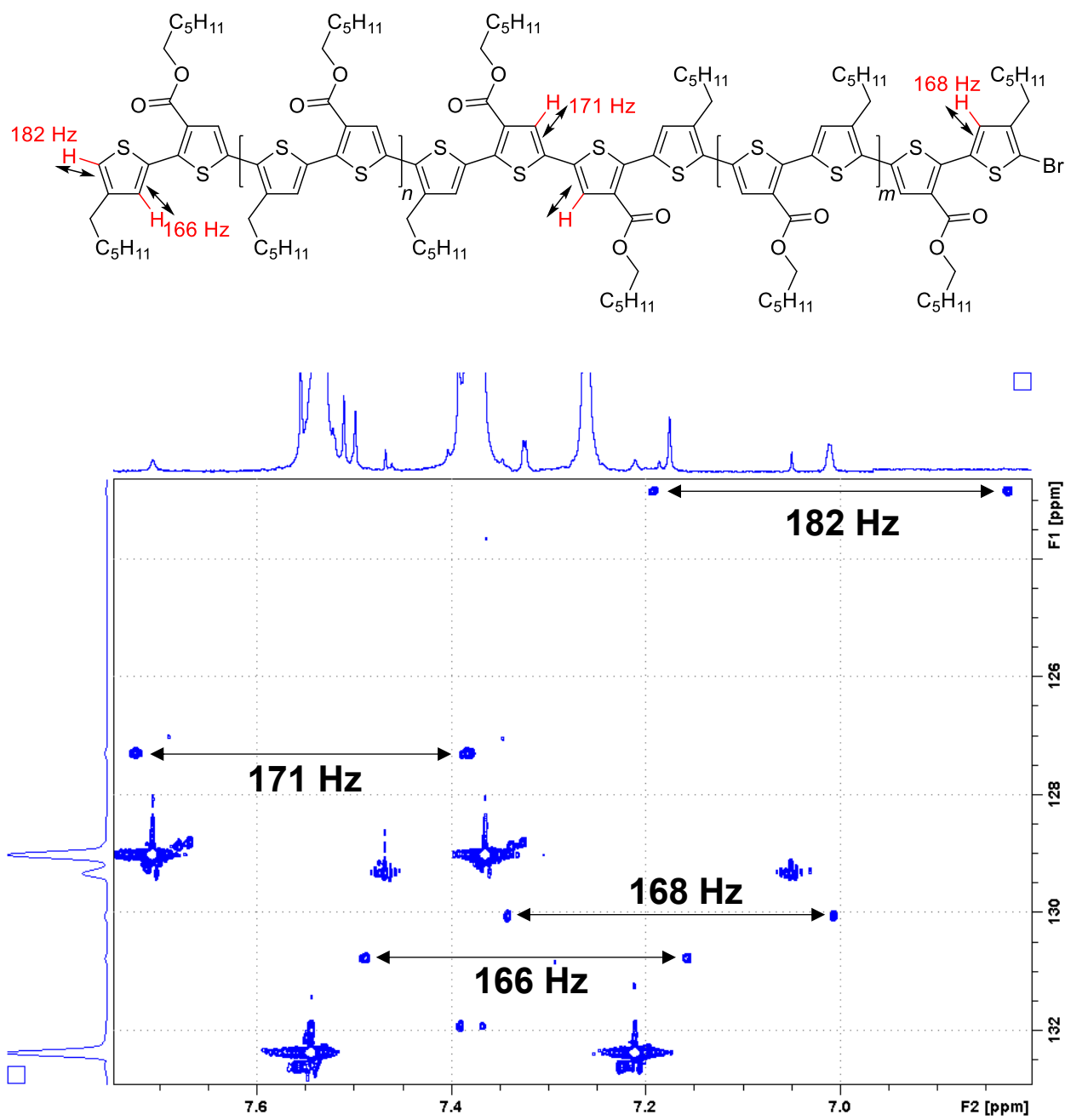


Figure A1.13. P3HET-*a*-P3HT high resolution HSQC illustrating the regioregular polymer backbone.

A1.3 Representative GPC Traces

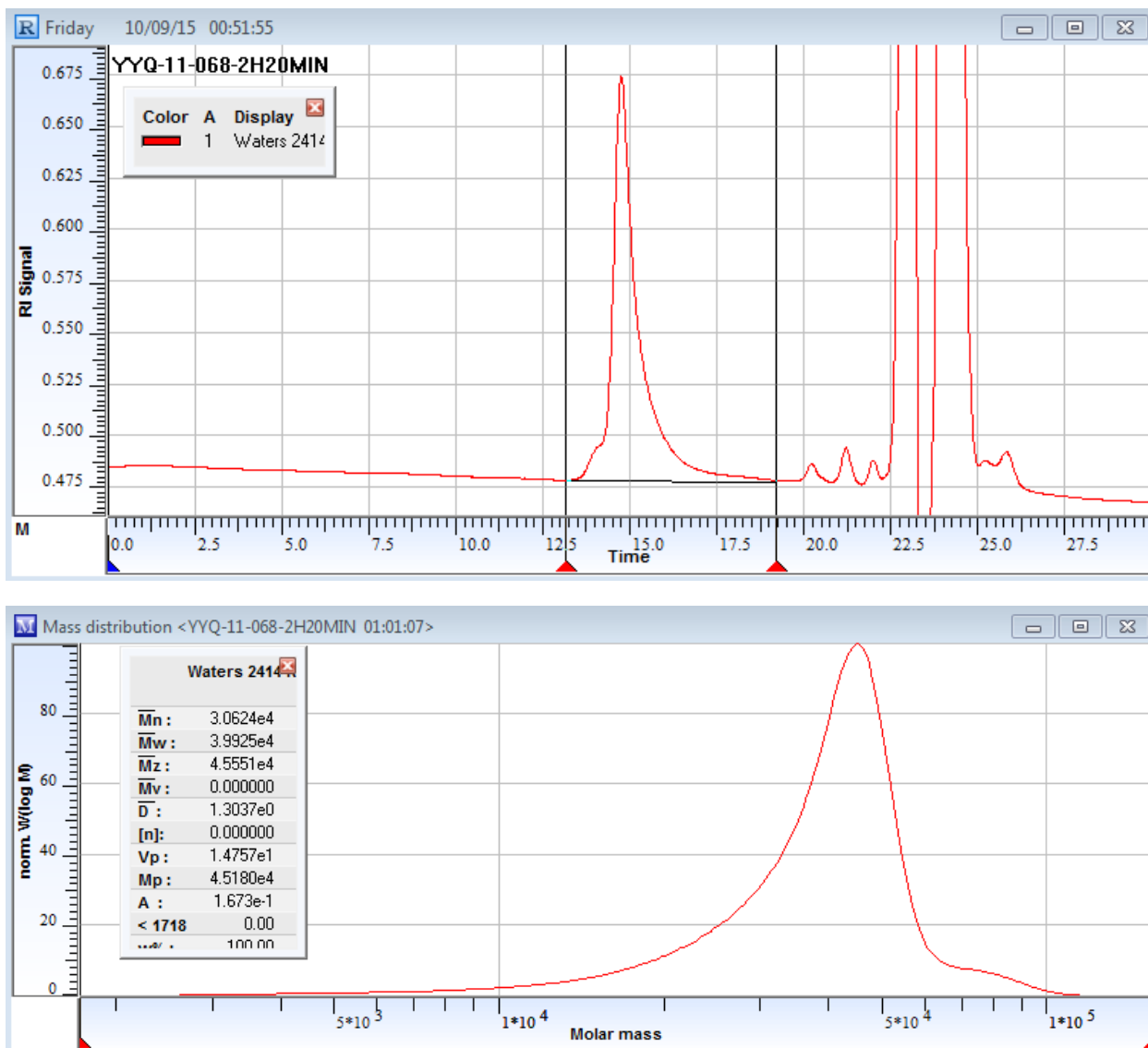


Figure A1.14. GPC Chromatogram and analysis of P3HET sample. Entry 3, Table 4.2 in Chapter 4.

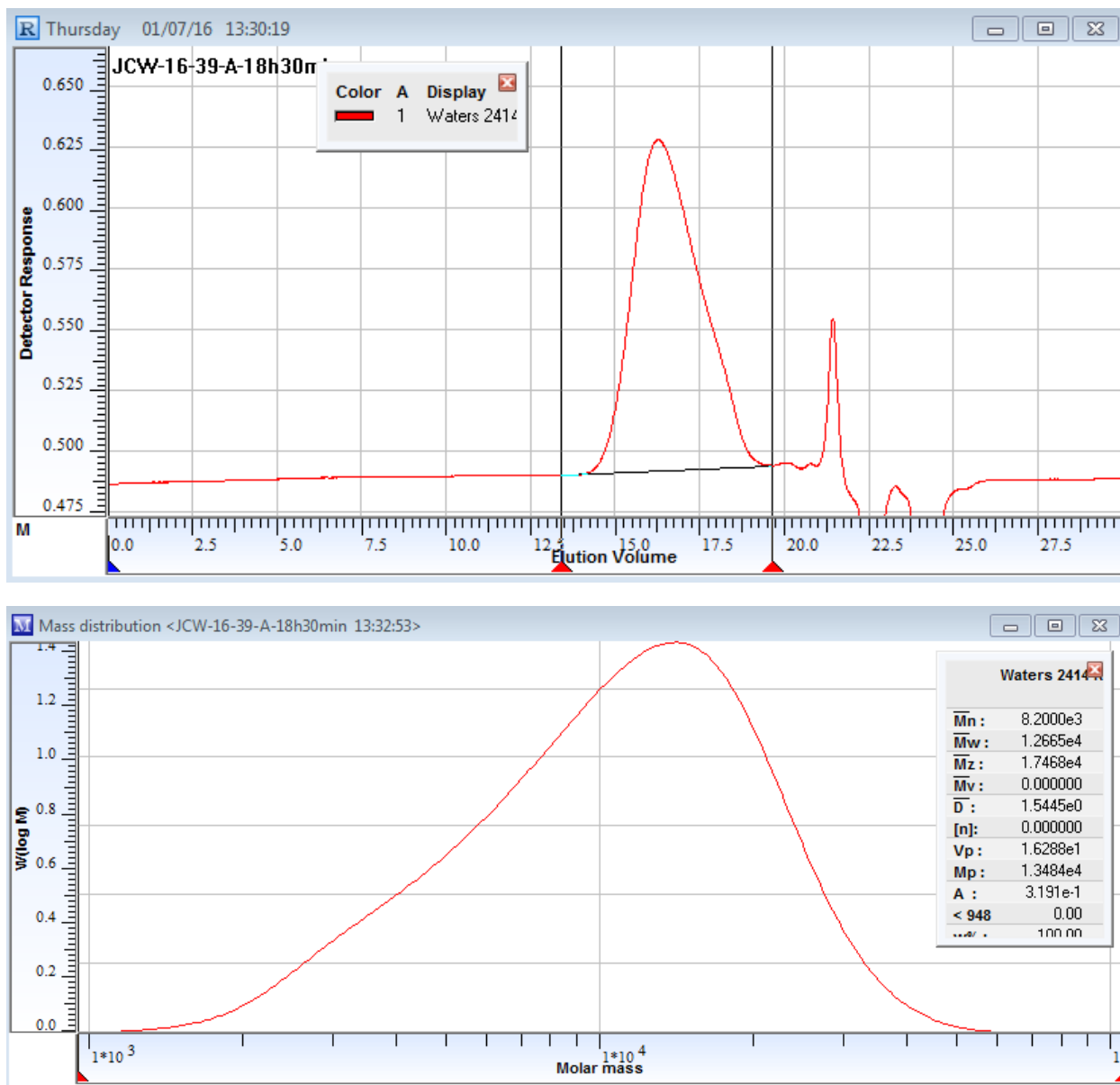


Figure A1.15. GPC Chromatogram and analysis of P3HT sample using Ni(dppp)Cl₂ as the catalyst without water.

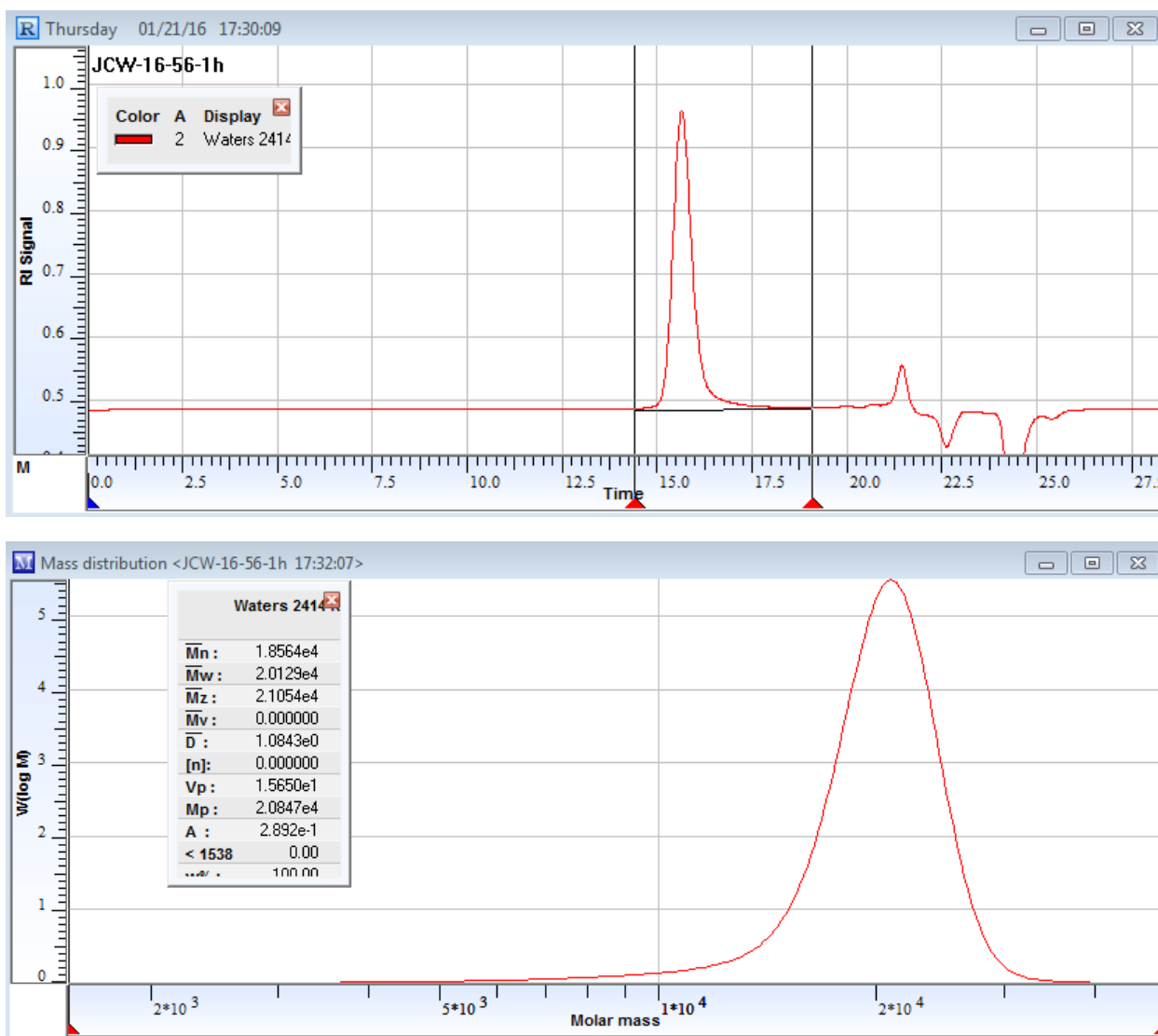


Figure A1.16. GPC Chromatogram and analysis of P3HT sample. Entry 9, Table 4.2 in Chapter 4.

Appendix 2

Supplementary Material for Chapter 5

A2.1 NMR Spectra Collected for Polymers

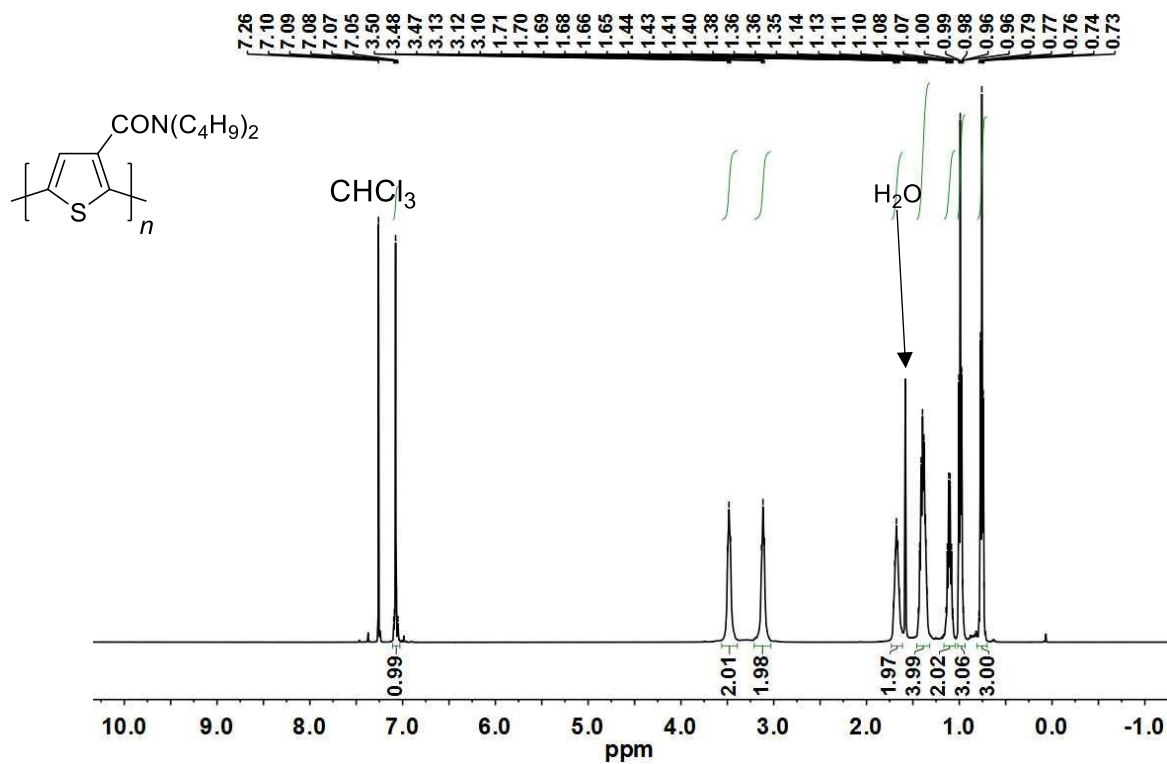


Figure A2.1. P3DBAT ^1H NMR Spectrum – 500 MHz, CDCl_3 .

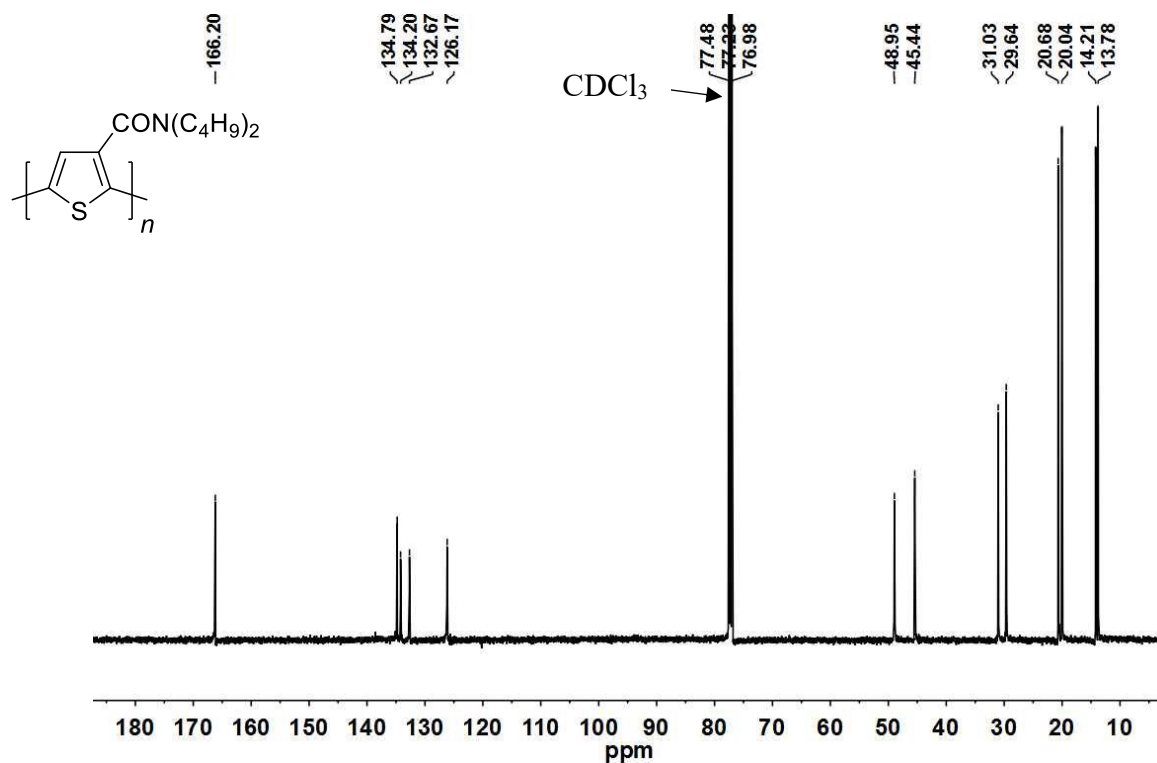


Figure A2.2. P3DBAT ^{13}C NMR Spectrum – 126 MHz, CDCl_3 .

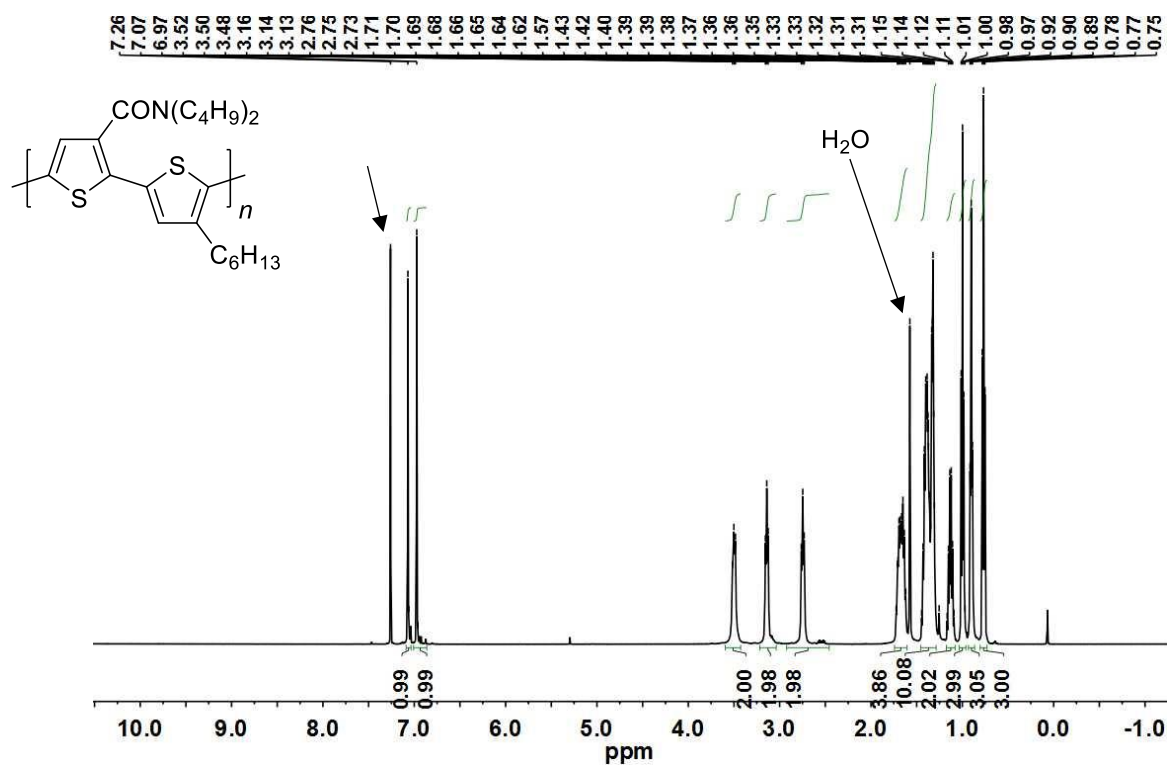


Figure A2.3. P3DBAT-*a*-P3HT ^1H NMR Spectrum – 500 MHz, CDCl_3 .

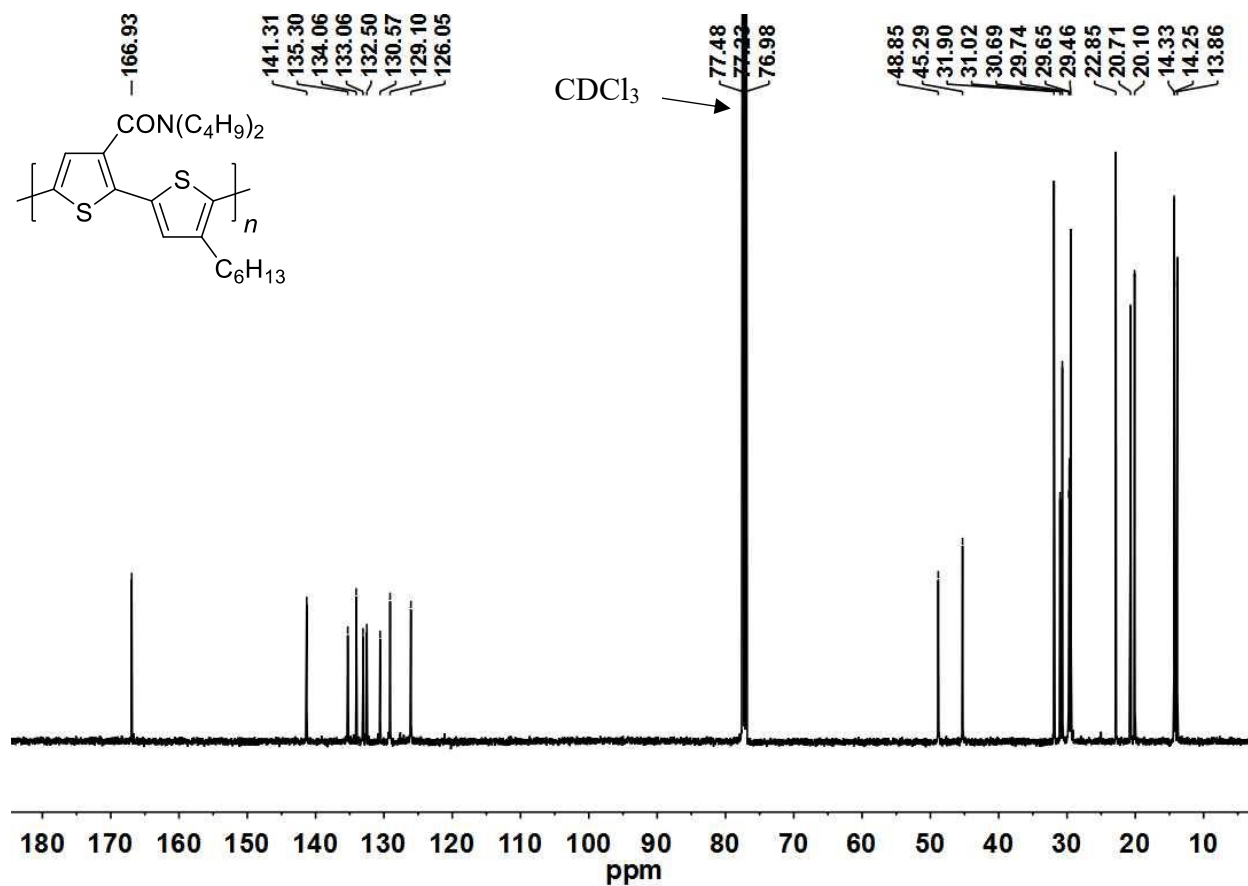


Figure A2.4. P3DBAT-*a*-P3HT ^{13}C NMR Spectrum – 126 MHz, CDCl_3 .

A2.2 Representative GPC Traces

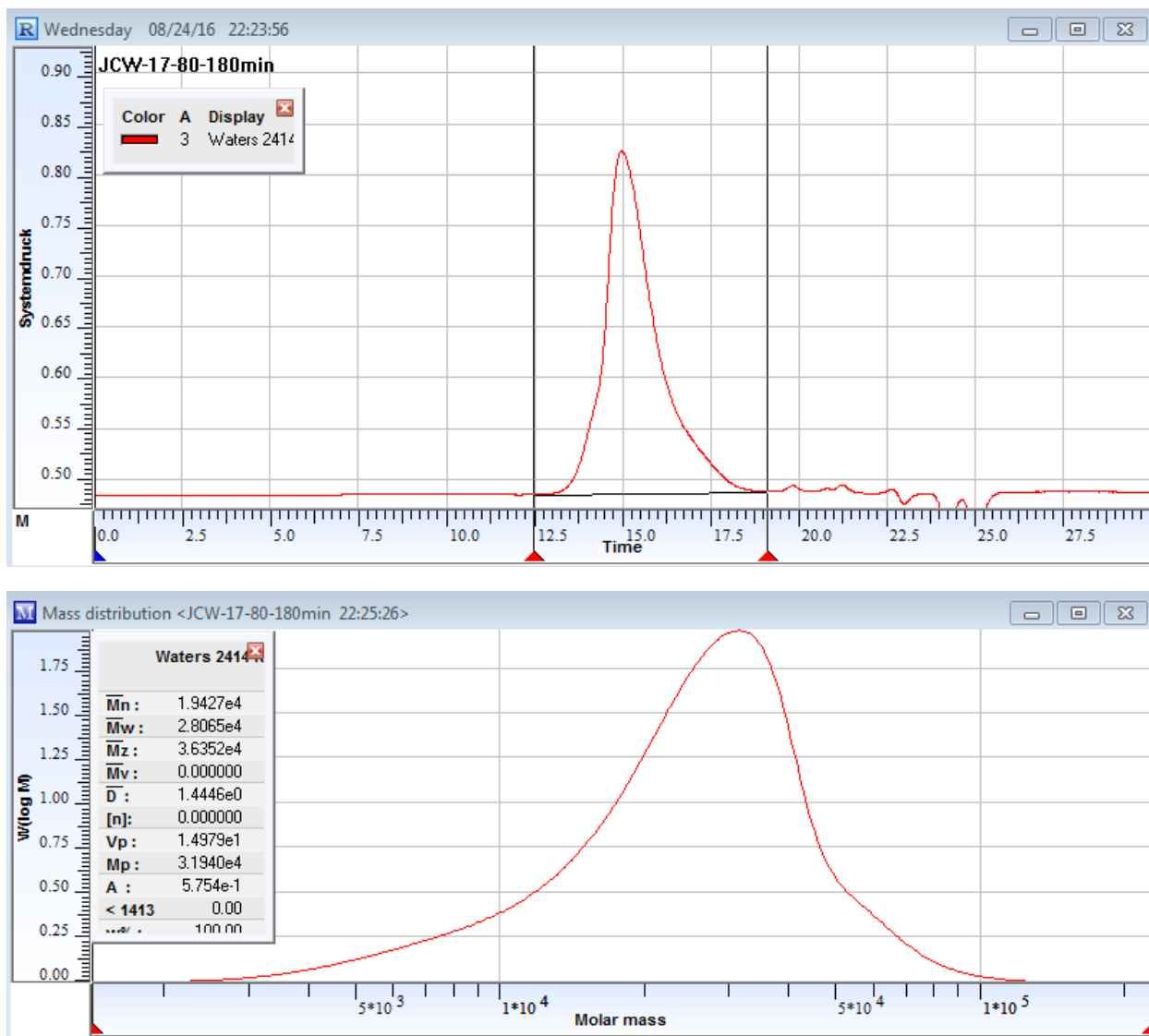


Figure A2.5. GPC Chromatogram and analysis of P3DBAT sample. Entry 3, Table 5.1 in Chapter 5.

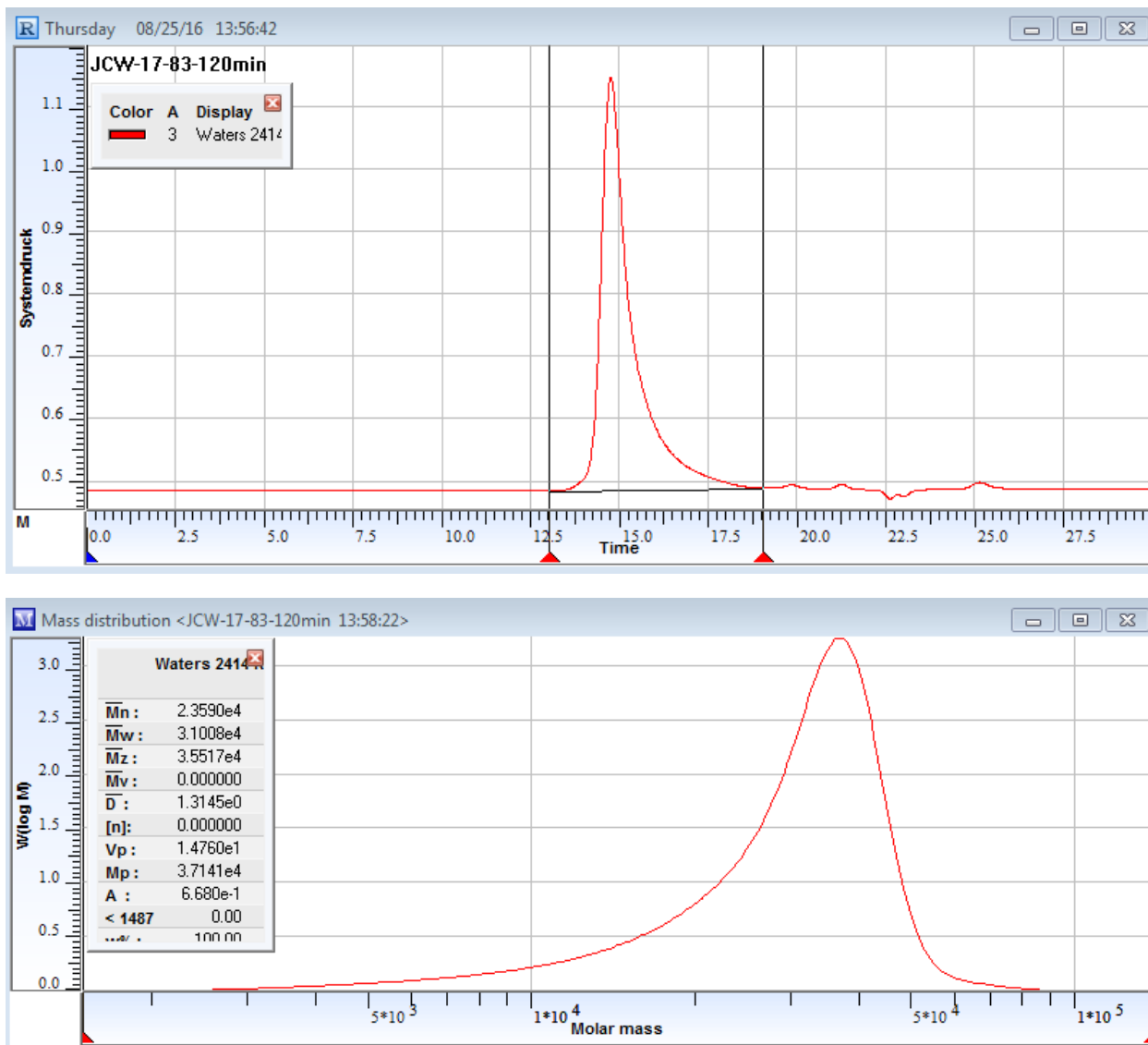


Figure A2.6. GPC Chromatogram and analysis of P3DBAT-*a*-P3HT sample. Entry 6, Table 5.1 in Chapter 5.

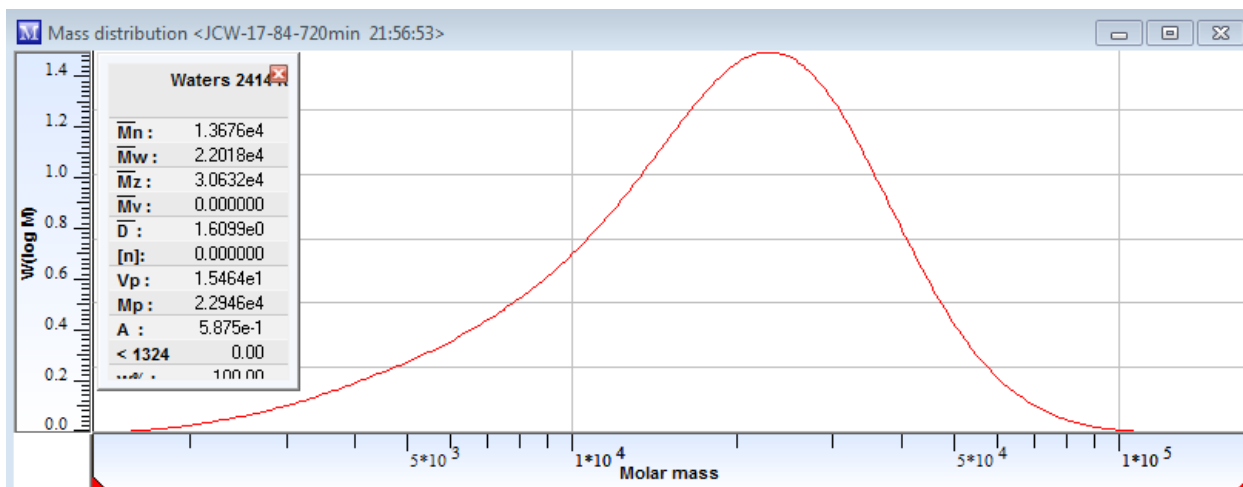
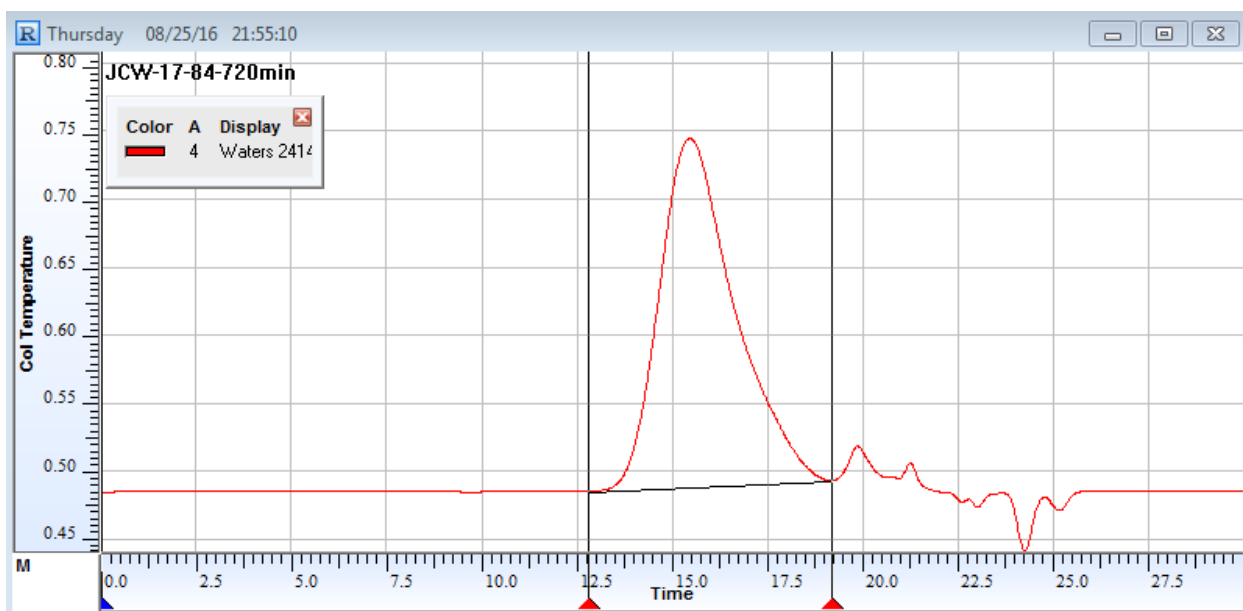


Figure A2.7. GPC Chromatogram and analysis of P3DBAT-*a*-P3HT sample. Entry 7, Table 5.1 in Chapter 5.